Spring 2020

Evaluation of the performance of different polymer gel systems as an in-depth gel treatment using numerical simulation

Tariq K. Khamees

Department: Geosciences and Geological and Petroleum Engineering

EVALUATION OF THE PERFORMANCE OF DIFFERENT POLYMER GEL SYSTEMS AS AN IN-DEPTH GEL TREATMENT USING NUMERICAL SIMULATION

by

TARIQ KHALAF KHAMEES

A DISSERTATION

Presented to the Graduate Faculty of the

MISSOURI UNIVERSITY OF SCIENCE AND TECHNOLOGY

In Partial Fulfillment of the Requirements for the Degree

DOCTOR OF PHILOSOPHY

in

PETROLEUM ENGINEERING

2020

Approved by:

Ralph E Flori, Advisor
Shari Dunn-Norman
Mingzhen Wei
J. David Rogers
Parthasakha Neogi

PUBLICATION DISSERTATION OPTION

This dissertation consists of the following three articles, formatted in the style used by the Missouri University of Science and Technology:

Paper I, found on pages 46-109, has been published in *Fuel Journal*.

Paper II, found on pages 110-151, has been published in *American Journal of Science, Engineering and Technology.*

Paper III, found on pages 152-202, has been published in SPE OnePetro.

ABSTRACT

Oil production from heterogeneous and naturally fractured reservoirs are usually hindered due to the presence of high-permeability streaks and natural fractures networks. Oil production could be more lowered if there is a crossflow from the high- to the low-permeability layers and high mobility ratio. These problems are called conformance problems and the treatment is called conformance improvement technologies (CITs). The aims of CIT is to correct the heterogeneity of the reservoir and to lower the unfavorable mobility ratio. These technologies are leading to the diversion of post-treatment water into the low-permeability layers and to increase the viscosity of the displacing fluid (e.g., water). Therefore, overall sweep efficiency, could be improved and an enhancement to oil production could occur.

Assessment of the potential of polymer flooding and gel treatment requires accurate modeling of different parameters that could affect these processes. Selecting of the best polymer gel system requires an understanding of its performance inside the reservoir. The main aim and principle contribution of this work is to build different models to simulate the performance of in-depth gel treatment with different scenarios and different gel systems, using different reservoir simulators.

In this study, we developed a separate model for each polymer gel system that has been investigated. Different parameters have been scrutinized and the optimum parameters have been concluded. By knowing these optimum parameters, a successful application of each polymer gel system could lead to maximum benefits and maximum oil production.

ACKNOWLEDGMENTS

First, thanks to almighty God (Allah) for giving me the many blessings, opportunities, and strength to complete this long journey. Second, I would like to express my sincere gratitude to my advisor, Dr. Ralph E. Flori Jr., for his invaluable support throughout my research. He has always been an excellent mentor, a contributor, a supporter, and a friend during different stages of this study.

I would also like to thank my committee members, Dr. Shari Dunn-Norman, Dr. Mingzhen Wei, Dr. J. David Rogers, and Dr. Parthasakha Neogi, for their valuable advice and recommendations. In addition, I am very grateful to Iraq Ministry of Oil and to the ExxonMobil Iraq for granting me a PhD scholarship and financial support through ExxonMobil Iraq Training, Technology and Scholars Program (EMITT&S Program). Moreover, I would like to extend my acknowledgement to Institute of International Education (IIE) for administering this program successfully.

I am highly appreciate the University of Texas at Austin for allowing me to use the UTGEL simulator. My appreciation is extended to Dr. Ali Goudarzi for his valuable advice, fruitful discussion, and invaluable information that he provided me during all stages of my research.

Ultimately, I would like to thank my beloved wife, Shadha, for her unimaginable support, without her great sacrifice I would not be able to complete this work. I extend my thankful words to my pretty princesses, Zahraa and Daniah, for their love and great patience throughout my study. Without my family's faithful support, sacrifices, and kind encouragement, this study would have never been completed.

TABLE OF CONTENTS

LIST OF ILLUSTRATIONS

SECTION Page

PAPER I

PAPER II

LIST OF TABLES

SECTION Page

PAPER I

PAPER II

NOMENCLATURE

Symbol	Description
E	Overall Sweep Efficiency
E_D	Displacement Efficiency
E_V	Volumetric Efficiency
E_A	Aerial Sweep Efficiency
E_I	Vertical Sweep Efficiency
S_{oi}	Initial Oil Saturation
S_{or}	Residual Oil Saturation
M	Mobility Ratio
λ_o, λ_w	Mobility of Oil and Water, respectively
k_o, k_w	Effective Permeability to Oil and Water, respectively
μ_o, μ_w	Viscosity of Oil and Water, respectively
k_{ro}, k_{rw}	End-Point Relative Permeability to Oil and Water, respectively
F_r	Resistance Factor
k_w, k_p	Water and Polymer permeability, respectively
μ_w, μ_p	Water and Polymer viscosity, respectively
F_{rrw}	Residual Resistance Factor

1. INTRODUCTION

1.1. STATEMENT AND SIGNIFICANCE OF THE PROBLEM

In oil production operations, early water breakthrough, excess water production, and poor sweep efficiency are indications of severe heterogeneity, high oil viscosity, fractures, oil wet rock, and residual oil saturation, which are shown in Figure 1.1. In 1996, Seright estimated the cost savings to the oil industry between $50-100 million per year for each 1% reduction in water production. As an average based on worldwide statistics, for each barrel of oil there are three barrels of water produced with a $40 billion annual cost of disposal. In the United States, for each barrel of oil there are seven barrels of water produced with $5-10 billion annual cost of disposal (Bailey et al., 2000; Veil et al., 2004).

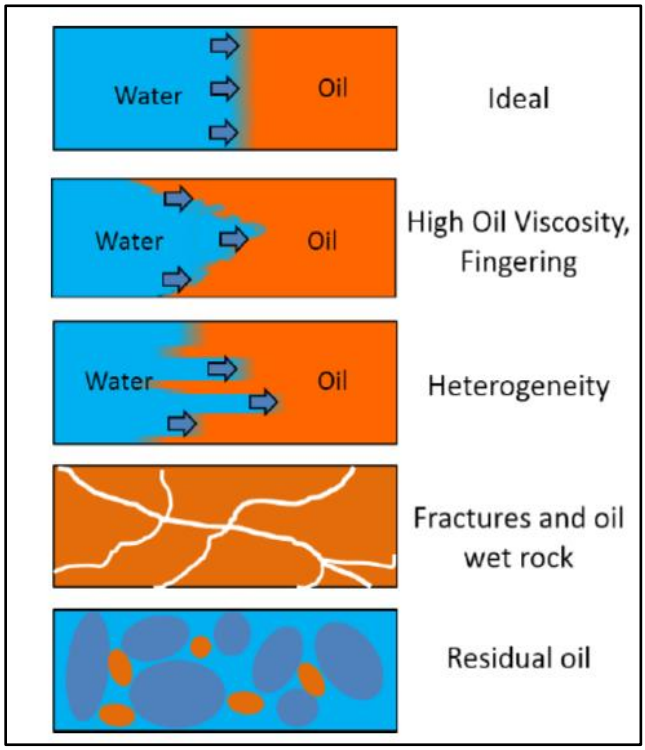

Figure 1.1. Key issues that affect oil recovery factor (Chen, 2016).

According to Green and Willhite (1998), only one third of oil in place can be recovered by the injection of chemicals, such as a surfactant or an alkaline that can increase the capillary number by lowering the interfacial tension. These chemicals aim to reduce the residual oil saturation. The process of targeting the one-third of the oil in place with these chemicals is called residual oil saturation recovery (RSOR). Another one-third of the oil in place can be recovered by primary and secondary oil recovery methods and is called conventionally recoverable mobile oil. The last one-third of oil in place can only be recovered by applying the improved recovery technologies. The latter one-third is called mobile oil and is not recoverable by conventional oil recovery, as shown in Figure 1.2 (Laherrere, 2003; Hirasaki et al., 2008; Sydansk and Romero-Zeron, 2011). In the United States, about 45% of discovered oil cannot be recovered by conventional technologies, which represents a target for improved recovery technologies.

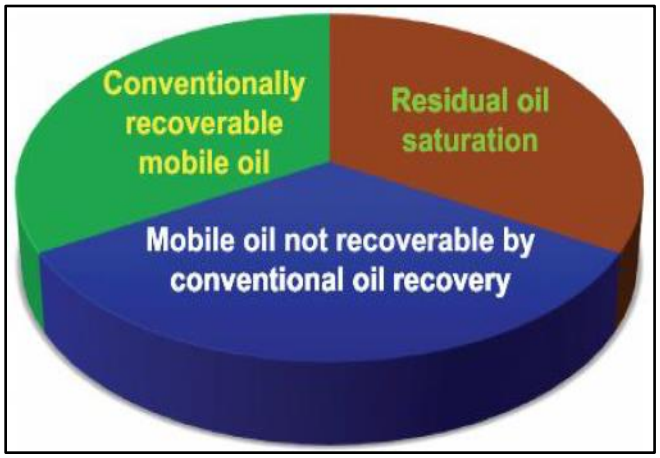

Figure 1.2. Categories of oil in place (Sydansk and Romero-Zeron, 2011).

Conformance improvement technologies (CITs) involve the injection of different chemicals such as polymer solutions, polymer in-situ gels, and polymer microgels to

correct the heterogeneity and to improve the mobility of oil, as well as to convert the wettability of the reservoir from oil-wet to moderate- or water-wet. However, the applications of these chemicals without thorough investigations of the parameters that could lead to the success or failure of the treatment may result in an over- or an under-estimation of the performance of these chemicals.

The use of these chemicals, which is considered a chemical enhanced oil recovery (CEOR) method, is varied according to the existing problems in the reservoir and the source of water production. Conformance problems caused by the existence of different layers with different permeability (e.g., highly heterogeneous or naturally fractured reservoirs) is one of the main sources of excess water production leading to unevenness in the flood front. Accordingly, extensive experimental works supported by pilot tests were carried out for more than three decades to select the best strategy to attack excess water production. In addition, huge efforts have been dedicated in order to select the best combination of chemical (e.g., polymer and crosslinker) concentration and type that is suitable for different reservoir conditions.

Numerical modeling is an alternative way to design and study a given combination of polymer and crosslinker that can be used in field applications. There are different commercial simulators such as CMG-STARS (Computer Modeling Group LTD), and ECLIPSE (Schlumberger), in adition to in-house simulators such as UTCHEM, and UTGEL (University of Texas at Austin) that can be used to model chemical enhanced oil recovery methods. The use of these simulators includes validating a given experimental work, building a conceptual model, and building a pilot model based on real field data supported by experimental work.

In this study, different polymer gel systems have been designed and modeled as an in-depth gel treatment using CMG-STARS and UTGEL simulators. Both simulators have the capability of modeling different CEOR processes. The UTGEL simulator has the capability to model a preformed gel as one component and an in-situ gel as a reaction between different components. On the other hands, the CMG-STARS simulator can model both preformed and in-situ gel systems as a reaction between different components only.

The main objective of this study is to provide a guide to successfully design, implement, and evaluate different polymer gel systems. Table 1.1 shows the polymer gel systems that have been studied and modeled in this study.

Table 1.1. Types of polymer gels modeled in this study.

Model #	Gel system	Gelation process occurs at	Components of the gel system	Simulator
1	Colloidal Dispersion Gel (CDG)	Reservoir	HPAM and Aluminum citrate	CMG-STARS
2	Polymer/chromium chloride gel	Reservoir	HPAM, Sodium dichromate, thiourea	UTGEL
3	Polymer/chromium malonate gel	Reservoir	HPAM, Cr(III), and Malonate ion	UTGEL
4	Sodium silicate gel	Reservoir	Sodium-silica, HCl, and Aluminum	CMG-STARS
5	Preformed particle gel (PPG)	Surface	Superabsorbent crosslinked polymer	UTGEL
6	Thermally activated polymer (TAP)	Surface	Superabsorbent crosslinked polymer	UTGEL

1.2. EXPECTED IMPACTS AND CONTRIBUTIONS

By using reservoir simulations, this study aims to develop a thorough understanding of the most influential parameters that could affect the application of different polymer gel systems in both heterogeneous and naturally fractured reservoirs. After fulfilling the main objectives, the sub-objectives were accomplished. These sub-objectives are as follows:

(a) Comparison between different polymer gel systems at same reservoir setup to show the potential of each gel system.

(b) Modeling a combination injection of low-salinity water flooding (LSWF), polymer solution, and surfactant with the gel treatment.

(c) Investigating the ability of a polymer solution's shear-thickening behavior to compete with gel treatment in order to improve the sweep efficiency.

In this study, parameters are recognized to be of two categories, which can affect the ultimate recovery factor and the maximum oil production:

(a) Reservoir parameters: represent the reservoir and fluid properties that cannot be physically controlled on location. The reservoir properties includes:

   i) Heterogeneity: the degree of contrast between the permeability of the thief zones compared to the permeability of the matrix.

   ii) Crossflow: the ratio of the permeability in the vertical direction to the permeability in the horizontal direction.

   iii) Wettability: the tendency of one reservoir fluid to adhere or spread on the rock surface in the presence of another reservoir fluid.

   iv) Thickness of the thief zones.

   v) Fluid viscosity.

vi) Reservoir temperature.

vii) Salinity and the hardness of the reservoir brine.

viii) Clay content.

(b) Operating parameters: these represent the parameters that we do have physical control over on location, which include, but are not limited to the following:

i) Polymer and crosslinker properties such as concentration and molecular weight.

ii) Volume of the treatment.

iii) Injection rate.

iv) Injection pressure.

The outcomes from this study will help the engineers to identify the most and least influential parameters.

1.3. STATEMENT OF WORK

In this research the following objectives and work scope are investigated:

1.3.1. Objectives. This study is designed to model different polymer gel systems separately, which could lead to higher oil recovery and better sweep efficiency.

The models are designed as full-scale field models to make the results applicable to the field applications. The data used to build the models were taken from published literatures that contain field and experimental works. The purpose of using real data was to mimic the performance of the polymer gel systems in real life.

1.3.2. Work Scope. This research is primarily a numerical simulation study using two simulators: CMG-STARS and UTGEL. Table 1.2 presents the parameters that have been investigated for each polymer gel system using either the CMG-STARS or the UTGEL simulators.

Table 1.2. Objective parameters.

Polymer Gel Type	Study the effect of	Publication/Year	Simulator
• Colloidal Dispersion Gel (CDG)	• Bullhead injection • Zonal isolation • Heterogeneity • Crossflow • Initiation time of the treatment • Alternate injection of gel and polymer • Sensitivity analysis	SPE-185716-MS / 2017	CMG-STARS
• Polymer/Chromium Chloride Gel	• Polymer solution vs. polymer gel • Polymer rheology • Salinity • Injection schemes • Cation exchange capacity (CEC) • Reservoir wettability • Gravity segregation and dip angle • Mobility ratio • Skin factor in the injector	Fuel Journal / 2018	UTGEL
• Polymer/Chromium Malonate Gel	• Polymer solution vs. gel treatment • Gel rheology • Salinity • Hardness	SPE-190046-MS / 2018	UTGEL
• Sodium Silicate Gel	• Sensitivity analysis of the gridblocks • Injecter vs. producer • Placement technology • HCl concentration • Pre-flush	SPE-191200-MS / 2018	CMG-STARS

Table 1.2. Objective parameters (Cont.).

• Sodium Silicate Gel	• Volume of pre-flush • Gel adsorption • Mixing gel with polymer solutions • Temperature and activation energy • Shut-in time • Reservoir wettability	SPE-191200-MS / 2018	CMG-STARS
• Polymer/Chromium Chloride Gel	• Mixing surfactant-polymer with gel • Reservoir temperature • Polymer rheology • Surfactant concentration • Injection scheme • Salinity and hardness	SPE-193011-MS / 2018	UTGEL
• Polymer solution • CDG • Polymer/Chromium Chloride Gel • Polymer/Chromium Malonate Gel	• Uinified Viscosity Model (UVM) vs. shear thinning polymer rheology	SPE-193592-MS / 2019	UTGEL
• CDG	• Polymer vs. CDG • Shear thinning behavior of CDG • Adsorption of CDG • Degradation of CDG • Salinity of the brine • In-depth vs. near-wellbore treatments • Alternate injection of CDG and polymer • Reservoir wettability • Polymer/crosslinker ratio • Hydrolysis of polymer solution	American Journal of Science, Engineering, and Technology / 2019	CMG-STARS
• Preformed Particle Gel (PPG)	• Width of fracture • Salinity of brine • Reservoir wettability • Number of fracture segments	Unpublished	UTGEL

Table 1.2. Objective parameters (Cont.).

• Thermally Activated Polymer (TAP)	• TAP concentration and slug size • Heterogeneity and crossflow • Reservoir wettability • Location of the thief zone • Mobility ratio • Initiation time of the treatment • Reservoir and activation temperatures • Salinity of brine • Applying the optimum parameters	SPE-198048-MS/2019	UTGEL

2. LITERATURE REVIEW

2.1. RECOVERY MECHANISMS

Oil recovery from petroleum reservoirs involves three recovery mechanisms: primary, secondary, and tertiary, as shown in Figure 2.1. The primary recovery mechanism is the production of oil by the natural energy of the reservoir, which decreases rapidly after the start of production. The recovery factor from this stage does not exceed 25% OOIP if the reservoir is saturated with light oils, and only 5% OOIP if the reservoir is saturated with heavy oils as shown in Figure 2.2. By the end of the primary recovery stage, the reservoir pressure is unable to push more oil out of the pores. At this point, a water flood or a gas injection is normally initiated to support the reservoir pressure and push more oil out of the pores. Gas is injected into the gas cap to support pressure or into the oil column in the wellbore to lift oil to the surface. The differences of the permeability of the reservoir layers and the differences of fluid viscosities (i.e., unfavorable mobility ratio), make water tends to move faster than oil and bypass large quantities of hydrocarbons in place. The recovery factor from secondary recovery mechanisms is 30% OOIP for light oil reservoirs and only 5% OOIP for heavy oil reservoirs. Schulte (2005) estimated the worldwide recovery factor is only 34% OOIP from the primary and secondary recovery mechanisms.

Due to the increasing demands of oil consumption, rapidly declining oil production, and low recovery factors from primary and secondary methods, a third stage recovery mechanism should be implemented with a target of approximately either 45% OOIP if the reservoir oils are light, or 90% OOIP if the reservoirs are saturated with heavy oils as shown in Figure 2.2. This stage is called enhanced oil recovery (EOR), which may be considered

as a first or second stage if the reservoir oils are heavy (Ahmed and Meehan, 2012). Thus, EOR is not necessarily tertiary recovery processes.

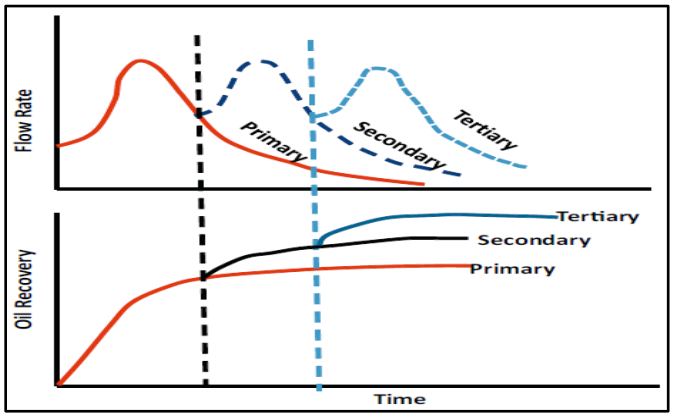

Figure 2.1. Classification of oil recovery mechanisms (Ahmed and Meehan, 2012).

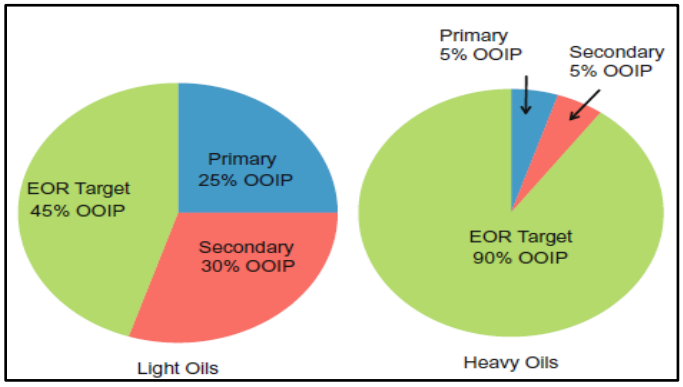

Figure 2.2. Percentage of oil recovery from each category of recovery mechanism (Ahmed and Meehan, 2012).

2.2. ENHANCED OIL RECOVERY PROCESSES

Enhanced oil recovery is defined as the injection of materials that do not normally exist in reservoirs to improve their recovery (Lake, 1989; Sydansk and Romero-Zeron, 2011). Another terminology that has been used interchangeably with EOR is improved oil

recovery (IOR). IOR processes include EOR in addition to water flooding, pressure maintenance, infill drilling, and horizontal wells. The latter processes could be considered as a part of reservoir characterization and reservoir management (Green and Willhite, 1998; Alvarado and Manrique, 2010). EOR processes are divided into thermal and non-thermal techniques as shown in Figure 2.3.

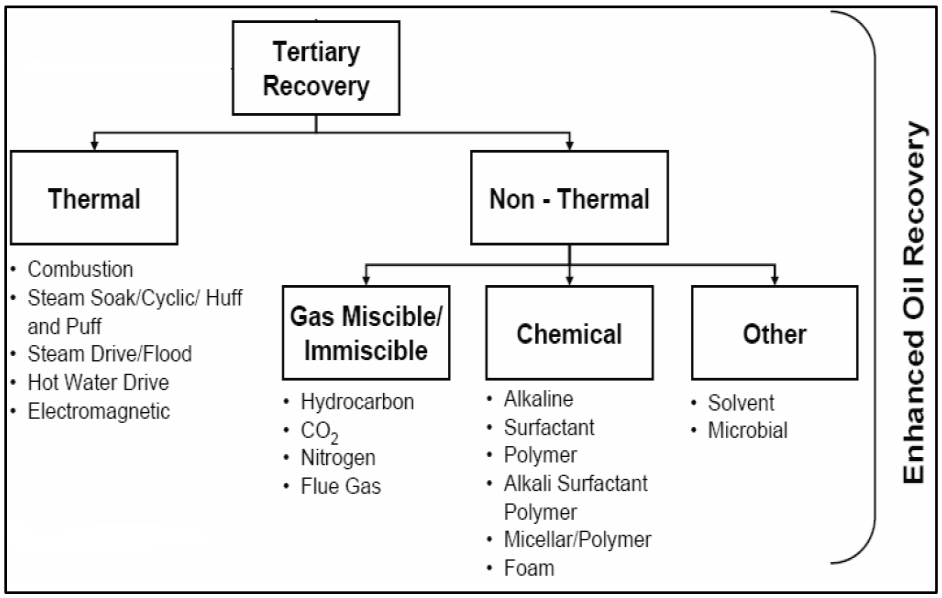

Figure 2.3. Classification of EOR methods (Lake, 1989).

EOR technologies aim to rejuvenate mature fields by injecting different chemicals such as polymers, surfactants, foams, or combinations such as alkaline / surfactant / polymer (ASP). These chemicals interact with reservoir rocks or reservoir fluids to control the mobility ratio such as using the polymers or to lower the interfacial tension between oil and water to thereby increase the capillary number, such as surfactant, surfactant-polymer, and/or Alkaline-Surfactant-Polymer, or to change the wetting characteristics of the carbonate rocks from oil-wet to water-wet, such as using the surfactants.

Another EOR technology is the use of crosslinked polymer to block the high-permeability layers and reduce the flow of water through these layers. Post-treatment water is diverted into the low-permeability layers in order to improve the sweep efficiency. Gel treatment can be divided into near-wellbore treatment and in-depth fluid diversion. This classification depends on reservoir characterization, such as the fluid crossflow from the high-permeability layers to the low-permeability layers. Different gel systems are available to satisfy different types of conformance control problems, such as colloidal dispersion gel (CDG) for heterogeneous reservoirs and preformed particle gels (PPG) for naturally fractured reservoirs with super K layers.

The main objective of injecting the previously mentioned chemicals is to improve the overall sweep efficiency E, which is composed of displacement (E_D) and volumetric sweep efficiency (E_V), as shown in Equations (2.1), (2.2) and (2.3):

$$E = E_D \times E_V \tag{2.1}$$

$$E_D = \frac{S_{oi} - S_{or}}{S_{oi}} \tag{2.2}$$

$$E_V = E_A \times E_I \tag{2.3}$$

2.3. SOURCES OF EXCESS WATER PRODUCTION

Water production during the production of oil can be divided into two categories: good water production and bad water production. Good water production (also known as necessary water production) refers to the quantity of water required to produce a commercial amount of oil without affecting the economic life of the well. Bad water (also known as unnecessary water production) happens when water competes with oil inside the reservoir. Eventually, water cut increases and oil production decreases, which affects the

economic life of the well. Bailey et al. (2000) divided water production into three categories:

- *"Sweep" water*: the source of this water is from an injector or an active water bearing zone (i.e., aquifer), which contributes to the sweeping of oil.
- *Good water*: necessary to the production of oil, which occurs due to the fractional flow in porous media (Seright et al., 2003; Sydansk and Romero-Zeron, 2011). This water is produced below the economic limit of the WOR, and reducing "good" water production will lower oil production correspondingly.
- *Bad water*: unnecessary to the production of oil. Water is produced above the WOR economic limit because it flows into the wellbore through thief zones or natural fractures (Seright et al., 2003; Sydansk and Romero-Zeron, 2011), which causes detrimental damages to oil production.

The last type of water production is the most challenging to operators because it causes severe problems, including but not limited to the following:

- Corrosion of casing and tubing.
- Fine migration.
- Increased cost of separation.
- Reduced oil production rate.
- Lowered productive life of the oil wells.
- Environmental issues.

Table 2.1 shows a classification of excess water production problems as suggested by Seright et al. (2003) and Baily et al. (2000). This classification was categorized according to the difficulty of treatment.

Table 2.1. Excess water production problems and treatment categories (Bailey et al., 2000; Seright et al., 2003; Sydansk and Romero-Zeron, 2011).

Category	Proposed Treatments
A: "Conventional" Treatments Normally are an Effective Choice 1. Casing leaks without flow restrictions. 2. Flow behind pipe without flow restrictions. 3. Unfractured wells with effective crossflow barriers.	Cement, mechanical patches, or a combination of gel placement followed by cement
B: Treatments with Gelants Normally are an Effective Choice 4. Casing leaks with flow restrictions. 5. Flow behind pipe with flow restrictions. 6. "2D coning" through a hydraulic fracture from an aquifer. 7. Natural fracture system leading to an aquifer.	Gelants, partially formed gels or preformed gels
C: Treatments with Preformed Gels are an Effective Choice 8. Faults or fractures crossing a deviated or horizontal well. 9. Single fracture causing channeling between wells. 10. Natural fracture system allowing channeling between wells.	Conventional gel treatments or preformed gels
D: Difficult Problems where Gels Treatments Should Not Be Used 11. 3D coning. 12. Cusping. 13. Channeling through strata (no fractures), with crossflow.	Gelants and gel treatments are not recommended.

Category D represents the most difficult conformance problems that are encountered in the reservoirs. Seright et al. (2009) recommended the isolation of hydrocarbon intervals during the placement of gelant in Category D to avoid any damage that could happen to these intervals. Sydansk and Romero-Zeron (2011) listed the treatment options for each category and divided the sources of excess water into three main

categories, as shown in Figures 2.4, 2.5, and 2.6. In this study, the far-wellbore reservoir conformance problems are the target of the numerical modeling.

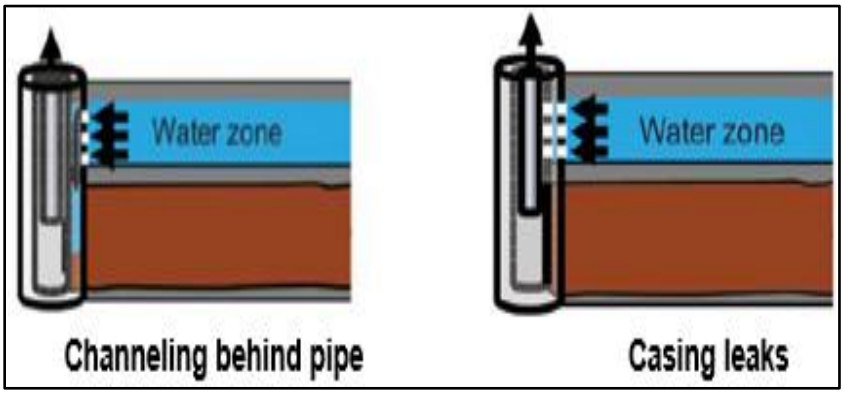

Figure 2.4. Wellbore-related problems (Sydansk and Romero-Zeron, 2011).

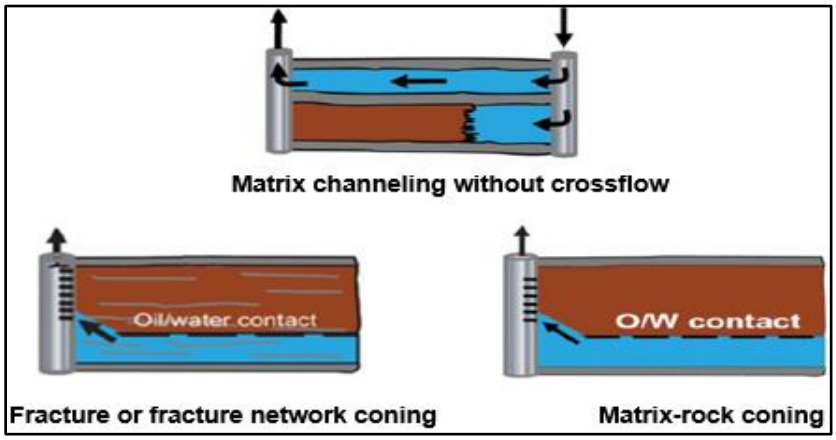

Figure 2.5. Near wellbore-related problems (Sydansk and Romero-Zeron, 2011).

2.4. TYPES OF CONFORMANCE IMPROVEMENT TECHNOLOGY

The placement of the treatment, the type of the conformance problem, and the reservoir characteristics (e.g., crossflow versus no crossflow) are factors that determine the

type of treatment. According to Liu et al. (2006), five types of the treatment can be characterized:

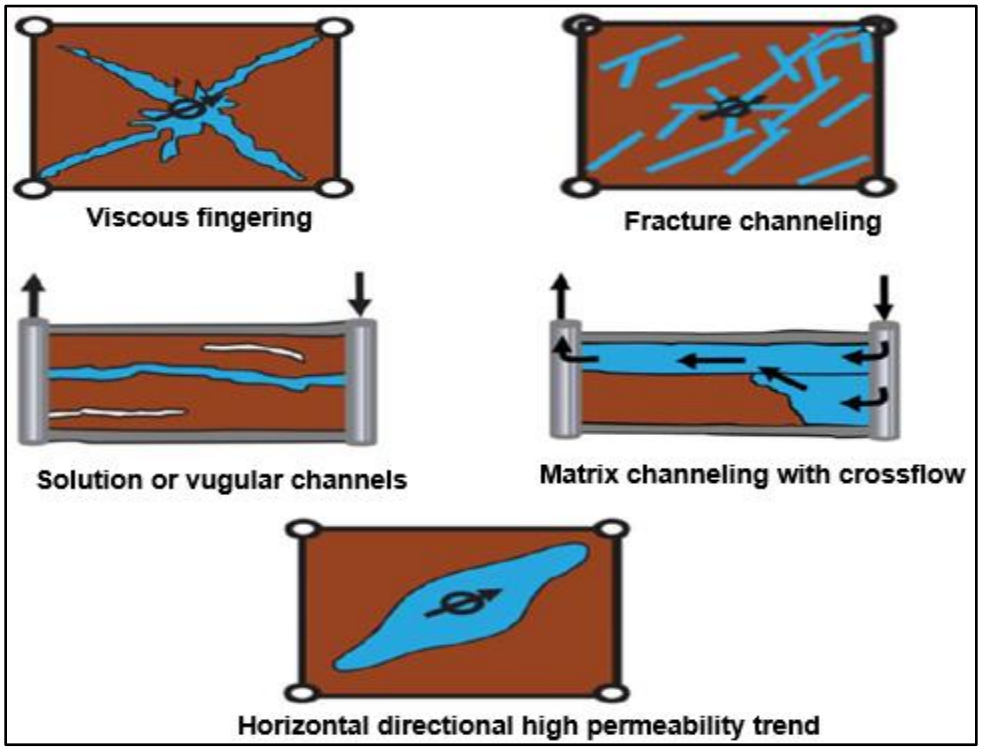

Figure 2.6. Far wellbore-related problems (Sydansk and Romero-Zeron, 2011).

2.4.1. Water Shutoff. This type of treatment was used during the 1950s to 1970s (Liu et al., 2006). The treatment is placed in the production wells, as shown in Figure 2.7. The purpose is to reduce the production of water without affecting oil production. The plugging agents have the ability to reduce the permeability of water without affecting the permeability of oil; these materials are called (RPM) or (DPR).

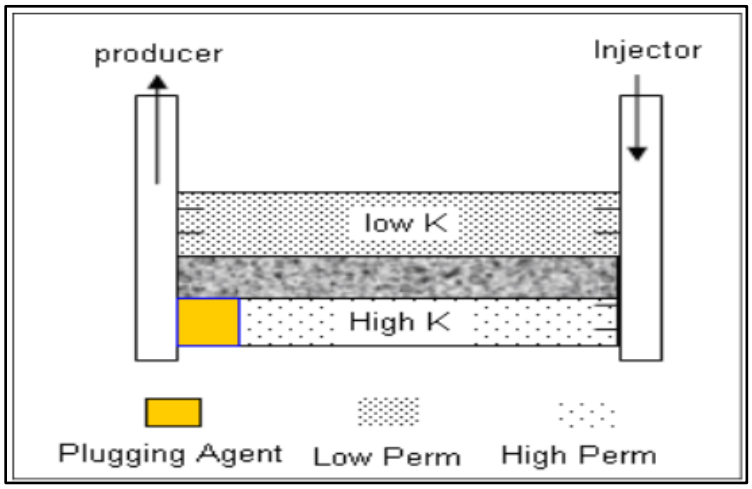

Figure 2.7. Water shutoff in a producer (Liu et al., 2006).

2.4.2. Profile Control. This type of treatment was used in the 1980s and used into mid-1990s (Liu et al., 2006). If the reservoir is composed of layers with different permeability with a barrier that prevents the crossflow between these layers, then the best placement strategy is to place the gelant solution or plugging agent near the wellbore of the injection wells, as shown in Figure 2.8.

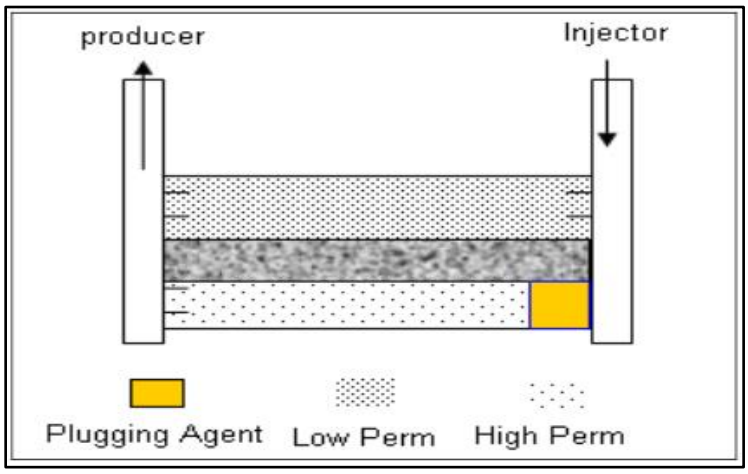

Figure 2.8. Profile control in an injector (Liu et al., 2006).

2.4.3. Water Shutoff and Profile Control. In this treatment, a plugging agent is placed simultaneously near the wellbore of the producer to modify the fluid production and near the wellbore of the injector to modify the injection profile, as shown in Figure 2.9.

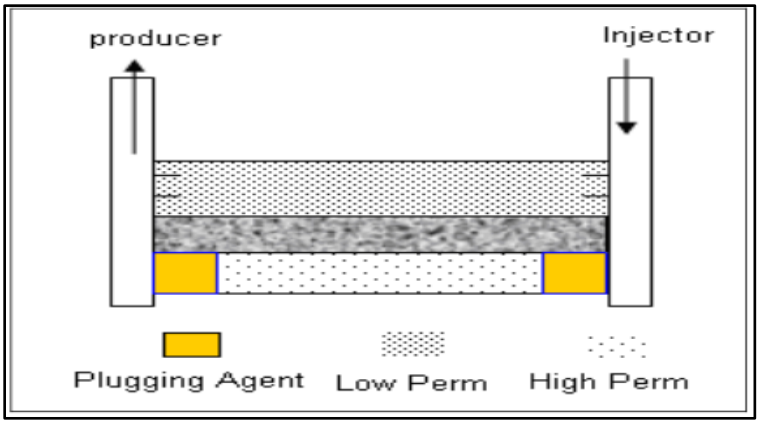

Figure 2.9. Water shutoff and profile control (Liu et al., 2006).

In water shutoff and profile modification treatments, a strong plugging agent is normally injected, while gel is formed in the vicinity of the wellbore. The strong gel is composed of high concentrations of polymer and crosslinker, which is characterized by high reaction rates (i.e., short gelation time). These treatments are easy to perform with a high success rate and at a low cost (Sydansk and Romero-Zeron, 2011).

2.4.4. Multi-well Treatment at One Block. This type of treatment was started in the 1990s and used into the early of 2000s (Liu et al., 2006). Figure 2.10 shows how several injectors and producers are treated at the same time in one block to enhance the sweep efficiency from this block.

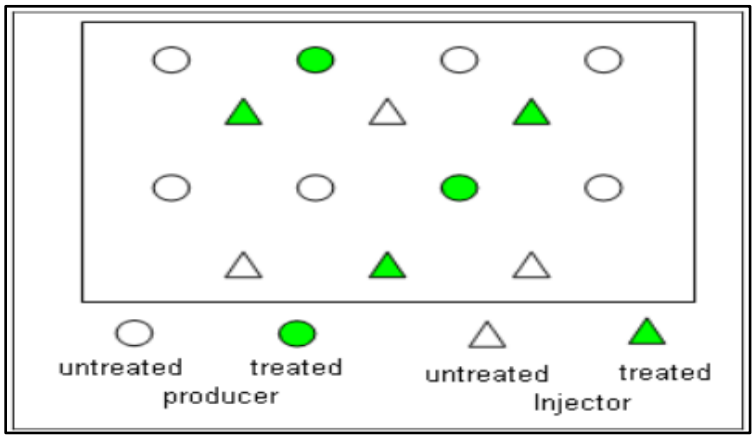

Figure 2.10. Multi-well treatment in one block (Liu et al., 2006).

2.4.5. In-Depth Fluid Diversion. This type of treatment was started in the 1990s and is still in use (Liu et al., 2006). If the reservoir is characterized by high permeability contrast with free pressure communication (i.e., free crossflow) between the high- and low-permeability layers, then near-wellbore treatment (i.e., profile control) is not the best option because post-treatment water will bypass the plugging agent and flow back in the high-permeability layers, as shown in Figure 2.11. Therefore, low concentrations of polymer and crosslinker are injected in order to place the plugging agent in the middle of the thief zone (i.e., far away from the injector), as shown in Figure 2.12. This gel system is characterized by long gelation time and low reaction rate between the reactants. The concentrations of the reactants are dependent on the type of the polymer gel system.

The treatment showed in Figure 2.12 is also called in-depth gel treatment, where the polymer gels or polymer microgels are injected deep into the thief zones to force post-treatment water to divert into oil-rich low-permeability layers, which represents the core of this study. Han et al. (2014) presented a comparison between water shutoff, profile modification, and in-depth fluid diversion, as shown in Table 2.2.

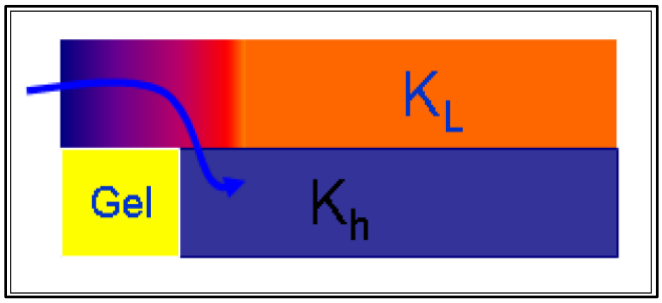

Figure 2.11. Profile control with crossflow (Liu et al., 2006).

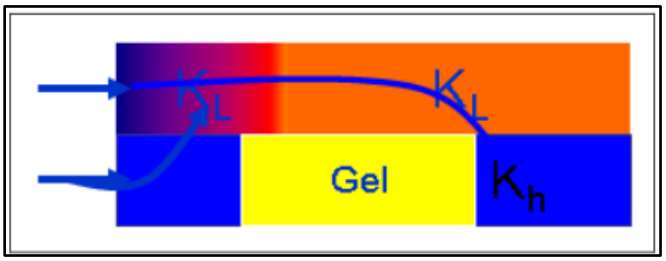

Figure 2.12. In-depth fluid diversion (Liu et al., 2006).

2.5. TYPES OF CHEMICALS USED IN EOR PROCESSES

In this study, chemical enhanced oil recovery (CEOR), specifically polymer gel treatment, is the focus of the numerical simulation models. Therefore, a description of each polymer gel system that has been used in this research is presented in the subsequent sections. Moreover, since the polymer solution represents the main component of any polymer gel system, a brief description of different types of polymer solutions and their rheological properties is also presented and reviewed.

2.5.1. Polymer Solutions. Pye (1964) and Sandiford (1964) were among the first reserachers who tested the potential of the polymer solution by laboratory works and pilot projects to lower the mobility ratio and to increase oil production. Therefore, polymer solution is considered a mature EOR process with more than 50 years of successful field applications

(Needham and Doe, 1987; Liu et al., 1996; Sheng, 2011; Standnes and Skjevrak, 2014). In the United States, 40 polymer flooding projects out of 46 were considered successful. In China, the first application of polymer solution was in the Liaojunmiao oil field in 1957, followed by 31 flooding projects in the Daqing oil field (Chang et al., 2006), in addition to uses in Canada and Germany (Standnes and Skjevrak, 2014). The incremental oil recovery that can be achieved using polymer solution ranges from 8% to 22% (Maitin, 1992). Furthermore, polymer flooding in the Daqing oil field in China is considered one of the most successful and largest applications of that solution with an incremental oil recovery of 12% OOIP (Chang et al., 2006). Polymer flooding has been used recently for improving oil recovery in heavy oil reservoirs, particularly in Canada, where oil viscosities range from 430 cp to 80,000 cp (Wang and Dong, 2009; Guo et al., 2013; Rego et al., 2017).

Table 2.2. Comparison between different conformance improvement technologies (Han et al., 2014).

Technique	Treated well	Diameter of treatment	Targeted problem	Advantage	Disadvantage
Water shutoff	Producer	(3–30) ft.	Water coning and thief zones	Immediate response	45% success rate; risk of reducing oil production
Profile control	Injector	(30–100) ft.	High perm. zones	High success rate	Average effective period of 6 months
In-depth fluid diversion	Injector	(0.1–0.5) PV	Diverting flow to un-swept reservoir zones	In-depth reservoir treatment	Large volumes

The main objective of polymer flooding used in the tertiary stage of oil recovery is to increase the viscosity of the injected water, which will eventually improve macroscopic (volumetric) displacement efficiency. The injection of polymer solution is aimed to

improve the mobility of water and to lower the unfavorable mobility ratio. Mobility ratio is defined as the ratio between the mobility of the *displacing fluid* (e.g., water) to the mobility of the *displaced fluid* (e.g., oil) (Ahmed, 2001). The definition of mobility ratio is shown in Equations (2.4) and (2.7), while the mobility of oil and water is shown in Equations (2.5) and (2.6), respectively.

$$M = \frac{\lambda_{displacing}}{\lambda_{displaced}} \tag{2.4}$$

$$\lambda_o = \frac{k_o}{\mu_o} = \frac{kk_{ro}}{\mu_o} \tag{2.5}$$

$$\lambda_w = \frac{k_w}{\mu_w} = \frac{kk_{rw}}{\mu_w} \tag{2.6}$$

$$M = \frac{krw@_{sor}}{kro@_{swi}} \frac{\mu_o}{\mu_w} \tag{2.7}$$

Mobility ratio should be close to or less than one to be considered as favorable; otherwise, it is unfavorable, as shown in Figure 2.13. Figures 2.14 and 2.15 show the effect of mobility ratio on both areal and vertical sweep efficiencies, respectively. Sorbie (1991) considered the reservoirs characterized by one-dimension flood with mobility ratio more than five, polymer flooding is the best selection to improve the sweep efficiency.

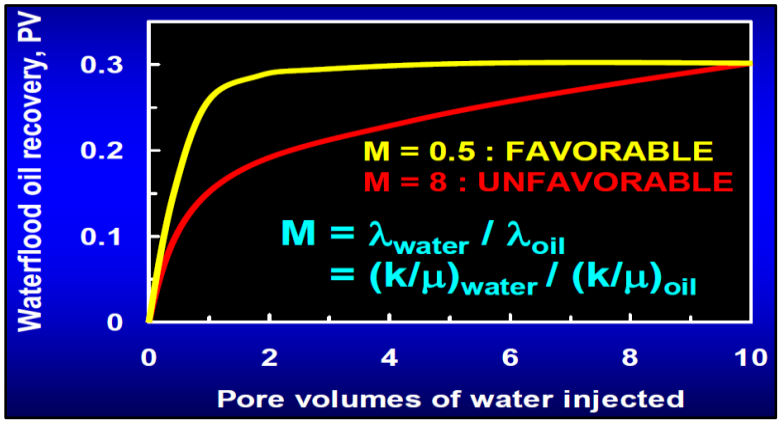

Figure 2.13. Effect of mobility ratio on waterflood oil recovery (Seright et al., 2009).

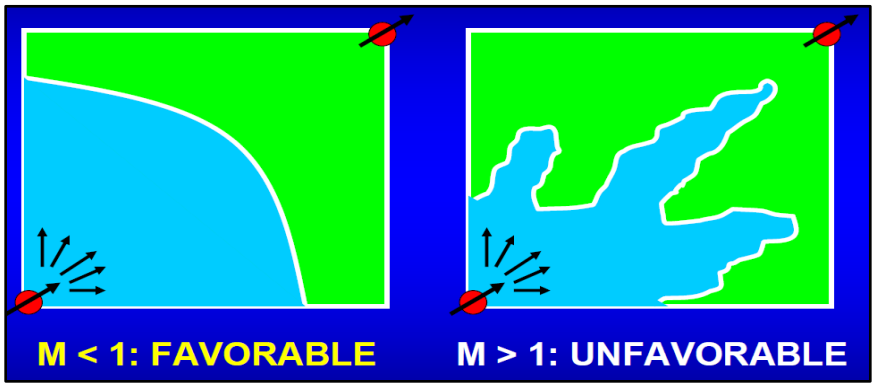

Figure 2.14. Effect of mobility ratio on areal sweep efficiency (Seright et al., 2009).

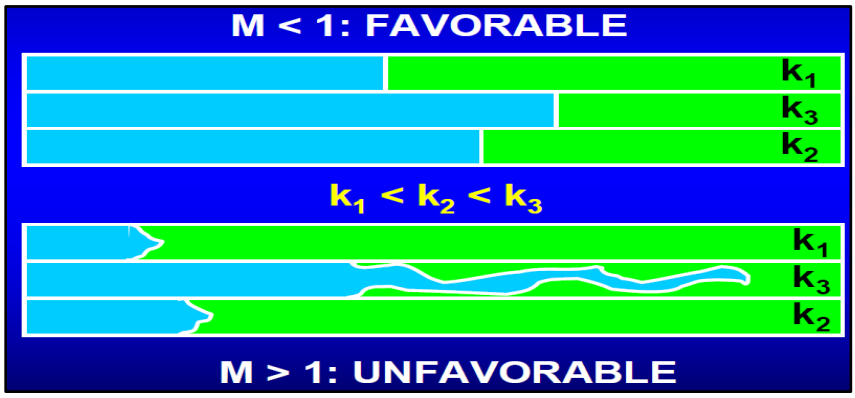

Figure 2.15. Effect of mobility ratio on vertical sweep efficiency (Seright et al., 2009).

Resistance factor is used to represent the reduction in the mobility ratio due to the injection of polymer (Chauveteau and Kohler, 1974). Resistance factor is defined as the *mobility of flooding water* to *the mobility of polymer solution*, as shown in Equation (2.8)

$$F_r = \frac{Mobility\ of\ Flooding\ Water}{Mobility\ of\ Polymer\ Solution} = \frac{\left(\frac{K_w}{\mu_w}\right)}{\left(\frac{K_p}{\mu_p}\right)} = \frac{\Delta P_p}{\Delta P_w} \qquad (2.8)$$

Equation (2.8) implies that if we assumed a water viscosity of 1.0 cp and applied the Darcy equation, then the resistance factor would represent apparent viscosity of polymer (μ_{app}).

Another parameter that is normally used to quantify the efficiency of polymer flooding and its effect on permeability is the residual resistance factor (Chauveteau and Kohler, 1974). Residual resistance factor is defined as the ratio of water permeability before and after the treatment, as shown in Equation (2.9):

$$F_{rrw} = \frac{Initial\,Water\,Mobility\,before\,Chemical\,Injection}{Final\,Water\,Mobility\,after\,Chemical\,Injection} = \frac{\left(\frac{K_w}{\mu_w}\right)_{initial}}{\left(\frac{K_w}{\mu_w}\right)_{final}} = \frac{\Delta P_{wa}}{\Delta P_{wb}} \qquad (2.9)$$

The higher the F_{rrw} values, the better the performance of the polymer flooding. The injection of polymer gel or polymer microgel will yield higher values of F_{rrw} compared to the injection of polymer solution. This is because the polymer solution is linear while polymer gel and polymer microgel are 3D networks due to the presence of crosslinkers (Mack and Smith, 1994).

Thus, the resistance factor is used to measure the reduction of mobility and the residual resistance factor is usually used to measure the reduction of permeability. The resistance factor is calculated during the treatment, while the residual resistance factor is calculated after the treatment. Polymer solution retention inside the porous media is the main cause of the permeability reduction that occurs after the injection of polymer solution. Polymer retention is divided into three types that can be either reversible or irreversible depending on the retention mechanism (Green and Willhite, 1998):

- Adsorption.
- Mechanical entrapment.
- Hydrodynamic retention.

Polymer adsorption is defined as the adhesion of polymer molecules onto the rock surfaces (Manichand and Seright, 2014). Hoteit et al. (2016) suggested that the

permeability reduction caused by polymer flooding might not be the same after post-treatment water injection; thus, the permeability reduction might be exaggerated. They explained that the irreversibility assumption indicates that the apparent viscosity of the chase water will be the water viscosity multiplied by the permeability reduction. Mechanical entrapment is irreversible and happens when the large polymer molecules are trapped in pores with a small exit pore-throat diameter. The polymer propagation is significantly affected by mechanical entrapment if the pore-throat size and permeability are too small (Wang et al., 2007). Hydrodynamic retention is reversible and occurs when flow rates are suddenly increased.

The adsorption of polymer solutions can affect both water and oil permeability. However, polymer solutions can reduce water permeability more than oil permeability. The polymer solutions lowered the endpoint of oil relative permeability by increasing the irreducible water saturation. Thus, effective permeability to oil is affected by polymer injection, especially in the low-permeability layers where oil saturation is high compared to the high-permeability layers (Seright et al., 2003).

Different factors can affect the polymer adsorption, and hence the permeability reduction. These parameters include polymer viscosity and polymer molecular weight, water salinity and hardness, and the porosity and permeability of the porous media (Hirasaki and Pope, 1974). The characteristics of the reservoirs will determine what type of chemicals should be used. For example, in reservoirs with high heterogeneity (high permeability contrast), polymer flooding might be not a good choice and other chemicals should be investigated, such as polymer gels or polymer microgels. Several reasons could

explain why polymer gels or polymer microgels are better candidates for heterogeneous reservoirs than polymer solution:

- Because of high adsorption characteristics of polymer gels, permeability reduction in the thief zones is higher compared to polymer solution (Abdulabaki et al., 2014).
- 3D structure of polymer gels yield high pressure drops after the treatment, which causes a high residual resistance factor; thus, more post-treatment water is diverted into less permeable layers.

Two types of polymer solutions are widely used in the petroleum industry: synthetic polymer, such as partially hydrolyzed polyacrylamide (HPAM) and xanthan biopolymer. HPAM is used more than xanthan biopolymer for several reasons:

- Permeability reduction achieved by HPAM solution is higher than xanthan biopolymer solution (Pope et al., 2003).
- HPAM is readily available, economic, and resistant to bacterial attack.
- Low adsorption on the rock surfaces due to their negatively charge.
- HPAM crosslinks well with crosslinkers such as Cr(III) (Han et al., 2014; Hasan et al., 2013).
- HPAM has an adjustable degree of hydrolysis (Sheng, 2011).
- HPAM polymer solution exhibit both shear thinning and shear-thickening behavior. While xanthan biopolymer exhibit only shear-thinning behavior during flowing inside the reservoir rocks (Wang et al., 2001; Delshad et al., 2008; Li and Delshad, 2014; Lotfollahi et al., 2016).

The development of shear-thickening behavior (polymer viscosity increases as shear rate increases) beyond a certain shear rate or flow velocity makes HPAM more

favorable than xanthan biopolymer. The shear-thickening behavior reduces the residual oil saturation by pulling the trapped or hard-to-displace oil from the small-scale pores (Wang et al. 2001; Delshad et al., 2008; Wang et al., 2010 and 2011). However, the shear-thickening behavior is associated with high molecular weight HPAM polymer solution (i.e., more than 15 million Daltons) (Delshad et al., 2008; Seright et al., 2009; Luo et al., 2015). Seright et al. (2011) concluded that HPAM polymer solution exhibit shear-thinning (pseudoplastic) behavior in the lab (viscometer), while it shows Newtonian and shear-thickening (pseudodilatant) behavior in porous rock. Moreover, they concluded that the shear-thinning behavior is negligible or unobserved during the flow of HPAM in porous media. Delshad et al. (2008) pointed out that the viscosity of polymer solution should be low near the wellbore (i.e., shear-thinning behavior) to facilitate its injection, while the polymer viscosity should be increased with flow velocity inside the porous media (i.e., shear-thickening behavior) to improve both displacement and volumetric sweep efficiencies.

2.5.2. Polymer Gels and Polymer Microgels. Due to maturity of most giant oil fields and scarcity of discoveries, polymer flooding is not capable of maintaining high enough recovery factors to meet the expectation of the oil supply demands.

The heterogeneity of the reservoir due to the existence of thief zones, high permeability streaks, and natural fracture networks that connect the injectors with the producers forces researchers to investigate other methods to mitigate these problems. The polymer gel system represents one of the methods to block off the high-permeability layers and divert subsequently injected water into the low-permeability layers, thus improving the sweep efficiency.

The permeability reductions achieved by 3D polymer gel systems are higher than the permeability reductions achieved by traditional linear polymer solutions. The immobile polymer gel system can create a high-pressure gradient through the thief zones, which yields a higher residual resistance factor (permeability reduction) compared to polymer solution. Needham et al. (1974) reported a water residual resistance factor of 3 when polymer solution was injected into Repetto sandstone cores that had a brine permeability of 200 – 400 md. Whereas, the residual resistance factor to brine was 16 to 18 when the polymer gel system was injected into the same cores. Once the polymer solution crosslinked with the crosslinkers by the gelation process, the formed gel could not flow through the porous rocks, while the polymer solution was able to flow through the porous media. In addition, formed gels are more stable thermally and mechanically under reservoir conditions than polymer solutions (Glenat et al., 1996; Seright et al., 2009). Moreover, the low-permeability layers should not be damaged during gel treatment. During polymer flooding, penetration into the low-permeability layers should be maximized as much as possible (Glenat et al., 1996; Seright et al., 2009), as shown in Figure 2.16. The formed gel should have the ability to penetrate selectively into the thief zones without affecting the low-permeability layers. Many researchers, such as Cozic et al. (2008), Seright et al. (2012), Bai et al. (2015), and Zaitoun et al. (2007), hypothesized that the low viscosity (e.g., 1-1.3 cp) and small size of polymer microgels and/or gelant solutions help these materials to invade and penetrate the thief zones during the injection process without damaging the low-permeability layers.

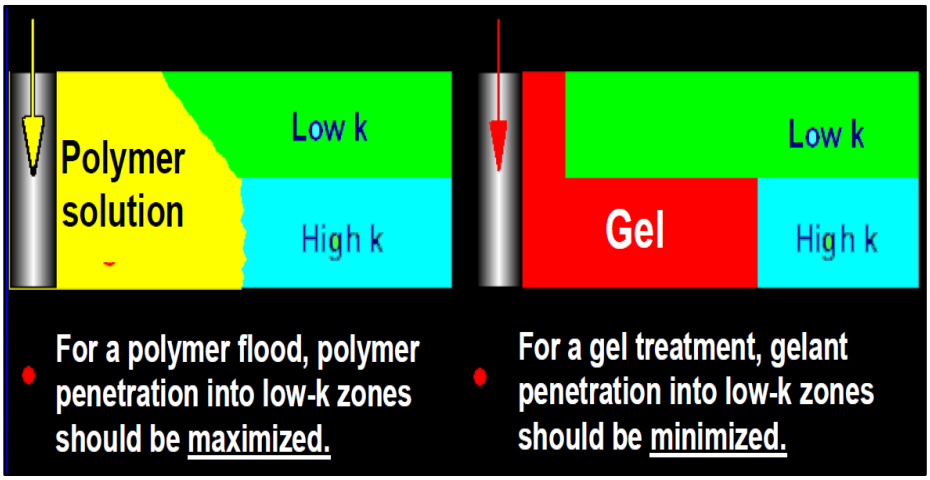

Figure 2.16. Comparison between polymer flooding and gel treatment (Seright et al., 2009).

2.5.3. Types of Polymer Gel Systems based on their Compositions. Different types of polymers and crosslinkers could be used to form a crosslinked polymer that could mitigate and alleviate heterogeneity or conformance problems. The following are commonly used polymer solutions (Glenat et al., 1996; Sheng, 2011; Bai et al., 2012):

- Synthetic polymers such as HPAM and polyvinyl alcohol. HPAM is partially hydrolyzed by converting some of its amide groups into carboxylate groups. The degree of hydrolysis ranges from 0% to 60%. Thus, HPAM is partially hydrolyzed to make HPAM carry a negative charge.
- Natural polymers, are also biopolymers, such as xanthan scleroglucan, curdlan, simusan, and succinoglycan.

Both synthetic and natural polymers are crosslinked with different types of crosslinkers, which include the following:

- Organic crosslinkers such as phenol-aldehyde, or resorcinol.

- Inorganic multivalent metal ions crosslinkers, such as Cr(III), Al(III), Zr(III), and Fe(III).

Organic crosslinkers are toxic and need to be handled carefully. Inorganic crosslinkers are chelated with organic acids, such as acetate, citrate, lactate, malonate, and propionate. The purpose of adding these acids is to delay the reaction rate between the reactants to achieve long gelation time. Therefore, the formed gel could be placed far away from the injector. Moreover, these acids are used to prevent the precipitation of crosslinkers on the rocks, which eventually lowers the adsorption (Glenat et al., 1996). The multivalent ions will crosslink with HPAM through the carboxyl group (Bai et al., 2015). Table 2.3 shows the type of gels commonly used in conformance improvement technology (CIT), which was prepared by Sydansk and Romero-Zeron (2011). Figure 2.17 shows an environmental scanning electron microscope (ESEM) for bulk gel, and Figure 2.18 shows the preformed particle gels (PPGs) before and after swelling.

Table 2.3. Types of gel for use in conformance improvement technology (Sydansk and Romero-Zeron, 2011).

- Inorganic based (bulk gels)
  - Silicate gels
  - Aluminum-based gels
- Organic-based polymers
  - Bulk gels
    - Synthetic or biopolymers
      - Arcylamide polymers (most widely used polymer)
      - Xanthan biopolymer
    - Organic crosslinkers

Table 2.3. Types of gel for use in conformance improvement technology (Sydansk and Romero-Zeron, 2011) (Cont.).

- ♦ Aldehydes
  - ▫ Phenol-formaldehyde and dervatives
- ♦ Polyethyleneimine
- o Inorganic crosslinkers
  - ♦ Al(III) based
  - ♦ Zr(IV) based
  - ♦ Cr based
    - ▫ Cr(VI) redox
    - ▫ Cr(III) with inorganic anions
    - ▫ Cr(III) with organic carboxylate complex ions
- ▪ Monomer gels (organic-monomer-based in-situ polymerization)
  - o Acrylamide monomer
  - o Acrylate monomer
  - o Phenolics
- ▪ Lignosulfonate gels
- ▪ Preformed particle gels
  - o Swelling organic-polymer “macroparticle” gels
- ➢ Mixed silicate and acrylamide-polymer gels
- ➢ Microgels
  - ▪ Microgels with narrow particle-size distribution
  - ▪ CDGs
    - o Alminum-citrate crosslinker
    - o Chromium-triacetate crosslinker
  - ▪ Delayed “popping”/swelling microgels (Bright Water™)

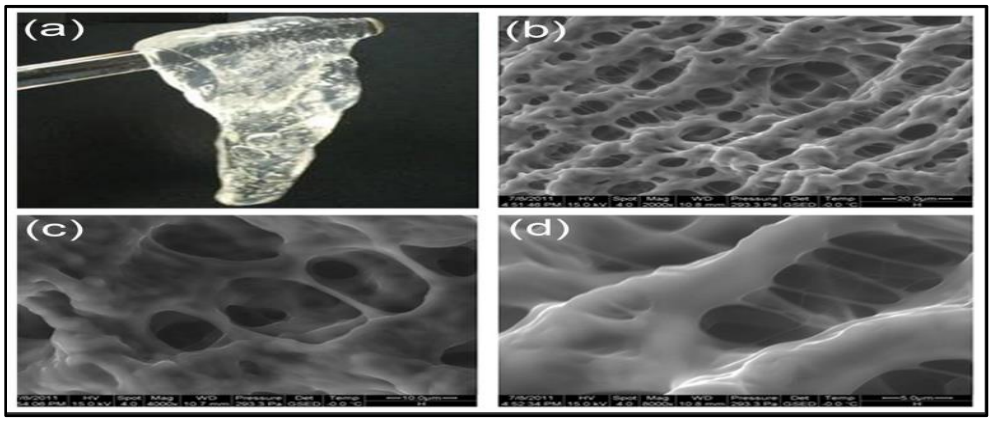

Figure 2.17. ESEM image of the morphology of bulk gel (Zhao et al., 2013).

Figure 2.18. PPG before and after swelling in seawater (Alhuraishawy et al., 2018).

2.5.4. Types of Polymer Gel Systems based on Gelation Process. Polymer gel systems are divided into three main categories based on their compositions (organic versus inorganic), applications (water shutoff, profile modification, or in-depth fluid diversion), strengths (weak versus rigid), and gelation process (in-situ versus preformed) (Bai et al., 2015):

- In-situ monomer-based gel (Water shutoff treatments).
- In-situ polymer-based gels. (Profile control and flow path diversion).
- Preformed particle gels. (In-depth fluid diversion).

2.5.4.1. In-situ polymer gels. The first in-situ polymer gel system was developed by Philips Co. (Currently ConocoPhillips) in 1970. This gel system was composed of HPAM and aluminum citrate (Needham et al., 1974). This technology attracted many researchers who developed more advanced in-situ polymer gel systems and applied them in field applications. Sydansk (1988) developed MARCIT™ (Marathon Conformance Improvement Technology), which is composed of HPAM and Cr(III) acetate and their gelation time is more controllable.

The injected components are called gelant solutions, where their viscosity is close to water viscosity, thus facilitating selective penetration into the thief zones. The gelant solution is composed of low concentrations of polymers/monomers, crosslinkers, and additives. The gelation process occurs inside the reservoir and is mainly affected by reservoir temperature in addition to other factors such as dilution, shear stress, and chromatographic degradation of gelant components. Moreover, the gelation process is affected by the pH level and brine inside the reservoir causing loss of control on the gelation process (Coste et al., 2000; Pritchett et al., 2003; Liu et al., 2006; Liu et al., 2010; Bai et al., 2015). However, these polymer gel systems have been applied in different field applications, where promising and successful results have been obtained (Seright and Martin, 1993; Sydansk and Moore, 1990; Southwell and Posey, 1994; Sydansk and Southwell, 2000; Bai et al., 2004; Herbas et al., 2004; Spildo et al., 2009).

To prolong the gelation time of the in-situ gel system and to control the gelation process, a redox agent is normally added to the gelant solution to slowly convert the inert Cr(VI) into active Cr(III) (Bai et al., 2015). This redox reaction system was first introduced to the oil industry by Clampitt and Hessert (1974) and Hessert and Fleming (1979).

Different types of reducing agents are used to reduce Cr(VI) to Cr(III), such as thiourea, sodium bisulfite, H_2S (in reservoir and injected brine) and sodium thiosulfate. Thiourea is the most widely used because it slowly reduces Cr(VI) to Cr(III) producing longer gelation time (Terry et al., 1981; Bhaskar et al., 1988). In field applications of this gel system, two polymer slugs are injected:

- The first polymer slug contains Cr(VI).
- The second polymer slug contains a reducing agent (e.g., thiourea).

When these two slugs are injected, a kinetic reaction occurs where Cr(VI) slowly reduces to Cr(III), which allows for deep penetration of the in-situ gel system into the thief zones. The last kinetic reaction involves the crosslinking of Cr(III) with a polymer solution normally HPAM. These slugs are injected in two ways:

- Sequential injection: this process includes a long-term injection of polymer, followed by a short-term injection of a slug of multivalent cations, and is then followed by a long-term injection of polymer (Needham et al., 1974; Mack and Smith 1994).
- Simultaneous (concurrent) injection: the polymer and crosslinker are injected together at the same time and the gel is formed at a fixed time (Shiyi et al., 2000). This method is adopted in this study.

In this study, different polymer gel systems have been modeled, such as:

- Polymer/chromium chloride gel (Table 2.4).
- Polymer/chromium malonate gel (Table 2.5).
- Sodium silicate gel (Table 2.6).

The NG indexes are codes used by the UTGEL simulator to assign the components of the selected gel system, which is defined by a KGOPT keyword. However, only the first and second gel systems were modeled using the UTGEL simulator, while the third gel system was modeled using the CMG-STARS simulator.

Table 2.4. Composition and kinetic reaction of polymer/chromium chloride gel system (UTGEL Technical Manual, 2015).

	Gel Index	KGOPT = 1	Kinetic reaction and advantage
Polymer/chromium chloride gel	NG_1	$Na_2Cr_2O_7.2H_2O$ (sodium dichromate) (PPM)	• Sodium dichromate (source of Cr(VI)) • Thiourea (reducing agent) • Cr(VI) + Thiourea = Cr(III) • Cr(III) + HPAM = Gel • High pH affects the concentration of the crosslinker. • Dependency of gel reaction on pH should be accounted for (Lockhart, 1994; Seright and Martin, 1993). • Hydrogen ion is implemented in the model to represent the dependency of gel reactions on pH. • Has relatively short gelation time.
	NG_2	$(NH_2)_2CS$ (thiourea) (PPM)	
	NG_3	Cr^{3+} (PPM)	
	NG_4	Gel (PPM)	
	NG_5	Hydrogen (meq/ml)	

Another in-situ gel type is colloidal dispersion gel (CDG), also known as weak gel, microgel dispersion, weak viscoelastic fluid, crosslinked polymer, linked polymer solution, deep diverting gel, or low concentration flowing gel (Sheng, 2011). CDG is applied only to injection wells and is composed of mixing low concentrations of high molecular weight partially hydrolyzed polyacrylamide and metal ions such as inorganic crosslinkers (e.g., chromium or aluminum) (Ranganathan et al., 1998). Thus, there is not enough polymer to

form an intermolecular bulk gel or continuous network; instead, an intramolecular weak gel is formed, as shown in Figure 2.19 (Sydansk, 1988; Shiyi et al., 2000; Diaz et al., 2008; Sheng, 2011; Abdulbaki et al., 2014). The molecular weight of the HPAM is from 8 to 17 million Daltons, and the polymer/crosslinker (P/X) ratio ranges from 30/1 to 60/1 (Sheng, 2011). However, this ratio could be in the range of 20/1 to 100/1 (Mack and Smith, 1994). In addition, CDG could be considered a mid-point between easily flowing uncrosslinked polymer and difficulty flowing bulk gel (Smith et al., 2000; Sheng, 2011; Abdulbaki et al., 2014).

Table 2.5. Composition and kinetic reaction of polymer/chromium malonate gel system (UTGEL Technical Manual, 2015).

	Gel Index	KGOPT = 2	Kinetic reaction and advantage
Polymer/Chromium Malonate Gel	NG_1	_	• Polymer, crosslinker, and malonate ion • Malonate ion (delaying ligand). • Two types of polymers, HPAM and HE-100, were used. • Longer gelation time than polymer/chromium chloride.
	NG_2	Malonate ion (PPM)	
	NG_3	Cr^{3+} (PPM)	
	NG_4	Gel (PPM)	
	NG_5	Hydrogen (meq/ml)	

Table 2.6. Composition and kinetic reaction of sodium silicate gel system (UTGEL Technical Manual, 2015).

	Gel Index	KGOPT = 3	Kinetic reaction and advantage
	NG_1		Condensation of monomer and dimer to form oligomers
	NG_2	SiO_2 (Silicate)	Intramolecular condensation of silanol groups leading to ring closure and eventual particle formation.

Table 2.6. Composition and kinetic reaction of sodium silicate gel system (UTGEL Technical Manual, 2015) (Cont.).

Silicate gel	NG_3	OH^- (PPM)	Aggregation of individual particles to form chains and microgel.
	NG_4	Gel (PPM)	Low initial viscosity (good for deep penetration)
	NG_5		Inexpensive.
			Environmental friendly
			Good thermal and chemical stability
			Easy to remove in case of any failure.
			Rate of gelation is a function of:
			1. Silicate concentration.
			2. pH.
			3. Ionic strength.
			4. Temperature.

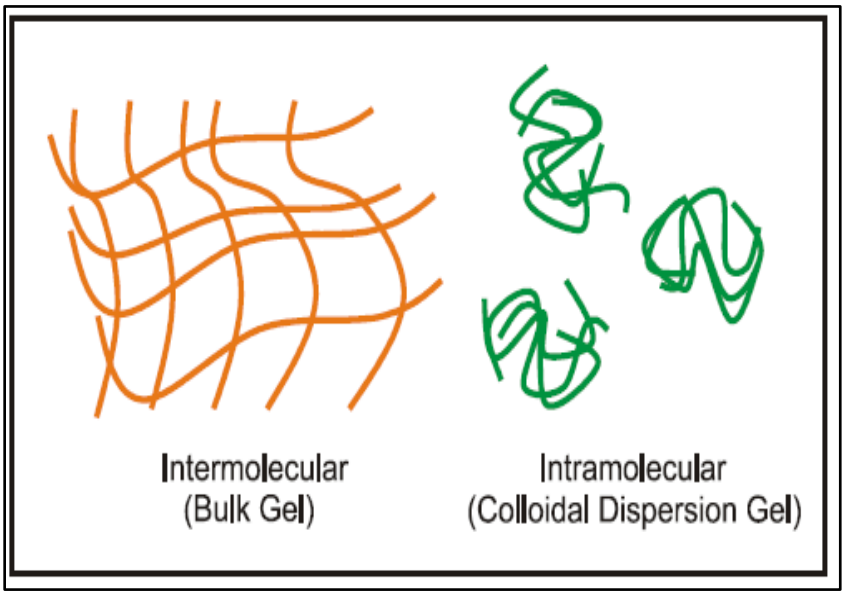

Figure 2.19. Comparison between the molecular structure of bulk gel and CDG (Diaz et al., 2008).

2.5.4.2. Polymer microgels. In this type of microgel, the gelation process occurs outside the reservoir, where the gel is prepared at the surface and then injected into thief zones. This is called a preformed gel, and it can divided into subcategories based on size and propagation mechanisms, such as preformed particle gels (PPG) (Bai et al., 2008; Coste et al., 2000; Zhang and Bai, 2011), thermally activated polymer (TAP) (also known as BrightWater®) (Frampton et al., 2004; Garmeh et al., 2012; Pritchett et al., 2003; Yanez et al., 2007; Izgec and Shook, 2012; Onbergenov, 2012), and pH-sensitive polymer microgel (Al-Anzi and Sharma, 2002; Choi et al., 2006; Huh et al., 2005; Onbergenov, 2012). The development of PPG began in 1996 when PetroChina initiated this conformance control technology (Bai et al., 2015). Preformed particle gel (PPG), a super absorbent polymer (SAP) (Bai et al., 2007a; Sheng, 2011), is one of the chemicals that has attracted attention during the last two decades for the purpose of controlling excess water production and correcting the heterogeneities in mature oil fields (Seright et al., 2003; Feng et al., 2003; Coste et al., 2000; Bai et al., 2007b). The gelation process occurs on the surface, and the gel is composed of one component; therefore, there is no need to install additional surface facilities during the injection process. Moreover, the size of PPG can become 200 times bigger than its original size when it mixes with brine (Bai et al., 2007a). Since the gelation process occurs on the surface, the gelation process is more controllable than in an in-situ gelation system where the gelation process occurs inside the reservoir. In addition, the effects of shear degradation, dilution by formation water, and modification of gel compositions are overcome when using PPG (Coste et al., 2000; Bai et al., 2015).

Another type of microgel is BrightWater®, also known as thermally activated (or active) polymer (or particles), or temperature-sensitive microgels. BrightWater® was

developed by BP, Chevron, Texaco and Nalco (an industry consortium) and is characterized by its un-swelled submicron size (0.1-1 nm) (Abdulbaki et al., 2014). Its initial viscosity was close to that of water, which enabled it to selectively penetrate deep into the high-permeability layers before expansion.

The first field trial was in November 2001, when this newly developed technology was injected in the Minas field in Indonesia, where 42,000 barrels were injected to test the potential of TAP to block off the thief zones and improve the sweep efficiency (Pritchett et al., 2003; Frampton et al., 2004). The injection of BrightWater® was intended to correct the heterogeneity of the heterogeneous matrix reservoirs that are characterized by radial flow; therefore, it was not designed for naturally fractured reservoirs where linear flow is the dominating flow regime (Pritchett et al., 2003; Mustoni et al., 2010; Galli et al., 2012). During the treatment, the injection well is not required to shut down, which represents one of the advantages of this technology. More importantly, this technology is benign with zero risk to both reservoir and environment (Garmeh et al., 2012). Furthermore, BrightWater® is not affected by chromatographic separation since it is composed of one component (Pritchett et al., 2003).

The sizes of TAP are smaller than the pore throats they move through; therefore, they selectively enter the thief zones. Because of the temperature profile (i.e., thermal front) inside the reservoir, TAPs pick up heat gradually from the reservoir. Once they reach a predetermined temperature, these small particles (or kernels) expand and “pop” like popcorn by swelling water irreversibly, and their size becomes ten times larger than their original size, as shown in Figure 2.20 (Ohms et al., 2010; Garmeh et al., 2012; Salehi et al., 2012; Abdulbaki et al., 2014).

Colloidal dispersion gel (CDG), preformed particle gel (PPG), and thermally activated polymer (TAP) are modeled using the UTGEL simulator. Table 2.7 summarizes the components of each polymer gel and polymer microgel system that was used in the UTGEL simulator. Note that KGOPTs 1 to 3 are in-situ polymer gel systems, while KGOPTs 4 to 6 are polymer microgel systems. Moreover, KGOPTs 4 and 5 are preformed polymer microgels, whereas KGOPT6 is an in-situ polymer microgel.

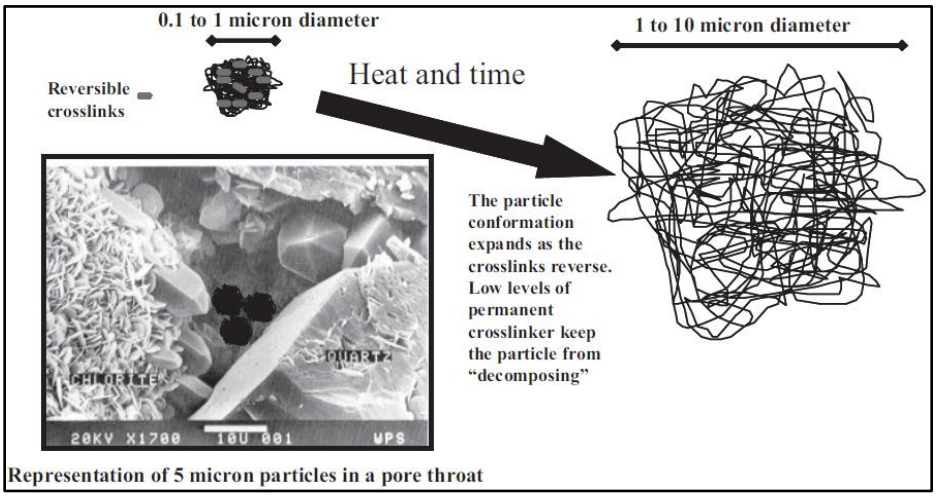

Figure 2.20. Activation of BrightWater® particulates (Ohms et al., 2010).

Table 2.7. Polymer gels and polymer microgels components and units in UTGEL simulator (UTGEL Technical Manual, 2015).

Gel Index	KGOPT = 1	KGOPT = 2	KGOPT = 3	KGOPT = 4	KGOPT = 5	KGOPT = 6
NG_1	$Na_2Cr_2O_7.2H_2O$ (Sodium dichromate),(PPM)	—	—	—	—	—
NG_2	CSN_2H_4 (thiourea) (PPM)	Malonate ion (PPM)	SiO_2 (Silicate)	—	—	—

Table 2.7. Polymer gels and polymer microgels components and units in UTGEL simulator (UTGEL Technical Manual, 2015) (Cont.).

NG_3	Cr^{3+} (PPM)	Cr^{3+} (PPM)	OH^- (Hydroxyl ion) (PPM)	—	—	—
NG_4	Gel (PPM)	Gel (PPM)	Gel (PPM)	—	—	—
NG_5	Hydrogen (meq/ml)	Hydrogen (meq/ml)	—	—	—	—
NG_6	—	—	—	PPG (PPM)	—	—
NG_7	—	—	—	—	CDG (PPM)	—
NG_8	—	—	—	—	—	TAP (PPM)

2.6. TYPES OF SIMULATORS USED IN THIS STUDY

Many commercial and in-house simulators have been developed to model different chemical EOR processes, such as polymer (P), alkaline/surfactant/polymer (ASP), and surfactant/polymer (SP), in addition to polymer gels and polymer microgels. Some of these simulators, such as STARS (Computer Modeling Group), ECLIPSE-100 (Schlumberger), and Reveal (Petroleum Experts), use friendly user interface (FUI) environments to input the data. These simulators have a post-processing software to process the results On the other hand, the UTCHEM and UTGEL simulators (The University of Texas at Austin), use a free format to input the data and require an external software to display and process the

results, such as S3GRAF (http://www.sciencesoft.com/products/s3graf/) and Kraken 2 (http://www.esss.com.br/kraken/) (Sheng, 2015). Furthermore, additional code is required to handle the simulation of naturally fractured reservoirs. However, the latter simulators (i.e., the UTCHEM and UTGEL) were designed specifically to model chemical EOR processes because they are equipped with the necessary equations to capture major physical phenomena such as the following (UTGEL Technical Manual, 2015):

- Adsorption of surfactant, polymer, and gel.
- Capillary pressure.
- Interfacial tension reduction by surfactant.
- Wettability alteration by surfactant.
- Cation exchange.
- Partitioning of chemical species between oil and water.
- Non-Newtonian polymer rheology (shear thinning model and UVM model).
- Permeability reduction and adsorption by polymer flooding and by gel treatment.
- Gel kinetic reactions as a function of temperature.

The UTGEL simulator can simulate in-situ gel systems as a reaction inside the reservoir between different species and can simulate preformed polymer microgels as one component (one species). Other simulators, such as CMG-STARS and ECLIPSE-100, can only simulate in-situ gel systems and preformed polymer microgels as reaction between different species. Moreover, the UTGEL simulator has been validated by comparing its results with actual lab and field data (Goudarzi, 2015). On the other hand, CMG-STARS can model permeability reductions due to fine migration during low-salinity waterflooding. The UTGEL simulator cannot model any mechanism during low-salinity waterflooding.

The improvement that occurred during the injection of low-salinity water is due to the effect of salinity on the viscosity and the adsorption of polymer. Thus, as salinity increases, polymer viscosity decreases and polymer adsorption increases, which affects the strength and plugging efficiency of the formed gel. Goudarzi et al. (2016) reviewed and compared polymer, surfactant/polymer, and alkaline/surfactant/polymer using different reservoir simulators and listed the properties that can be modeled using these simulators.

Since all polymer gels are composed of polymer solution as the main component, and since UTCHEM and UTGEL simulators are almost the same regarding polymer and surfactant modeling, Table 2.8 shows a comparison between UTCHEM, CMG-STARS, and ECLIPSE simulators. Moreover, in this study, a combined simulation of polymer, surfactant, and polymer gel treatments have been modeled; thus, Table 2.9 shows a comparison of the surfactant model options of these three simulators. The UTGEL technical manual is a good reference for a full description of the UTGEL simulator.

Table 2.8. Comparison of polymer model options between different reservoir simulators (Goudarzi et al., 2016)

Polymer module	UTCHEM	CMG-STARS	ECLIPSE
Viscosity vs. polymer conc.	√	√	√
Viscosity vs. shear rate	√	√	√
Adsorption	√	√	√
Permeability reduction	√	√	√
Inaccessible pore volume	√	√	√
Effect of salinity on viscosity and adsorption	√	√	√
Effect of hardness on viscosity and permeability reduction	√	Not included	Not included

Table 2.9. Comparison of surfactant model options between different reservoir simulators (Goudarzi et al., 2016).

Surfactant module	UTCHEM	CMG-STARS	ECLIPSE
Microemulsion (ME) viscosity	√	Not included	Not included
Interfacial tension	√	Included (Tabular format)	Included (Tabular format)
Phase behavior	√	Not included	Not included
Surfactant adsorption	√	√	√
Ion exchange effect	√	√	√
Effective salinity window	√	Not included	Not included

PAPER

I. A COMPREHENSIVE EVALUATION OF THE PARAMETERS THAT AFFECT THE PERFORMANCE OF IN-SITU GELATION SYSTEM

Tariq K Khamees and Ralph E Flori

Department of Geosciences, Geological, and Petroleum Engineering, Missouri University of Science and Technology, Rolla, MO 65409

ABSTRACT

This study investigates the effects of different parameters on the in-situ gelation of a polyacrylamide/chromium (VI)/thiourea solution using numerical modeling. The effects of polymer rheology, water salinity of the system on polymer viscosity and polymer adsorption, presence of divalent cations (hardness), injection schemes, wettability of the formation, cation exchange capacity (CEC), mobility ratio, and dip angle of the reservoir were investigated by a 3D model using UTGEL simulator. The injection pattern was one quarter of five-spot with eight layers. The model had two thief zones that were located in the middle of the model. The permeability of the thief zones was 1,500 md, with a permeability contrast (heterogeneity) of 15/1. The ratio of vertical to horizontal permeability was 0.01.

The results showed that regardless the salinity of the brine, considering both shear-thinning and shear-thickening behavior (i.e., UVM model) always yielded better results than assuming shear-thinning behavior only. The results also showed that the higher the salinity of the system, the lower the recovery factor. Thus, low salinity post-treatment water

improved the results, especially when the initial salinity of the system was too high. Moreover, the presence of divalent cations (hardness) affected the efficiency of gel treatment; therefore, low-salinity chase water floods improved the recovery. In addition, if the pore volume of the post-treatment water was not high, the optimum injection scheme would be the injection of the polymer solution before the gel treatment. However, if the pore volume of the post-treatment water was high, the ultimate oil recovery would not affected by the injection scheme and the treatment using only the gel would be the most viable scheme. In addition, damage in the low-permeability layer adjacent to the thief zone was significant for oil-wet conditions compared to water-wet conditions. Furthermore, the presence of the clays in the formation (i.e., increasing the cation exchange capacity) lowers the amount of the crosslinkers that are available for polymer to form gel due to the removal of the crosslinkers from the gelant solution. Therefore, no gel will form with a high value of CEC. Increasing the mobility ratio will lower the efficiency of gel treatment; thus, injection of the polymer solution after the gel treatment was the best option. The dip angle from the injector to the producer assisted the gel placement, which resulted in high oil recovery. Finally, the effect of the skin factor should be taken into consideration in designing the gel treatment, especially at high injection rate.

1. INTRODUCTION

In oil production operations, early water breakthrough, excess water production, and large amounts of unrecovered oil indicate the presence of severe heterogeneity and/or viscous oil. One of the methods to mitigate these problems is the injection of polymer gel

to block off the high permeability streak and divert subsequently injected water into less-permeable, oil-bearing strata. This method is called gel treatment in the injection wells (Sorbie and Seright, 1992).

Different types of polymer gel have been used, both in field applications and in laboratory experiments, such as the in-situ gelation of polyacrylamide / chromium (IV) / thiourea solution. Two types of polymer solutions are used commonly in the oil industry: xanthan biopolymer and synthetic polymer (e.g., partially hydrolyzed polyacrylamide (HPAM)). The rheology of these polymer solutions are different in porous media. Xanthan biopolymer exhibits only shear-thinning behavior inside porous media, whereas synthetic polymer solution exhibits both shear-thinning behavior at low to moderate shear rate and shear-thickening behavior at high shear rate (Li and Delshad, 2014). The shear-thickening behavior of HPAM prevails when polymer solution has high molecular weight (i.e., greater than 20 million) (Delshad et al., 2008). Moreover, the shear-thinning behavior in HPAM polymer solution is not as important as Newtonian and shear-thickening behavior (Seright et al., 2010). Chauveteau (1981) noted that HPAM polymer solution showed shear-thickening behavior at moderate to high velocities in porous media. However, he speculated that at moderate to low flux values in capillary constrictions or in porous media, HPAM resistance factor might show shear-thinning behavior and ultimately show Newtonian behavior at very low velocities. Thus, the rheology of polymer solution plays an important role of success or failure of the polymer gel treatment. These polymer gels are viscoelastic fluids that exhibit both viscous and elastic properties and are characterized by elastic modulus (G') and viscous modulus (G") (Liu and Seright, 2001). Therefore, in-situ shear rate imposed by the flow affects the gelation process (McCool et al., 1991).

The importance of considering shear-thinning and shear-thickening behavior of HPAM is based on the enhancement of both displacement and volumetric sweep efficiencies (Huh and Pope, 2008; Urbissinova et al., 2010; Luo et al., 2015). The researchers in Daqing oil field observed that during the experiments on cores and after prolonged waterflooding, an additional oil could be recovered due to the viscoelasticity of HPAM polymer solution (Wang et al., 2001). Thus, Delshad et al. (2008) have developed a unified viscosity model (UVM) that covers a full spectrum of Newtonian, shear-thinning, and shear-thickening behavior of HPAM polymer solution flowing in porous media as a function of the Deborah number.

Gao and Burchfield (1995) used the in-situ gelation of polyacrylamide / Cr(VI) / thiourea in a hypothetical reservoir that consisted of two layers with equal layer thickness. The oil and water viscosities were 3 cp and 0.8 cp, respectively. In their study, they investigated four gel systems that have different concentrations and reaction constants and compared their results with polymer flooding. They concluded that higher oil recovery was obtained with a lower value of $\left(\frac{k_v}{k_h}\right)$ for the combined polymer flooding and gel treatment. In addition, if the reservoir had a high crossflow, the results would be unpromising. Lee et al. (2013) modeled in-situ gelation of polymer/chromium chloride gel using UTCHEM simulator. In their study, the permeability distribution is generated using IGW software by multiscale correlation. They concluded that the performance of gel treatment was dependent on permeability distribution; therefore, gel placement was mainly in the thief zones. In addition, the longer the preflush period, the higher the reduction in water-oil ratio, which depends on the heterogeneity index and connectivity. The salinity of the reservoir brine and/or the salinity of the makeup brine has great effects on the treatment. If

the salinity increased, the polymer viscosity would decrease and polymer adsorption would increase (Dong et al., 2008; Sheng, 2011; Mungan, 1969). Thus, lowering the salinity of the brine would increase the polymer viscosity, which would lower the cost of the treatment, since low polymer concentration would be required (Mohammadi and Jerauld, 2012). Polymer gels, on the other hand, swell when in contact with low-salinity water inside the reservoir (Tu and Wisup, 2011; Brattekas et al., 2016) or dehydrate when in contact with high-salinity water (Asghari, 2002). Furthermore, the presence of divalent cations (i.e., hardness) could jeopardize the success of the gel treatment by increasing the precipitation of polymer solution (Chauveteau and Sorbie, 1991; Mohammadi and Jerauld, 2012).

Cation exchange capacity (CEC) of the resident clays, which causes slow transport of Cr^{3+} due to its consumption by the clays (Garver et al., 1989), could prevent crosslinking of the crosslinkers with the polymer solution to form gel. Thus, gel treatment should be applied with precaution in the presence of high clays in the reservoir rock.

Romero-Zeron and Kantzas (2007) presented the microscale experiments of foamed gels, which showed a higher blocking efficiency in strongly oil-wet conditions than in strongly water-wet conditions. In addition, they concluded that combining both foam and gel would produce an agent that is excellent as a mobility control and plugging agent. Shen et al. (2013 and 2014) used UTCHEM simulator to study the effect of wettability and temperature on gel treatment in a two-layer model with permeability of 100 and 1,000 md. The results indicated that oil-wet conditions caused an increase in water-oil ratio more than water-wet conditions. In addition, both oil- and water-wet conditions showed that gel treatment is not effective at elevated temperatures. Moreover, the results showed that the

wettability of the reservoir affected gel treatment by causing wider distribution of gel in oil-wet conditions than in water-wet conditions.

In this study, UTGEL (UT Austin) simulator was used to simulate these parameters and to study their effects on the in-situ gelation process. The output results were processed by S3GRAF software that was developed and licensed by Sciencesoft Ltd.

2. POLYMER GEL SYSTEM

The selection of polymer gel system is dependent upon the reservoir conditions such as salinity, temperature, pH, hardness, and type of lithology. Polymer/chromium chloride gel, which consists of polyacrylamide, sodium dichromate, and thiourea, was used in this study. This system is an in-situ gel (i.e., the gelation process occurred inside the reservoir), which considered one of the most popular methods for in-depth gel treatments. The kinetics reaction will be present later in the kinetics reaction section. This polymer gel has advantages over other types of polymer gel systems based on the following:

- Availability, low cost (2-4 dollars per kilogram, Zhu et al., 2017), and resistance to bacterial attack are among the properties of HPAM polymer solutions, which makes them superior to other polymers.
- Xanthan biopolymer solutions are more costly than HPAM polymer solutions. Moreover, it is susceptible to bacterial degradation. However, xanthan is insensitive to brine salinity and hardness (Sheng 2011).
- HPAM solution is stable at all hardness levels up to 167°F (Moradi-Araghi and Doe, 1987).

- The polyacrylamide polymer solutions can reduce water permeability without affecting much oil permeability (Sparlin, 1976; Terry et al., 1981).
- HPAM could lose its viscosity due to shear degradation near-wellbore region. Huang et al. (1986) showed that the gelation time of polyacrylamide/sodium dichromate/thiourea system decreased from 10 days in a beaker (without shearing effect) to 85 hours in a porous media (with shearing effect). However, Sparlin (1976) concluded that the permeability reduction caused by polyacrylamides does not affected by shear degradation.
- Xanthan does not affected by shear degradation; however, the permeability reduction caused by xanthan is low (Sheng, 2011).
- HPAM polymer solutions are negatively charged, which can reduce the polymer adsorption.
- HPAM polymer solution is widely used for both polymer flooding and gel treatment (Sheng, 2011).
- The presence of carboxyl groups (COO^-) in HPAM is essential for the reaction with Cr(III) (Han et al., 2014; Hasan et al., 2013). The hydrolysis process converted some of the amide groups ($CONH_2$) to carboxyl groups (Sheng, 2011).
- The degree of hydrolysis ranges from 15-35% in commercial products of HPAM polymer solution. Thus, by adjusting the degree of hydrolysis, the reaction rate, the chemical stability and adsorption could be controlled (Sheng, 2011).
- HPAM/Cr(III) is used not only in heterogeneous reservoirs, but also in fractured reservoirs (Zhang et al., 2016).

- No preference of HPAM polymer over xanthan biopolymer if the reservoir temperature is higher than 80°C (176 °F) because both solutions are not stable thermally at elevated temperature (Zhu et al., 2017). However, HPAM could withstand temperature ranged from 99 to 110 °C (210-230 °F) depending on the brine hardness (Achim et al., 2015; Sheng, 2011).
- HPAM polymer solutions have important characteristics: shear-thinning behavior at low to moderate flow velocity and shear-thickening behavior beyond certain shear rate. These characteristics could improve overall sweep efficiency (Delshad et al., 2008; Seright et al., 2008; Luo et al., 2015).
- Xanthan biopolymer exhibits shear-thinning behavior only.
- If the polymer was a polyacrylamide, the metal ion would usually be Cr(VI) (Bhaskar et al., 1988).
- Some of the metal ions, such as aluminum citrate, decreases the permeability at the inlet of the core samples as shown by a laboratory experiment conducted by Willhite et al. (1986).
- The non-toxicity nature of polyacrylamide and Cr(III) to both human and aquatic life, especially at low concentrations, make them suitable for gel treatment (Sydansk, 1990).
- In general, there are two categories of crosslinkers: inorganic and organic. Inorganic crosslinkers such as Cr(III), Al(III), and Zr(IV) are widely used in the United States, while organic crosslinkers are widely used in China (Caili et al., 2010; Zhang et al., 2015).

- The gelation time obtained from the experimental works of different polymer gel systems is lower than the gelation time of HPAM/Cr(III). For instance, the gelation time of xanthan/Cr(III) ranged from 1 to 7 hours (Hubbard et al. 1988). Moreover, the gelation time ranged from 18-72 hours at 149 °F for polyethyleneimine (PEI) crosslinking HPAM (Jia et al. 2012). By contrast, the gelation time of polyacrylamide/chromium(VI)/thiourea ranged from 200 to 250 hours (McCool et al., 1991). Moreover, Bhaskar et al. (1988) concluded that a gelation time from weeks to months is possible.
- The parameters that affect the gelation time, such as HPAM and Cr(III) concentration, are controllable (Marty et al., 1991).
- The permeability reduction could be achieve deeply in the thief zones by selection of low injection rate and low concentrations of polymer and crosslinker (Marty et al., 1991).
- Normally, gel is formed by fast reaction between the polymer and the Cr(III). Therefore, adding thiourea as a reducing agent, lower the rate of the reaction and produce gel with long gelation time and deep penetration into the thief zones.
- There are several reducing agents such as thiourea [$(NH_2)_2CS$] and sodium bisulfite ($NaHSO_3$); however, thiourea has a slow reaction rate than sodium bisulfite. Thus, adding thiourea to the gel system would yielded a longer gelation time, which enables deep penetration of the solution before forming a 3D gel network (Terry et al., 1981; Bhaskar et al., 1988).
- Some of the in-situ gelation of polyacrylamide polymer solutions with crosslinker such as zirconium is used for water shutoff (Chauveteau et al., 1999).

- Polyacrylamide/aluminum citrate is a non-toxic gel; however, the retention of aluminum on rock, precipitate when mixed with formation water, and a requirement for fresh water are considered disadvantages of this gel system (Sparlin, 1976).

For more information regarding different polymer solutions, Sheng (2011) listed the characteristics of these polymers such as polyoxyethylene, sodium alginate, HPAM, and xanthan gum among others.

3. UTGEL RESERVOIR SIMULATOR

UTGEL simulator stems from UTCHEM simulator where they both developed at the University of Texas at Austin. The UTGEL simulator can be used to simulate a wide range of displacement processes at both field and laboratory scales (UTGEL Technical Manual, 2014). In addition, non-Newtonian polymer rheology, the adsorption of polymer and gel, cation exchange, and several gel kinetics can be modeled. In addition, in-situ and preformed gels can be model using UTGEL simulator (Goudarzi, 2015).

3.1. KINETIC REACTION

Regardless of the gelation process (i.e., in-situ or preformed gel), the reaction chemistry includes the reactions of polymer solution with a crosslinker to form the gel (Garver et al., 1989; Kim, 1995). In polymer/chromium chloride gel, the first reaction of the in-situ gelation is a redox reaction of the sodium dichromate with the reducing agent (i.e., thiourea (CSN_2H_4)) to produce trivalent chromium. Then, the trivalent chromium crosslinks with HPAM polymer solution to form the gel, as shown in Equations 1 and 2.

$$Cr(VI) + Reducing\ Agent \rightarrow Cr(III) \quad (1)$$

$$Cr(III) + Polyacrylamide \rightarrow Gel \quad (2)$$

3.2. POLYMER RHEOLOGY IN POROUS MEDIA

The rheology of a polymer solution in porous media is essential to the injectivity and sweep efficiency of enhanced oil recovery (EOR) processes. HPAM polymer solution, exhibits non-Newtonian flow behavior, which involves both shear-thinning (pseudoplastic, shearing) and shear-thickening (dilatant, elongation) behaviors, as shown in Figure 1.

If the polymer solution such as xanthan biopolymer has only shear-thinning behavior inside porous media, then Meter's equation (Equation 3) is used in UTCHEM and UTGEL simulators:

$$\mu_{app} = \mu_{\infty} + \frac{\mu_p^{\circ} - \mu_{\infty}}{1 + (\frac{\gamma_{eff}}{\gamma_{1/2}})^{P\alpha - 1}} \quad (3)$$

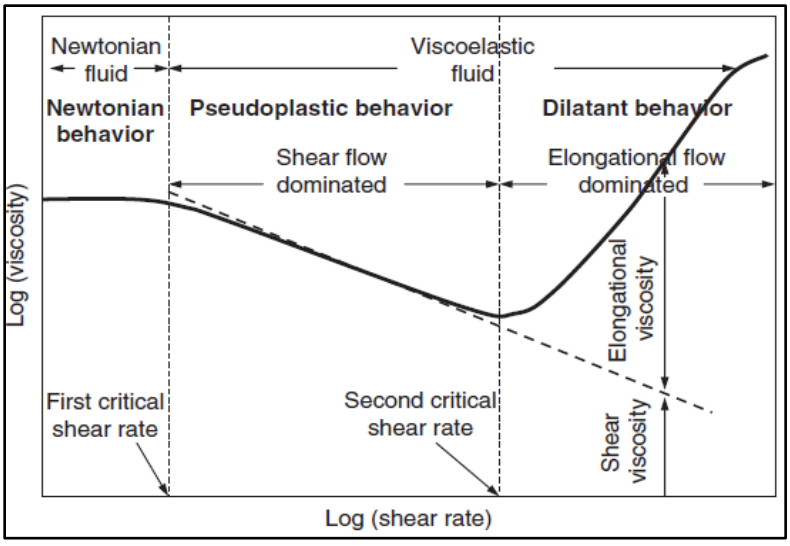

Figure 1. Polymer viscosity as a function of shear rate for shear thinning and UVM (Sheng, 2011).

where μ_{app} is the apparent viscosity of the polymer solution; μ_∞ is the polymer solution viscosity at an infinite shear rate, which is approximated by brine viscosity; and μ_p° is the viscosity at a very low shear rate and calculated using the modified Flory-Huggins equation (Flory, 1953) as presented in Equation 4. $\gamma_{1/2}$ is the shear rate at which the apparent viscosity is the average of μ_p° and μ_∞ and is a function of polymer concentration (C_p), where P_α is another fitting parameter.

$$\mu_p^\circ = \mu_w \left[1 + \left(A_{P1}C_p + A_{P2}C_p^2 + A_{P3}C_p^3\right)C_{SEP}^{S_p}\right] \quad (4)$$

where μ_w is the brine viscosity; $A_{P1}, A_{P2},$ and A_{P3} are the fitting parameters obtained from matching laboratory data; and $C_{SEP}^{S_p}$ represents the dependence of the polymer viscosity on the salinity and hardness (i.e., anion and divalent cation concentrations) (Li and Delshad, 2014). S_p represents the slope of $\left(\frac{\mu_p^\circ - \mu_\infty}{\mu_\infty}\right)$ vs. C_{SEP} on a log-log plot.

$$C_{SEP} = \frac{C_{anion} + (\beta_p - 1)C_{cation}^{++}}{C_w} \quad (5)$$

where C_{anion}, C_{cation}^{++}, and C_w are total anion, divalent cation, and water concentrations in the aqueous phase, and β_p is measured in the laboratory and is an input model parameter.

3.3. UNIFIED VISCOSITY MODEL (UVM)

As mentioned previously, Delshad et al. (2008) have proposed unified viscosity model (UVM). This model consists of (Lotfollahi et al., 2016):

$$\mu_{app} = \mu_{sh} + \mu_{el} \quad (6)$$

The shear-thinning component is calculated using Carreau's model (Carreau, 1968):

$$\mu_{sh} = \mu_\infty + \left(\mu_p^\circ - \mu_\infty\right)\left(1 + \left(\lambda_1 \dot{\gamma}_{eff}\right)^2\right)^{(n_1-1)/2} \quad (7)$$

where n_1 is a model parameter, and λ_1 is a function of polymer concentration (C_p), which is calculated from Equation 8.

$$\lambda_1 = \beta_1 \exp(\beta_2 c_p) \tag{8}$$

where β_1 and β_2 are model parameters that obtained by matching the measured polymer solution viscosity versus the shear rate for several concentrations at a given temperature and brine viscosity (Lotfollahi et al., 2016). The shear-thickening component of the UVM model is calculated as follows:

$$\mu_{el} = \mu_{max} \left\{1 - \exp[-\left(\lambda_2 \tau_r \dot{\gamma}_{eff}\right)^{n_2 - 1}]\right\} \tag{9}$$

where n_2 and λ_2 are model parameters and τ_r is the polymer relaxation time, which, for simplicity, is assumed to be a linear function of the polymer concentration c_p as:

$$\tau_r = \tau_o + \tau_1 C_p \tag{10}$$

μ_{max} is the plateau viscosity of the shear-rate thickening and is modeled with an empirical correlation on the basis of laboratory measurements:

$$\mu_{max} = \mu_w \left(AP_{11} + AP_{22}\, ln\, C_p\right) C_{SEP}^{S_p} \tag{11}$$

where AP_{11} and AP_{22} are model parameters. If these two parameters were zeros, Equation 6 would be consisted from only shear thinning part.

3.4. POLYMER ADSORPTION

Polymer adsorption is defined as the interaction between polymer molecules and the porous media, which leads to the attachment of polar groups along the polymer chain to many different polar points on the rock surface (Manichand and Seright, 2014). Several isotherms such as the widely used Langmuir isotherm could be best describes the

adsorption of polymer solution (Ali and Ben Mahmud, 2015), as shown in Equation 12:

$$C_p^{\wedge} = \frac{aC_p}{1+bC_p} \tag{12}$$

$$a = (a_1 + a_2 C_{SEP})\sqrt{\frac{k_{ref}}{k}} \tag{13}$$

where a_1, a_2, and b are adsorption model parameters that are specified at a reference permeability (k_{ref}). The maximum level of adsorbed polymer is represented by (a/b).

3.5. PERMEABILITY REDUCTION FACTOR

Jennings et al. (1970) stated that the residual resistance factor (i.e., permeability reduction), is a measure of water mobility after polymer solution relative to water mobility before polymer solution. The permeability reduction is measured by the permeability reduction, R_k, calculated by:

$$R_k = \frac{k_w}{k_p} \tag{14}$$

The permeability reduction factor in UTGEL simulator is modeled as:

$$R_k = 1 + (R_{kmax} - 1)\frac{b_{rk}C_p}{1+b_{rk}C_p} \tag{15}$$

where

$$R_{kmax} = [1 - \frac{C_{rk}\left(AP_1 C_{SEP}^{Sp}\right)^{\frac{1}{3}}}{\sqrt{k/\phi}}]^{-4} \tag{16}$$

b_{rk} and C_{rk} are the input parameters. In UTGEL simulator, the polymer and gel adsorptions are considered to be irreversible, i.e., it does not decreases as the polymer concentration decreases. Thus, $R_{RF} = R_k$ (UTGEL Technical Manual, 2014; Stavland et al., 1994).

3.6. GEL VISCOSITY, ADSORPTION, AND PERMEABILITY REDUCTION

Using the Flory-Huggins equation, the gel viscosity is modeled with additional terms for gel (Thurston et al., 1987).

$$\mu_1 = \mu_w \left[1 + \left(AP_1 C_p + AP_2 C_p^2 + AP_3 C_p^3\right) C_{SEP}^{Sp} + A_{g1} C_g + A_{g2} C_g^2\right] \quad (17)$$

where A_{g1} and A_{g2} are Flory-Huggins parameters for gel viscosity and C_g is the gel concentration. Langmuir isotherm is used to correlate the adsorbed concentration with the aqueous-phase concentrations, as shown below:

$$C_g^{\wedge} = \frac{a_g C_g}{1 + b_g C_g} \quad (18)$$

where a_g and b_g are gel adsorption parameters. A residual resistance factor is used to account for the effect of the gel on the aqueous-phase permeability reduction, as shown in Equation 19:

$$R_k = 1 + (R_{kmax} - 1) \frac{A_{gk} C_g}{1 + B_{gk} C_g} \quad (19)$$

where the maximum residual resistance factor is calculated by:

$$R_{kmax} = \left[1 - \frac{C_{rg}\left(AP_1 C_{SEP}^{Sp}\right)^{1/3}}{\left(\frac{\sqrt{k_x k_y}}{\phi}\right)^{1/2}}\right]^{-4} \quad (20)$$

where A_{gk}, B_{gk}, and C_{rg} are permeability-reduction parameters for gel that depends on the type of the gel.

4. MODEL DESCRIPTION

All runs were conducted on a 3D of one-quarter of a five-spot pattern, with one injection well and one production well located at opposite corners. The model dimensions

are 1,875×1,875×220 ft^3 with six layers that have different properties, as shown in Table 1. The high-permeability streaks (i.e., layers 3 and 4) were located in the middle of the model. Water and oil viscosities were 0.86 cp and 6 cp, respectively as shown in Table 2. The injection well was operated under an injection rate of 1070 bbl/day, which was constant for all runs. The selection of this injection rate was based on previous field applications (Bai et al., 2004). The producer was under bottomhole pressure constraints. For most simulation runs, the reservoir was represented by 19 gridblocks in the *x* and *y* directions and 6 gridblocks in the vertical direction as shown in Table 1 and Figure 1, whereas Figure 2 shows the relative permeability curves. The model was built with Cartesian coordinates with small sizes of gridblocks near wellbore, in order to eliminate the possible errors of calculating shear rate and polymer viscosity (Sharma et al., 2011; Li and Delshad, 2014). The ratio of vertical to horizontal permeability was set to be 0.01. This ratio was selected because the geological processes make the vertical permeability much lower than the horizontal permeability. To make the treatment more reliable and acceptable, criteria that proposed by Seright et al. (2012) were taken into consideration, which includes:

- High-permeability contrast (e.g., 10:1 and higher).
- High thickness ratio.
- Relatively low oil viscosity.

Thus, in this study the following criteria were considered:

- The permeability contrast was 15:1 (i.e., ratio of high to low permeability).
- The thickness ratio was 5:1 (i.e., ratio of thickness of low to high-permeability layer).

- Oil viscosity was 6 cp.

Other considerations were:

- As the purpose of this study is to model and observe the effects of different parameters on the in-situ gelation process of in-depth gel treatment, the reservoir is fictitious. However, the injection rate, the polymer and gel rheology parameters were taken from the published literatures such as Bai et al. (2004), Liu et al. (2006), Yuan (2012), and Kim (1995). Some of these data such as shear thinning parameters in Flory-Huggins equation and Langmuir isotherm parameters in polymer adsorption equation were modified according to polymer viscosity and polymer adsorption versus concentration curves.
- Only water and oil phases were presented in the model. No gas phase effect was considered.
- There was no aquifer support on the production; thus, the only water influence was from the injection well.
- The salinity in this study reflects the concentration of sodium chloride (NaCl) in the system, which was selected because of the compatibility of polymer solution with NaCl solution.
- The comparison of the results with water flooding scenario is not possible, because UTGEL simulator cannot model low-salinity water flooding mechanisms. Therefore, the enhancements that occurred in the recovery due to low-salinity reservoir brine or due to low-salinity chase water floods were resulted from the effects of salinity on both polymer viscosity and polymer adsorption.

4.1. INJECTION SCHEMES

To show the effect of the injection schemes on the results, three injection schemes were considered. For all injection schemes, the flooding started with pre-treatment water flooding; then, a designated fluid was injected. For example, in injection scheme1, the flooding started with a water injection, followed by a gelant solution injection, then post-treatment water. Tables 3 to 5 showed the injection schemes, which showed that a total of 0.23 PV (i.e., 7,300 days) was injected. The proposed injection rate (i.e., 1070 bbl/day) with the proposed duration for injection of the gelant solution (i.e., 50 days) will give an injected volume equal to 53,500 bbls (8506 m^3). Liu et al. (2006) stated that the typical injected volumes for this type of polymer gel ranged from 12,500 to 50,000 bbls (2000 m^3 to 8000 m^3).

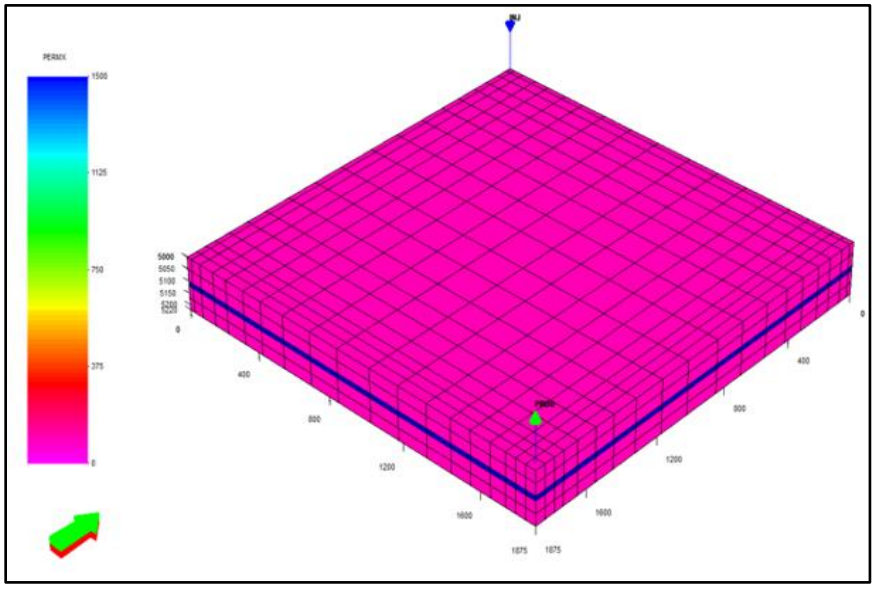

Figure 2. Representation of the simulation model showing thief zones located in the middle of the model.

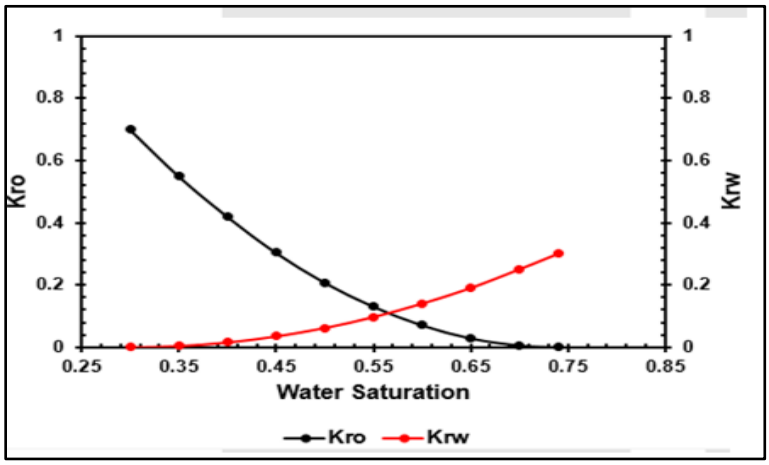

Figure 3. Relative permeability curves.

Table 1. Reservoir characteristics.

Initial reservoir pressure	2,500 psi
Length, *x*	1,875 ft.
Width, *y*	1,875 ft.
Thickness, *z*	220 ft.
NX	19
NY	19
NZ	6
Gridblock size in x and y directions	Variable
Low- and high-permeability layer thicknesses	50 ft. and 10 ft.
Low- and high-permeability layer porosities	0.25 and 0.20
Low and high permeability regions: $k_x = k_y$	100 md and 1,500 md
k_v/k_h	0.01
Injection rate	1,070 bpd
Producer BHP	500 psi
Well radius	0.4 ft.
Well pattern	¼ of 5-spot

Table 2. Fluid properties.

Water viscosity	0.86 cp
Oil viscosity	6.0 cp
Initial water saturation	0.30
Residual oil saturation	0.26
Endpoint Krw	0.3
Endpoint Kro	0.7
Water exponent	2.0
Oil exponent	2.0
Endpoint mobility ratio	3.0
Water density	62.4 lb/ft^3
Oil density	53.0 lb/ft^3
Water	2.7e-06
Oil	5.0e-05

Table 3. Injection scheme 1.

Sequence of the injected fluid	Injected PV	Injection duration, days	Injection duration, yrs.
Pre-treatment water	0.058	1,825	5.0
Gelant solution	0.0016	50	0.14
Post-treatment water	0.171	5,425	14.86
	0.23	7,300	20.0

4.2. VISCOSITY AND ADSORPTION PARAMETERS OF THE POLYMER SOLUTION

Since polymer solution represents the main component of any gel system. The polymer viscosity is affected by different parameters, which affect the gelation process and the strength of the formed gel. These parameters are (Sheng, 2011):

- Molecular weight.
- Polymer concentration.
- Salt concentration.
- Shear rate.
- Degradation.

Table 4. Injection scheme 2.

Sequence of the injected fluid	Injected PV	Injection duration, days	Injection duration, yrs.
Pre-treatment water	0.058	1,825	5.0
Gelant solution	0.0016	50	0.14
Polymer solution	0.012	365	1.0
Post-treatment water	0.1584	5,060	13.86
	0.23	7,300	20.0

Table 5. Injection scheme 3.

Sequence of the injected fluid	Injected PV	Injection duration, days	Injection duration, yrs.
Pre-treatment water	0.058	1,825	5.0
Polymer solution	0.012	365	1.0
Gelant solution	0.0016	50	0.14
Post-treatment water	0.1584	5,060	13.86
	0.23	7,300	20.0

To investigate the effect of salinity on polymer viscosity and polymer adsorption, the data that presented in Figures 4 and 5 were used. These data were taken from Aluhwal (2008).

Shear thinning parameters (A_{P1}, A_{P2}, A_{P3}) in Equation 4 were obtained using third-order polynomial fitting of polymer viscosity versus polymer concentration plot at different salinity values (Figure 4). Thus, these parameters are dependent on the salinity of the solvent, as shown in Table 6. The constant S_p in Equation 4 represents the slope of $\left(\frac{\mu_p - \mu_\infty}{\mu_\infty}\right)$ (i.e., specific viscosity or viscosity enhancement) versus C_{SEP} on a log-log plot as shown in Figure 6, while Table 7 showed S_p at different polymer concentrations. This constant is negative for hydrolyzed polyacrylamide (HPAM) and positive for polysaccharide (xanthan) (UTGEL User Guide). In this study, a 1,000-ppm polymer concentration was used; therefore, the constant S_p at this polymer concentration was selected.

The next step is to find the Langmuir isotherms. Equation 21 represents an equation of a straight line, which obtained after rearranging Equation 12. Thus, at each salinity value, $\left(\frac{1}{Ads}\right)$ versus $(\frac{1}{C_p})$ was plotted as a straight line and the values of (a), (b), and (a/b) can be obtained as shown in Table 8. These parameters were plotted versus the salinity as shown in Figure 7, which demonstrated the effect of salinity on polymer adsorption.

$$\frac{1}{Ads} = \frac{1}{a} \times \frac{1}{C_p} + \frac{b}{a} \tag{21}$$

Finally, Tables 9 and 10 show the polymer and gel input parameters, respectively, which were taken from Yuan (2012) and Kim (1995).

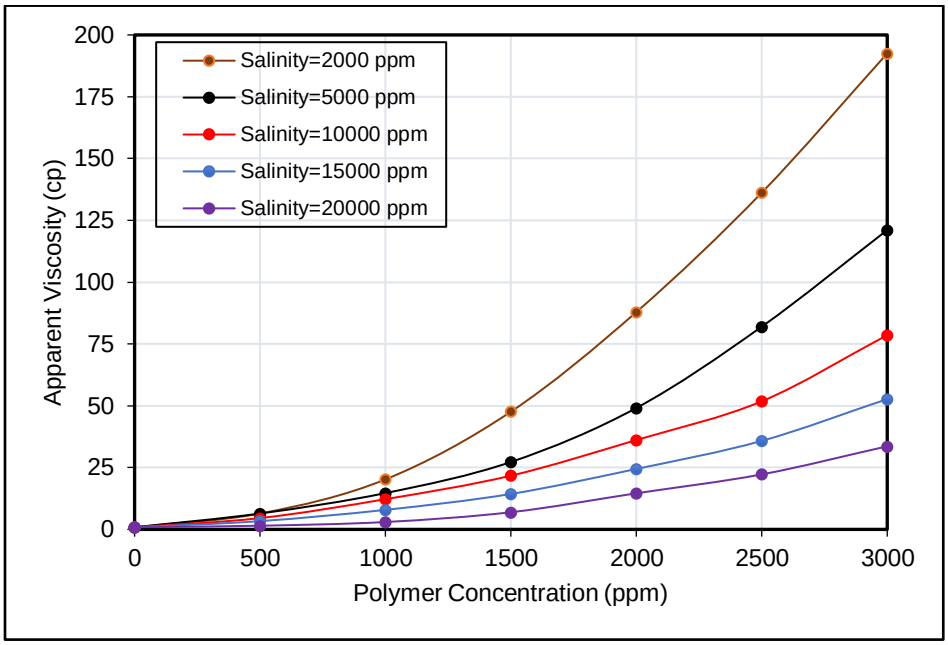

Figure 4. HPAM apparent viscosity as a function of polymer concentration and salinity (Aluhwal, 2008).

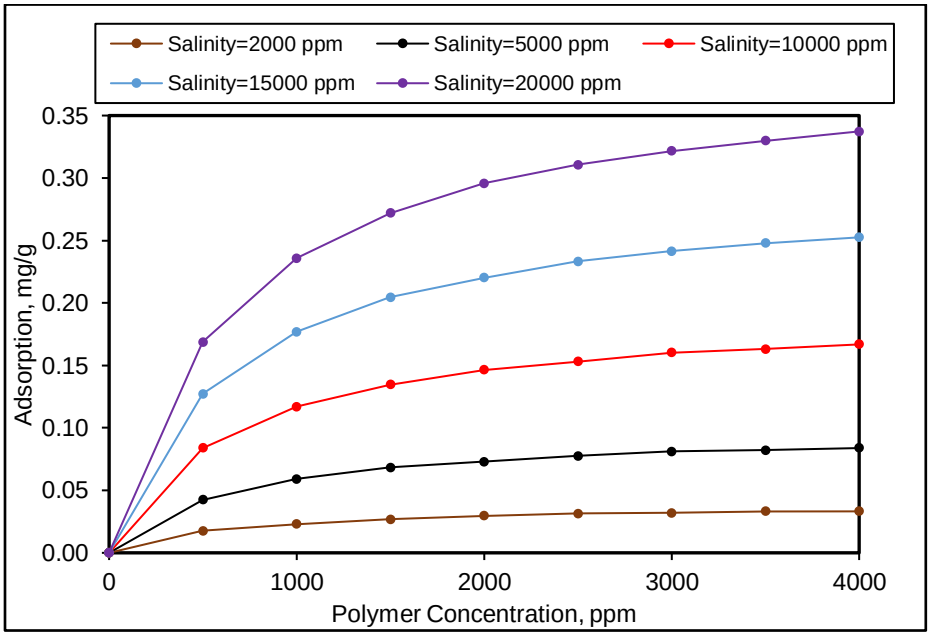

Figure 5. HPAM adsorption as a function of polymer concentration and salinity (Aluhwal, 2008).

Table 6. Shear thinning parameters of Flory-Huggins equation.

Salinity concentration, ppm	A_{P1}	A_{P2}	A_{P3}
1,000	144.4	2282.7	302.22
2,000	76.40	2844.6	1524.40
5,000	48.30	544.60	2253.30
10,000	65.04	273.14	1253.30
15,000	33.09	370.80	364.44
20,000	6.50	270.80	253.33

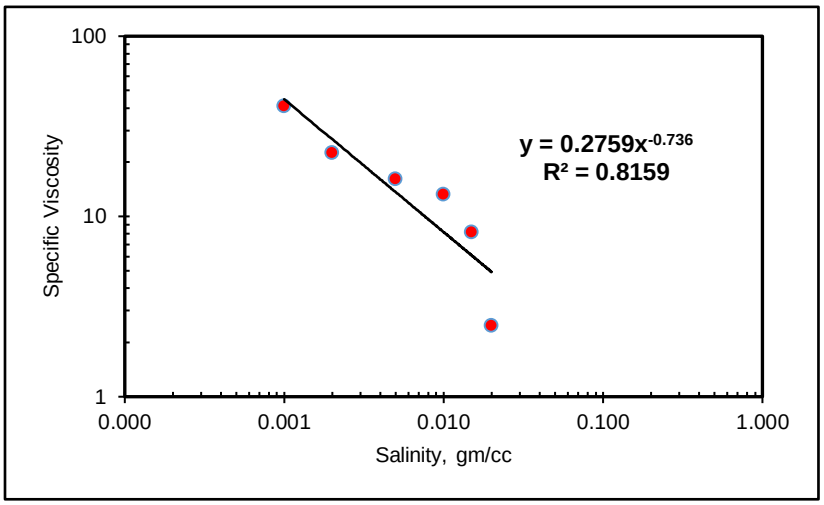

Figure 6. Specific viscosity versus salinity at 1000-ppm HPAM concentration to obtain S_p exponent for Flory-Huggins equation.

Table 7. S_p Exponent at different polymer concentrations.

Polymer conc., ppm	S_p
500	-0.573
1,000	-0.736
1,500	-0.720
2,000	-0.655

Table 7. S_p Exponent at different polymer concentrations (Cont.).

2,500	-0.656
3,000	-0.633

Table 8. Langmuir isotherm parameters.

Salinity, ppm	a, (L/g)×(mg/g)	b, L/g	$(\frac{a}{b})$, mg/g
2,000	0.06	1.75	0.034
5,000	0.15	1.78	0.084
10,000	0.30	1.80	0.167
15,000	0.48	1.83	0.262
20,000	0.61	1.86	0.328

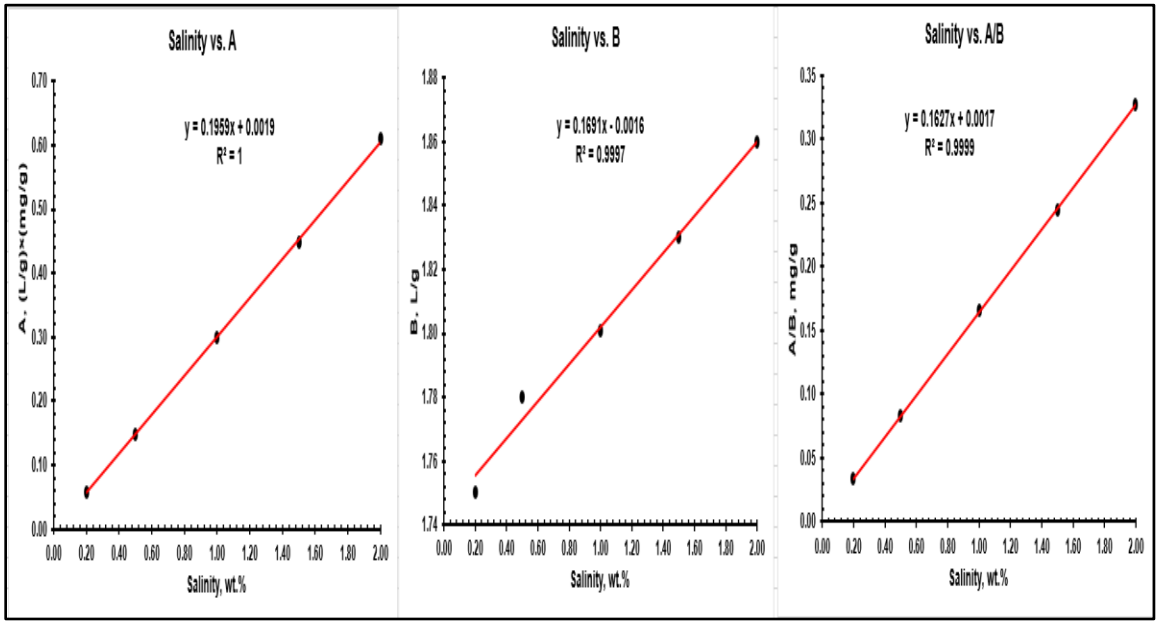

Figure 7. Langmuir adsorption parameters (A and B) and maximum adsorption parameter (A/B) vs. salinity.

Table 9. Polymer input parameters (data from Yuan 2012 with modifications to viscosity and adsorption parameters of polymer).

Parameter	Keyword in UTGEL simulator	Value
Polymer viscosity parameters:		
$AP_1,\ AP_2, AP_3, S_p$	AP1, AP2, AP3, SSLOPE	Tables 9 and 10
Polymer adsorption parameters:		
$a_{1,}\ a_{2,}\ b$	AD41, AD42, B4D	Table 11
Permeability reduction:		
$b_{rk},\ C_{rk}$	BRK, CRK	1000, 0.0186
UVM parameters:		
$\beta_1,\ \beta_2$	BETAV1, BETAV2	0.0192, 18.522
n_1	EXPN1	0.78
AP_{11}, AP_{22}	AP11, AP22	21.76, 3.49
τ_o, τ_1	TAU0, TAU1	0.0089, 0.2992
n_2,λ_2	EXPN2, TETAV	3.5, 0.01

5. NUMERICAL MODEL RUNS

To investigate the optimum conditions leading to successful deep gel placement, several scenarios were modeled in this study. These includes:

- Comparison between polymer flooding and gel treatment.
- Polymer rheology.
- Salinity and hardness.
- Injection schemes.
- Cation exchange capacity (CEC).
- Wettability of the model.
- Gravity segregation and dip angle of the model.

- Mobility ratio.
- Effect of the skin factor in the injection well.

5.1. COMPARISON BETWEEN POLYMER FLOODING AND GEL TREATMENT

To clarify the importance of gel treatment, polymer flooding was modeled and compared with gel treatment. The main objective of polymer flooding is to increase the viscosity of water and to improve sweep efficiency by lowering unfavorable mobility ratio. Invading of the polymer solution into low-permeability layers should be maximize during the flooding. Thus, in this study, polymer solution has access to all open layers. Whereas in gel treatment, the gelant solution should be injected into only high-permeability layers and the penetration into low-permeability layers should be minimized (Seright et al., 2012). Thus, in this study, the gelant solution was injected into the thief zones only. The polymer and the gelant were injected using the same injection rate (i.e., 1070 bbl/day); however, the injection duration was different. The polymer solution was injected for one year (i.e., 0.012 PV), while gel treatment was injected for 50 days (i.e., 0.0016 PV). Thus, the economy of the project would depend on the cost of the used chemicals, the slug size, and the incremental oil. Table 11 shows the recovery factor by water flooding, polymer flooding, and gel treatment. It seems that, in spite of the difference in the slug size of polymer and gelant solutions, gel treatment still the best option to plug and divert post-treatment water into low-permeability layers. In addition, the blocking efficiency of the gel treatment was higher compared to polymer flooding, which is clear from difference between the final water cut for both processes (Figure 8-right). The cost saving is remarkable by reducing the cost of the injected chemicals. Several reasons caused this difference which includes:

- Polymer flooding is used mainly as a mobility control, not for blocking the thief zones.
- In-situ gelation system is used mainly as a blocking agent (i.e., conformance control agent).
- In-situ gelation system yielded higher residual resistance factor (RFF) than polymer flooding, because of their crosslinked nature and greater permeability reduction capabilities.

Figure 8 shows a comparison of oil recovery factor and water cut between water flooding, polymer flooding, and gel treatment, respectively. As can be notice from Figure 9 that the blocking efficiency (i.e., permeability reduction) was higher during gel treatment compared to polymer flooding.

Table 10. Gel input parameters (Kim, 1995).

Parameter	Keyword in UTGEL simulator	Value
HPAM concentration		1,000 ppm
Sodium dichromate		500 ppm
Thiourea		700 ppm
HPAM MW		12 million
Gel viscosity parameters: $A_{g1}, A_{g2}, C_{rg}, A_{gk}, B_{gk}$	AG1, AG2, CRG, AGK, BGK	8E-03, 2.7E-05, 0.5, 0.1, 0.099
Gel retention parameters: a_g, b_g	A15D, B15D	2, 100
k_1	AK1	1E-05
k_{1ref}	AK2	303.6
SCR	SCR	0.25
X4	X4	2.6

Table 10. Gel input parameters (Kim, 1995) (Cont.).

X13	X13	1.6
X14	X14	1.0
X16	X16	0.3

Table 11. Comparison of oil recovery factor, incremental oil, and water cut at the end of post-water injection.

Run	Total injected PV	Slug injected, PV	RF, %	Cum. Oil, MM bbls	Incremental oil, MM bbls	Water cut at the end of chase water floods, %
Water Flooding	0.23		21.75	5.79		69.00
Polymer Flooding	0.23	0.012	23.13	6.16	0.37	72.00
Gel Treatment	0.23	0.0016	23.68	6.30	0.51	60.30

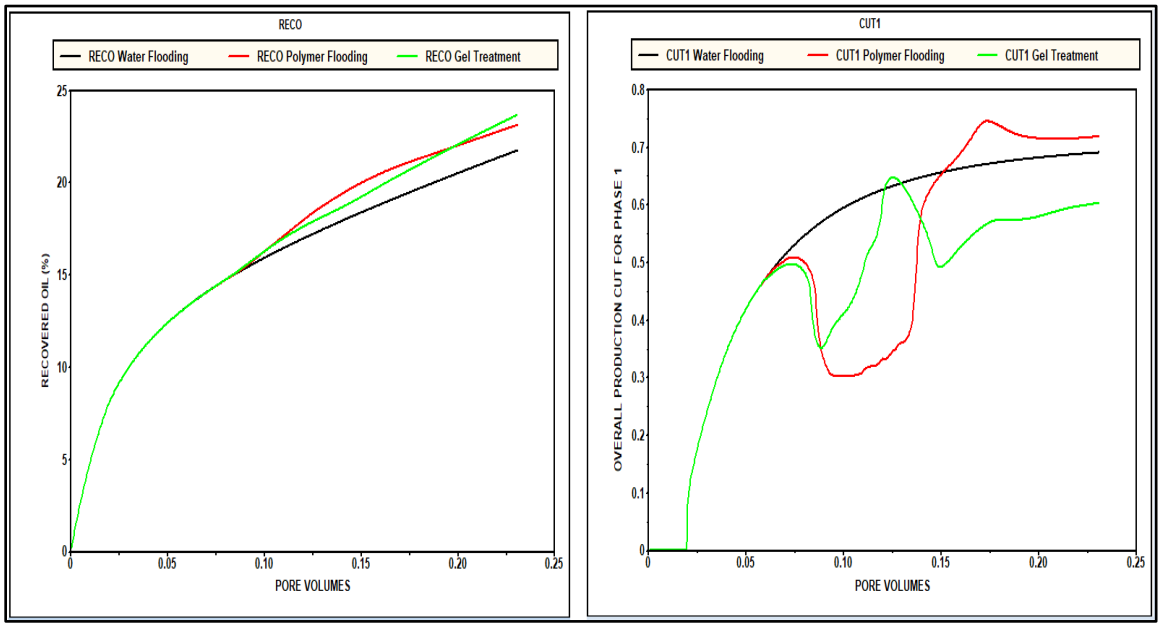

Figure 8. Comparison of oil recovery factor (left) and water cut (right) between water flooding, polymer flooding, and gel treatment.

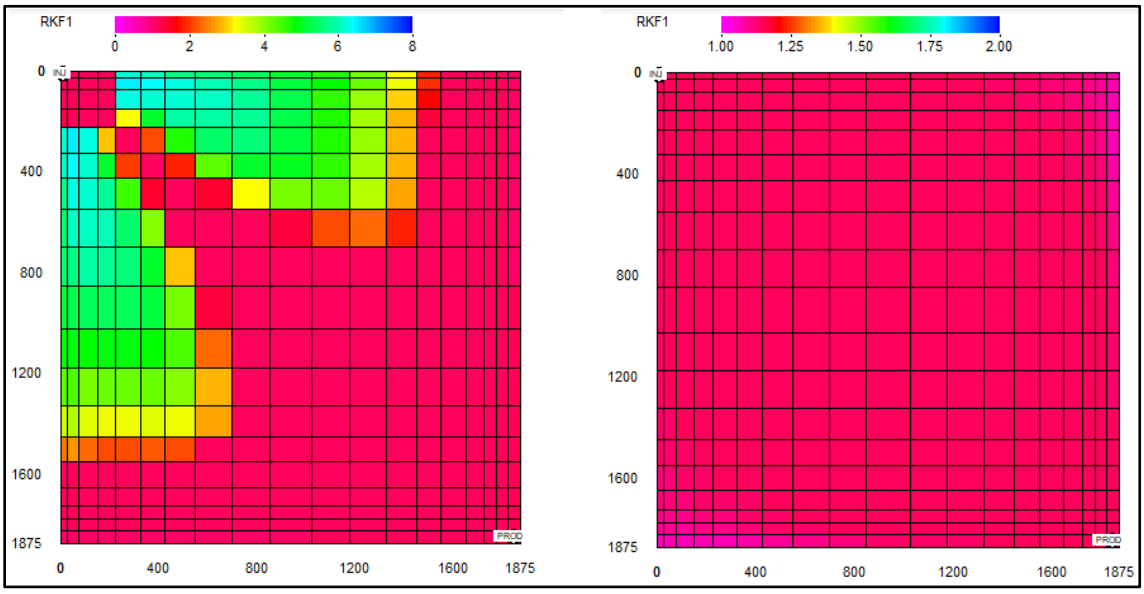

Figure 9. Comparison of water residual resistance factor (permeability reduction) in layer 4 between gel treatment (left) and polymer flooding (right).

5.2. EFFECT OF POLYMER RHEOLOGY

There is an increasing evidence from laboratory and field data that the viscoelastic characteristics of polymer solution improved the polymer flooding efficiency as well as the gel treatment. Shear-thinning behavior is important as it assisted the gelant solution injectivity at the perforations (Sheng, 2011; Lee, 2011). However, another behavior might develop as the gelant solution moves far away from the wellbore region. Thus, the flow velocity is reduce and the viscosity is restore and increase (i.e., shear-thickening behavior). To show the importance of the polymer rheology on the gel treatment, two models were run using polymer rheology with shear-thinning behavior only versus shear-thinning and shear-thickening behaviors together (unified viscosity model, UVM). In the subsequent sections and for comparison, shear-thinning curves represented the models that ran using shear-thinning behavior only, while UVM represented the models that ran using UVM

model. In addition, “S” refer to the salinity of the system. Table 12 shows a comparison of a system with 10,000-ppm salinity, which demonstrate the difference between UVM and shear-thinning behavior. Whereas, Fig. 10 shows the permeability reduction factor in layer 4 (i.e., thief zone), which also confirmed the importance of UVM rheology over shear-thinning behavior.

Table 12. Effect of polymer rheology.

Rheology	Recovery factor, %	Cumulative oil, MM bbls
Shear thinning only	22.43	5.97
UVM model	23.68	6.30

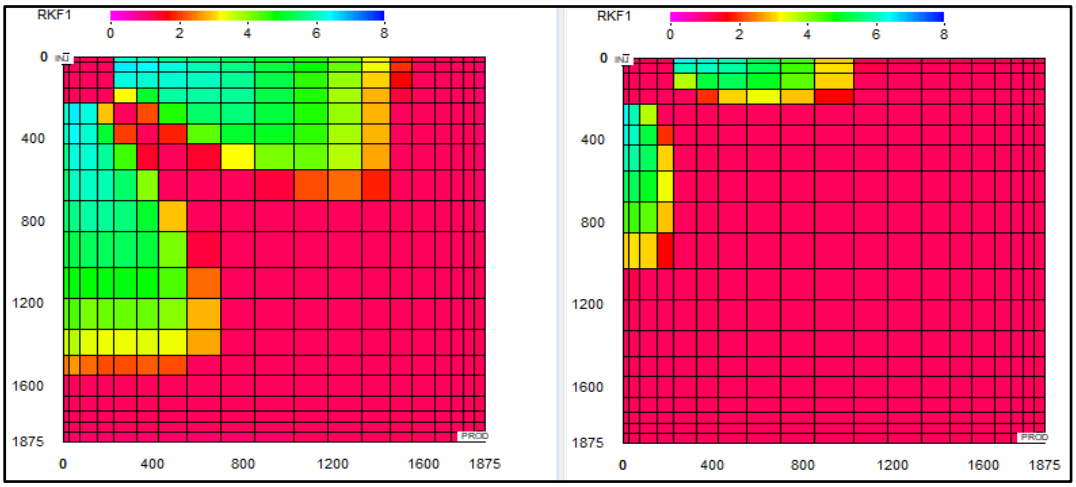

Figure 10. Comparison of permeability reduction factor (RKF1) in layer 4 between UVM run (left) and shear thinning run (right).

Figure 10 above showed the potential ability of shear-thickening behavior of improving the sweep efficiency by enhancing the blocking efficiency of the gel in the thief zone. Consequently, diverting more post-treatment water into low-permeability layers.

5.3. EFFECT OF

In this section, the effect of salinity, low-salinity post-treatment water, hardness (i.e., divalent cations), and low-salinity post-treatment water in the presence of hardness are investigated. The purpose is to show the effect of low-salinity brine on both polymer viscosity and polymer adsorption, which affects the strength of the formed gel.

5.3.1. Salinity. Sheng (2011) stated, "At low salinities, the negative charges on the polymer backbones repel each other and cause the polymer chains to stretch and incre -ease the viscosity of the polymer solution." When adding NaCl (i.e., an electrolyte) to the polymer solution, double layers of electrolytes shield the repulsive forces; thus, the stretch and the repulsion is reduce and decrease the viscosity of the polymer solution. Therefore, increasing the salinity would decrease the viscosity of the polymer, which affects the strength of the gel. The shear thinning parameters, A_{P1}, A_{P2}, and A_{P3}, obtained at different salinities were included in Equation 5. These parameters were used to calculate shear-thinning part of the UVM model (i.e., Equation 7), while constant S_p was concluded from Figure 6 at 1000-ppm polymer concentration. In addition, Langmuir isotherm parameters (i.e., *a*, *b*, and *a/b*) were included in Equation 13 to show the effect of salinity on polymer adsorption. Using UVM model, different models were run at different salinities as shown in Table 13. It is obvious that the gel treatment were more efficient at low-salinity water system due to the combined effects of salinity on both polymer viscosity and polymer adsorption. The effect of gel treatment in reducing the permeability in layer 3 (i.e., water residual resistance factor), was higher when the salinity of the system was 1,000 ppm (Figure 11-left) compared to 15,000-ppm salinity system (Figure 11-right). Thus, gel treatment with high-salinity water system was performed less efficient.

Table 13. Effect of salinity.

Salinity, ppm	Recovery factor, %	Cumulative oil, MM bbls
1,000	25.50	6.77
2,000	25.28	6.73
5,000	23.41	6.23
15,000	22.45	5.97
20,000	21.89	5.83

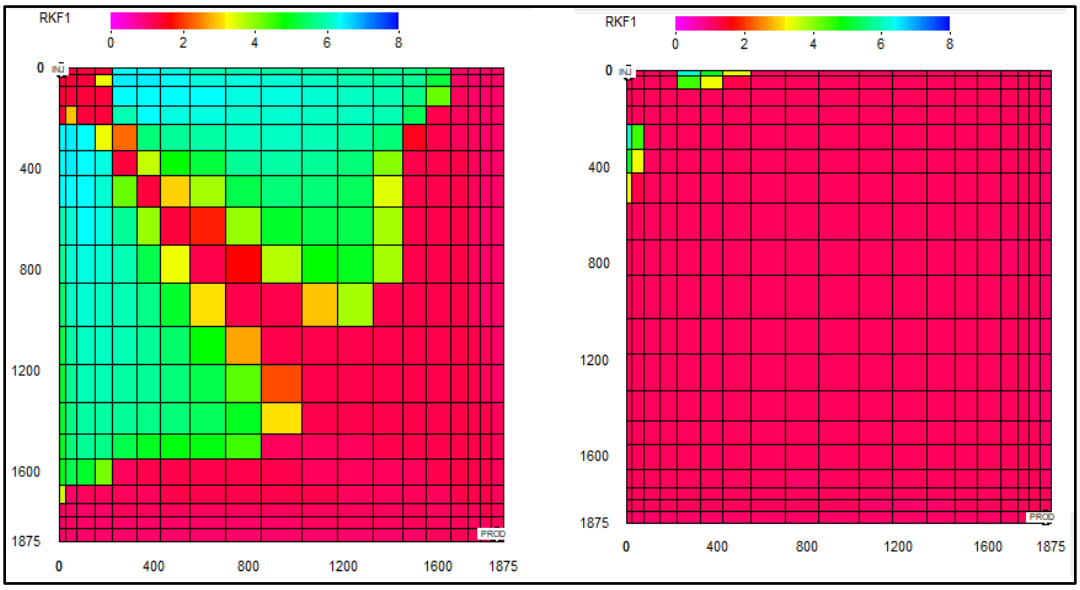

Figure 11. Comparison of permeability reduction factor in layer 3 between 1000-ppm salinity system (left) and 15,000-ppm salinity system (right).

5.3.2. Low-Salinity Post-Treatment Water Flooding. The reservoir brine and/or the makeup brine that used to prepare the gelant solution has tremendous effect on the performance and strength of the formed gel.

The gel systems that used for permeability modification of thief zones swell or dehydrate when in contact with brine. This phenomenon can increase or decrease the

volume of the gel and probably affect the long-term performance of gels placed in the reservoir (Asghari, 2002). Thus, gel volume increase due to swelling, which occur when the gel system is in contact with low-salinity water, or when gel is prepared with low-salinity water (Brattekas et al., 2016; Tu and Wisup, 2011). On the other hand, gel volume decrease or shrink (i.e., dehydrate), in which solvent is expelled from the gel network, when the gel system is in contact with high-salinity water.

In order to confirm if low-salinity post-treatment water has an effect on gel performance, three salinities were selected (i.e., 10,000, 15,000, 20,000 ppm). A comparison was made between no change in chase water salinity (i.e., NC run) versus runs where low-salinity post-treatment water (i.e., 2000-ppm salinity) is injected (i.e., LSWFA runs). Alotaibi et al. (2010) considered that the brine salinity between 500 to 5,000 ppm are considered as low-salinity water floods. Table 14 and Figure 12 showed the effects of low-salinity post-treatment water on the results. The highest incremental oil recovery was obtained when the initial salinity of the system was 15,000-ppm.

Table 14. Effect of low-salinity chase water floods with UVM model.

Initial sal_Chase water sal, ppm	RF, %	Cum. oil, MM bbls	Initial sal_Chase water sal, ppm	RF, %	Cum. oil, MM bbls	Incr. oil, MM bbls
10,000_10,000 (NC)	23.68	6.30	10,000_2,000 (LSWFA)	24.97	6.64	0.34
15,000_15,000 (NC)	22.45	5.97	15,000_2,000 (LSWFA)	24.37	6.49	0.52
20,000_20,000 (NC)	21.90	5.83	20,000_2,000 (LSWFA)	23.60	6.28	0.45

5.3.3. Hardness (Divalent Cations). The degradation of polymer and/or gel are caused by three ways: mechanical, biological, and chemical (Green and Willhite, 1998; Sheng, 2011). HPAM polymer is relatively resistance to bacterial attack; however, it degraded mechanically and chemically that would affect the gelation process.

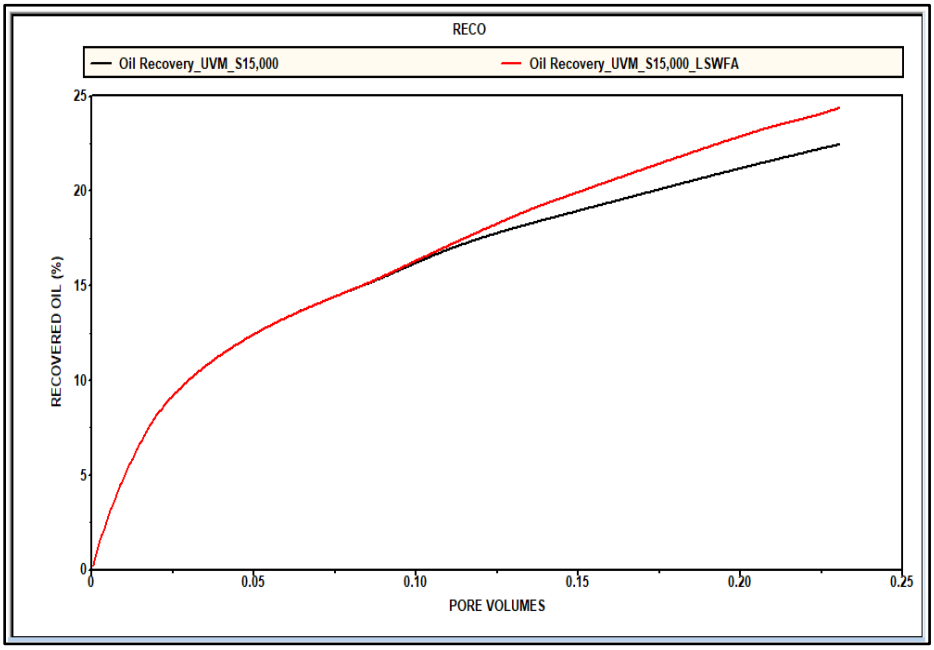

Figure 12. Comparison of oil recovery factor for 15,000-ppm salinity system with UVM model between initial run (NC, black curve) and low-salinity chase water floods (LSWFA, red curve).

The chemical degradation is triggered by the presence of monovalent and divalent cations. The viscosity of polymer and the strength of formed gel are highly affected by the presence of the monovalent (i.e., Na^{+} and K^{+}) and divalent (i.e., Ca^{++} and Mg^{++}) cations in the formation water, as the negative carboxyl groups in HPAM interact strongly with these cations (Sheng, 2011). Furthermore, Ca^{++} has more detrimental effect than Mg^{++}, and the divalent cations have more effect than monovalent cations. The presence of the divalent

cations causes the polymer chain to contract to its minimum size (Dang et al., 2015). The presence of the divalent cations could jeopardize the efficiency of the gel treatment, by precipitating of the polymer solution (Chauveteau and Sorbie, 1991; Mohammadi and Jerauld, 2012). Therefore, the presence of these cations in the mixing solution will shields the negative charge on the polymer chain and the repulsive forces will reduce.

Two models were compared: the first model with no hardness and the second model with 2,000-ppm hardness, both model with 10,000-ppm salinity and UVM rheology. The presence of divalent cations lower the recovery factor (Table 15) and lower the strength of the formed gel by increasing the precipitation of polymer, which reduces the blocking efficiency of in-situ gelation system (Figure 13).

5.3.4. Low-Salinity Post-Treatment Water Flooding In The Presence Of Hardness. The previous model with 2000-ppm hardness was run again; however, in the current model, low-salinity chase water floods was injected. The effect of the presence of divalent cations was reversed and the recovery factor was improved with low-salinity post-treatment water injection (Table 16). Figure 14 showed the improvement in recovery factor when low-salinity post-treatment water (i.e., LSWFA) was injected in the presence of hardness (green curve in Figure 14).

Table 15. Effect of the presence of hardness.

Salinity, ppm	Hardness, ppm	RF, %	Cumulative Oil, MM bbls	Reduction in cum. oil due to the presence of hardness, MM bbls
10,000	0	23.68	6.30	
10,000	2,000	22.41	5.96	0.34

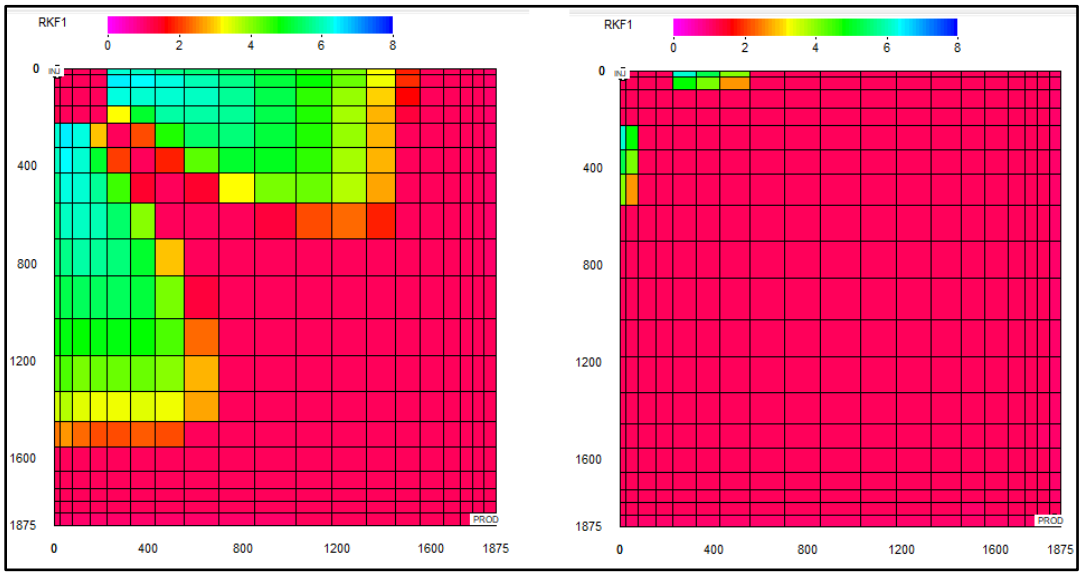

Figure 13. Comparison of permeability reduction between two models: 0-ppm hardness (left) and 2,000 ppm hardness (right) (both models have 10,000-ppm salinity and UVM rheology).

Table 16. Effect of low-salinity water floods in the presence of hardness.

Initial salinity_Chase water salinity, ppm	Hardness, ppm	RF, %	Cumulative Oil, MM bbls	Incremental oil due to low-salinity chase water floods, MM bbls
10,000_10,000	0	23.68	6.30	
10,000_10,000	2,000	22.41	5.96	
10,000_2,000 (LSW)	2,000	22.98	6.11	0.15

5.4. EFFECT OF INJECTION SCHEMES

The combination injection of the polymer and the gelant solutions are considered an important method to evaluate the effectiveness of the gel treatment. As mentioned previously, three injection schemes were investigated (Tables 3 to 5). The purpose of this section is to determine which injection sequence has a better EOR performance. Table 17 summarizes the results of these schemes.

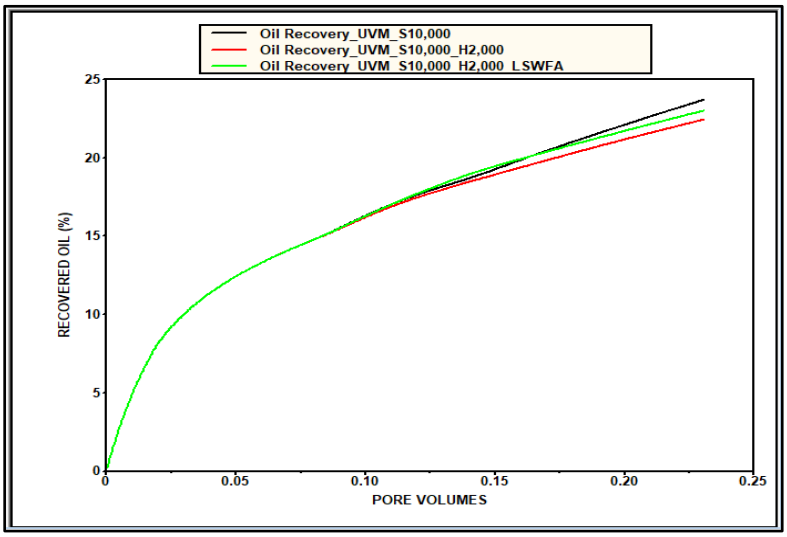

Figure 14. Comparison of oil recovery factor between 0-ppm hardness (black), 2,000-ppm hardness (red), and 2,000-ppm hardness with low-salinity chase water floods (green) (three models with 10,000-ppm salinity and UVM rheology).

The results showed that the injection of polymer solution before or after gel treatment yielded higher results. Gao and Burchfield (1995) conducted several numerical simulation models to simulate the combination injection of the polymer with the gel. They concluded that the injection of the polymer after the gel treatment caused an increase in permeability reduction in the thief zones due to the reaction of polymer with unreacted crosslinkers in the formation. However, in this study, the injection of the polymer solution before gel treatment yielded higher results, which could be attributed to the difference in oil viscosity between our study (i.e., 6 cp) and their study (i.e., 3 cp). Thus, in our study, the injection of the polymer solution before gel treatment will lower the mobility ratio and enhance the performance of the gel treatment. The salinity of these models was 10,000-ppm with UVM rheology behavior. Figure 15 shows a comparison of the gel treatment in layer 3 (thief zone) between the injection schemes 3 and 1. Consequently, the injection scheme 3 is the best scenario.

In order to confirm the efficiency of these schemes with prolonged post-treatment water injection, same schemes that shown in Table 17 were considered; however, the total injected pore volumes were 0.46 instead of 0.23. The purpose of these runs were to evaluate the necessity of injection of the polymer solution with the gel treatment. The results showed that the ultimate oil recoveries were almost the same in the injection schemes 1 and 3, while in the injection scheme 2 the recovery factor was lower compared to injection schemes 1 and 3. This behavior could be attributed to the production of the polymer solution and the gel from the production well due to the prolonged injection of post-treatment water. Table 18 and Figure 16 show these results. Thus, the injection of polymer solution with the gel treatment is not always a better option, especially with the prolonged post-treatment water injection.

Table 17. Comparison of the recovery factor and cumulative oil for different injection schemes.

Scheme	Sequence of injection	Injected PV	RF, %	Cum. Oil, MM bbls
1	Water_Gel_Water	0.23	23.68	6.30
2	Water_Gel_Polymer_Water	0.23	23.93	6.37
3	Water_Polymer_Gel_Water	0.23	24.41	6.50

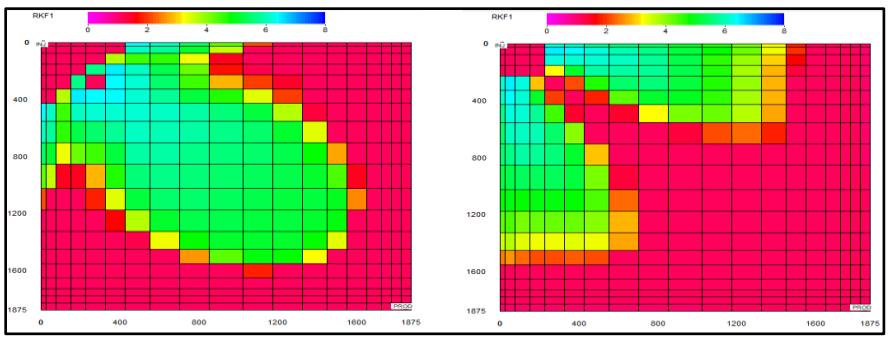

Figure 15. Comparison of RRF in layer 3 between scheme 3 (left) and scheme 1 (right).

Table 18. Comparison of the recovery factor and cumulative oil for different injection schemes with prolonged post-treatment water injection.

Scheme	Sequence of injection	Injected PV	RF, %	Cum. Oil, MM bbls
1	Water_Gel_Water	0.46	35.12	9.35
2	Water_Gel_Polymer_Water	0.46	32.83	8.74
3	Water_Polymer_Gel_Water	0.46	35.10	9.34

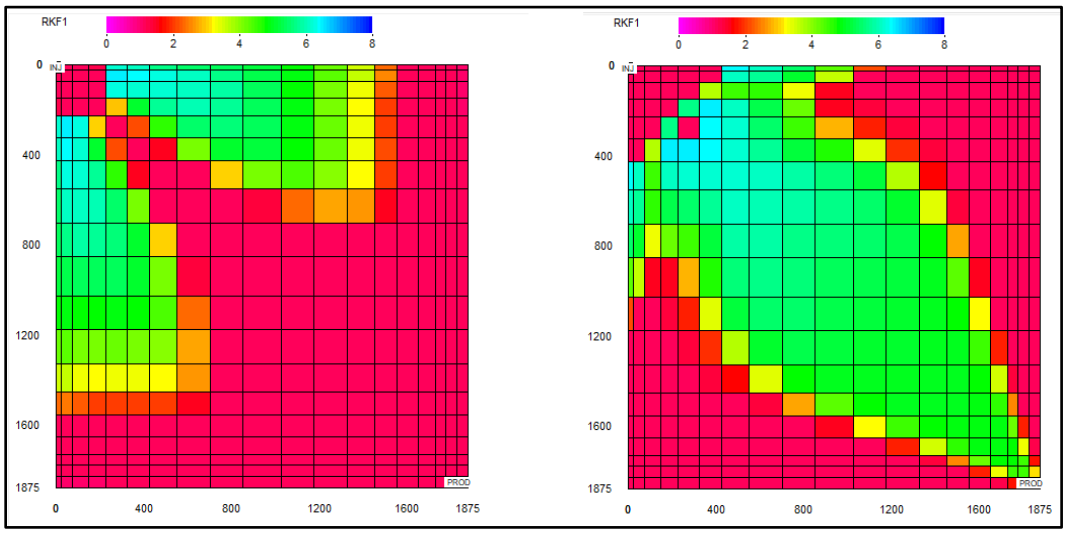

Figure 16. Comparison of permeability reduction in layer 4 between the injection scheme 1 (left) and the injection scheme 3 (right).

5.5. EFFECT OF CATION EXCHANGE CAPACITY (CEC)

If there is resident clays in the reservoir, there will be a competition for the crosslinkers (e.g., chromium) between those clays and HPAM polymer solution, which would affect and slow down the gelation process (Garver et al., 1989). The polymer solution requires the crosslinkers to form gel, while the clay tries to remove those crosslinkers from the gelant solution. Garver et al. (1989) showed that the retention of the

chromium was found to be high and on the order of the cation exchange capacity (CEC) of the clays in the sandstone. Thus, increasing CEC means that there is a high content of the clay in the reservoir. In addition, increasing the clay would increase the polymer retention (Sorbie, 1991); thus, the presence of the clay would have dual effects on the removal of the crosslinker from the gelant solution and the retention of the polymer solution. The objective of this section is to model the competition for chromium that exist between HPAM polymer solution and the clay. The default model (i.e., no clay) was compared with two models. The first model contains 0.5 meq/ml of PV CEC, while the second model contains 1.0 meq/ml PV CEC. Table 19 showed that the oil recovery factor and incremental oil were lower with higher values of CEC. The results proves the importance of determining the CEC value experimentally before the injection of the gelant solution, especially if the reservoir contains clays. The salinity of these models was 10,000-ppm with UVM rheology. The right-hand side of Figure 17 proves that when the CEC was 1.0 meq/ml, the crosslinker was removed from the gelant solution. Thus, no gel was formed and the treatment was a polymer flooding, which shows the devastating effect of the presence of the clays on the gelation process. Garver et al. (1989) attributed that behavior to the decrease of chromium concentration due to the reactions with the clays. Thus, if the resident clays in the formation was high, it would be better to increase the reaction rate between the reactants by lowering the reducing agent (i.e., thiourea) concentration. Consequently, a faster reaction would make the sodium dichromate to produce more trivalent chromium that would crosslink faster with the HPAM polymer solution to form gel. Therefore, the rate of crosslinking between the HPAM polymer solution and the Cr(III) will be faster than the rate of removal of the Cr(III) by the resident clays in the formation.

To confirm this hypothesis, a comparison was made between two models that have same value of CEC (i.e, 1.0 meq/ml) with different reaction rate. Table 20 showed the improvement that would occurred by increasing the rate of reaction compared to slow reaction rate. The right hand side of Figures 17 and 18 are the same, while the left-hand side of Figure 18 showed the permeability reduction in layer 4 after implementing higher-reaction rate in that model. Thus, a faster reaction rate implicitly means that we would have a high concentration of crosslinkers. Consequently, a gelation process would take place between the polymer solution and the crosslinker to form gel even in the presence of clay.

Table 19. Comparison of RF and incr. oil at different values of CEC.

Run	RF, %	Cum. oil, MM bbls
UVM_0 CEC (no clay)	23.68	6.30
UVM_0.5 CEC	23.08	6.14
UVM_1.0 CEC	22.80	6.07

Table 20. Comparison of RF and inc. oil at same CEC with different rate of reaction.

Run	RF, %	Cum. oil, MM STB
UVM_1.0 CEC_Low Reaction Rate	22.80	6.07
UVM_1.0 CEC_High Reaction Rate	23.14	6.16

5.6. EFFECT OF WETTABILITY

The reservoir wettability could range from water-wet conditions to oil-wet conditions; however, mixed or intermediate wettability conditions could be exist. The

reservoir wettability affects capillary pressure, relative permeability curves, and distribution and location of the fluids inside the pores (Ahmed, 2001).

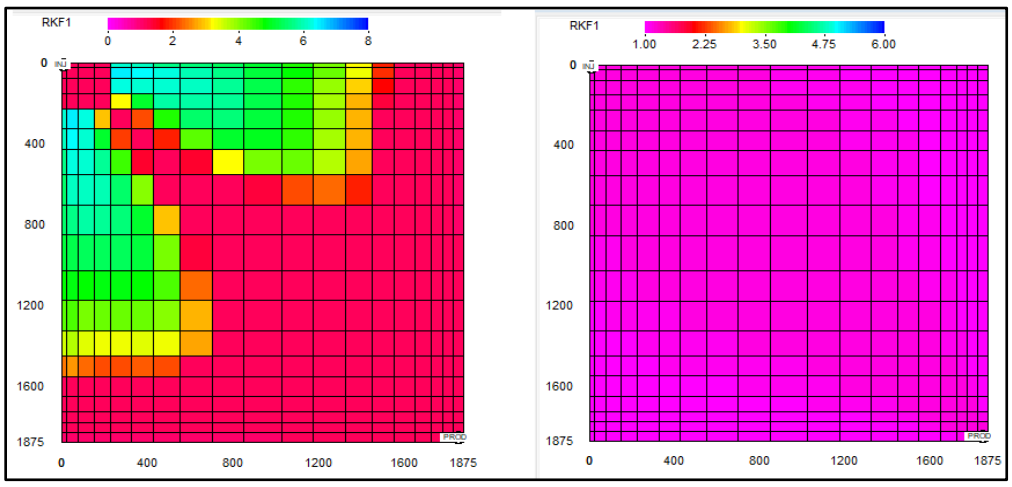

Figure 17. Comparison of the permeability reduction in layer 4 between model with 0 CEC (left) and model with 1.0 CEC (right).

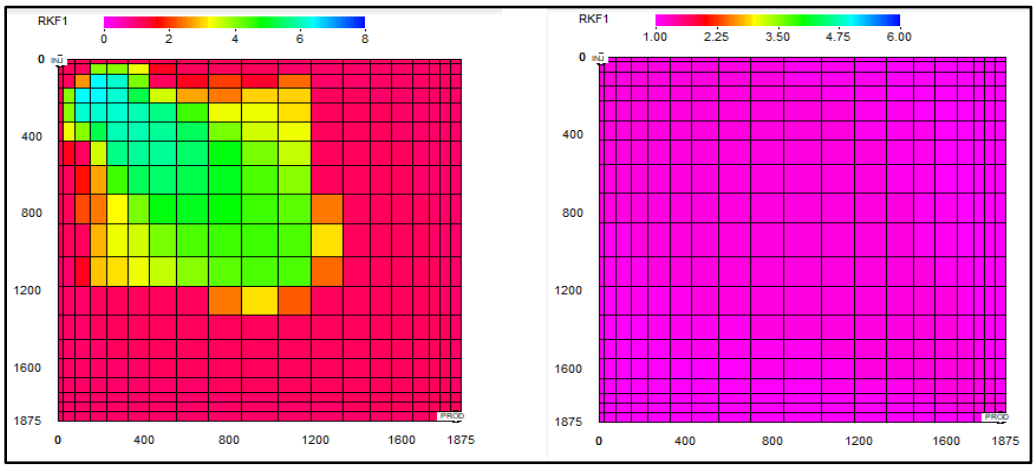

Figure 18. Comparison of water residual resistance factor in layer 4 between high-reaction rate (left) and low-reaction rate (right) (both models with 1.0 meq/ml CEC).

Wettability conditions of a reservoir determine which fluid is preferentially wetting the rock surfaces. Thus, in water-wet cores, the oil is located in the center of the pores,

while water surrounds oil and cover the grain surface; therefore, it is easier to recover the oil when the reservoir wettability is a water-wet. In addition, wettability affects the capillary desaturation curve (CDC). Figure 19 shows the typical CDC, which shows that high capillary number is required to mobilize wetting phase than non-wetting phase.

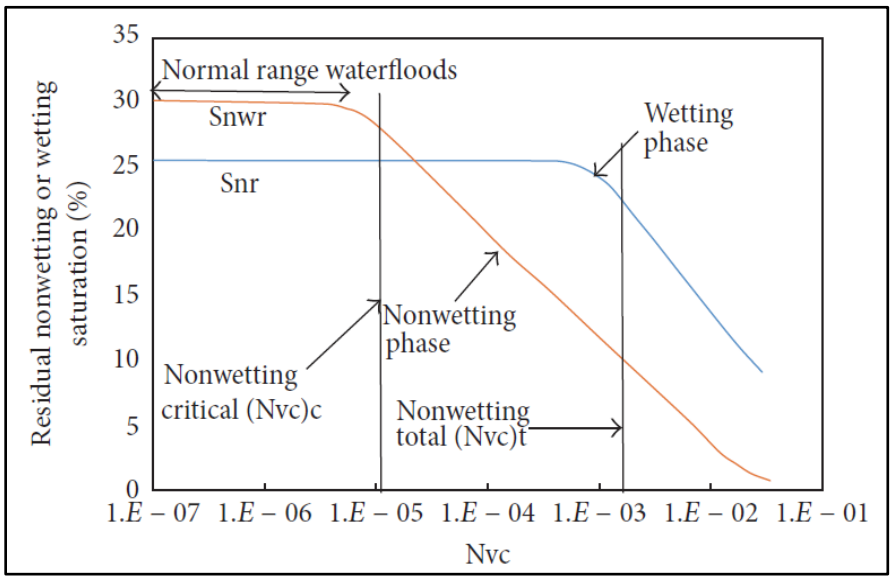

Figure 19. Typical capillary desaturation curve (CDC) and the effect of wettability (Green and Willhite, 1998).

Shen et al. (2013 and 2014) investigated the effects of temperature and wettability on the gel treatment. The results showed that the water-oil ratio increased rapidly in an oil-wet system compared to water-wet system. The results also showed that the gel is distributed more in the oil-wet conditions compared to the water-wet conditions. However, the authors did not report the effect of the wettability due to the gel treatment on the low-permeability layers. Thus, to investigate the importance of reservoir wettability on the performance of the gel treatment and the damage that could occur to low-permeability

layers, especially those layers that are adjacent to the thief zones, two scenarios with water-wet conditions and oil-wet conditions were modeled. Both models with 10,000-ppm salinity and UVM rheology. Table 21 shows that the gel performed better and yielded higher recovery factor with water-wet condition. The right-hand side of Figure 20 showed that a damage was occurred in low-permeability layer (layer 2) when the reservoir rock was oil-wet conditions. Moreover, the right-hand side of Figure 21 showed that the relative permeability of water decreased when the reservoir rock was oil-wet conditions. Thus, if the reservoir wettability is an oil-wet, the gelant would penetrated and the gel would formed in the low-permeability layer.

Table 21. Comparison of RF and incremental oil between oil-wet and water-wet.

Run	RF, %	Cum. Oil, MM STB
UVM_Water wet	23.68	6.30
UVM_Oil wet	21.88	5.88

5.7. EFFECT OF GRAVITY SEGREGATION AND DIP ANGLE OF THE MODEL

There are two types of gravity segregation: gravity underride (when the displacing fluid density is higher than the displaced fluid density), and gravity override (when the displacing fluid density is lower than the displaced fluid density). Increasing the density difference would increase the gravity segregation between the fluids and would decrease the vertical sweep efficiency. In addition, the gravity segregation is more pronounced with a thick reservoir and in the existence of dip angle. In this study, a gravity underride would

occur since the density difference between water and oil is relatively high (i.e., $\rho_w = 62.4\ lb/ft^3$ and $\rho_o = 52.99\ lb/ft^3$). In addition, the gravity difference would be more pronounced because the low-permeability layers are thicker than the thief zones.

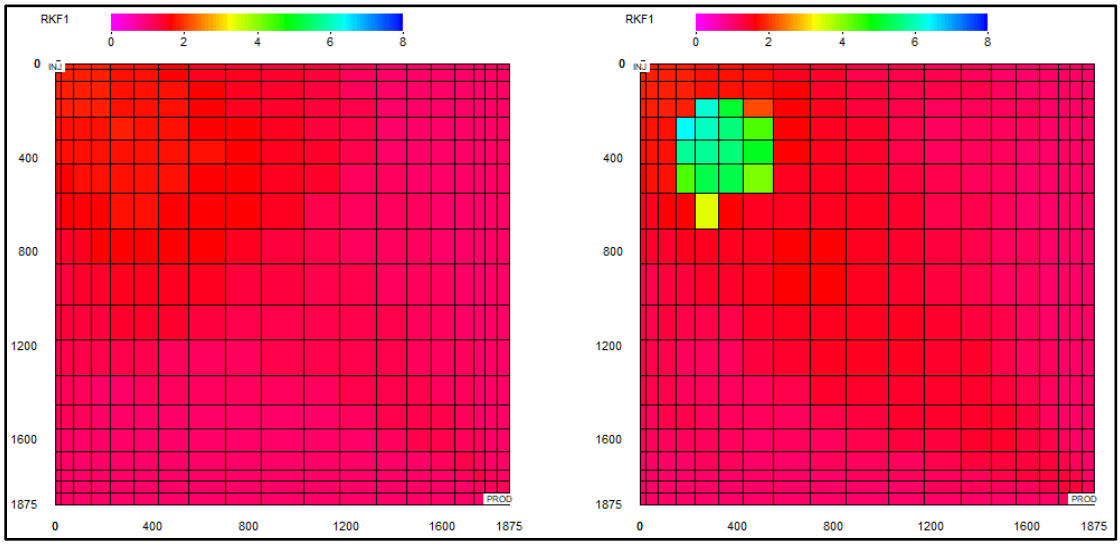

Figure 20. Comparison of permeability reduction in layer 2 between oil-wet (right) and water-wet (left).

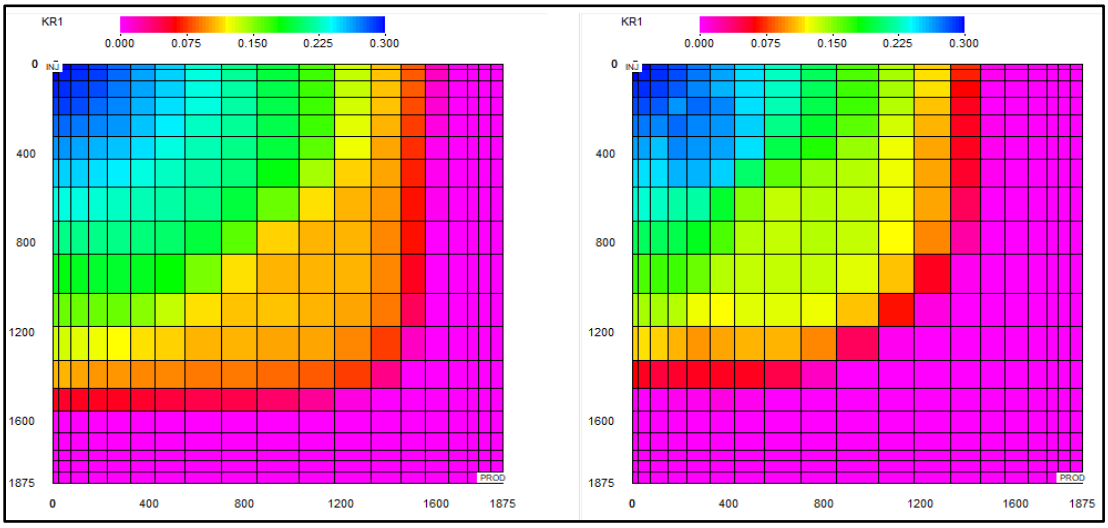

Figure 21. Comparison of water relative permeability in layer 2 between oil-wet (right) and water-wet (left).

The dip angles are classified according to the slope of the reservoir. If the slope of the formation was from the injector to the producer (i.e., down dip), a “positive” dip angle would occurred, which would assisted of displacing more oil by the water after the treatment (i.e., it is easier for the displacing fluid to move downward from the injector to the producer and sweep more oil). While if the slope of the model was from the producer to the injector (i.e., up dip), a “negative” dip angle would occurred. In this case, the water will face resistance by the gravity forces and it would be harder to flow upward from the injector to the producer and displace oil; thus, lowering the sweep efficiency. To clarify these concepts, the default model with “no dip” angle was compared with two models that have “positive” and “negative” dip angles. Table 22 shows the difference in recovery factor between these three models. While Figure 22 shows a comparison of water saturation between “positive” dip angle (left) and “negative” dip angle (right). It is clear that with the “positive” dip angle, of the water would flow easier and displace more oil from the low-permeability layer (layer 5) compared to “negative” dip angle. Figure 23 shows a comparison of water residual resistance factor in layer 4 between these models. Apparently, the blocking efficiency of gelant solution was increased when the dip angle was “positive”.

Table 22. Comparison of recovery factor and incremental oil between “no, positive, and negative” dip angle models.

Scenario	RF, %	Cum. oil, MM bbls
UVM_No Dip Angle	23.68	6.30
UVM_Positive Dip Angle	24.06	6.40
UVM_Negative Dip Angle	23.53	6.26

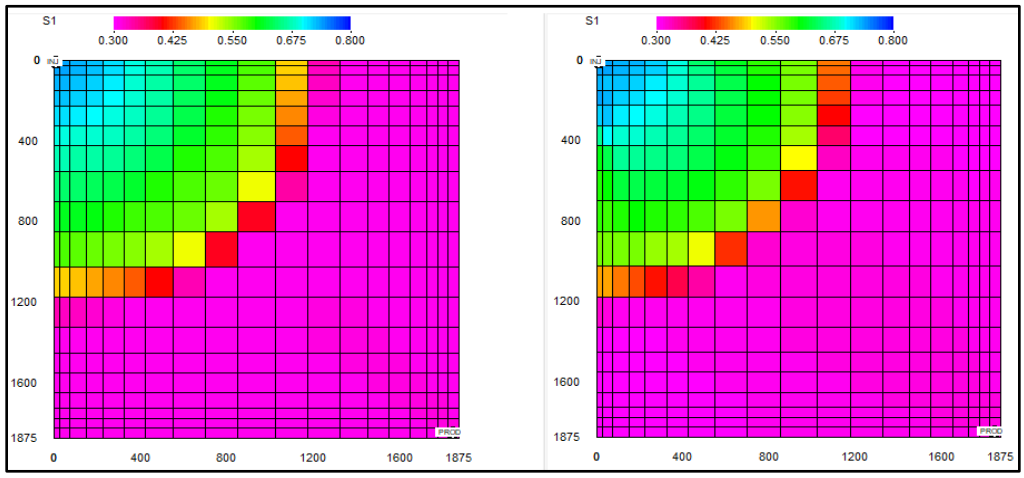

Figure 22. Comparison of water saturation in layer 5 between "positive" (left) and "negative" dip angle (right).

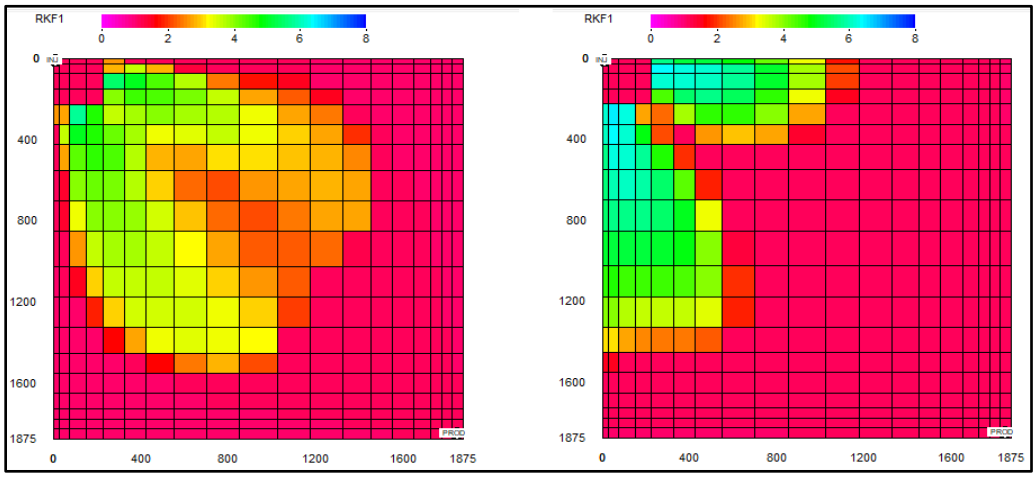

Figure 23. Comparison of water residual resistance factor in layer 4 between positive (left) and negative dip angle (right).

5.8. EFFECT OF MOBILITY RATIO

In general, the mobility λ of any fluid is defined as the ratio of the effective permeability of a fluid to the viscosity of that fluid, i.e.:

$$\lambda_o = \frac{k_o}{\mu_o} = \frac{kk_{ro}}{\mu_o} \qquad (22)$$

$$\lambda_w = \frac{k_w}{\mu_w} = \frac{kk_{rw}}{\mu_w} \quad (23)$$

where

λ_o, λ_w = Mobility of oil and water, respectively.

k_o, k_w = Effective permeability to oil and water, respectively.

μ_o, μ_w = Viscosity of oil and water, respectively.

k_{ro}, k_{rw}= End-point relative permeability to oil and water, respectively.

The mobility ratio (M) is defined as the mobility of the *displacing fluid* (e.g., water) to the mobility of the *displaced fluid* (e.g., oil) (Ahmed 2001):

$$M = \frac{\lambda_{displacing}}{\lambda_{displaced}} \quad (24)$$

If the oil viscosity was low and there was no heterogeneity in the reservoir, then water floods would be the best and economic option of producing oil. Thus, the heterogeneity of the reservoir and the viscosity of the crude oil are considered the most important factors that determine the success or the failure of any water-flooding project. Areal and vertical sweep efficiencies are highly influenced by the mobility ratio (M) among other factors. In this model, the mobility ratio is the endpoint mobility ratio. It means that the relative permeability of water and oil were taken to be at the initial saturation of the water and residual saturation of the oil, respectively. Thus, the mobility ratio is:

$$M = \frac{krw@_{sor}}{kro@_{swi}} \frac{\mu_o}{\mu_w} \quad (25)$$

Therefore, three endpoint mobility ratios were selected to investigate their roles on the gel treatment. Highest oil viscosity that considered was 24 cp, while the lowest oil viscosity was 6 cp (base value). Thus, increasing the mobility ratio will cause displacement instabilities and affects both the areal and the vertical sweep efficiencies. Consequently,

the water channeling will exacerbate and cause an earlier water breakthrough, which would cause a decrease in the incremental oil and the oil recovery. The results that are presented in Table 23 showed that the oil recovery factor and the cumulative oil are decreased with the increasing of the mobility ratio; however, the incremental oil was higher in case of high mobility ratio (i.e., 12) compared to lower mobility ratio (i.e., 6).

Table 23. Comparison of recovery factor and incremental oil between different values of mobility ratio.

			RF, %		Cumulative oil, MM bbls		Incremental oil, MM bbls
μ_w, cp	μ_o, cp	M	WF	Gel	WF	Gel	
0.86	3.0	1.5	21.75	23.68	5.79	6.30	0.51
0.86	12.0	6.0	18.90	19.60	5.03	5.21	0.18
0.86	24.0	12.0	15.30	16.60	4.07	4.42	0.35

To reverse the poor performance of gel treatment associated with high mobility ratio, a 0.1 PV of the polymer was injected after gel immediately. In these runs, dual actions of plugging thief zone (by gel) and increasing the viscosity of the injected water (by polymer) are took place. Table 24 showed the enhancement that was occurred when a 0.1 PV of the polymer solution was injected after the gel treatment. In this table, the lower mobility ratio (i.e., 6) was affected more by the injection of the polymer solution after the gel treatment compared to higher mobility ratio (i.e., 12). The left- and the right-hand sides of Figure 24 showed a comparison of water viscosity in layer 5 between gel injection only and gel injection followed by 0.1 PV of polymer, for 6.0 mobility ratio.

Table 24. Comparison of recovery factor and incremental oil between gel treatment only and gel treatment followed by 0.1 PV polymer for two values of mobility ratios.

	RF, %			Cumulative oil, MM bbls			Incremental oil, MM bbls	
M	WF	Gel only	Gel then 0.1 PV Polymer	WF	Gel only	Gel then 0.1 PV polymer	Gel	Gel-0.1 PV Polymer
6.0	18.90	19.60	22.24	5.03	5.21	5.92	0.18	0.89
12.0	15.30	16.60	17.62	4.07	4.42	4.69	0.35	0.62

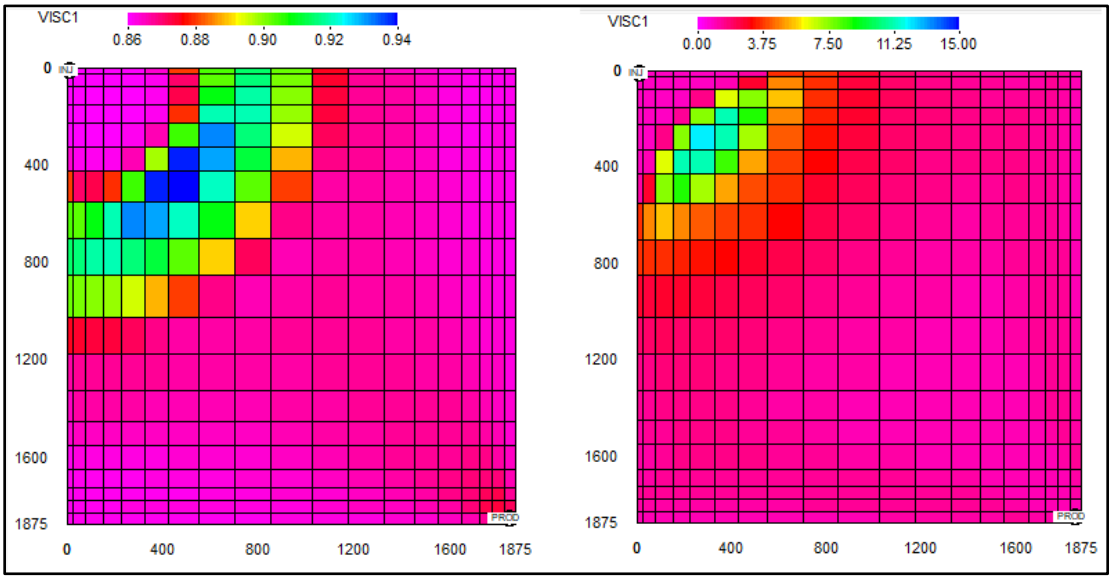

Figure 24. Comparison of water viscosity in layer 5 between gel treatment only (left) and gel treatment followed by 0.1 PV polymer flooding (right) (both cases with mobility ratio = 6.0).

Therefore, these runs strongly suggested that when an unfavorable mobility ratio existed, a mobility control fluid (i.e., polymer) has to be injected to modify the mobility ratio.

5.9. EFFECT OF THE SKIN FACTOR IN THE INJECTION WELL

Skin factor is defined as the restriction to the flow (i.e., a positive skin factor) due to the drilling and the completion operations, or an enhancement of the flow (i.e., an negative skin factor) due to the acidizing process. Positive skin factor causes an additional pressure drop near-wellbore region due to the lowering of the permeability in this region. In addition, a damage in near-wellbore region of the injection well could occur due to prolonged injection of materials that plug the formation and reduce the permeability around wellbore. Thus, the default model with zero skin factor (i.e., no enhancement or damage) was compared with two models having negative skin factor (i.e., stimulated well) and positive skin factor (i.e., damaged well). Table 25 shows a comparison of oil recovery and cumulative oil for these three models. In these models, there is no big differences in the results regarding the effect of skin factor.

Table 25. Comparison of recovery factor and incremental oil between "zero, positive, and negative" skin factor models.

Scenario	Injected PV	RF, %	Cum. oil, MM bbls
UVM_Zero Skin Factor	0.23	23.68	6.30
UVM_Positive Skin Factor	0.23	23.61	6.28
UVM_Negative Skin Factor	0.23	23.67	6.29

To investigate the effect of another factor that could affect the results in the presence of negative or positive skin factor, two scenarios were modeled and compared; however, higher injection rate was implemented. The injection rate was 2,500 bbl/day

instead of 1,070 bbl/day (i.e., the default value). The results were presented in Table 26, which shows a difference in oil recovery and cumulative oil between negative and positive skin factor. Thus, changing the injection rate would have tremendous effect on the performance of gel treatment in cases of stimulated or damaged wells. In Figure 25, the water is invaded more in the low-permeability layer (e.g., layer 1) with negative skin factor (i.e., stimulated well) compared to the positive skin factor (i.e., damaged well).

Table 26. RF and increm. oil between "zero, positive, and negative" skin factor models.

Scenario	Injected PV	RF, %	Cum. oil, MM bbls
UVM_Positive Skin Factor	0.54	37.54	9.99
UVM_Negative Skin Factor	0.54	36.25	9.64

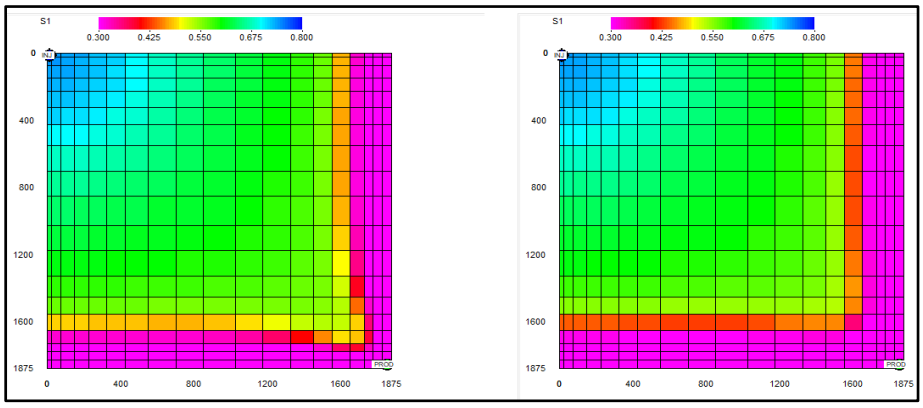

Figure 25. Water saturation in layer 1 for negative (left) and positive skin factors (right).

Thus, the injection rate has big impacts on the results, especially when there is a damage or an improvement in permeability around the wellbore because it would prevent or assist the placement of the gelant solution.

6. CONCLUSIONS

1. Regardless of the salinity, it is important to consider shear-thinning and shear-thickening behavior together (UVM model).
2. The higher the salinity of the injected brine and/or the brine of the reservoir, the lower the recovery factor.
3. Low-salinity post-treatment water greatly improve the sweep efficiency, especially when the initial reservoir salinity was too high.
4. The presence of divalent cations (hardness) in the brine lowers the recovery factor; however, low-salinity post-treatment water improves the recovery in the presence of hardness.
5. With the suggested pore volume of the post-treatment water (i.e., 0.16 PV); the best injection scheme was the injection of polymer solution before the gelant.
6. By increasing the pore volume of the post-treatment water to 0.39 PV, the injection of polymer solution with the gel treatment is not always the best option.
7. The presence of the clays in the reservoir affected the crosslinking process by removal of the crosslinkers from the gelant solution. Thus, no gel will be formed in the presence of the clay.
8. If there are clays in the reservoir, the reaction rate between the crosslinkers and polymer solution to form gel must be high enough to overcome the removal of the crosslinkers by the clay.
9. If the treatment was applied in a reservoir with water-wet condition, it would yielded higher recovery factor and higher incremental oil compared to oil-wet conditions.

10. The dip angle has a great impact on the treatment. Thus, higher recovery factor was yielded if the dip angle was from the injector to the producer (i.e., positive dip angle).
11. The higher the mobility ratio, the lower the recovery factor and incremental oil. However, injection of polymer solution after gel treatment improves the performance of gel treatment in case of unfavorable mobility ratio.
12. The negative or the positive skin factor in the injection well would increase or decrease the recovery factor after the gel treatment if a high injection rate was used (e.g., 2,500 bbl/day) compared to low injection rate (e.g., 1070 bbl/day).

NOMENCLATURE

μ_{app} = Apparent viscosity of the polymer solution, cp.

μ_∞ = Polymer viscosity at infinite shear rate, which is equal to water viscosity, cp.

μ_p° = Polymer viscosity at very low (approximately zero) shear rate; function of polymer concentration & effective salinity, cp.

$\dot{\gamma_{eff}}$ = In-situ shear rate, sec^{-1}.

$\dot{\gamma}_{1/2}$ = Shear rate at which apparent viscosity is the average of μ_p° and μ_∞ and is a function of polymer concentration(C_p), sec^{-1}.

P_α = Fitting parameter, $dimensionless$.

μ_w = Brine viscosity, cp.

$AP_1,\ AP_2,\ AP_3$ = Shear thinning viscosity model parameters, $(wt\%)^{-1},\ (wt\%)^{-2},\ (wt\%)^{-3}$.

C_p = Polymer concentration in water phase, $wt\%$.

S_p = Slope of specific viscosity vs. salinity plot, $dimensionless$.

C_{SEP} = Effective salinity, meq/ml.

C_{anion} = Total anions conc., meq/ml.

C_{cation}^{++} = Divalent cations concentration, meq/ml.

C_w = Water concentration.

β_p = Input parameter measured in the laboratory, $dimensionless$.

n_1 = Shear-thinning viscosity model parameters, $dimensionless$.

λ_1 = Polymer relaxation time.

β_1, β_2 = Shear-thinning viscosity model parameters,sec, $(wt\%)^{-1}$.

υ_w = Darcy velocity of the polymer solution.

k = Permeability, md.

k_{rw} = Water relative permeability, $dimensionless$.

ϕ = Porosity, $fraction$.

s_w = Water saturation, $fraction$.

λ_2 = Shear-thickening viscosity model parameter, sec.

n_2 = Shear-thickening viscosity model parameter, $dimensionless$.

τ_r = Rotational relaxation time.

τ_o, τ_1 = Shear-thickening viscosity model parameters,$dimensionless$, $(wt\%)^{-1}$.

AP_{11}, AP_{22} = Shear-thickening viscosity model parameters,$dimensionless$, $(wt\%)^{-1}$

$C_p^{\wedge}$ = Adsorbed polymer concentration, $wt\%$.

b = Polymer adsorption parameter, $\frac{volume\ of\ water}{wt\%\ polymer}$.

a_1 = Polymer adsorption parameter, $dimensionless$.

a_2 = Polymer adsorption parameter, ml/meq.

a/b = Maximum level of adsorbed polymer.

b_{rk} = Permeability-reduction parameter for polymer, $\frac{volume\ of\ polymer}{wt\%\ polymer}$.

C_{rk} = Permeability-reduction parameter for polymer, $\sqrt{darcy}\ (100g/g)^{-1/3}$.

A_{g1} = Flory-Huggins parameters for gel viscosity, $cp\ ppm^{-1}$.

A_{g2} = Flory-Huggins parameters for gel viscosity, $cp\ ppm^{-2}$.

C_g = Gel concentration, $wt\%$.

$C_g^{\wedge}$ = Adsorbed gel concentration, $wt\%$.

a_g = Gel adsorption parameter, $\frac{volume\ of\ water}{ppm\ gel}$.

bg = Gel adsorption parameter, $\frac{volume\ of\ water}{ppm\ gel}$.

A_{gk} = Permeability-reduction parameter for gel, $dimensionless$.

B_{gk} = Permeability-reduction parameter for gel, $dimensionless$.

C_{rg} = Permeability-reduction parameter for gel, $\sqrt{darcy}\ (wt\%)^{1/3}$.

R_{kmax} = Maximum residual resistance factor.

ACKNOWLEDGMENTS

The authors would like to acknowledge the Ministry of Oil of Iraq and the ExxonMobile Iraq (Training Technology & Scholars Program) for financial support. The authors also would like to acknowledge The University of Texas at Austin for allowing them to use UTGEL simulator.

REFERENCES

Achim, N., Alias, N.H., Ghazali, N.A. et al. 2015. Polymer Gelled Technology to Improve Sweep Efficiency in Enhanced Oil Recovery: A literature Review. *Advanced Materials Research* **1113**: 690-694. https://doi.org/10.4028/www.scientific.net/AMR.1113.690.

Ahmed, T. 2001. *Reservoir Engineering Handbook* 2nd Edition, Gulf Professional Publishing.

Ali, M. and Ben Mahmud, H. 2015. The Effects of Concentration and Salinity on Polymer Adsorption Isotherm at Sandstone Rock Surface. *Materials Sci & Eng* **78** (1). http://dx.doi.org/10.1088/1757-899X/78/1/012038.

Alotaibi, M.B., Azmy, R.M., and Nasr-El-Din, H.A. 2010. A Comprehensive EOR Study Using Low Salinity Water in Sandstone Reservoirs. Presented at the SPE Improved Oil Recovery, Tulsa. Oklahoma, USA. 24-28 April. SPE-129976-MS. https://doi.org/10.2118/129976-MS.

Aluhwal, O. 2008. *Simulation Study of Improving Oil Recovery by Polymer Flooding in a Malaysian Reservoir*. Master Thesis, Universiti Teknologi Malaysia. Kualampur, Malaysia (2008).

Asghari, K. 2002. Performance and Properties of KUSP1-BORIC Acid Gel System for Permeability Modification Purposes. *J Petrol Sci & Tech* **20** (9-10): 1141-1150. http://dx.doi.org/10.1081/LFT-120003702.

Bai, B., Wang, Q., Du, Y. et al. 2004. Factors Affecting In-Depth Gel Treatment for Reservoirs with Thick Heterogeneous oil Layers. Presented at the 55th Annual Technical Meeting, Calgary, Alberta, Canada, 8-10 June, PETSOC-2004-140. https://doi.org/10.2118/2004-140.

Bhaskar, R.K., Stinson, J.A., Willhite, G.P. et al. 1988. The Effect of Shear History on the Gelation of Polyacrylamide/ Chromium (VI) /Thiourea Solutions. *SPE Res Eng J* **3** (04): 1251-1256. SPE-17472-PA. https://doi.org/10.2118/17472-PA.

Brattekas, B., Graue, A., and Seright, R.S. 2016. Low-Salinity Chase Waterfloods Improve Performance of Cr (III)-Acetate Hydrolyzed Polyacrylamide Gel in Fractured Cores. *SPE Res Eval & Eng* **19** (02). SPE-173749-PA. https://doi.org/10.2118/173749-PA.

Broseta, D., Marquer, O., Alain, Z. et al. 2000. Shear Effect on Polyacrylamide/Chromium (III) Acetate Gelation. *SPE Res Eval & Eng* **3** (03): 204-208. SPE-64500-PA. https://doi.org/10.2118/64500-PA.

Caili, D., Qing, Y., and Fulin, Z. 2010. In-Depth Profile Control Technologies in China—A Review of the State of the Art. *Petrol Science & Technol* **28** (13): 1307-1315. https://doi.org/10.1080/10916460903419164.

Chauveteau, G. 1981. Molecular Interpretation of Several Different Properties of Flow of Coiled Polymer Solutions through Porous Media in Oil Recovery Conditions. Presented at the SPE 56th Annual Technical Conference and Exhibition, San Antonio, Texas, USA. 5-7 October. SPE-10060-MS. https://doi.org/10.2118/10060-MS.

Chauveteau, G. and Sorbie, K.S. 1991. Mobility Control by Polymers. In *Basic Concepts in Enhanced Oil Recovery Processes*, Critical Reports on Applied Chemistry Volume 33, Baviere, Chapter 2, 43. Essex, England: Elsevier Science Publishers LTD.

Chauveteau, G., Tabary, R., Renard, M. et al. 1999. Controlling In-Situ Gelation of Polyacrylamides by Zirconium for Water Shutoff. Presented at the SPE International Symposium on Oilfield Chemistry, Houston, Texas, USA. 16-19 February. SPE-50752-MS. https://doi.org/10.2118/50752-MS.

Dang, T.Q.C., Chen, Z., Nguyen, T.B.N. et al. 2015. Rheological Modeling and Numerical Simulation of HPAM Polymer Viscosity in Porous Media. *Energy Sources* **37** (20): 2189-2197. http://doi.org/10.1080/15567036.2011.624156.

Delshad, M., Kim, D.H., Magbagbeola, O.A. et al. 2008. Mechanistic Interpretation and Utilization of Viscoelastic Behavior of Polymer Solutions for Improved Polymer-Flood Efficiency. Presented at the 2008 SPE/DOE Improved Oil Recovery Symposium, Tulsa, Oklahoma, USA. 19-23 April. SPE-113620-MS. http://doi.org/10.2118/113620-MS.

Dong, H.Z., Fang, S.F., Wang, D.M. et al. 2008. Review of Practical Experience and Management by Polymer Flooding at Daqing. Presented at SPE/DOE Improved Oil Recovery Symposium, Tulsa, Oklahoma, USA. 19-23 April. SPE-114342-MS. https://doi.org/10.2118/114342-MS.

Gao, H.W. and Burchfield, T.E. 1995. Effects of Crossflow and Layer Permeability on the Effectiveness of Gel Treatment in Polymer Floods and Waterfloods. *SPE Res Eng* **10** (02): 129-135. SPE-25453-PA. https://doi.org/10.2118/25453-PA.

Garver, F. J., Sharma, M. M., and Pope, G. A. 1989. The Competition for Chromium between Xanthan Biopolymer and Resident Clays in Sandstones. Presented at the SPE Annual Technical Conference and Exhibition, San Antonio, Texas, USA. 8-11 October. SPE-19632-MS. https://doi.org/10.2118/SPE-19632-MS.

Goudarzi, A. 2015. *Modeling Conformance Control and Chemical EOR Processes Using Different Reservoir Simulators*. PhD dissertation, The University of Texas at Austin, Austin, Texas, USA (2015).

Green, D.W. and Willhite, G.P. 1998. *Enhanced Oil Recovery*, SPE Textbook Series **6**. Richardson, Texas, USA: SPE.

Han, M., Alshehri, A.J., Krinis, D. et al. 2014. State-of-the-Art of In-Depth Fluid Diversion Technology: Enhancing Reservoir Oil Recovery by Gel Treatments. Presented at the SPE Saudi Arabia Section/ ATSE, AL-Khober, Saudi Arabia, 21-24 April. SPE-172186-MS. https://doi.org/10.2118/172186-MS.

Hasan, S.F., Han, M., Zhou, X. et al. 2013. Study of Polyacrylamide/Cr(III) Hydrogels for Conformance Control in Injection Wells to Enhance Chemical Flooding Process. Presented at the SPE Saudi Arabia Section/ ATSE, AL-Khober, Saudi Arabia, 19-22 May. SPE-168069-MS. https://doi.org/10.2118/168069-MS.

Huang, C.G, Green, D.W., and Willhite, G.P. 1986. An Experimental Study of the In-Situ Gelation of Chromium (+3)/Polyacrylamide Polymer in Porous Media. *SPE Res Eng* **1** (06): 583-592. SPE-12638-PA. https://doi.org/10.2118/12638-PA.

Hubbard, S., Roberts, L.J., and Sorbie, K.S. 1988. Experimental and Theoretical Investigation of Time-Setting Polymer Gels in Porous Media. *SPE Res Eng* **03** (04): 1257-1267.SPE-14959-PA. https://doi.org/10.2118/14959-PA.

Huh, C. and Pope, G.A. 2008. Residual Oil Saturation from Polymer Floods: Laboratory Measurements and Theortical Interpretation. Presented at the SPE Improved Oil Recovery Symposium, Tulsa, Oklahoma, USA. 19-23 April. SPE-113417-MS. https://doi.org/10.2118/113417-MS.

Jia, H., Zhao, J.Z., Jin, F.Y. et al. 2012. New Insights into the Gelation Behavior of Polyethyleneimine Crosslinking Partially Hydrolyzed Polyacrylamide Gels. *Ind Eng Chem Res* **51** (38): 12155–12166. http://dx.doi.org/10.1021/ie301818f.

Jennings, R.R., Rogers, J.H., and West, T.J. 1970. Factors Influencing Mobility Control by Polymer Solutions. *J Pet Technol* **23** (03): 391-401. JPT-2867-PA. https://doi.org/10.2118/2867-PA.

Kim, H. S. 1995. *Simulation Study of Gel Conformance Treatments*. PhD dissertation, The University of Texas at Austin, Austin, Texas, USA (1995).

Lee, K.S. 2011. Performance of a Polymer Flood with Shear-Thinning Fluid in Heterogeneous Layered Systems with Crossflow. *Energies* **4** (8):1112-1128. http://dx.doi.org/10.3390/en4081112.

Lee, J.H., Shen, G.X., and Lee, K.S. 2013. Performance of Gel Treatments in Reservoirs with Multiscale Heterogeneity. *Journal of Chemistry* **2013**: 86-93. http://dx.doi.org/10.115/2013/416328.

Li, Z., and Delshad, M. 2014. Development of an Analytical Injectivity Model for Non-Newtonian Polymer Solutions. *SPE J.* **19** (3): 381-389. SPE-163672-PA. http://doi.org/10.2118/163672-PA.

Liu, Y., Bai, B., and shuler, P.J. 2006 Application and Development of Chemical-Based Conformance Control Treatments in China Oilfields. Presented at the SPE/DOE Symposium on Improved Oil Recovery, Tulsa, Oklahoma, USA. 22-26 April. SPE-99641-MS. https://doi.org/10.2118/99641-MS.

Liu, J. and Seright, R.S. 2001. Rheology of Gels Used For Conformance Control in Fractures. *SPE J.* **6** (02): 120-125. SPE-70810-PA. https://doi.org/10.2118/70810-PA.

Lotfollahi, M., Farajzadeh, R., Delshad, M., et al. 2016. Mechanistic Simulation of Polymer Injectivity in Field Tests. *SPE J.* **21** (4): 1178-1191. SPE-174665-PA. http://doi.org/10.2118/174665-PA.

Luo, H.S, Delshad, M., Li, Z.T. et al. 2015. Numerical simulation of the impact of polymer rheology on polymer injectivity using a multilevel local grid refinement method. *Petrol Science* **13** (01): 110-125. https://doi.org/10.1007/s12182-015-0066-1.

Manichand, R.N. and Seright, R. 2014. Field vs. Laboratory Polymer-Retention Values for a Polymer Flood in the Tambaredjo Field. *SPE Res Eval & Eng* **17** (03): 314-325. SPE-169027-PA. https://doi.org/10.2118/169027-PA.

Marty, L., Green, D.W., and Willhite, G.P. 1991. The Effect of Flow Rate on the In-Situ Gelation of a Chrome/Redox/Polyacrylamide System. *SPE Res Eng* **6** (02): 219-224. SPE-18504-PA. https://doi.org/10.2118/18504-PA.

McCool, C.S., Green, D.W., and Willhite, G.P. 1991. Permeability Reduction Mechanisms Involved in In-Situ Gelation of a Polyacrylamide/Chromium (VI)/Thiourea. *SPE Res Eng* **6** (01): 77-83. SPE-17333-PA. https://doi.org/10.2118/17333-PA.

Mohammadi, H. and Jerauld, G.R. 2012. Mechanistic Modeling of the Benefit of Combining Polymer with Low Salinity Water for Enhanced Oil Recovery. Presented at the Eighteenth SPE Improved Oil Recovery Symposium, Tulsa, Oklahoma, USA. 14-18 April. SPE-153161. https://doi.org/10.2118/153161-MS.

Moradi-Araghi, A and Doe, P.H. 1987. Hydrolysis and Precipitation of Polyacrylamides in Hard Brines at Elevated Temperatures. *SPERE J* **2** (02): 189-198. SPE-13033-PA. https://doi.org/10.2118/13033-PA.

Mungan, N. 1969. Rheology and Adsorption of Aqueous Polymer Solutions. *J Can Pet Technol* **8** (02): 45-50. PETSOC-69-02-01. PETSOC-69-02-01. http://dx.doi.org/10.2118/69-02-01.

Seright, R.S., Seheult, M., and Talashek, T. 2008. Injectivity Characteristics of EOR Polymers. *SPE Res Eval & Eng* **12** (05): 783-792. SPE-115142-PA. https://doi.org/10.2118/115142-PA.

Seright, R.S., Fan, T., Wavrik, K. E. et al. 2010. New Insights into Polymer Rheology in Porous Media. Presented at the 2010 SPE Improved Oil Recovery Symposium, Tulsa, Oklahoma, USA. 24-28 April. SPE-129200-MS. https://doi.org/10.2118/129200-MS.

Seright, R. S, Zhang, G., Akanni, O. et al. 2012. A Comparison of Polymer Flooding with In-Depth Profile Modification. *J Can Pet Technol* **51** (05): 393- 402. SPE-146087-PA. https://doi.org/10.2118/146087-PA.

Sharma, A., Delshad, M., Huh, C. et al. 2011. A Practical Method to Calculate Polymer Viscosity Accurately in Numerical Reservoir Simulators. Presented at the SPE Annual Technical Conference and Exhibition, Denver, Colorado, USA. 30 October-2 November. SPE-147239-MS. https://doi.org/10.2118/147239-MS.

Shen, G.X., Lee J.H., and Lee, K.S. 2013. The Effects of Wettability on Gel Performance in Layered Heterogeneous Reservoirs. *Applied Mechanics and Materials* **448-453**: 4028-4032. http://doi.org/10.4028/www.scientific.net/AMM.448-453.4028.

Shen, G.X., Lee J.H., and Lee, K.S. 2014. Influence of Temperature on Gel Treatment under Various Reservoir Wettability Conditions. Presented at the Offshore Technology Conference Asia. Kuala Lumpur, Malaysia, 25-28 March. OTC-24853-MS. https://doi.org/10.4043/24853-MS.

Sheng, J.J. 2011. *Modern Chemical Enhanced Oil Recovery: Theory and Practice*. Burlington, MA, USA: Gulf Professional Publishing.

Sheng, J. J. 2014. A Comprehensive Review of Alkaline-Surfactant-Polymer (ASP) Flooding. *Asia-Pac J Chem Eng* **9:** 471-489. http://dx.doi.org/10.1002/apj.1824.

Sorbie, K.S. 1991. *Polymer-Improved Oil Recovery*. Boca Raton, Florida, USA: CRC Press.

Sorbie, K. S., and Seright, R. S. 1992. Gel Placement in Heterogeneous Systems with Crossflow. Presented at the SPE/DOE Enhanced Oil Recovery Symposium, Tulsa, Oklahoma, USA. 22-24 April. SPE-24192-MS. https://doi.org/10.2118/24192-MS.

Sparlin, D.D. 1976. An Evaluation of the Polyacrylamides for Reducing Water Production. *J Pet Technol* **28** (08): 906-914. SPE-5610-PA. https://doi.org/10.2118/5610-PA.

Stavland, A., Kvanvik, B.A., and Lohne, A. 1994. Simulation Model for Predicting Placement of Gels. Presented at the SPE Annual Technical Conference and Exhibition. New Orleans, Louisiana, USA. 25-28 September. SPE-28600-MS. https://doi.org/10.2118/28600-MS.

Sydansk, R.D. 1990. A Newly Developed Chromium (III) Gel Technology. *SPE Res Eng* **5** (03): 346-352. https://doi.org/10.2118/19308-PA.

Terry, R.E., Huang, C.G., Green, D.W. et al. 1981. Correlation of Gelation Times for Polymer Solutions Used as Sweep Improvement Agents. *SPE J* **21** (02): 229-235. https://doi.org/10.2118/8419-PA.

Thurston, G. B., Ozon, P. M., and Pope, G. A. 1987. The Viscoelasticity and Gelation of Some Polyacrylamide and Xanthan Gum Solutions, Presented at the AICHE meeting.

Tu, T.N. and Wisup, B. 2011. Investigating the Effect of Polymer Gels Swelling Phenomenon under Reservoir Conditions on Polymer Conformance Control Process. Presented at the International Petroleum Technology Conference, Bangkok, Thailand, 15-17 November. IPTC-14673-MS. http://dx.doi.org/10.2523/14673-MS.

Urbissinova, T.S., Trivedi, J., and Kuru, E. 2010. Effect of Elasticity during Viscoelastic Polymer Flooding: A possible Mechanism of Increasing the Sweep Efficiency. *J Can Pet Technol* **49** (12): 49-56. SPE-133471-PA. https://doi.org/10.2118/133471-PA.

UTGEL User Guide, V.0l, 2011_2.

UTGEL Technical Manual, 2014.

Wang, D., Xia, H., Liu, Z. et al. 2001. Study of the Mechanism of Polymer Solution with Visco-Elastic Behavior Increasing Microscopic Oil Displacement Efficiency and the Forming of Steady 'Oil Threads' Flow Channels. Presented at the SPE Asia Pacific Oil and Gas Conference and Exhibition, Jakarta, Indonesia, 17-19 April. SPE-68723-MS. https://doi.org/10.2118/68723-MS.

Willhite, G.P., Green, D.W., Young, T.S. et al. 1986. Evaluation of Methods of Reducing Permeability in Porous Media by In-Situ Polymer Treatments. DOE/BC/10354-16.

Yuan, C. 2012. *Commercial Scale Simulations of Surfactant/Polymer Flooding.* PhD dissertation, University of Texas, Austin, Texas, USA (2012).

Zhang, L., Zheng, L., Pu, J. et al. 2016. Influence of Hydrolyzed Polyacrylamide (HPAM) Molecular Weight on the Cross-Linking Reaction of the HPAM/Cr3+ System and Transportation of the HPAM/Cr3+ System in Microfractures. *Energy Fuels* **30** (11): 9351-9361. http://doi.org/ 10.1021/acs.energyfuels.6b02230.

Zhang, L., Pu, C., Zheng, L. et al. 2015. Study and Application of Deep profile Control and Oil Displacement Technology in the Fractured Tight Oil Reservoir. *IFEESM* : 120-126. https://doi.org/10.2991/ifeesm-15.2015.25.

Zhu, D., Baojun, B., and Hou, J. 2017. Polymer Gel Systems for Water Management in High-Temperature Petroleum Reservoirs: A Chemical Review. *Energy Fuels* **31** (12): 13063-13087. https://doi.org/10.1021/acs.energyfuels.7b02897.

II. INVESTIGATING THE PROPAGATION OF THE COLLOIDAL DISPERSION GEL (CDG) IN THICK HETEROGENEOUS RESERVOIRS USING NUMERICAL SIMULATION

Tariq K Khamees and Ralph E Flori

Department of Geosciences, Geological, and Petroleum Engineering, Missouri University of Science and Technology, Rolla, MO 65409

ABSTRACT

Over the last few decades, there has been a dispute regarding the ability of colloidal dispersion gels (CDG) to improve sweep efficiency more than polymer flooding. In this study, a numerical model was built using the CMG-STARS simulator to investigate the behavior of injecting 0.1 PV of CDG slug into one quarter of inverted nine-spot pattern. This slug was composed of 0.1 wt. % HPAM polymer solution with a polymer-to-crosslinker ratio (P/X) of 50/1. The model was represented by a thick heterogeneous reservoir with high water cut caused by high heterogeneity and adverse mobility ratio. Different experimental results from published literatures have been implemented in the numerical model to study the effect of these parameters on the propagation of the CDG. The results confirmed that CDG could propagate deep into the thief zones and reduce their permeability more than polymer solution. Moreover, the results showed that the shear-thinning behavior of CDG could assist the selective penetration into the high-permeability streaks only, thus reducing the cost of isolating the thief zones by mechanical methods. In addition, the results showed that the wettability had tremendous effects on the treatment. Therefore, the water-wet system yielded higher results with less damage to the low-

permeability layers compared to the oil-wet system. The results showed an overestimation of the performance of post-treatment water when considering irreversible adsorption of CDG. However, the prolonged injection of post-treatment water would not remove the permeability reduction caused by CDG flooding, even with reversible adsorption. The results revealed that the higher the degradation of the CDG, the lower the recovery factor. The results showed the importance of considering a combination injection of polymer and CDG. The results also revealed that the higher the salinity of the reservoir brine and/or the makeup water, the lower the recovery factor. In addition, as the polymer/crosslinker ratio increases, the recovery factor decreases, while as the polymer hydrolysis increases, the recovery factor and residual resistance factor increases.

1. INTRODUCTION

Prolonging the life of mature reservoirs and reducing excess water production are big challenges in the oil industry because high water cut causes serious economic and environmental impacts. Different conformance treatment methods have been utilized to mitigate this problem, such as the injection of dispersion microgels to reduce water production and to improve sweep efficiency.

Colloidal dispersion gel (also known as weak gel, microgel dispersion, weak viscoelastic fluid, crosslinked polymer, deep diverting gel, or low concentration flowing gel) [1], is applied only to injection wells. The colloidal dispersion gel is composed of mixing low concentrations of high molecular weight of partially hydrolyzed polyacrylamide (HPAM) and inorganic crosslinkers, such as chromium or aluminum; thus,

there is no enough polymer to form a bulk gel or continuous network [1, 2, 3, 4, 5]. The molecular weight of the HPAM is from 8 to 17 million Daltons, and the polymer/crosslinker (P/X) ratio is from 30/1 to 60/1 [1]. However, this ratio could be in the range from 20/1 to 100/1 [6]. CDG could be considered a mid-point between easy to flow uncrosslinked polymer and not easy to flow bulk gel [1, 2, 7].

The successful field applications of CDG introduce it as a substitute to uncrosslinked polymer solution, with the ability to achieve high level of permeability reduction in the high-permeability layers. Until 2011, more than 70 CDG floods were implemented in the United States and worldwide, such as the Rocky Mountain Region (USA), Loma Alta Sur and the El Tordillo fields (Argentina), the Dina Cretaceous field (Colombia), and the Daqing, the Shengli, and the Karamay oil fields (China) [6, 7, 8, 9, 10, 11, 12]. These field applications proved the ability of large volumes of CDG to propagate deep into the reservoir without injectivity problems and can generate higher viscosity and increase the resistance factor substantially compared to uncrosslinked polymer [6, 7, 9, 13, 14, 15, 16, 17]. However, there is a debate about the mechanism, propagation, and economics of CDG as an in-depth gel treatment [3, 18, 19, 20]. The main question is about the propagation of the CDG aggregate deep into the high-permeability layers, which could cause a permeability reduction in these layers more than polymer solution. Those authors claim that once the gel particles have grown to the size of the pore throats, the gel will not be able to propagate deep through porous rock.

Different factors should be taken into account when selecting CDG in field applications, such as shear rate and salinity. Shear rate affects the formation of CDG, which makes the CDG demonstrate shear-thinning behavior [6, 18, 21]. This shear-thinning

behavior is important from the injectivity standpoint, which is very favorable in field applications of chemical-enhanced oil recovery [1]. Moreover, the gelant solution can flow as uncrosslinked polymer near the wellbore and enter selectively into the high-permeability layers [6]. On the other hand, CDG strength decreases when the salinity increases because of the buckle of polymer coils boosted by the presence of salt [6, 22]. Diaz et al. (2008) stated that, at low polymer concentrations fresh water was not necessary to form CDG that was used in the Loma Alta Sur field in the Neuquén Basin of Argentina. However, oil fields with high salinity were considered unsuitable for the application of CDG.

In this study, a 3D model, including one injector and three producers, was built using CMG-STARS simulator. The main objective of this study was to examine the role of different parameters on the propagation of CDG and to compare the obtained results with polymer flooding to ensure that CDG could increase the resistance factor more than polymer flooding.

2. CMG-STARS SIMULATOR

2.1. GEL MODELING

The gel modeling in STARS is mainly based on the interaction of chemicals and adsorption/retention of a blocking agent. To form gel, a chemical reaction needs to be defined. When gelant is injected, it should contain an adsorbing polymer and non-adsorbing crosslinking agent. The gelation process depends mainly on gelation time and the reaction rate.

2.2. GELATION TIME

Gelation time can be defined as the time it takes for the injected solution to gel (when viscosity starts to increase). It depends on the reaction rate of the gel [23]. The start of gelation can be recognized as the inflection point on the viscosity versus time curve. Gelation time is a function of the concentration of polymer and crosslinker, temperature of the reservoir, and salinity and pH of the formation water. Gelation time can be increased by using low polymer concentration, which produces weak gel that is capable of penetrating deep into thief zones. On the other hand, gelation time decreases with increasing the concentration of the crosslinker [24]. For in-depth gel treatment, a long gelation time is required. On the contrary, a short gelation time is required for near-wellbore gel treatment. In the latter case a high concentration of polymer and crosslinker is used to form a strong gel that is suitable for blocking high permeability layers without crossflow. Therefore, accurate estimation of the gelation time is vital for the success of deep gel placement. Because, a too short gelation time may results in pre-mature gelation of the gel system. On the other hand, a too long gelation time may result in the production of the gel system from the producer where even the gelation process could not take place.

2.3. REACTION RATE

The reaction rate is the speed of the reaction [23]. A simplified reaction scheme for gel formation might be modeled by assuming the reaction is of the form that shown in Eq. (1):

$$polymer\ (C1) + Crosslinker\ (C2) \rightarrow Gel\ (C3) \qquad (1)$$

where C1, C2, and C3 refer to the mass concentrations in the aqueous phase [25]. Reaction

rates are characterized through the frequency factor (the rate constant) in CMG-STARS simulator [26]. The concentration of polymer is taken to decline according to a first order reaction scheme [27], as in Eq. (2):

$$K = \frac{\ln(2)}{\tau_{1/2}} \tag{2}$$

where K represent the first order rate constant, and $\tau_{1/2}$ is the half-life of the component (i.e., polymer and crosslinker). In modeling the reaction of polymer/crosslinker to form gel, it is assumed that both components are in stoichiometric ratios. Moreover, the time taken for the conversion of half of these components is given by second order reaction [25], as follows:

$$K = \frac{5*10^7}{\tau_{1/2}} \tag{3}$$

As a summary, the reaction rate is affected by the concentration of the reactants and the order of reaction. A reaction occurs mainly because of the collisions between the molecules of the reactants. Increasing the concentration of the reactants would result in more collisions of molecules and thereby a faster reaction is obtained.

2.4. GEL KINETIC MODEL IN STARS (REACTION KINETICS)

As discussed previously, the gel modeling in STARS depends on the interaction of chemicals and the injected fluid which should contain adsorbing polymer and non-adsorbing crosslinker agent. The reaction kinetics in CMG-STARS simulator [26] is given by:

$$r_k = k \prod_{i=1}^{n_c} C_i^{e_k} \tag{4}$$

$$k = r_{rk.}\, e^{-\frac{E_a}{RT}} \tag{5}$$

Substituting Eq. (5) in Eq. (4), yields:

$$r_k = r_{rk.}\, e^{-(\frac{E_a}{RT})}.\prod_{i=1}^{n_c} C_i^{e_k} \quad (6)$$

Note that the definitions of all parameters are available in the nomenclature section at the end of this article. Eq. (6) demonstrate that the reaction rate is affected by the reactants' concentration and the order of reaction. A reaction occurs mainly because of the collisions between the molecules of the reactants. Increasing the concentrations of the reactants would result in more collisions of molecules and thereby a faster reaction is obtained. In CMG-STARS simulator [26], Eq. (6) is used to model the creation of gel and Table 1 shows the representation of these variables as a keyword in STARS.

Table 1. Keywords connected to gel modeling in CMG-STARS simulator [26].

Variables in Eq. (6)	Keyword in STARS
e_k	RORDER
r_{rk}	FREQFAC
E_a	EACT

2.5. RESISTANCE FACTOR & RESIDUAL RESISTANCE FACTOR

Mobility reduction, because of polymer flooding, can be quantified using a 'mobility reduction factor', otherwise known as the 'resistance factor' [28] and can be expressed as:

$$RF = \frac{k_w/\mu_w}{k_p/\mu_p} = \frac{Mobility\ of\ flooding\ water}{Mobility\ of\ polymer\ or\ gelant} \quad (7)$$

Resistance factor is equivalent to the effective viscosity of the gelant in porous media relative to that of water [29]. On the other hand, the permeability reduction as a

result of polymer flooding and/or gel treatment can be quantified using a 'permeability reduction factor', otherwise known as 'resistance residual factor' [28]. The residual resistance factor can be expressed as [28, 30, 31]:

$$RRF = \frac{(\frac{k_w}{\mu_w})_{initial}}{(\frac{k_w}{\mu_w})_{final}} = \frac{\textbf{\textit{Initial}}\ Water\ Mobility\ \textbf{\textit{Before}}\ Treatment}{\textbf{\textit{Final}}\ Water\ Mobility\ \textbf{\textit{After}}\ Treatment} \quad (8)$$

The permeability reduction factor or RRF is related to the adsorption level as given in Eq. (9). The mobility of water phase is divided by RK_w, thus accounting for blockage [26]:

$$RK_w = 1.0 + (RRF - 1.0)(\frac{Ads_i}{Ads_{max}}) \quad (9)$$

As mentioned previously, the residual resistance factor in low-permeability layers is higher than that in the thief zones. The latter assumption reflects the fact that low-permeability layers will have higher blocking and there will be a severe damage if gel enters or formed in these layers [25].

3. BUILDING THE MODEL

3.1. DESCRIPTION OF THE MODEL

A 3D representation of the model was presented in Figure 1 and the wells are completed through all layers. The selected pattern will maximize the production rate because it has a higher ratio of producer to injector. The model dimensions were 1170 ×1170×164 ft^3 with 30 × 30 × 3 gridblocks. The size of each gridblock was 39 feet and the thickness of the layers were different as shown in Table 2. Two rock types were considered: rock type 2 for layers 1 and 2 (i.e., the thief zones), in which a linear dependence relative

permeability was assumed and rock type 1 for layer 3 as shown in Figure 2. In addition, Table 3 shows the basic parameters of the reservoir, while Table 4 shows the fluid properties. In this study, the injection rate was 1,070 barrels per day for all runs and the models were run for 25 years. Table 5 represent the properties of the polymer solution, while Table 6 represent the properties of gel. Other considerations were:

- All fluids are incompressible.
- Only water and oil phases were considered and gas phase was not considered.
- No aquifer was attached, the injected water was from the injector only.
- The model is isothermal (activation energy is not required).
- Polymer exists in the water phase.
- Chemical reactions only occur between polymer and crosslinker.
- Water density does not affected by polymer.
- No biological degradation is modeled.
- The injection of chemicals was started at 80% water cut.

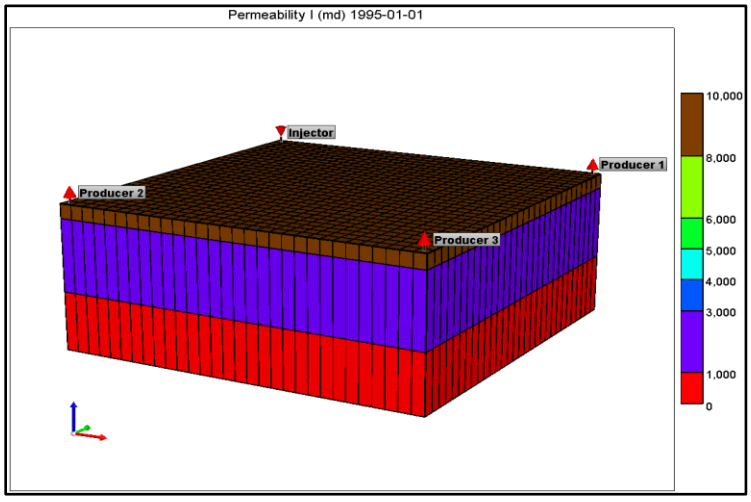

Figure 1. 3D visualization of the model.

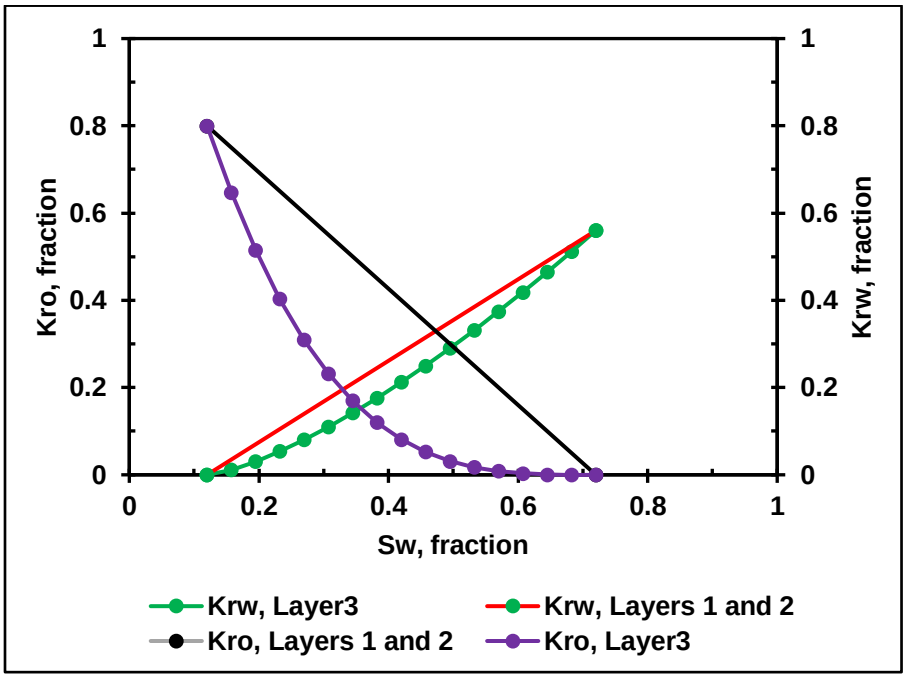

Figure 2. Water and oil relative permeability curves [25].

Table 2. Basic parameters of the model [32].

Layer	Thickness (ft.)	Porosity (%)	Permeability (mD)
1	16	32	10,000
2	82	30	2000
3	66	28	780

Table 3. Basic parameters of the reservoir [32].

Reservoir temperature	149 °F
Initial reservoir pressure	2031 psi
K_v/K_h	0.1
Initial water saturation	0.22
Rock type 1	Layer 3
Rock type 2	Layers 1 and 2

Table 4. Fluid properties.

Water viscosity and density	0.6 cp, 62.4 lb/ft^3
Oil viscosity and density	78.0 cp, 59.31 lb/ft^3
Polymer viscosity and density	30.0 cp, 62.4 lb/ft^3
Crosslinker viscosity and density	30.0 cp, 62.4 lb/ft^3
Polymer molecular weight	18,000 lb/lbmole
Crosslinker molecular weight	206 lb/lbmole
CDG molecular weight	18,206 lb/lbmole
Polymer concentration	1,000 ppm
Crosslinker concentration	20 ppm

Table 5. Properties of polymer solution [32].

Polymer conc., wt.%	Viscosity, cp	Adsorption density, lb/ft^3	Frr
0	0.6	0	1.0
0.04	12.2	20.5	1.6
0.08	26.4	35.1	2.1
0.12	34.5	40.8	2.6

Table 6. Properties of gel [32].

Polymer conc., wt.%	Retention density, mg/l	Frr
0.0	0	1
0.04	400	4
0.08	800	12
0.12	1200	28

3.2. INJECTION OF COLLOIDAL DISPERSION GEL

CDG is injected by two methods:

1. Sequential injection: this process includes an alternative injection of long-term slug of polymer and short-term slug of crosslinker [6].
2. Simultaneous injection: the polymer and crosslinker are injected at the same time (i.e., concurrent or co-injection) and the gel is formed at a fixed time [1].

In this study, we modeled the injection of CDG based on the simultaneous injection method. The field experience proved that when using the sequential injection method, the polymer and crosslinker might not come together at the same time inside the thief zones, which leads to the failure of the treatment.

3.3. INJECTION SCHEDULES

The injected volumes of CDG are measured by pore volumes and can be compared with polymer flooding. Therefore, CDG is a flooding operation rather than treatment. In the Loma Alta Sur field in Argentina, the total volume of the injected CDG is 391,094 barrels, which represents 3.06% of the pore volume of the LAS-58 pilot area [33]. In the Daqing oil field, they injected 0.53 PV of chemical slugs (0.18 PV CDG, 0.15 PV polymer, and 0.2 PV CDG) over a period of four years (i.e., 0.14 PV/yr.) [8]. In this study, the total injected volumes of CDG was 1,177,000 barrels within three years, which represented 0.10 of the total PV. Thus, the longtime of the CDG injection was based on the previous field applications. Two methods of placing the gelant solution are normally used: bullhead and zonal isolation. In the bullhead method, the gelant solution has access to all three layers

without isolation, while in zonal isolation method the gelant solution has access to layers 1 and 2 only.

4. RESULTS AND DISCUSSIONS

4.1. COMPARISON BETWEEN POLYMER AND CDG FLOODING

The success of any gel treatment depends on the recovery factor and sweep efficiency before applying the treatment [34]. In this study, a thick heterogeneous reservoir, with crossflow between layers and high oil viscosity, was considered. It seems from Table 7 that the recovery factor obtained from water flooding was 27.8% only. Therefore, applying gel treatment should improve the sweep efficiency from the reservoir. The purpose of injecting the polymer solution is to reduce the high mobility ratio, whereas the purpose of injecting gel is to reduce or block off the high-permeability layers. However, CDG and polymer flooding share multiple similarities; yet, oil production response occurred immediately during the polymer flooding and the oil production declined slowly after the treatment. During CDG flooding, the increase in the oil production rate lasted much longer [35]. Moreover, the oil recovery by polymer flooding from flooded-out layers is insignificant [31]. The aim of this comparison is to prove that CDG is more preferable than uncrosslinked polymer flooding and to prove that the residual resistance factor (RRF) generated by CDG is higher compared to RRF from the polymer solution only. This comparison will determine the technical feasibility of implementing CDG injection in field applications. The same pore volume (i.e., 0.1) of polymer solution is injected into all three layers without zonal isolation. Table 7 show a large difference between polymer flooding

and CDG flooding, while Figure 3 compares RRF between polymer flooding (left) and CDG injection (right), which proves that CDG yielded RRFs 4-5 times higher than uncrosslinked polymer. Thus, CDG must be used to block this thief zone and divert subsequent water injection into the low-permeability layer.

Table 7. Recovery factor and incremental oil from polymer and CDG flooding.

Scheme	RF, %	Cum. oil, MM STB	Incremental oil, MM STB	Water cut during the treatment	Final water cut	Max. RRF
WF	27.80	2.55			94.5	
Polymer	29.30	2.69	0.14	83.0	94.5	1.62
CDG	40.30	3.70	1.15	40.0	90.6	7.80

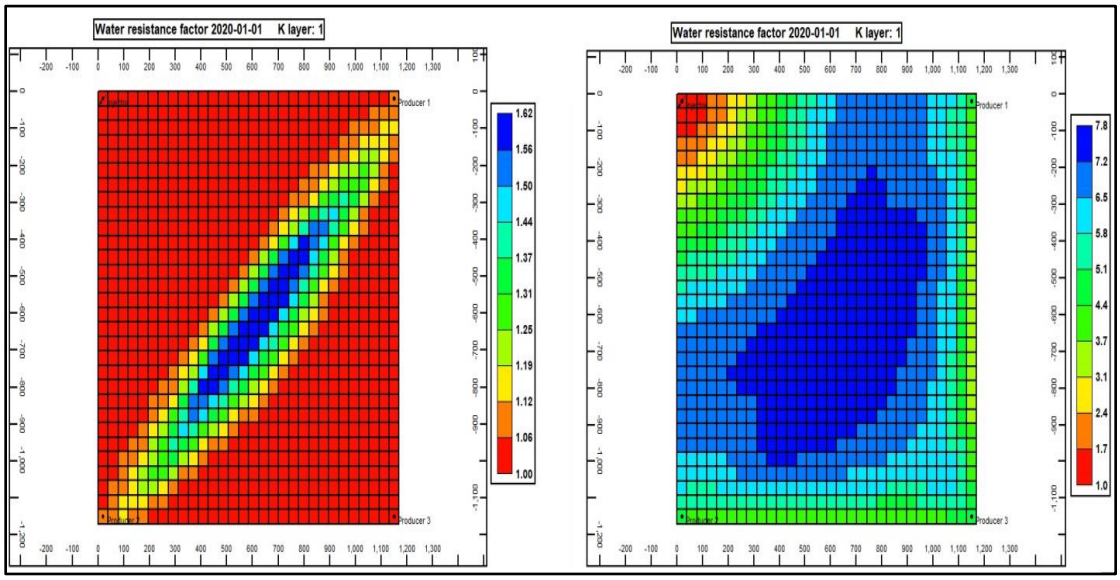

Figure 3. Comparison of water residual resistance factor between polymer (left) and CDG (right).

4.2. EFFECT OF SHEAR-THINNING BEHAVIOR OF CDG ON THE SELECTIVE PENETRATION

There is always a debate regarding the ability of CDG to enter the thief zones without damaging the low-permeability layers. If the gel treatment is performed in unfractured wells (i.e., radial flow), the zonal isolation is more likely to be needed [36, 37, 38]. However, if the gelling agent has a water-like viscosity and the resistance factor is unity, minimum damage to the low-permeability layers could happen because the low viscosity fluids penetrate less into the low-permeability layers [37]. Thus, mechanical isolation is the most effective way of protecting the low-permeability layers during gelant solution placement. Moreover, the bullhead injection will always cause a damage to the less permeable layers.

Shear-thinning fluids such as CDG or xanthan-based polymer gels might have a higher tendency to flow in the high-permeability layers due to the lower viscosity near the wellbore, which provides more favorable injectivity [6, 39, 40]. Thus, the shear-thinning behavior could assist the placement of CDG solution without the necessity of zonal isolation (i.e., mechanical packer). In order to show the effect of shear-thinning behavior of the placement of CDG, two scenarios were considered where CDG was injected using the bullhead method. In the first scenario, the shear rate was not considered to have any effect on the viscosity of CDG, which is a hypothetical assumption, whereas in the second model, a real CDG rheology model was considered (i.e., shear-thinning behavior). Table 8 shows the incremental oil achieved by the shear-thinning model, which assisted the gelant solution to enter and block the thief zones only (Figure 4).

When shear-thinning behavior of CDG is considered, layer 3 (the less permeable layer in this model) is not affected by gelant solution placement even when gelant has

access to all open layers as shown in the left-hand side of Figure. 4. Therefore, shear-thinning rheology of the CDG, supported by the difference of saturation of the fluids in heterogeneous reservoir's model, can further assist CDG to penetrate selectively into low-permeability layers. These results confirmed the ability of shear-thinning gelant solution to penetrate into thief zones without damaging the less permeable layer; thus, reducing the cost of mechanical isolation of the low-permeability layer. However, the maximum residual resistance factor was higher when the shear-thinning rheology model was not considered.

Table 8. Effect of shear thinning on selective penetration.

Scheme	Rheology	RF, %	Cum. oil, MM STB	Incremental oil, MM STB
WF		27.80	2.55	
CDG	Shear rate is not consider	39.08	3.58	1.03
CDG	Shear-thinning behavior	39.50	3.62	1.07

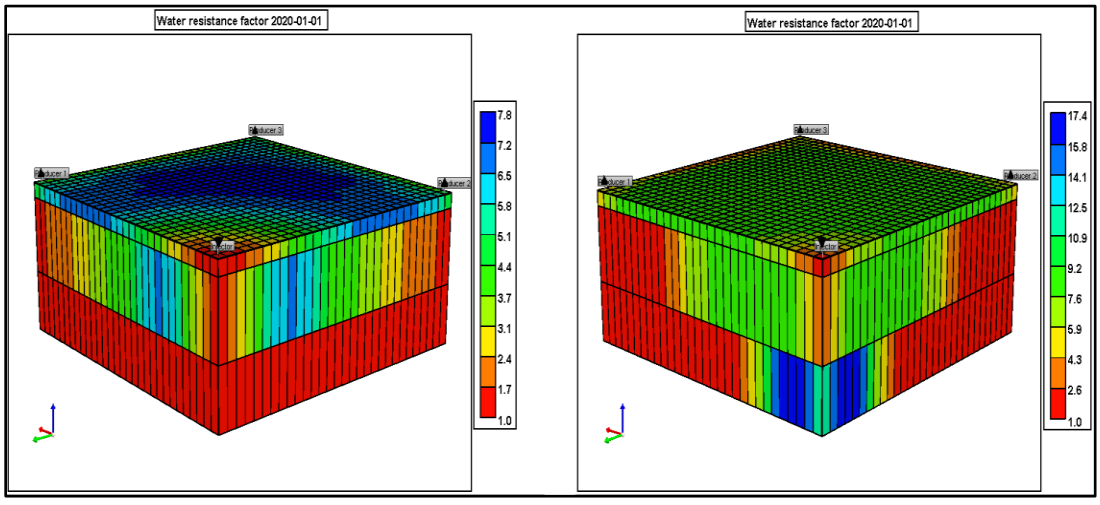

Figure 4. Damage in layer 3 when shear-thinning behavior is not considered (right) compared to no-damage in this layer when shear-thinning model is considered (left).

4.3. EFFECT OF CDG ADSORPTION

Polymer, which is the main component of any gel system, has three types of retention when it flows inside the porous media. These mechanisms are adsorption, mechanical entrapment, and hydrodynamic retention [41]. Mechanical entrapment is irreversible and happens when the large polymer molecules are trapped in pores with small exit pore-throat diameter. The polymer propagation, and hence gel propagation, is significantly affected by mechanical entrapment if the pore-throat sizes are too small [42]. In this study, mechanical entrapment is not important because the permeability was too high. The hydrodynamic retention is reversible and occurs when flow rates are suddenly increased. Thus, polymer adsorption is the most important mechanism, which is defined as the adhesion of the polymer molecules onto the rock surfaces [43]. A recent study suggested that the permeability reduction caused by polymer flooding might not be the same after post-treatment water injection and the performance of the reservoir after the treatment might be exaggerated [44]. In addition, the permeability reduction caused by CDG injection could be removed with prolonged injection of chase water [9]. Thus, to prove whether permeability reduction generated by CDG injection could be removed or not, three assumptions for adsorption were suggested. Therefore, three models with irreversible, partially reversible, and reversible adsorptions were considered. The results shown in Table 9 suggest that assuming irreversibility of polymer adsorption will give higher results compared to other options (i.e., partial reversible and reversible adsorption).

To show if the permeability reduction caused by the gel treatment will vanish and be removed as concluded by other researchers [9, 44], an extension of post-treatment water injection until year 2050 was considered (the default end date of the simulation run was

2020). Figure 5 (left-hand side) shows that after prolonged injection of post-treatment water for the reversible adsorption model, there was still permeability reduction in the thief zone (layer 1) and the gel treatment was not removed completely.

Table 9. Recovery factor and cumulative oil for different degrees of adsorption.

Scheme	Adsorption	RF, %	Cum. oil, MM STB	Incremental oil, MM STB
WF		27.80	2.55	
CDG	Reversible	36.11	3.31	0.76
CDG	Partial Reversible	37.00	3.40	0.85
CDG	Irreversible	40.25	3.70	1.15

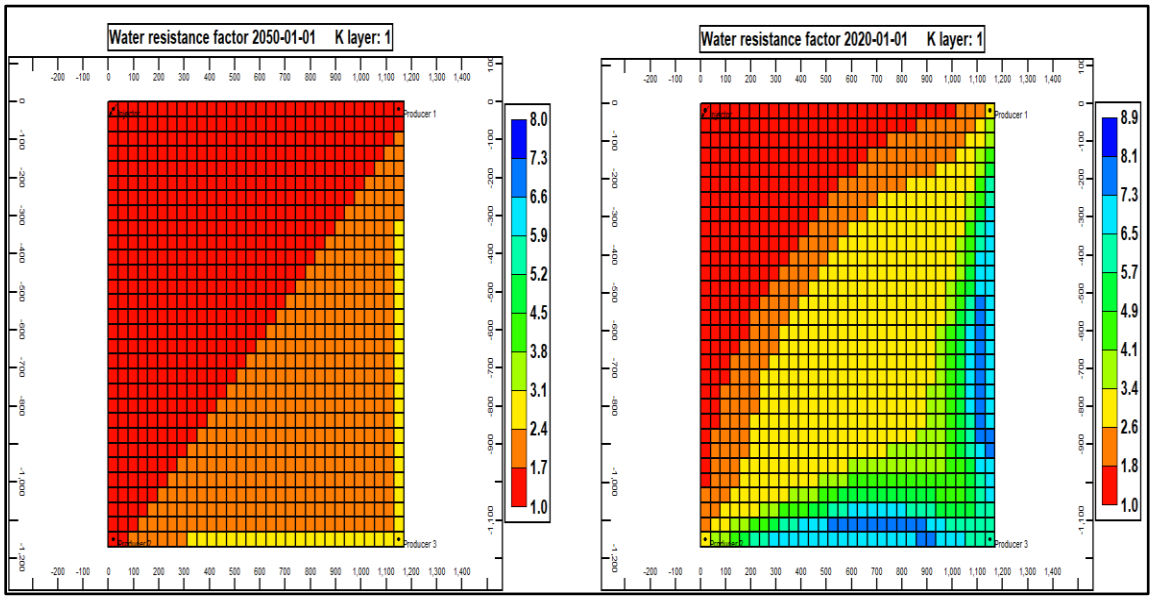

Figure 5. Comparison of water residual resistance factor in layer 1 between prolonged injection (left) and default run (right).

4.4. EFFECT OF CDG DEGRADATION

4.4.1. Chemical Degradation. Gel degradation is related in one way or another with polymer degradation. Polymer solutions such as HPAM and xanthan are subjected to thermal, microbial, mechanical, and chemical degradations. However, HPAM polymer solution is relatively more tolerant to microbial (bacterial) attack than xanthan biopolymer solution. On the other hand, the presence of oxygen and other contaminants such as iron is considered the main cause of chemical degradation [1].

In this section, a gel degradation time was used to represent the chemical degradation. The gel degradation time refers to the time at which gel viscosity is same as water viscosity and it has no effect on blocking the permeability of the thief zones [32]. Four scenarios were modeled, which include no degradation, 1-year, 2-year, and 4-year gel degradation. Table 10 shows the difference in recovery factors and incremental oil. The longer the gel degradation time, the lower the chemical degradation, the higher the recovery factor, the higher the residual resistance factor, and the deeper the gel can penetrate into the thief zone. Figure 6 shows how far CDG can penetrate deep into layer 1 when there is no gel degradation compared to 1, 2, and 4 year degradation time.

Table 10. Recovery factor and cumulative oil under different chemical degradation times.

Scheme	Degradation	RF, %	Cum. oil, MM STB	Incremental oil, MM STB	Max. Frr
WF		27.80	2.55		
CDG	Nil	40.25	3.70	1.15	9.0
CDG	1 year	34.19	3.13	0.58	3.5
CDG	2 year	37.72	3.46	0.91	4.4
CDG	4 year	38.62	3.54	0.99	5.3

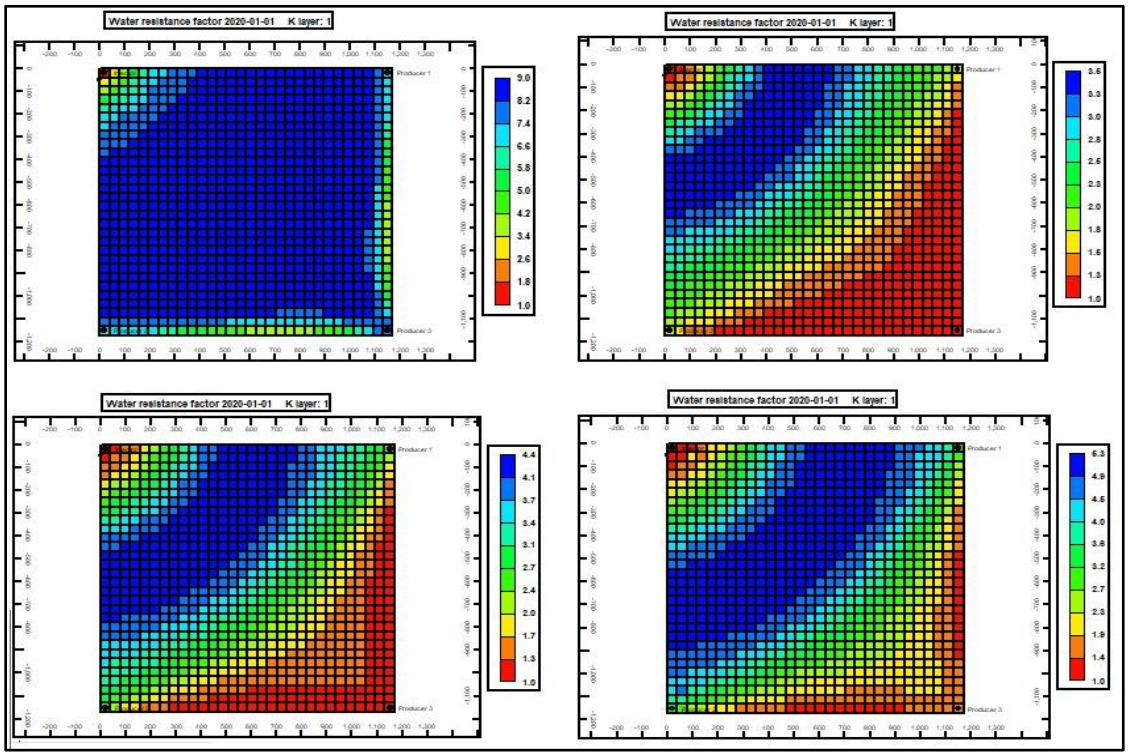

Figure 6. Comparison of water residual resistance factor in layer 1 between no degradation (upper left), 1-year (upper right), 2-year (lower left), and 4-year degradation (lower right).

4.4.2. Mechanical Degradation. Flow of polymer and gelant solutions through restricted areas such as valves, pumps, pore throats, and perforations is the main factor that initiates the mechanical (shear) degradation. Mechanical degradation occurs when the shear rate is increased above the critical shear rate of the polymer (i.e., polymer stretch rate) [45, 46]. This degradation depends on the molecular weight of the polymer, therefore the higher the molecular weight the longer the molecule chain and the higher the degradation rate [47, 48, 49]. Thus, long chains are subjected to cut through its center, which leads to decrease of polymer viscosity and eventually poor sweep efficiency.

Two investigators [50] developed a model to calculate polymer viscosities as a function of shear rate taking into account the effect of mechanical degradation, which uses

molecular weight distributions of the polymer solution, as shown in Figure 7. These data were used, modeled, and compared to show the effect of mechanical degradation on the propagation of the CDG.

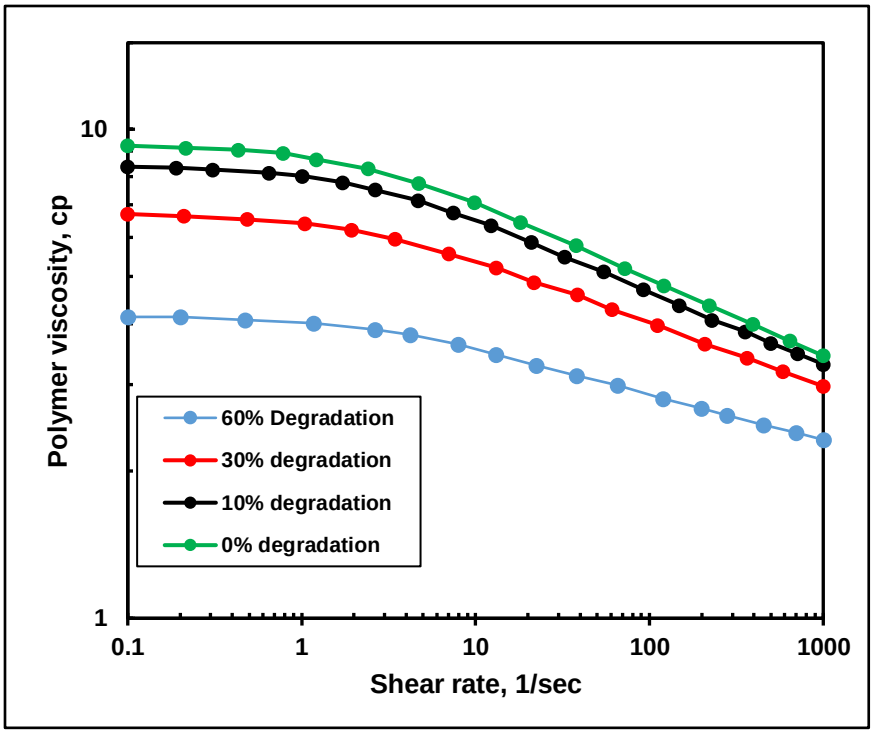

Figure 7. Polymer viscosity vs. shear rate at different levels of degradation [50].

In our model, the pore throats are large because of the high permeability of the thief zones. However, the polymer solution is still subject to mechanical degradation because of the existence of the restricted areas, as mentioned previously. It is obvious from Table 11 and Figure 8 that water saturation was distributed more evenly in layer 1 for 0% and 10% mechanical degradation than for 30% and 60% cases. The latter findings proved that CDG has higher strength in 0% and 10% degradations than in 30% and 60% degradations.

Table 11. Recovery factor and cumulative oil under different mechanical degradation criteria.

Scheme	Degradation	RF, %	Cum. oil, MM STB	Incremental oil, MM STB
WF		27.80	2.55	
CDG	0%	39.00	3.60	1.05
CDG	10%	38.66	3.55	1.00
CDG	30%	37.99	3.50	0.95
CDG	60%	37.09	3.40	0.85

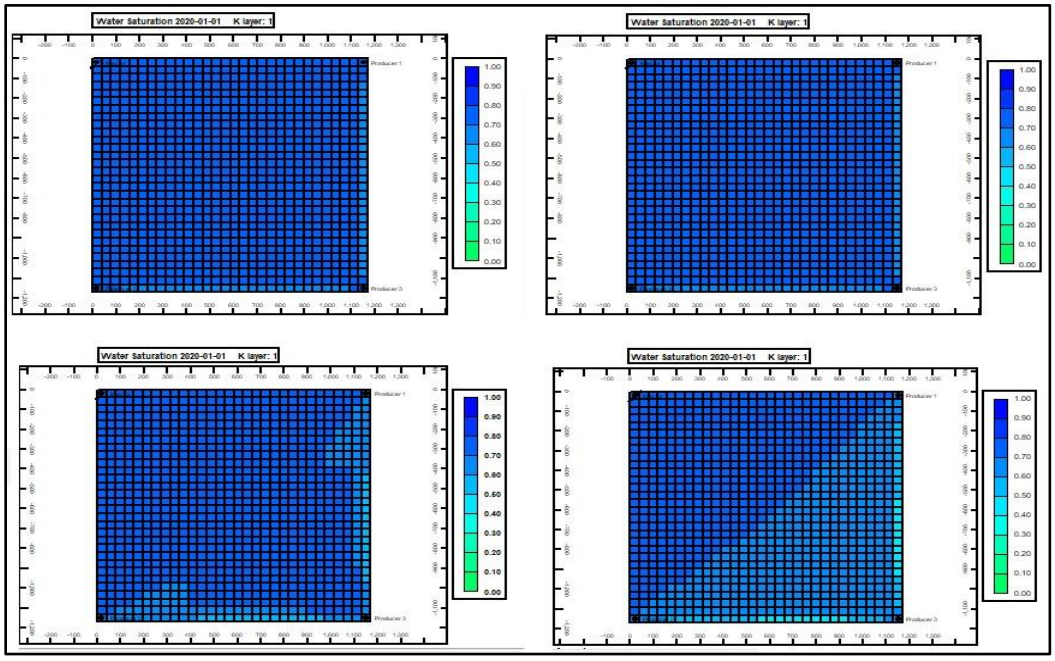

Figure 8. Comparison of water saturation in layer 1 between 0% (upper left), 10% (upper right), 30% (lower left), and 60% mechanical degradation (lower right).

4.5. EFFECT OF SALINITY ON THE PERFORMANCE OF CDG

In field applications, the long history of water injection make the reservoir brine salinity similar to the salinity of the injected water before the initiation of injection of any

chemicals [51]. In addition, the makeup water and/or the reservoir brine that is used to prepare the treatment have an effect on the performance of the chemical enhanced oil recovery processes. As mentioned previously, the strength of CDG decreases as the salinity increases. A previous study suggested that the CDG can tolerate a water salinity up to 30,000 mg/l without any problems [6]. However, a recent screening criteria suggested that CDG could tolerate between 3,000 mg/l to 130,000 mg/l of water salinity in the field applications [52]. Hence, in order to demonstrate the effect of salinity on CDG, the effect of salinity on the viscosity of HPAM polymer solution should be investigated. Sheng (2011) stated, "An HPAM flexible chain is compressed in saline water, resulting in low viscosity" (Ch. 5, page no. 106). This is because when the salinity is high, the polymer molecules tend to compact due to the loss of water to the more saline environment that surround the solution [53]. However, at low salinities, polymer molecules tend to stretch, which causes high polymer viscosity. Several researchers [54, 55] presented data of polymer viscosity versus polymer concentration and shear rate at different salinities, which was used in this section.

In the formulation of a CDG, a range of polymer concentrations from 0.01 wt. % to 0.12 wt. % polymer is used [1]. In all previous sections, a 0.10 wt. % polymer concentration was used. Thus, a new model with a new polymer concentration (i.e., 0.12 wt. %) was used with the same polymer to crosslinker ratio (i.e., 50/1). The HPAM polymer solution was prepared using NaCl with different salinities that range from fresh water up to 30,000 mg/l salinity as shown in Figure 9 and these mixture were modeled individually with the specified polymer to crosslinker ratio. It is obvious that the higher the salinity of the makeup water, the lower the viscosity of the polymer solution. Consequently, this will

affect the strength of the formed CDG, which lowers the sweep efficiency and permeability reduction in the thief zone as shown in Table 12 and Figure 10.

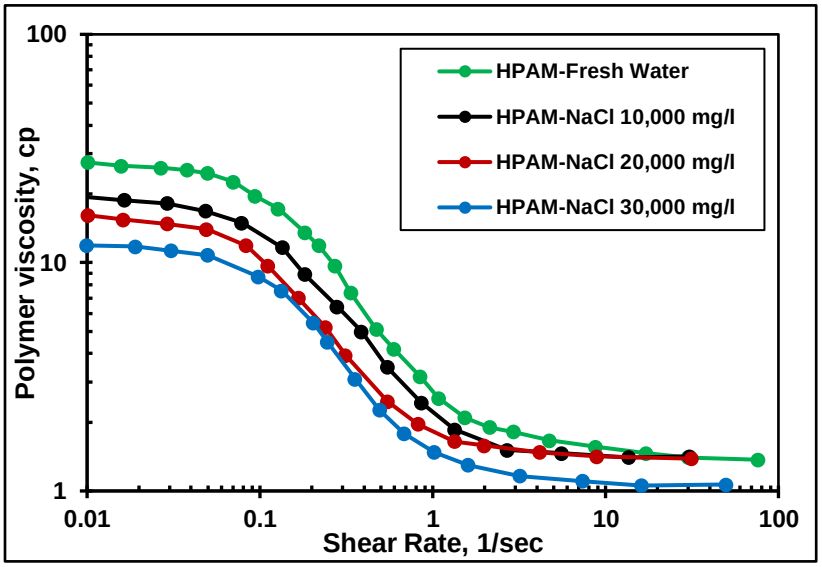

Figure 9. Polymer viscosity vs. shear rate at different levels of salinity [55]

Table 12. Recovery factor and cumulative oil under different salinities.

Scheme	NaCl salinity, mg/l	RF, %	Cum. oil, MM STB	Incremental oil, MM STB	Max. Frr
WF		27.80	2.55		
CDG	Fresh water	40.90	3.75	1.20	8.9
CDG	10,000	40.17	3.68	1.13	8.6
CDG	20,000	39.46	3.62	1.07	8.5
CDG	30,000	38.72	3.55	1.00	8.3

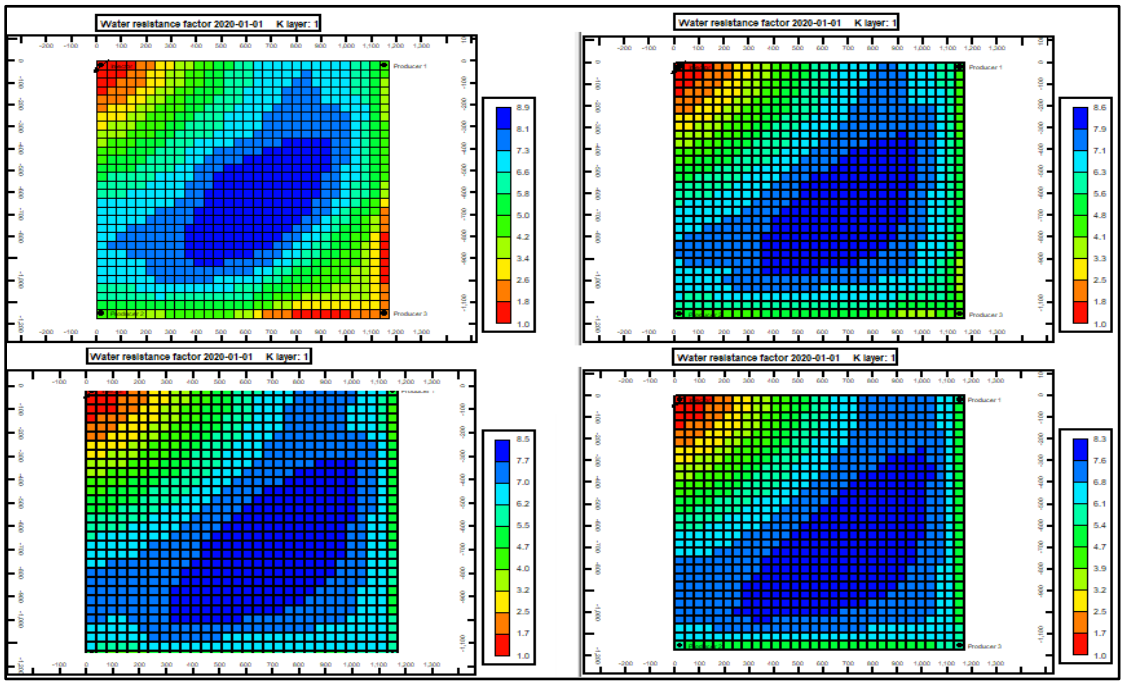

Figure 10. Comparison of residual resistance factor in layer 1
HPAM+fresh water (upper left), HPAM+10,000 mg/l NaCl (upper right), HPAM+20,000 mg/l NaCl (lower left), and HPAM+30,000 mg/l NaCl (lower right).

4.6. COMPARISON BETWEEN IN-DEPTH AND NEAR-WELLBORE GEL TREATMENT

When flooding a thick heterogeneous reservoir with crossflow between layers, it is imperative to inject the gelant solution to penetrate deep into the thief zones. Near-wellbore (NWB) treatment in the order of fifty feet is sufficient to reduce the permeability of layered reservoir without crossflow by a factor of 100 or more [56]. To demonstrate the importance of in-depth gel treatment for this type of reservoir, a near-wellbore (NWB) gel treatment is considered. During NWB gel treatment, high concentrations of polymer and crosslinker were used to form a strong gel, as compared to the deep fluid diversion method where low concentrations of the reactants were used to yield long gelation time. If there was a crossflow, the post-treatment water injection could move around the gel and back into the

thief zone with minimum impact on pattern performance as compared to in-depth treatment. Figure 11 shows the residual resistance factor in layer 1, which represents the depth of gel penetration by in-depth (left) and near-wellbore (right) treatments, while Table 13 shows a comparison between oil recovery and incremental oil between these two cases. Therefore, in NWB gel treatment the maximum residual resistance factor was 22.3, compared to 9.0 in case of in-depth gel treatment; however, the effect of NWB gel treatment was limited to the cell around the injection well only. Thus, NWB gel treatment was not as efficient as in-depth gel treatment.

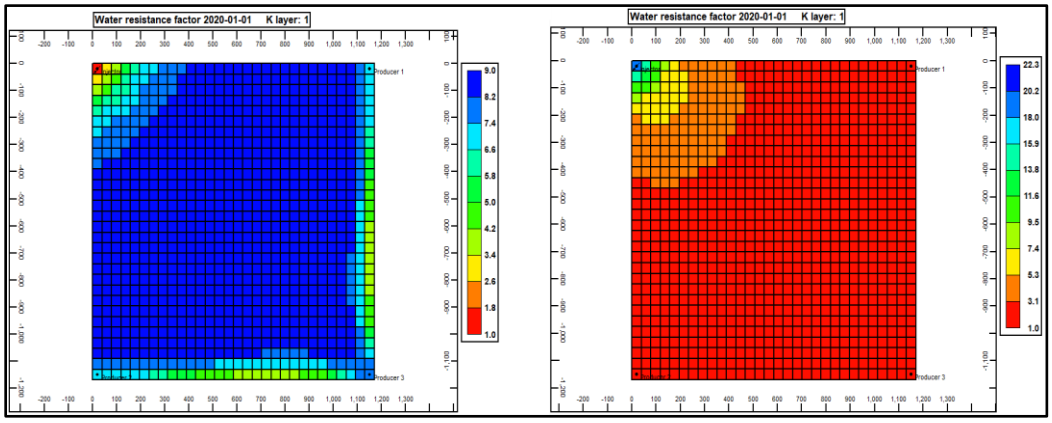

Figure 11. Comparison of residual resistance factor generated from in-depth (left) vs near-wellbore gel treatment (right).

Table 13. Comparison of recovery factor and cumulative oil between in-depth and NWB treatment.

Scheme	Injected Fluid	PV, injected gel	RF, %	Cum. oil, MM STB	Incremental oil, MM STB
WF			27.80	2.55	
CDG	In-depth	0.1	40.25	3.70	1.15
CDG	Near-wellbore	0.1	32.76	3.00	0.45

4.7. EFFECT OF THE ALTERNATIVE INJECTION OF CDG AND POLYMER

To enhance the recovery from this heterogeneous thick reservoir with viscous oil, it would be preferable to inject polymer either before or after the treatment. The injected polymer slug size was 0.1 PV. Therefore, two scenarios were compared with CDG treatment alone. Table 14 shows the results of this comparison.

Table 14. Recovery factor and cumulative oil under combination injection of gel and polymer.

Scheme	Sequence of injection	RF, %	Cum. oil, MM STB	Incremental oil, MM STB
WF		27.80	2.55	
CDG	Gel only	40.25	3.70	1.15
PF_CDG	Polymer-gel	42.72	3.92	1.37
CDG_PF	Gel-polymer	43.81	4.02	1.47

As can be seen from this table, injection of polymer with CDG always yielded higher results regardless of the sequence of the injection. However, the injection of polymer after CDG was better than injection of polymer before CDG. The increase in recovery was attributed to the high degree of permeability reduction in the theif zones, resulting from the interaction of polymer that followed the gel treatment with the unreacted crosslinkers.

4.8. EFFECT OF RESERVOIR WETTABILITY ON THE PERFORMANCE OF CDG

CDG or any other type of gel are composed of polymer, crosslinker, and additives where water represents more than 90% of these mixtures. Capillary forces, interfacial tension, and wettability of the reservoir rocks govern the distribution of fluids inside the

reservoir [57]. Thus, in oil-wet conditions, oil phase is located in the small pores and covers the pore surfaces, while water phase is located in the larger pores. In water-wet system, the water phase is located in the smaller pores and covers the pore surfaces, while oil phase is located in the larger pores. In an oil-wet system, the water-oil ratio increased more rapidly than in a water-wet system [58, 59]. In our previous works [60, 61], we concluded that the recovery factor from gel treatment in water-wet conditions was higher and the damage to the low permeability layer was less compared to oil-wet system. To assess the effects of rock wettability on the performance of CDG floods, wettability data presented in Table 15 were used, and two scenarios were compared. A linear saturation dependence was used for the high-permeability layers [25].

Table 15. Relative permeability parameters [58, 60, 61].

Wettability	S_{wi}	S_{or}	k°_{rw}	k°_{ro}	n_w	n_o
Water-wet	0.12	0.25	0.26	1	3	1.3
Oil-wet	0.12	0.28	0.56	0.8	1.4	3.3

$$k_{rw} = k^{\circ}_{rw}\left(\frac{S_w - S_{wi}}{1 - S_{or} - S_{wi}}\right)^{n_w} \quad (10)$$

$$k_{ro} = k^{\circ}_{ro}\left(\frac{S_o - S_{oi}}{1 - S_{or} - S_{wi}}\right)^{n_o} \quad (11)$$

The results of these scenarios are presented in Table 16 and Figure 12. This table shows that the incremental oil achieved by CDG flooding under the water-wet system was higher compared to the oil-wet system. In addition, for oil-wet system, Figure 12 shows that the less permeable layer (i.e., layer 3) was damaged and that CDG penetrated and

reduced the permeability of this layer compared to the water-wet system. This could be due to the dispersion of CDG into layer 3 in oil-wet conditions, because the water phase is normally located in the larger pores under these conditions. Thus, CDG flooding was more efficient and the damage to layer 3 was less when wetting conditions of the system were water-wet.

Table 16. Recovery factor and cumulative oil under oil-wet and water-wet condition systems.

Scheme	RF, %	Difference of RF%	Cum. oil, MM STB	Incremental oil, MM STB
WF_Water-wet	31.40		3.25	
CDG_Water-wet	43.70	12.30	4.51	1.26
WF_Oil-wet	25.70		2.66	
CDG_Oil-wet	37.40	11.70	3.86	1.20

4.9. EFFECT OF POLYMER/CROSSLINKER (P/X) RATIO

As mentioned previously, a reaction occurs mainly because of the collisions between the molecules of the reactants. Increasing the concentrations of the reactants would result in more collisions of molecules and would thereby obtain a faster reaction and a shorter gelation time. In this section, different polymer to crosslinker ratio were utilized, where the polymer concentration was 0.05 wt. % [22]. Table 17 presented the results of these scenarios, which demonstrated that increasing the P/X ratio would result in a lower recovery factor and lower incremental oil. This behavior is attributed to the fact that increasing P/X ratio would increase the viscosity of the formed CDG; therefore, there is a

shorter penetration into the high-permeability layer, as shown in Figure 13. In addition, at higher P/X ratios, the crosslinking reaction rate would increase [6]. Thus, the higher the P/X ratio, the lower the viscosity of the formed CDG and the higher the penetration into thief zones. However, the higher the P/X ratio, the higher the residual resistance factor (i.e., permeability reduction).

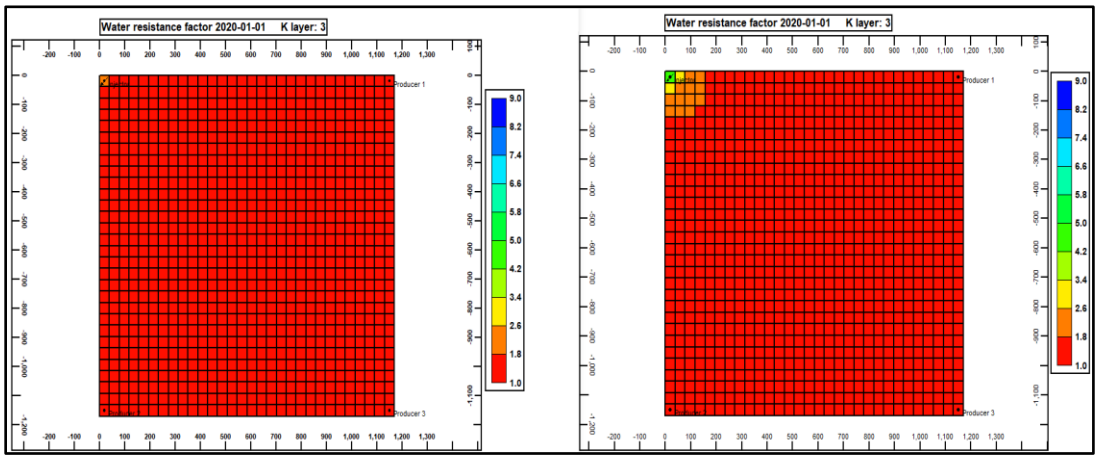

Figure 12. Comparison of residual resistance factor in layer 3 (low-permeability layer) between water-wet (left) and oil-wet conditions (right).

Table 17. Recovery factor and cumulative oil under different polymer/crosslinker values.

Polymer Conc. wt.%	P/X ratio	RF%	Cum. oil, MM STB	Incremental oil, MM STB	RRF
WF		27.80	2.55		
0.05	10/1	40.40	3.70	1.15	6.8
0.05	20/1	40.00	3.67	1.12	10.7
0.05	30/1	36.10	3.31	0.76	18.9
0.05	40/1	34.20	3.13	0.58	21.9

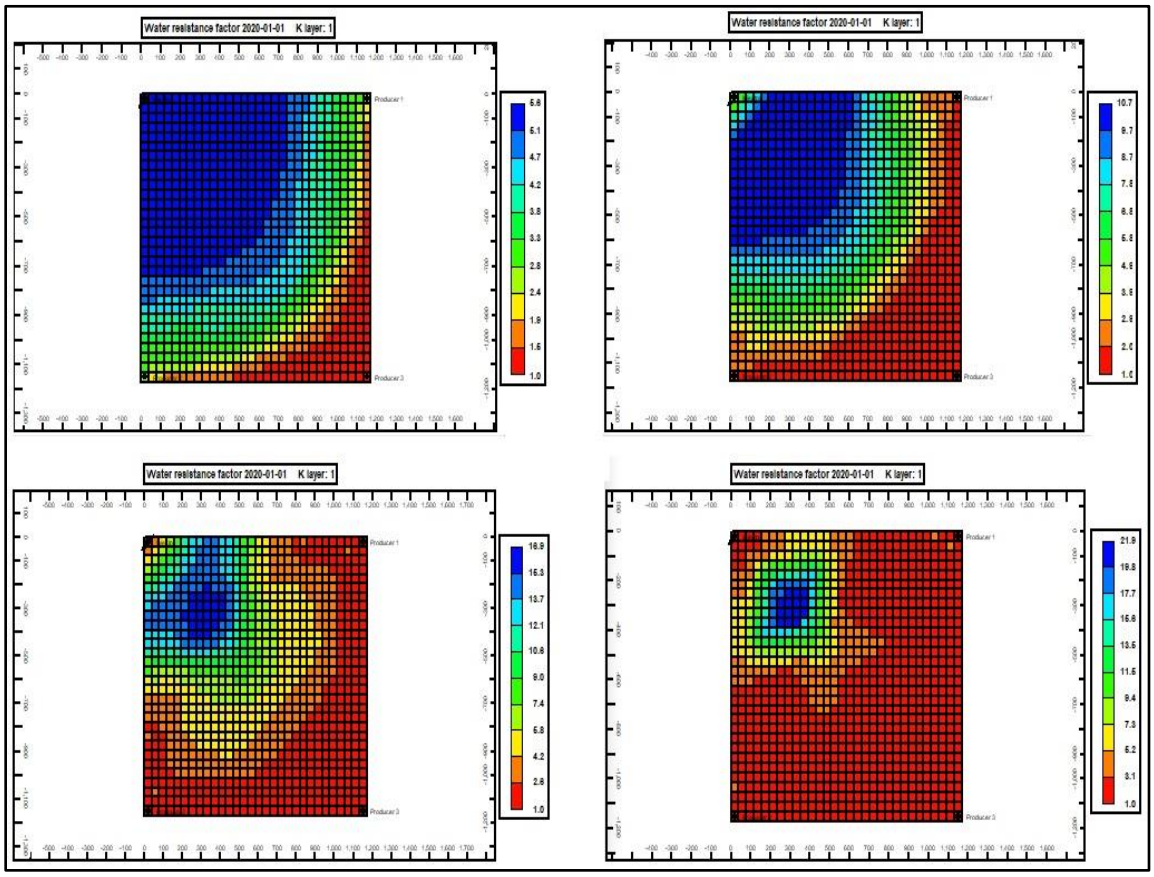

Figure 13. Comparison of residual resistance factor in layer 1 at different levels of P/X ratio (10/1 P/X (upper left), 20/1 P/X (upper right), 30/1 P/X (lower left), and 40/1 P/X (lower right)).

4.10. EFFECT OF POLYMER HYDROLYSIS ON THE FORMULATION OF CDG

Since HPAM polymer solution contains nonionic amide groups ($CONH_2$) and anionic carboxyl groups (COO^-); thus, the hydrolysis process converts some of amide groups to carboxyl groups, which can by represented by the degree of hydrolysis. In general, HPAM polymer solution that used in field applications has a degree of hydrolysis ranges from 15-35 % [1]. Converting some of amide groups to carboxyl groups will introduce negative charges on the backbones of polymer chains. In addition, increasing

hydrolysis will increase the viscosity and reduce the adsorption; however, the chemical stability is reduced due to the losing of amide groups. On the other hand, low degree of hydrolysis will give high chemical stability to the polymer but the adsorption will increase due to high content of amide groups [1]. Moreover, the degree of hydrolysis could affect the retention of HPAM polymer solution in unconsolidated sandpacks [62] and the data presented by those researchers were used in this section. Thus, degree of hydrolysis plays an important role in the chemical stability of polymer, which in turn will affect the gelation process between the polymer and the crosslinker.

Table 18 and Figure 14 shows that increasing the polymer hydrolysis from 0% (unhydrolyzed) to 35% would resulted in an increase of the recovery factor and the residual resistance factor. These results proved the importance of the degree of hydrolysis on the formulation and performance of the CDG.

Table 18. Recovery factor and cumulative oil under oil-wet and water-wet condition systems.

Polymer Conc. wt. %	Degree of polymer hydrolysis	RF%	Cum. oil, MM STB	Incremental oil, MM STB	RRF
WF		27.80	2.55		
0.06	Unhydrolyzed	40.00	3.75	1.20	8.8
0.06	15% hydrolyzed	41.20	3.77	1.22	9.0
0.06	25 % hydrolyzed	42.10	3.79	1.24	9.1
0.06	35% hydrolyzed	43.60	3.83	1.28	9.1

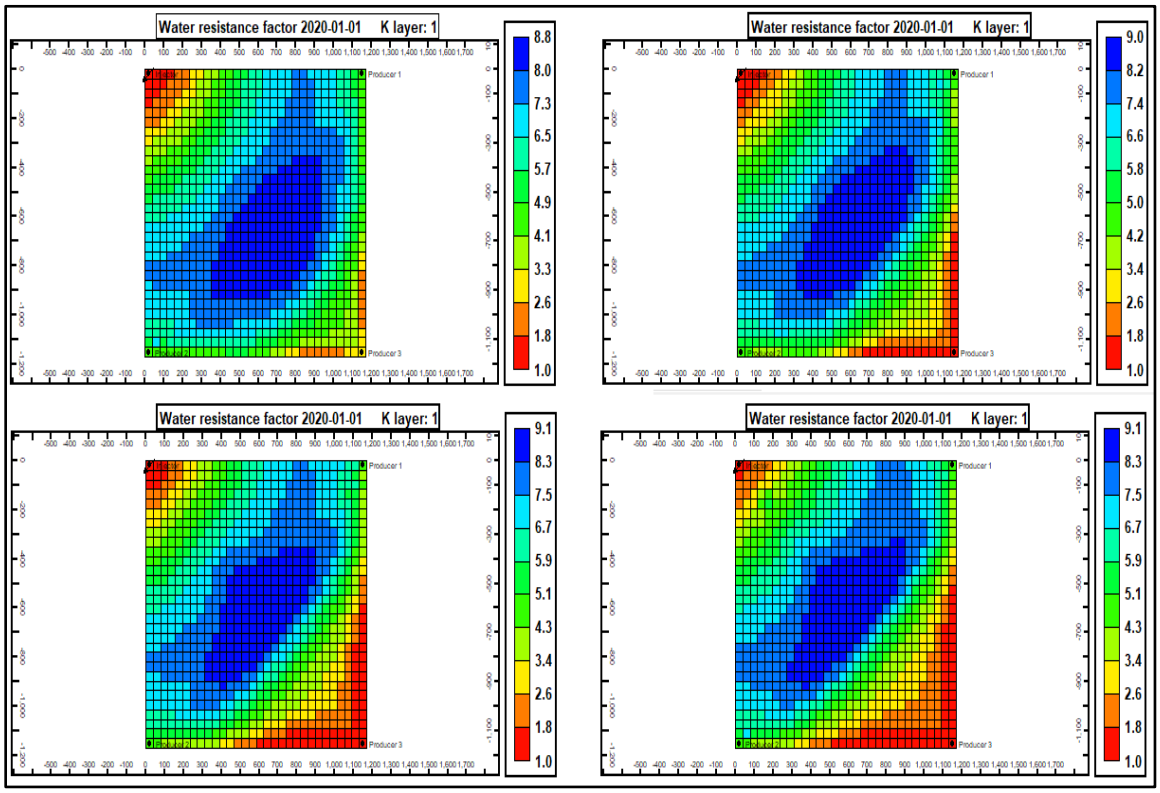

Figure 14. Comparison of permeability reduction (residual resistance factor) in layer 1 at 0% (upper left), 15% (upper right), 25% (lower left), and 35% (lower right) polymer hydrolysis.

5. CONCLUSIONS

1. CDG propagated deeper and generated higher residual resistance factor than polymer solution in the high-permeability layers.
2. Shear-thinning behavior of CDG assisted the selective penetration into the high-permeability layers only.
3. The permeability reduction generated by CDG was not easy to remove, even with reversible adsorption and prolonged post-treatment water injection.

4. Two types of gel degradations affected the performance of CDG: chemical and mechanical degradations.
5. For both types of gel degradation, the higher the degree of degradation, the lower the recovery factor.
6. Increasing the salinity of the reservoir brine and/or the makeup water lowers the strength of the formed CDG and lower the recovery factor.
7. In-depth gel treatment should be considered the only method of blocking high-permeability layers and diverting the post-treatment water injection into the low-permeability layer for thick heterogeneous reservoir with crossflow.
8. Starting the treatment with gel followed by polymer makes the remaining crosslinkers from gel treatment attach to the subsequent injected polymer; therefore, it creates a higher recovery factor and higher incremental oil.
9. Regardless of the sequence of gel and polymer injection, the combination injection of gel and polymer always yielded higher results than using the gel treatment alone.
10. Water-wet conditions are more favorable than oil-wet conditions for the application of the CDG treatment.
11. The lower the polymer/crosslinker ratio, the higher the penetration into the high permeability layers, which leads to high recovery factor and low RRF.
12. The higher the degree of HPAM hydrolysis, the higher the recovery factor, and the higher the permeability reduction in the thief zones.

NOMENCLATURE

CDG	=	Colloidal dispersion gel
C1, C2, and C3	=	Mass concentrations in the aqueous phase
K	=	The first order rate constant
$\tau_{1/2}$	=	The half-life of the component (i.e., polymer and crosslinker)
r_k	=	Reaction rate, kg/ (min.cm^3)
k	=	Rate constant, 1/min
C_i	=	Reactant i concentrations [kg/cm^3]
e_k	=	Order of reaction for the ith component, dimensionless
n_c	=	Total number of reactant components
r_{rk}	=	Reaction frequency factor (must be non-negative), 1/min
E_a	=	Activation energy, J/gmole or BTU/lbmole
R	=	Molar gas constant, 8.3145 J/ (^{o}K. mole)
T	=	Temperature, ^{o}K
k_w	=	Effective water permeability, md
μ_w	=	Water viscosity, cp
k_p	=	Effective polymer permeability, md
μ_p	=	Polymer viscosity, cp
RK_w	=	Water phase permeability-reduction factor
RRF	=	Residual resistance factor
Ads_{max}	=	Maximum adsorption level at maximum concentration, gm/cm^3 PV
Ads_i	=	Adsorption level of component i at concentration C, gm/cm^3 PV

k_{rw} = Water relative permeability, $dimensionless$

k_{ro} = Oil relative permeability, $dimensionless$

k_{rw}° = Water relative permeability at endpoint saturation, $dimensionless$

k_{ro}° = Oil relative permeability at endpoint saturation, $dimensionless$

S_w = Water saturation, $fraction$

S_{wi} = Irreducible water saturation, $fraction$

S_o = Oil saturation, $fraction$

S_{or} = Residual oil saturation, $fraction$

n_w , n_o = Corey exponents for water and oil phases, respectively

ACKNOWLEDGMENTS

The financial support of The Iraq Ministry of Oil and ExxonMobil Iraq (Training Technology & Scholars Program) is gratefully acknowledged.

REFERENCES

[1] Sheng, J.J. 2011. Modern Chemical Enhanced Oil Recovery: Theory and Practice. Burlington, MA, USA: Gulf Professional Publishing.

[2] Abdulbaki, M., Huh, C., Sepehrnoori, K., et al. 2014. A Critical Review on use of Polymer Microgels for Conformance Control Purposes. *J Petrol Sci & Eng* **122**: 741-753. https://doi.org/10.1016/j.petrol.2014.06.034.

[3] Ranganathan, R. Lewis, R., McCool, C.S. et al. 1998. Experimental Study of the Gelation Behavior of a Polyacrylamide/Aluminum Citrate Colloidal-Dispersion Gel System. *SPE J* **03** (04): 337-343. SPE-52503-PA. https://doi.org/10.2118/52503-PA.

[4] Shiyi, Y., Dong, H., Qiang, W. et al. 2000. Numerical Simulation Study on Weak Gel Injection. Presented at the SPE Asia Pacific Oil and Gas Conference Exhibition, Brisbane, Australia, 16-18 October. SPE-64291-MS. https://doi.org/10.2118/64291-MS.

[5] Sydansk, R.D. 1988. A New Conformance-Improvement-Treatment Chromium (III) Gel Technology. Presented at the SPE Enhance Oil Recovery Symposium, Tulsa, Oklahoma, USA, 16-21 April. SPE-17329-MS. https://doi.org/10.2118/17329-MS.

[6] Mack, J.C. and Smith, J.E. 1994. In-Depth Colloidal dispersion Gels Improve Oil Recovery Efficiency. Paper SPE/DOE 27780 Presented at the SPE/DOE Ninth Symposium on IOR, Tulsa, Oklahoma, USA, 17-20 April. SPE-27780-MS. https://doi.org/10.2118/27780-MS.

[7] Smith, J.E., Liu, H., and Guo, Z. D. 2000. Laboratory Studies of In-Depth Colloidal Dispersion Gel Technology for Daqing Oil Field. Presented at the SPE/AAPG Western Regional Meeting, Long Beach, California, USA, 19-22 June. SPE-62610-MS. https://doi.org/10.2118/62610-MS.

[8] Chang, H.L, Sui, X. Xia, L. et al. 2006. Successful Filed Pilot of In-Depth Colloidal Dispersion Gel (CDG) Technology in Daqing Oil Field. *SPE Res Eval & Eng* **09** (06): 664-673. SPE-89460-PA. https://doi.org/10.2118/89460-PA.

[9] Diaz, D. Saez, N. et al. 2015. CDG in a Heterogeneous Fluvial Reservoir in Argentina: Pilot and Field Expansion Evaluation. Presented at the SPE/EOR Kuala Lumpur, Malaysia, 11-13 August. SPE-174704-MS. https://doi.org/10.2118/174704-MS.

[10] Manrique, E. and Lantz, M. 2011. Colloidal Dispersion Gels (CDG) and their Application in Wyoming and Elsewhere. The 3rd Annual Wyoming IOR/EOR Conference, Jackson Hole, Wyoming, USA.

[11] Muruaga, E., Flores, M.V., Norman, C. et al. 2008. Combining Bulk Gels and Colloidal Dispersion Gels for Improved Volumetric Sweep Efficiency in a Mature Waterflood. Presented at the SPE Symposium on Improved Oil Recovery, Tulsa, Oklahoma, USA, 20-23 April. SPE-113334-MS. https://doi.org/10.2118/113334-MS.

[12] Sandoval, J.R., Manrique, E.J., Perez, H.H. et al. 2010. Dina Cretaceo Field Chemical EOR: From Screening to Pilot Design. Presented at the SPE Latin American and Caribbean Petroleum Engineering Conference, Lima, Peru, 1-3 December. SPE-139200-MS. https://doi.org/10.2118/139200-MS.

[13] Castro, R., Maya, J. et al. 2013a. Colloidal Dispersion Gels (CDG) in Dina Cretaceous Field: From Pilot Design to Field Implementation and Performance. Presented at the SPE Enhanced Oil Recovery Conference, Kuala Lumpur, Malaysia, 2-4 July. SPE-165273-MS. https://doi.org/10.2118/165273-MS.

[14] Castro, R., Maya, G.A., Sandoval, J.E. et al. 2013b. Colloidal Dispersion Gel (CDG) To Improve Volumetric Sweep Efficiency in WaterFlooding Processes. *CTF Cienc Tecnol Futuro* **05** (03): 61-78.

[15] Fielding Jr., R.C., Gibbons, D.H., and Legrand, F.P. 1994. In-Depth Drive Fluid Diversion Using an Evaluation of Colloidal Dispersion Gels and New Bulk Gels: An Operational Case History of North Rainbow Ranch Unit. Presented at the SPE/DOE IOR Symposium, Tulsa, Oklahoma, USA, 17-20 April. SPE-27773-MS. https://doi.org/10.2118/27773-MS.

[16] Manrique, E., Reyes, S., Romero, J. et al. 2014. Colloidal Dispersion Gels (CDG): Field Projects Review. Presented at the SPE EOR Conference at Oil and Gas West Asia, Muscat, the Sultanate of Oman, 31 March-2 April. SPE-169705-MS. https://doi.org/10.2118/169705-MS.

[17] Wang, W. Gu, Y., and Liu, Y. 2003. Applications of Weak Gel for In-Depth Profile Modification and Oil Displacement. J Can Pet Technol 42 (06): 54-61. PETSOC-03-06-04. https://doi.org/10.2118/03-06-04.

[18] Al-Assi, A.A., Willhite G.P., Green, D.W. et al. 2009. Formation and Propagation of Gel Aggregates using Partially Hydrolyzed Polyacrylamide and Aluminum Citrate. *SPE J* **14** (03): 450-461. SPE-100049-PA. https://doi.org/10.2118/100049-PA.

[19] Seright, R.S. 1994. Propagation of an Aluminum Citrate-HPAM Colloidal Dispersion Gel through Berea Sandstone. In Seright, R. 1995. Improved Techniques for Fluid Diversion in Oil Recovery Processes. Annual Report. Report No. DOE/BC/14880-10. U.S. DOE, Office of Fossil Energy, Washington, D.C., USA, September 1994 and March 1995. 51-64.

[20] Seright, R.S., Han, P., and Wang, D. 2006. Current Colloidal Dispersion Gels are not Superior to Polymer Flooding. *Petrol Geol & Oilfield Develop in Daqing* **25** (05): 71-80. Article ID: 1000-3754 (2006) 05-0071-10.

[21] Diaz, D., Somaruga, C., Norman, C. et al. 2008. Colloidal Dispersion Gels Improve Recovery in a Heterogeneous Argentina Waterflood. Presented at the SPE Symposium on IOR, Tulsa, Oklahoma, USA, 20-23 April. SPE-113320-MS. https://doi.org/10.2118/113320-MS.

[22] Alvand, E., Aalaie, J., Hemmati, M. et al. 2016. Colloidal dispersion gels based on sulfonated polyacrylamide and chromium triacetate for harsh-environment. Korean J Chem Eng 33 (06): 1654-1963. http://doi.org/10.1007/s11814-016-0025-6.

[23] Helleren, J. 2011. *Numerical Simulation of Chemical Flow-Zone Isolation*. M.Sc. Thesis, University of Stavanger, Faculty of Science and Technology, Department of Petroleum Engineering. http://hdl.handle.net/11250/183325.

[24] Al-Muntasheri, G.A., Nasr-El-Din, H.A., and Zitha, P.L.J. 2008. Gelation kinetics of an Organically Cross-Linked Gel at High Temperature and Pressure. *SPE J* **13** (03): 337-345. SPE-104071-PA. http://dx.doi.org/10.2118/104071-PA.

[25] Scott, T., Roberts, L.J., Sharpe, S.R., et al. 1987. In-situ Gel Calculations in Complex Reservoir Systems using a New Chemical Flood Simulator. *SPE Res Eng* **02** (04): 634-646. SPE-14234-PA. https://doi.org/10.2118/14234-PA.

[26] CMG-STARS User Guide, 2015.

[27] Clifford, P.J. and Sorbie, K.S. 1985. The Effects of Chemical Degradation on Polymer Flooding. Presented at the International Symposium on Oilfield and Geothermal Chemistry, Phoenix, Arizona, USA, 9-11 April. https://doi.org/10.2118/13586-MS.

[28] Chauveteau, G., and Kohler, N. 1974 Polymer Flooding: The Essential Elements for Laboratory Evaluation. Presented at SPE/IOR Symposium, 22-24 April. Tulsa, Oklahoma, SPE-4745-MS. https://doi.org/10.2118/4745-MS.

[29] Seright, R.S. and Martin, F.D. 1993. Impact of Gelation pH, Rock Permeability, and Lithology on the Performance of a Monomer-Based Gel. *SPE Res Eng* **08** (01): 43-50. SPE-20999-PA. https://dx.doi.org/10.2118/20999-PA.

[30] Jennings, R.R., Rogers, J.H., and West, T.J. 1970. Factors Influencing Mobility Control by Polymer Solutions. *J Pet Technol* **23**, (03): 391-401, SPE-2867-PA. https://doi.org/10.2118/2867-PA.

[31] Needham, R.B. and Doe, P.H. 1987. Polymer Flooding Review. *J Pet Technol* **39** (12):1503-1507. SPE-17140-PA. https://doi.org/10.2118/17140-PA.

[32] Bai, B., Wang, Q., Du, Y. et al. 2004. Factors Affecting In-Depth Gel Treatment for Reservoirs with Thick Heterogeneous Oil Layers. Presented at the fifth Canadian International Petroleum Conference, Calgary, Alberta, Canada, 8-10 June. PETSOC-2004-140. https://doi.org/10.2118/2004-140.

[33] Carpenter, C. 2016. Colloidal-Dispersion Gel in a Heterogeneous Reservoir in Argentina. *J Pet Technol* **68** (06): 82-83. SPE-0616-0082-JPT. https://doi.org/10.2118/0616-0082-JPT.

[34] Seright, R. S, Zhang, G., Akanni, O. et al. 2012. A Comparison of Polymer Flooding with In-Depth Profile Modification. *J Can Pet Technol* **51** (5): 393- 402. SPE-146087-PA. https://doi.org/10.2118/146087-PA.

[35] Zhidong, G. et al. 2011. Comparison of Oil Displacement Characteristics between CDG and Polymer Flooding in the Daqing Oilfield. Presented at SPE EOR Conference, Malaysia, 19-21 July. SPE-144119. https://doi.org/10.2118/144119-MS.

[36] Seright, R.S. 1988. Placement of Gels to Modify Injection Profiles. Presented at the SPE Enhanced Oil Recovery Symposium, Tulsa, Oklahoma, USA, 16-21 April. SPE-17332-MS. https://doi.org/10.2118/17332-MS.

[37] Seright, R.S. 1991. Effect of Rheology on Gel Placement. *SPE Res Eng* **06** (02): 212-218. SPE-18502-PA. https://doi.org/10.2118/18502-PA.

[38] Seright, R.S. 1996. Improved Methods for Water Shutoff. PRRC Report 96-23, Semi-Annual Technical Report, Submitted to BDM-OKLAHOMA/The US DOE.

[39] Hoefner, M.L., Seetharam, R.V., Shu, P. et al. 1992. Selective Penetration of Bioploymer profile-Control Gels: Experiment and Model. *J of Petrol Sci & Eng* 07 (1-2): 53-66. https://doi.org/10.1016/0920-4105(92)90008-O.

[40] Lee, K.S. 2011. Performance of a Polymer Flood with Shear-Thinning Fluid in Heterogeneous Layered Systems with Crossflow. *Energies* **04** (08): 1112-1128. https://doi.org/10.3390/en4081112.

[41] Green, D.W. and Willhite, G.P. 1998. *Enhanced Oil Recovery*, Society of Petroleum Engineers, Richardson, Texas, USA.

[42] Wang, D., Seright, R., Zhenbo, S. et al. 2007. Key Aspects of Project Design for Polymer Flooding. Presented at the SPE Annual Technical Conference and Exhibition, Anaheim, California, USA, 11-14 November. SPE-109682-MS. https://doi.org/10.2118/109682-MS.

[43] Manichand, R.N. and Seright, R. 2014. Field vs. Laboratory Polymer-Retention Values for a Polymer Flood in the Tambaredjo Field. *SPE Res Eval & Eng* **17** (03): 314-325. SPE-169027-PA. https://doi.org/10.2118/169027-PA.

[44] Hoteit, H., Alexis, D., Adepoju, O.O. et al. 2016. Numerical and Experimental Investigation pf polymer-Induced Resistance to Flow in Reservoirs Undergoing a Chemical Flood. Presented at the SPE Annual technical Conference and Exhibition, Dubai, UAE, 26-28 September. SPE-181720-MS. https://doi.org/10.2118/181720-MS.

[45] Asen, S.M., Stavland, A., Strand, D. et al. 2018. An Experimental Investigation of Polymer Mechanical Degradation at cm and m Scale. Presented at the SPE Improved Oil Recovery Conference, Tulsa, Oklahoma, USA, 14-18 April. SPE-190225-MS. https://doi.org/10.2118/190225-MS.

[46] Morris, C.W. and Jackson, K.M. 1978. Mechanical Degradation of Polyacrylamide Solutions in Porous Media. Presented at the SPE Symposium on Improved Oil Recovery, Tulsa, Oklahoma, USA, 16-17 April. SPE-7064-MS. https://doi.org/10.2118/7064-MS.

[47] Sorbie, K.S. 1991. *Polymer-Improved Oil Recovery*, CRC Press, Boca Raton, Florida, USA (1991).

[48] Sorbie, K.S. and Roberts, L.J. 1984. A Model for Calculating Polymer Injectivity Including the Effects of Shear Degradation. Presented at the SPE Enhance Oil Recovery Symposium, Tulsa, Oklahoma, USA, 15-18 April. SPE-12654-MS. https://doi.org/10.2118/12654-MS.

[49] Zaitoun, A., Makakou, P., Blin, N. et al. 2012. Shear Stability of EOR Polymers. SPE J 17 (02): 335-339. SPE-141113-PA. https://doi.org/10.2118/141113-PA.

[50] Brakstad, K. and Rosenkilde, C. 2016. Modelling Viscosity and Mechanical Degradation of Polyacrylamide Solutions in Porous Media. Presented at the SPE Improved Oil Recovery Conference, Tulsa, Oklahoma, USA, 11-13 April. SPE-179593-MS. https://doi.org/10.2118/179593-MS.

[51] Sheng, J.J. 2015. Status of surfactant EOR technology. *J. Petrol* **01** (02): 97-105. https://doi.org/10.1016/j.petlm.2015.07.003.

[52] Aldhaheri, M.N., Wei, M., and Bai, B. 2016. Comprehensive Guidelines for the Application of In-Situ Polymer Gels for Injection Well Conformance Improvement Based on Field Projects. Presented at the SPE Improved Oil Recovery Conference, Tulsa, Oklahoma, USA, 11-13 April. SPE-179575-MS. https://doi.org/10.2118/179575-MS.

[53] Abdulbaki, M.R. 2012. *Simulation Study of Polymer Microgel Conformance Treatments*. Master Thesis. The University of Texas at Austin, Austin, Texas, USA (2012).

[54] Aluhwal, O. 2008. Simulation Study of Improving Oil Recovery by Polymer Flooding in a Malaysian Reservoir. Master Thesis, Universiti Teknologi Malaysia. Kuala Lumpur, Malaysia (2008).

[55] Sedaghat, M.H., Ghazanfari, M.H., Masihi, M. et al. 2013. Experimental and numerical investigation of polymer flooding in fractured heavy oil five-spot systems. *J Petrol Sci Eng* 108: 370-382. https://doi.org/10.1016/j.petrol.2013.07.001.

[56] Vossoughi, S. 2000. Profile modification using in-situ gelation technology- A review. *J Petrol Sci & Eng* **26** (1-4): 199-209. https://doi.org/10.1016/S0920-4105(00)00034-6.

[57] Ahmed, T. 2001. *Reservoir Engineering Handbook* 2nd Edition, Gulf Professional Publishing.

[58] Shen, G.X., Lee J.H., and Lee, K.S. 2013. The Effects of Wettability on Gel Performance in Layered Heterogeneous Reservoirs. Applied Mechanics and Materials 448-453: 4028-4032. http://doi.org/10.4028/www.scientific.net/AMM.448-453.4028.

[59] Shen, G.X., Lee J.H., and Lee, K.S. 2014. Influence of Temperature on Gel Treatment under Various Reservoir Wettability Conditions. Presented at the Offshore Technology Conference Asia. Kuala Lumpur, Malaysia, 25-28 March. OTC-24853-MS. https://doi.org/10.4043/24853-MS.

[60] Tariq K. Khamees and Ralph E. Flori 2018. A comprehensive evaluation of the parameters that affect the performance of in-situ gelation system. *Fuel* 225: 140-160. https://doi.org/10.1016/j.fuel.2018.03.115.

[61] Tariq K. Khamees, Ralph E. Flori, Ahmed A. Alsubaih et al. 2018. Modeling the Effects of Salinity, Polymer Rheology, Temperature, and Reservoir Wettability on the Performance of In-Depth Gel Treatment Coupled with Surfactant and Polymer Flooding. Presented at the Abu Dhabi Petroleum Exhibition & Conference, Abu Dhabi, UAE, 12-15 November. SPE-193011-MS. https://doi.org/10.2118/193011.

[62] Martin, F.D. and Shrewood, N.S. 1975. The Effect of Hydrolysis of Polyacrylamide on Solution Viscosity, Polymer Retention and Flow Resistance Properties. Presented at the SPE Rocky Mountain Regional Meeting, Denver, Colorado, USA. 7-9 April. SPE-5339-MS. https://doi.org/10.2118/5339-MS.

III. NUMERICAL MODELING OF WATER-SOLUBLE SODIUM SILICATE GEL SYSTEM FOR FLUID DIVERSION AND FLOW-ZONE ISOLATION IN HIGHLY HETEROGENEOUS RESERVOIRS

Tariq K Khamees, Ralph E Flori, and Sherif M Fakher

Department of Geosciences, Geological, and Petroleum Engineering, Missouri University of Science and Technology, Rolla, MO 65409

ABSTRACT

This study presents a numerical modeling of a sodium silicate gel system (inorganic gel) to mitigate the problem of excess water production, which is promoted by high heterogeneity and/or an adverse mobility ratio. A numerical model of six layers was represented by one quarter of five spot pattern with two thief zones. CMG-STARS simulator was used that has the capabilities of modeling different parameters. The gelation process of this gel system was initiated by lowering the gelant's pH, and then the reaction process proceeded, which is dependent on temperature, concentration of the reactant, and other factors. An order of reaction of each component was determined and the stoichiometric coefficients of the reactants and product were specified. The purpose of this study is to develop a thorough understanding of the effects of different important parameters on the polymerization of a sodium silicate gel system.

This study was started by selecting the optimum gridblock number that represents the model. A sensitivity analysis showed that the fewer the number of gridblocks, the better the performance of the gel system. This model was then selected as a basis for other comparisons. Different scenarios were run and compared. The results showed that the gel

system performed better in the injection well compared to the production well. In addition, the treatment was more efficient when performed simultaneously in injection and production wells. Placement technology was among the parameters that affected the success of the treatment; therefore, zonal isolation and dual injection were better than bullhead injection. Lower activator concentration is more preferable for deep placement. Pre-flushing the reservoir to condition the targeted zones for sodium silicate injection was necessary to achieve a higher recovery factor. Moreover, different parameters such as adsorption, mixing sodium silicate with different polymer solutions, effects of temperature and activation energy, effects of shut-in period after the treatment, and effects of reservoir wettability were investigated. The obtained results were valuable, which lead to apply a sodium silicate gel successfully in a heterogeneous reservoir.

1. INTRODUCTION

To mitigate and alleviate water channeling through high permeability streaks or thief zones, a conformance improvement technology (CIT) should be implemented. Conformance improvement technology refers to the treatment that is applied to a heterogeneous or a naturally fractured reservoir to lower their heterogeneities by the injection of crosslinked polymer gels into high permeability streaks, or an injection of a polymer solution to lower the mobility ratio between displacing and displaced phases. The purpose of CIT is to distribute the post-treatment injected water more evenly between layers and to direct it into new unswept areas in the reservoir, thus increasing production and improving sweep efficiency.

Since the 1960s, different gel systems have been proposed in the oil industry for various purposes depending on their gelation mechanisms (i.e., in-situ versus performed) and chemical nature (i.e., organic versus inorganic). Silicate gels are inorganic-based gels that can be classified as an internal activated silicate (IAS), which can be used for conformance control applications, or an external activated silicate (EAS), which can be applied in the drilling operations (e.g., lost circulation). Silicate gels were first recognized by Mills in 1922 to modify reservoir permeability. Later, Robertson and Oelefein (1967) used silica acid gel for selectively plugging thief zones in an injection well in the Inglewood oil field in California. Their results showed the potential of silica gel to improve waterflooding efficiency. The applications of these silicate gels were used primarily for water shut-off in near-well treatments (Herring et al., 1984; Nasr-El-Din et al., 1998; Hatzignatiou et al., 2014). There are different field applications for using polymer silicate gel for water shut-off, such as in Hungarian oil fields (Lakatos et al., 1999) and the offshore Statfjord field (Boreng and Svendsen, 1997). The latter field is located in the boundary line between the Norwegian and British continental shelves, in which a reduction of 16% in watercut has been achieved due to the treatment.

In recent years, silicate gels received a great deal of attention for their deep penetration into thief zones (Krumrine and Boyce, 1985; Stavland et al., 2011; Helleren, 2011; Hamouda and Amiri, 2014; Amiri et al., 2014; Hatzignatiou et al., 2014). The success of the sodium silicate as an in-depth reservoir treatment in the Snorre field, offshore of Norway, in which a 40 m permeability restriction away from the wellbore was achieved, justified the using of this inorganic system for water management (Skrettingland et al., 2012). The use of the sodium silicate (Na-silicate) for an in-depth reservoir treatment was

motivated by the following factors (Lakatos et al., 1999; Lakatos and Lakatos-Szabo, 2012: Hamouda and Amiri, 2014):

- Low initial viscosity (suitable for injectivity).
- Inexpensive chemicals with thermal stability (suitable for high temperature reservoirs).
- Resistance to chemical and biological attack.
- Long gelation time (i.e., up to several days).
- Low to moderate cost.
- Green chemicals (environmentally benign).
- It does not damage the formation in case of failure.

However, this gel system has disadvantages: (Hamouda and Amiri, 2014; Pham and Hatzignatiou, 2016):

- Weak gel system.
- Fluid is expelled out of solution (i.e., syneresis).
- Long-term shutoff capability is questionable.
- Precipitates of silicate may form instead of gels.
- Gelation time is hard to control.
- The gelation mechanism is complicated because of its chemistry.

However, the popularity of using sodium silicate as a conformance control agent started 20 years ago, when Norwegian authorities gave their permission to use it in the Norwegian continental shelf of the North Sea (Amiri, 2014).

2. TYPES OF SILICATE SYSTEM

2.1. ACIDIC GEL SYSTEM

High acid concentrations, mainly HCl and H_2SO_4, are used in acidic gels; thus, the pH value ranges from 4.0 to 6.0. Acidic silicate gels are stiff, rigid, and opalescent materials. The main advantages of acid gel are good thermal stability in reservoirs with temperatures up to 200 °F and low to moderate cost. This gel system is characterized by rapid gelation. Thus, the applications of these types of gels are useful for near-wellbore regions within an area of 20 ft (Krumrine and Boyce, 1985).

2.2. ALKALINE SILICA GELS

Compared to acidic gel systems, considerably less acid or a weaker acid is used to make alkaline silica gel systems. This gel system uses the same silicate concentration and molar ratio as acidic gel systems; however, the main difference is in the gelation mechanism. Smith et al. (1969) reported that this gel system has a longer gelation time, which makes this gel suitable for deep reservoir treatment.

3. SODIUM-SILICATE CHEMISTRY

Commercial sodium silicate is a clear and a stable solution with a pH in the range of 11-13 (Pham and Hazignatiou, 2016). Sodium silicate (also known as water glass), identified by $(SiO_2)n.Na_2O$, is produced by heating silica and sodium carbonate to a very high temperature (i.e., above 1300°C). The molar ratio (n) of SiO_2 to Na_2O plays an important role in the chemical behavior of Na-silicate (Iler, 1979). In addition, the molar

ratio affects the alkalinity. Thus, the tolerance of the gel system to significant amounts of acid is indicated by a low molar ratio (Hatzignatiou et al., 2014). In general, the molar ratio ranges from 1.6 to 3.9, and the alkalinity increases by decreasing this value (Pham and Hatzignatiou, 2016). The polymerization, occurs as follows (Krumrine and Boyce, 1985; Hatzignatiou et al., 2014; Pham and Hazignatiou, 2016):

- Monomer and dimer silicate species are condensed to form particles.
- Growth of particles.
- Linking of individual particles together into branched chains.
- Extension of the network through liquid medium, thickening it to gel.

Thus, instead of crosslinking, the gelation occurs due to polymerization and condensation. Figure 1 shows the polymerization process of silica (Iler, 1979). The initiation of the gelation happens once the gelant's pH value is reduced below 11.0 (Pham and Hatzignatiou, 2015). When the pH of the solution is above 11.0, the particles repel each other. Thus, no gel is formed in mixtures with a pH greater than 11.0 (Krumrine and Boyce, 1985).

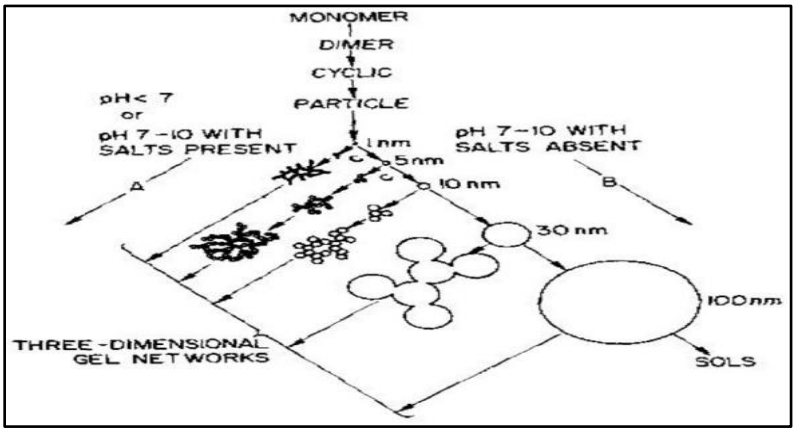

Figure 1. Polymerization process of silicate system (Iler, 1979).

4. FACTORS AFFECTING GELATION TIME

Long gelation time is considered as the most important parameter for in-depth gel treatment. However, for silicate gel systems, a longer gelation time leads to a weaker gel (Hamouda and Amiri, 2014), which could jeopardize the deep reservoir treatment. Gelation time is defined as the time when the viscosity deviates from linearity on the viscosity versus time curve, which indicates the start of gelation or transition from solution to gel (Pham and Hatzignatiou, 2016). In addition, the gelation time depends on the reaction rate of the gel (Hatzignatiou et al., 2014). In general, the reaction rate and the gelation time are related to each other, in which the reaction rate depends on the concentration of the reactants (i.e., polymer, crosslinker, and additives), temperature, and interactions with the reservoir fluids and rocks (Hatzignatiou et al., 2016). Increasing the concentration of the reactants will decrease the gelation time (Prud'homme and Uhl, 1984; Southard et al., 1984; Al-Muntasheri et al., 2008). For a sodium-silicate gel, inorganic and organic compounds control the gelation. In addition, the gelation time and gel strength depend on the following (Krumrine and Boyce, 1985; Yang et al., 2007: Stavland et al., 2011; Hamouda and Amiri, 2014; Hatzignatiou et al., 2014; Pham and Hatzignatiou, 2016):

- Silicate content: gelation time decreases with increasing silicate content.
- Solution pH: small changes in pH had a large effect on the gelation time. To control the gelation time, HCl concentration should be adjusted.
- Temperature: an increase in temperature promotes more rapid gelation, which reduces the gelation time.

- Salinity and divalent cations (Ca^{++} and Mg^{++}): increases the possibility of precipitation, which reduces the gelation time (e.g., Ca^{++} increase precipitation via ion exchange).
- Shear rate: silicate gel displays a viscoelastic behavior. Dynamic results show shear-thickening behavior at a high shear rate, and Newtonian behavior at a low shear rate. In general, gelation time decreased as the shear rate increased.

Krumrine and Boyce (1985) stated that the hostile environment of the reservoir (e.g., high salinity, hardness, and high temperature) palys an important role of accelerating the gel formation. Kim (1995) stated that the effect of pH on gelation time is much higher than the effect of temperature.

5. SILICATE GEL KINETICS

Jurinak and Summers (1991) assumed the gelation time of the silicate gel follows a first-order Arrhenius temperature dependence; thus, Stavland et al. (2011) presented the following equation:

$$t_{gel} = A.e^{\propto[Si]}.e^{\beta[HCl]}.e^{\gamma[Ca^{2+}]}.e^{\frac{E_a}{RT}} \quad (1)$$

where:

t_{gel} = Gelation time, days

A = Gelation time tunning parameter (2.1×10^{-8})

Si = Silicate concentration, wt%

HCl = Hydrochloric acid concentration, wt%

Ca^{2+} = Calcium concentration, ppm

$\propto$ = -0.6, 1/wt.%

β = -0.7, 1/wt.%

γ = -0.1, 1/wt.%

E_a = Activation energy, 77 kJ/mol

R = Molar gas constant, 8.3145 J/°K.mol

T = Temperature (°K)

In general, for modeling the gel treatment using numerical simulators, the gel is formed according to the following simple reaction:

$$Polymer\ (C_1)\ + Crosslinker\ (C_2)\ \rightarrow Gel\ (C_3) \qquad (2)$$

where $C_i's$ represent the the mass concentrations of th reactants in the aqueous phase (Scott et al., 1987). The reaction kinetics of silicate gel occurs due to polymerization; thus, there is no crosslinking of polymer with crosslinker. However, the concept of forming gel using numerical modeling still follows Equation 2; the reactant componenets are reacting together to form the gel.

In CMG-STARS, the stoichiometric coefficients of the reactants and the product should be in mass equilibrium:

$$\sum_i(\omega_{1,i})(MW_i)\ =\ \sum_i(\omega_{2,j})(MW_j) \qquad (3)$$

where MW_i and MW_j represent the molecular mass of reactants and product, respectively (kg/gmol). The silicate-solution chemistry to form gel is complex and not fully understood (Iler, 1979). However, Hatzignatiou et al. (2014), proposed the following simplified chemical reaction to describe the interaction between the chemicals, which resembles Equation 2:

$$\omega_{1,Si}.S_i + \omega_{1,HCl}.HCl + \omega_{1,Al^{3+}}.Al^{3+} + \omega_{1,Ca^2}\,Ca^{2+} \rightarrow \omega_{2,Gel}.Gel \qquad (4)$$

where $\omega_{1,i}$ is the stoichiometric coefficient of the reactants (i.e., silicate, HCl, aluminum, and calcium) and $\omega_{2,Gel}$ is the stoichiometric coefficient of the formed gel. Thus, the stoichemtric coefficients of the reactants that are shown in Equation 4 were concluded to represents the transformation of the injected components to 100% gel that has a molecular mass equal to 0.119 kg/gmol (Hatzignatiou et al., 2014):

$$15\ S_i + 47.6\ HCl + 0.015\ Al^{3+} \rightarrow 62.615\ Gel \qquad (5)$$

6. RESERVOIR AND MODEL DESCRIPTION

A three-dimensional model representing one quarter of a five spot pattern was used in all runs. The model represents a heterogeneous reservoir that consisted of six layers, with two thief zones (layers 3 and 4) located in the middle of the model as shown in Figure 2. The dimensions of the model were 625×625×120 ft^3 with one injection well and one production well located at opposite corners and drilled through all reservoir layers. The thickness of each layer was 20 ft and the porosity of the model was 20%. The horizontal permeability of the thief zones and low permeability layers were 10,000 md and 100 md, respectively. In all runs, the vertical/horizontal permeability ratio ($\frac{k_v}{k_H}$) was set at 0.01. The oil viscosity was 5.0 cp, and the water viscosity was 0.86 cp. These values yielded an end-point mobility ratio of 1.94.

The reservoir was represented by 25 gridblocks in the *x* and *y* directions and 6 gridblocks in the vertical direction. The fluid injection rate was 535 bbl/day (3004 ft^3/day), and a sodium silicate solution was injected at the same injection rate for 30 days. Tables 1 and 2 provide the reservoir and fluid characteristics used in the numerical modeling of the

sodium silicate gel. In addition, two rock types were used: rock type 1 for low-permeability layers, and rock type 2 for high-permeability layers, as shown in Figure 3. For both rock types, the same saturation and relative permeability end-point were used. However, a linear saturation dependence was used in theif zones as proposed by Scott et al. (1987). STARS™, an application of CMG (Computer Modeling Group), was used to run different scenarios to study the effects of different parameters on the performance of sodium silicate gel.

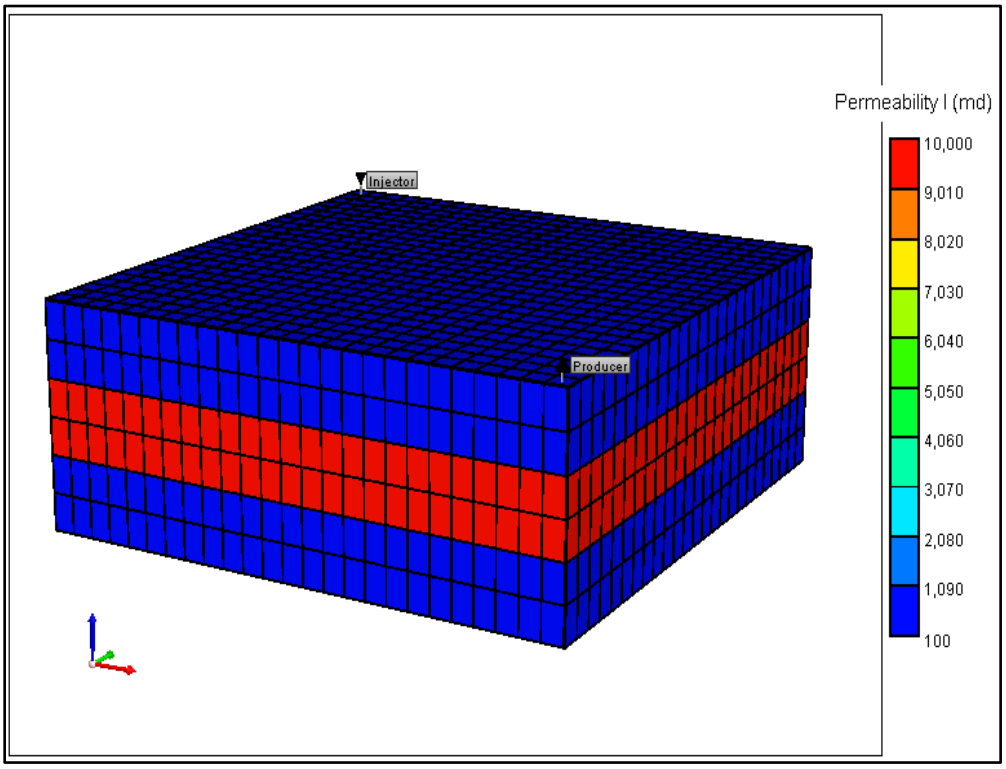

Figure 2. Six-layer heterogeneous reservoir model.

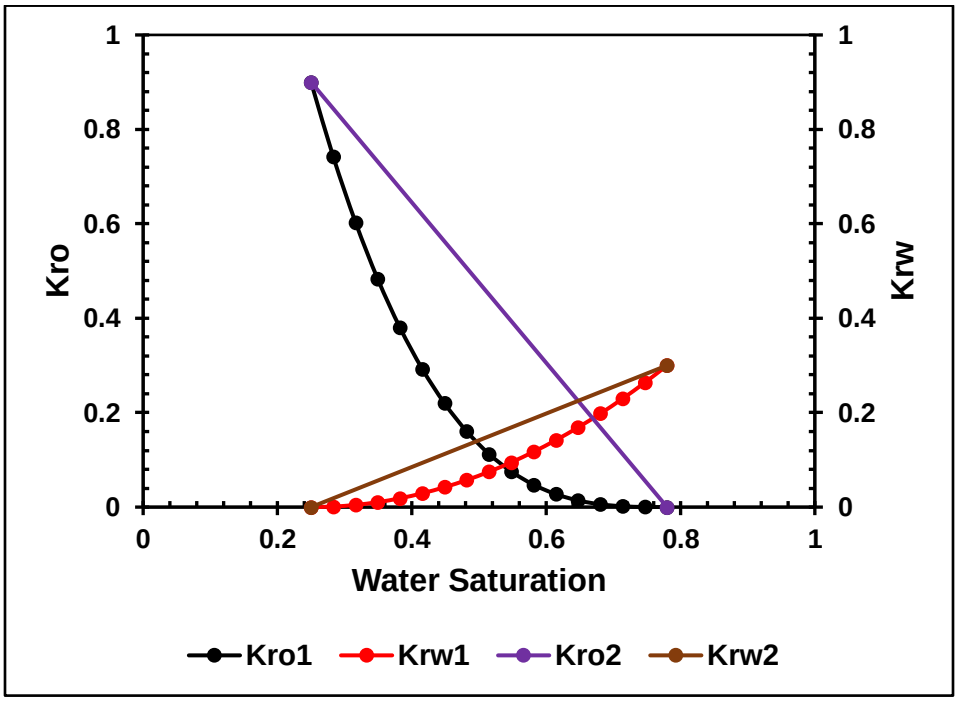

Figure 3. Relative-permeability curves for the two rock types in the model (Scott et al., 1987).

Table 1. Reservoir characteristics.

Initial reservoir pressure	3,000 psi
Initial reservoir temperature	120 °F
Length, *x*	625 ft
Width, *y*	625 ft
Thickness, *z*	120 ft
NX	25
NY	25
NZ	6
Gridblock size in x and y directions	25 ft
Layers thickness	20 ft
Layers porosity	20%
Low- and high-permeability regions: $k_x = k_y$	100 md and 10,000 md

Table 1. Reservoir characteristics (Cont.).

k_v/k_h	0.01
Well constraints:	
Injection rate	535 bbl/day
Well radius	0.4 ft.
Well pattern	One quarter of 5-spot

Table 2. Fluid properties.

Viscosity data:	
Water viscosity	0.86 cp
Oil viscosity	5.0 cp
Saturation data:	
Initial water saturation	0.25
Residual oil saturation	0.22
Relative permeability data:	
Endpoint Kr_w	0.3
Endpoint Kr_o	0.9
Corey exponent:	
Water exponent	2.0
Oil exponent	2.0
Endpoint mobility ratio	1.94
Fluid densities:	
Water density	62.4 lb/ft^3
Oil density	44.0 lb/ft^3

7. INJECTION SCHEMES

For all scenarios, a 0.33 PV of pre-treatment water was injected until the water cut in the producing well reached 97%. The sodium silicate solution injection was preceded by pre-flushing the reservoir for 60 days (i.e., 0.02 PV) with monovalent ions such as NaCl or KCl. A 1.0 wt% of KCl brine was used in the pre-flush stage with the purpose to eliminate or reduce the concentration of divalent cations (e.g., Ca^{++}). The presence of divalent cations caused a chemical reaction with the sodium silicate, which caused faster gelation and promoted the precipitation of $Mg(OH)_2$ from the silicate solution (Hatzignatiou et al., 2014). Moreover, the effect of cation exchange necessistated the pre-flush stage before the treatment (Stavland et al., 2011a). The injection of sodium silicate solution was initiated immediately after the pre-flush, which continued for 30 days (i.e., 0.029 PV). The total volume of 2 wt% sodium silicate solution was equal to 16,585 bbls, which was calculated based on volume sizing strategy (Smith 1999). In this strategy, 3-5% of moveable pore volume (MPV) of the thief zones should be considered to calculate the slug size of the gelant solution. In this study, the injected pore volume of the sodium silicate solution was computed based on the pore volume of the high permeability streaks only since this solution was injected into these two thief zones (i.e., layers 3 and 4). The pore volumes of pre- and post-treatment water were calculated based on the total pore volume of the model, because water had access to all open layers. Thus, 3% of MPV of layers 3 and 4 was used to fill a portion of these thief zones. The injection well was shut-in for 30 days as recommended in field applications to allow the completion of the gelation process and to produce a strong gel (Pham and Hatzignatiou, 2016). Finally, post-treatment water

injection was resumed for the rest of the simulation time, in which 1.38 PV was injected. The injection process and injected pore volumes are presented in Table 3.

Table 3. Injection schedule.

Sequence of the injected fluid	Status of the injection well	Injected PV	Time of injection (from-to) mm/dd/yr
Pre-treatment water	Open for injection	0.330	01/01/95-11/01/97
Pre-flush with KCl	Open for injection	0.020	11/01/97-12/31/97
Sodium-silicate solution	Open for injection	0.030	01/01/98-01/31/98
	Shut-in	0.00	02/01/98-03/01/98
Post-treatment water	Open for injection	1.380	03/01/98-01/01/2010

8. FORMATION OF GEL

The formation of gel in a sodium silicate system is initiated by reducing the pH of the solution (Pham amd Hazignatiou, 2016). Therefore, adding acid such as HCl will decrease the gelant's pH and initiate the gelation process. In addition, reducing the pH of the solution could happen by decreasing the alkalinity by reservoir rocks and ion exchange, which accelerate the gelation process. This alkalinity consumption increases at high temperatures. The latter gel system is often referred to as an acidic gel system. However, the gelation of a silicate system still happened when the pH of the solution remained under 11.0 (Pham amd Hazignatiou, 2016). This gel system is called an alkaline gel system, which is characterized by short gelation time; thus, it is not suitable for deep placement (Hamouda and Amiri, 2014). On the other hand, another silicate system has been tested by

Stavland et al. (2011a, 2011b) in which the gelation is not triggered by pH. The resultant gels had a strong resistance to acid breakdown.

8.1. CHEMICAL REACTION

Based on the simplified chemical reaction that was presented in Equation 4, the stoichiometric coefficients of HCl, silicate, and aluminum were established as 167, 70.05, and 0.06, respectively, and the stoichiometric coefficient of the resultant gel was 63.09 with a molecular mass of 225 lb/lbmole. Hence, Equation 4 can be expressed as:

$$70.05\, S_i + 167 HCl + 0.06 Al^{3+} \rightarrow 63.09\, Gel \qquad (6)$$

This equation stated that the reacting components should have the abovementioned stoichiometric coefficients to produce a gel with a stoichiometric coefficient equal to 63.09. However, the reaction rate is affected by the concentration of reactants and the order of reactions as explained in the next section.

8.2. GEL KINETIC MODEL IN STARS SIMULATOR (REACTION KINETICS)

The gel modeling in the STARS simulator depends on the interaction of at least two chemical components in the injected gelant, which should react together to form the gel. Then, the produced gel is adsorbed/retained in the formation (CMG-STARS Technical Manual, 2015). The reaction kinetics in the STARS simulator is given by:

$$r_k = k \prod_{i=1}^{n_c} C_i^{e_k} \qquad (7)$$

$$k = r_{rk.}\, e^{-\frac{E_a}{RT}} \qquad (8)$$

Substituting Equation 8 in Equation 7 yields:

$$r_k = r_{rk.}\, e^{-(\frac{E_a}{RT})} . \prod_{i=1}^{n_c} C_i^{e_k} \quad (9)$$

where

r_k = Reaction rate, kg/ min.cm^3.

k = Rate constant, 1/min.

C_i = Reactant i concentrations, kg/cm^3.

e_k = Order of reaction for the ith component, dimensionless.

n_c = Total number of reactant components.

r_{rk} = Reaction frequency factor (must be non-negative), 1/min.

E_a = Activation energy, J/g.mol or BTU/lb.mol.

R = Molar gas constant, 8.3145 J/^{o}K.mol.

T = Temperature, ^{o}K.

Reaction rate and gelation time are dependent on the concentrations of the reactants. Higher concentrations would result in higher collisions between the molecules, which would result in shorter gelation time. In STARS simulator, Equation 9 is used to model the creation of the gel. Table 4 presents a summary of mass fractions, concentrations, and an order of reactions for the reactant components. Note that calcium is not involved directly in the chemical reaction as suggested by Hatzignatiou et al. (2014); thus, the order of the reaction of calcium is set equal to zero.

9. PLACEMENT METHODS

In field applications of gel technology, there are several methods of injecting these chemicals. Two of the methods that are widely used are mechanical packer and bullhead

placements. In the first method, the gelant or preformed gel is injected into high permeability layers only (i.e., the gel has access to thief zones only). To achieve this goal, mechanical packers or bridge plugs are used to protect the oil zones and to ensure that the treatment will enter only the fractures or the thief zones. This method is very useful in the placement of gel in unfractured wells that are characterized by radial flow in matrix near-wellbore region because the protection of hydrocarbon productive zones is necessary during the treatment (Seright, 1996). Bullhead placement is considered the simplest and most economical placement method in which the treatment is injected without isolating the targeted zone (i.e., the gel has access to all open layers or perforations) (Bai et al., 2004).

Despite the differences between these two placement technologies, the researchers used both methods to inject sodium silicate gel. Rolfsvag et al. (1996) presented the results of the second treatment in Gullfaks, in which 4000 m^3 of gelant solution was injected after installing packer between the two perforated intervals (i.e., zonal isolation). Hatzignatiou et al. (2014) showed the experimental and numerical modeling results of sodium silicate gel, in which the gelant solution is bullheaded at a sufficiently large injection rate at a bottomhole pressure less than the fracture pressure of the formation. Moreover, Lakatos et al. (2011) used bullhead injection for placement of the silicate system.

Therefore, in this study, two placement technologies were used and the results were compared. In addition, another placement method (i.e., dual-injection), was also investigated. In this method, the sodium silicate solution had access to high permeability layers only through the well's tubular, while water had access to low permeability layers only through the annulus (while there is free crossflow between these layers). To model this method in the simulator, another well with the same location as the injection well was

assumed. This well was only operating during gel treatment with sodium silicate gel to mimic the injection of nondamaging water into the oil zone through the annulus.

Table 4. Mass fractions, concentrations, and order of reactions.

Parameter	H_2O	Na-Silica	Ca^{2+}	HCL	AL^{3+}
MW, lb/lbmole	18.015	225.0	40.078	72.9	26.98
Mass Fraction, Wi	0.9561785	2e-02	1.0e-05	2.38e-02	1.15e-05
Order of Reaction	0.0	0.1	0.0	3.0	0.1

10. RETENTION AND PERMEABILITY REDUCTION

Chemical loss during flow in porous media is classified into three mechanisms: adsorption, mechanical entrapment, and hydrodynamic retention (Willhite and Dominguez, 1977). Adsorption is instantaneous and irreversible, mechanical trapping is irreversible and hydrodynamic retention is reversible (Green and Willhite, 1998). However, it is difficult to differentiate these three mechanisms; thus, the term retention is normally used to describe the chemical loss (Sheng, 2011). In numerical modeling of chemical enhanced oil recovery using the STARS simulator, two keywords are used to describe the blocking of the porous media. These keywords are represented in Table 5.

The permeability reduction factor or RRF is related to the adsorption level as given in Equation 10. The mobility of the water phase is divided by RK_w, thus accounting for blockage (CMG-STARS Technical Manual, 2015):

$$RK_w = 1.0 + (RRF - 1.0)\left(\frac{Ads_i}{Ads_{max}}\right) \quad (10)$$

where

RK_w = Water phase permeability-reduction factor

RRF = Residual resistance factor

Ads_{max}= Maximum adsorption level at maximum concentration, gm/cm^3 PV

Ads_i = Adsorption level of component i at concentration C, gm/cm^3 PV

The adsorption of sodium silicate gel and RRF that proposed by Rolfsvag et al. (1996), were used in this study, as shown in Tables 6 and 7.

Table 5. Retention keywords in CMG-STARS simulator.

Keywords in STARS	Types	Explanation
ADMAXT (max. adsorption level)		Maximum adsorption capacity (gmole/ft3, kg/cm3) Included in the flow equation as, $\frac{\partial}{\partial t}\ [\varphi Adi]$
ADRT (residual adsorption level)	• Irreversible adsorption • Reversible adsorption • Partially reversible adsorption	• ADRT=ADMAXT • ADRT=0 • 0<ADRT<ADMAXT
PORFT	Accessible PV=(1-Inaccessible PV)	Molecules are larger than some pores in porous rock

In this study, RRF value in high permeability layers was assumed equal to 24, whereas in less permeable layers the value of RRF was assumed equal to 48, because resistance factors, residual resistance factors, and chemical retention vlaues ususally increase with decreasing permeability (Seright, 1996). The latter assumption reflects the

fact that severe damage could happen to low permeability layers if gel enters in these zones (Scott et al., 1987).

Table 6. Adsorption of sodium silicate gel (Rolfsvag et al., 1996).

Sodium silicate (weight fraction in solution	Irreversible adsorption (mg/g rock)	Reversible adsorption (mg/g rock)
0.00	0.20	0.00
0.02	0.20	0.42
0.04	0.20	0.80
0.06	0.20	1.17
0.10	0.20	2.00

Table 7. RRF as a function of the amount of gel (Rolfsvag et al., 1996).

Amount of gel (mg gel/ g rock)	RRF
0.0	1
1.6	8
3.2	16
4.8	24
6.4	32
8.0	40

11. SCENARIOS OF THE TREATMENT

A thorough investigation of different parameters was modeled to fully understand their effects on sodium silicate efficiency. These scenarios included the following:

- Sensitivity analysis of the model's gridblock.
- Injector versus producer treatment.
- Injector treatment versus simultaneous treatment of injector and producer.
- Placement technology.
- Effect of HCl concentration.
- Effect of pre-flush.
- Effect of adsorption.
- Comparison of sodium silicate and xanthan biopolymer mixture model versus sodium silicate and HPAM synthetic polymer mixture model.
- Effect of temperature and activation energy.
- Effect of shut-in time.
- Effect of reservoir wettability.

12. NUMERICAL SIMULATION RESULTS

12.1. SENSITIVITY ANALYSIS OF THE MODEL'S GRIDBLOCK

Before running the model, it was crucial to investigate the effect of the number of gridblocks of the model on the results. Two models were taken into account: a 25×25×6 model and a 50×50×6 model. The results showed how sensitive the sodium silicate treatment was on the number of gridblocks; the higher the gridblock number, the lower the recovery, as shown in Table 8 and Figure 4. Thus, the model that yielded a higher recovery factor (i.e., 25×25×6) will be used in the forthcoming sections.

Table 8. Effects of the number of gridblock of the model.

Model Dimension	25×25×6		50×50×6	
Parameter	WF	Na-silicate gel	WF	Na-silicate gel
Recovery Factor, %	29.00	34.90	29.10	33.70
Cumulative Oil, Bbl.	363,101	437,393	363,836	421,482
Incremental Oil, Bbl.		74,292		57,646

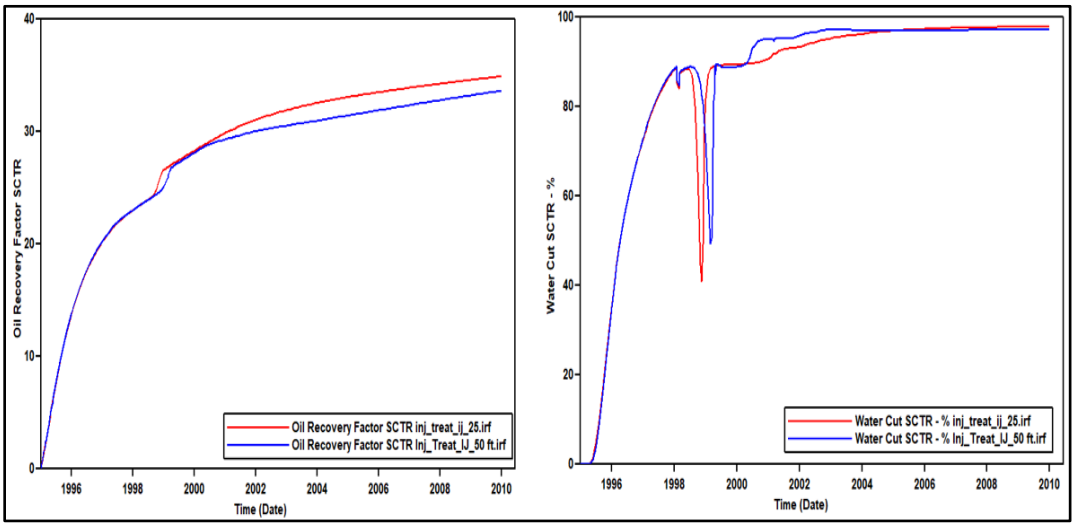

Figure 4. Oil recovery factor (left) and water cut (right) for (25×25×6) model (red curve) versus (50×50×6) model (blue curve).

12.2. INJECTOR, PRODUCER, AND COMBINED INJECTOR AND PRODUCER TREATMENTS

In field applications, silicate gel systems were used primarily for water shut-off in near-wellbore treatments (Herring et al., 1984; Hatzignatiou et al., 2014; Lakatos et al., 1999; Boreng and Svendsen, 1997). In water shut-off, the treatment is injected in the production well to lower the relative permeability to water without affecting oil relative permeability. However, in recent years, the application of sodium silicate as a profile

modification or in-depth reservoir treatment has attracted more attention (Krumrine and Boyce, 1985; Stavland et al., 2011; Helleren, 2011; Skrettingland et al., 2012; Hamouda and Amiri, 2014; Amiri et al., 2014; Hatzignatiou et al., 2014). In this section, an injector versus a producer treatment was modeled, in addition to simultaneous treatment of injector and producer. Tables 9 and 10 represent these results, which clearly demonstrated that sodium silicate gel was more efficient as a blocking agent when it was used in the injector. Moreover, the concurrent treatment of the injector and the producer was even more efficient than the injector treatment only.

Table 9 is presented graphically in Figure 5, which shows that producer treatment is not promising in increasing the recovery factor. Therefore, injector treatment is much easier and more convenient than producer treatment because the injector treatment does not require shut-in of the production (Fletcher et al., 1992). In addition, when treatment was applied in the producer, the propagation of sodium silicate into high permability streaks was less than the propagation in the injector (Figure 6). This figure demonstrates that sodium silicate treatment in the producer behaves like a water shut-off agent, while in the injector it behaves like an in-depth reservoir treatment agent. Moreover, if sodium silicate acts as a disproportionate permeability reduction agent, it will allow oil to flow, but not water. In this case, water saturation will increase close to or beyond the gel bank, which will reduce the relative permeability of oil (Seright et al., 2003). Table 10 is presented graphically in Figure 7, which shows that the recovery factor and incremental oil were more noticable when applying the treatment in both sides (i.e., injector and producer) due to the dual effect of in-depth treatment and water shut-off.

Table 9. Sodium silicate behavior in injector versus producer.

Parameter	Water flood	Injector treatment	Producer treatment
Recovery factor, %	29.00	34.90	32.10
Cumulative oil, Bbl.	363,101	437,393	402,507
Incremental oil, Bbl.		74,292	39,406

Table 10. Sodium silicate behavior in injector only versus producer and injector together.

Parameter	Water flood	Injector treatment	Inj. and prod. treatment together
Recovery factor, %	29.00	34.90	40.80
Cumulative oil, Bbl.	363,101	437,393	510,862
Incremental oil, Bbl.		74,292	147,761

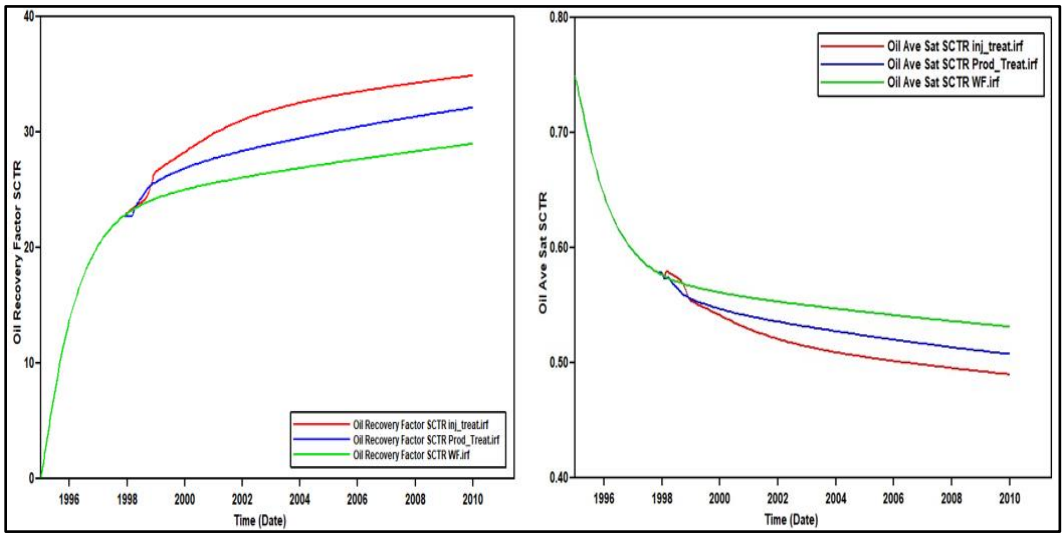

Figure 5. Oil recovery factor (left) and oil saturation reduction (right) for injector treatment (red) versus producer treatment (blue) compared with water flood (green).

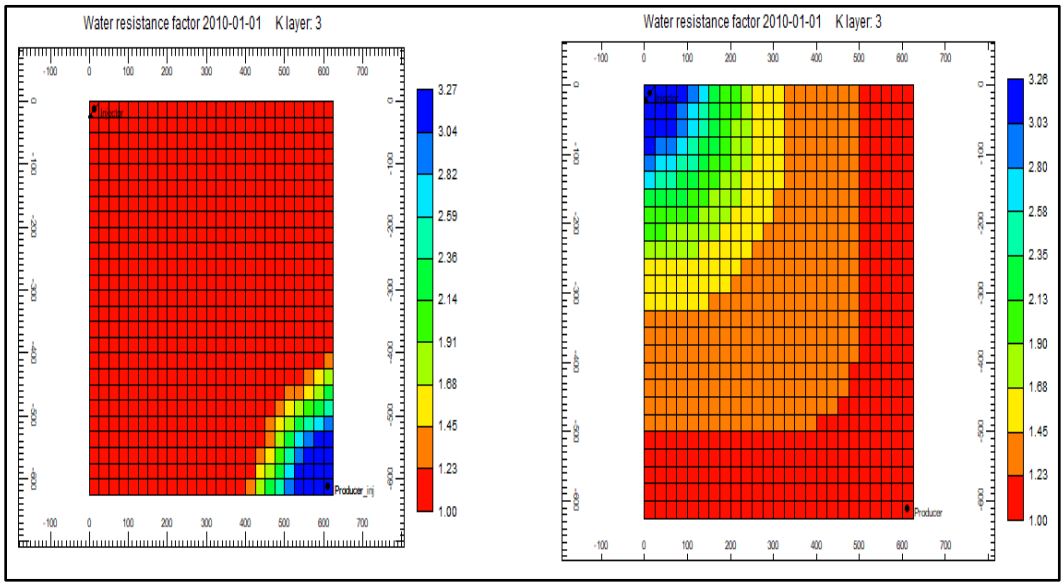

Figure 6. Water residual resistance factor in layer 3 in producer (left) versus injector (right).

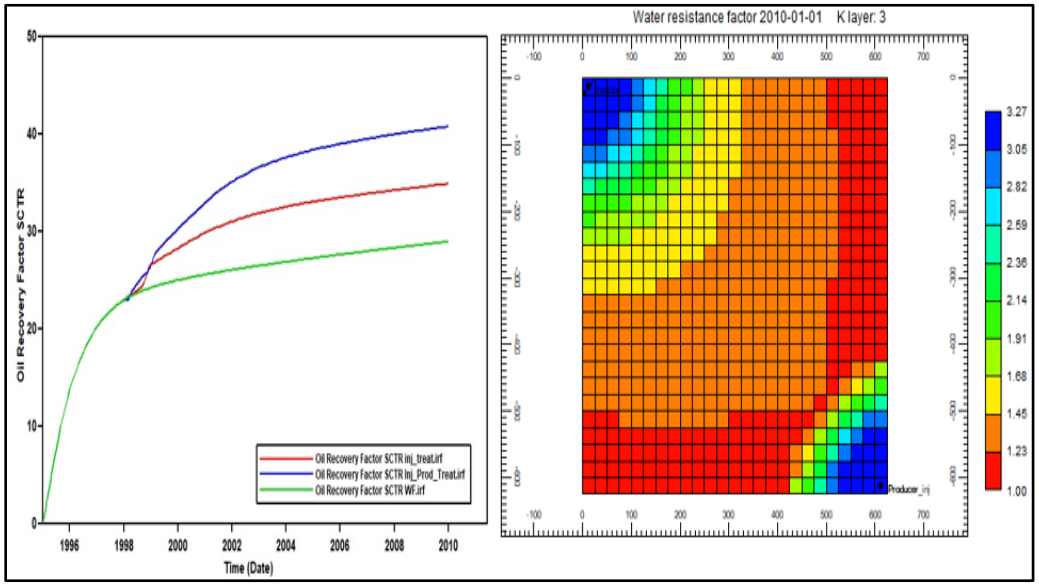

Figure 7. Oil recovery factor (left) and permeability reduction in layer 3 (right) when applying treatment in both sides.

12.3. PLACEMENT TECHNOLOGY

As mentioned previously, both zonal isolation and bullhead placement methods were used in field applications of the sodium silicate gel. In general, using zonal isolation as a placement method was more efficient in improving recovery factor and reservoir performance than bullhead injection (Bai et al., 2004; Khamees et al., 2017). Seright (1996) stated that neither the severe heterogeneity of the reservoir nor capillary pressure eliminated the need to isolate high-permeability from low-permeability layers during the treatment. Based on these evidences and due to the importance of placement methods, three models were simulated. Table 11 and Figure 8 show the results of these models (i.e., zonal isolation, bullhead, and dual injection).

Table 11. Dependence of recovery factor and cumulative oil on placement techniques.

Parameter	Water flood	Bullhead injection	Zonal isolation	Dual injection
Recovery factor, %	29.00	33.60	34.90	35.42
Cumulative oil, Bbl.	363,101	420,176	437,393	443,592
Incremental oil, Bbl.		57,075	74,292	80,491
Average oil saturation at the end of post-treatment water	53.20	50.10	49.00	48.95

Therefore, a sodium silicate solution should not be considered as a selective penetration agent (i.e., the solution does not selectively enter high-permeability layers). Thus, damage to low permeability layers occurred if the gelant had access to all open layers, as shown in Figure 9.

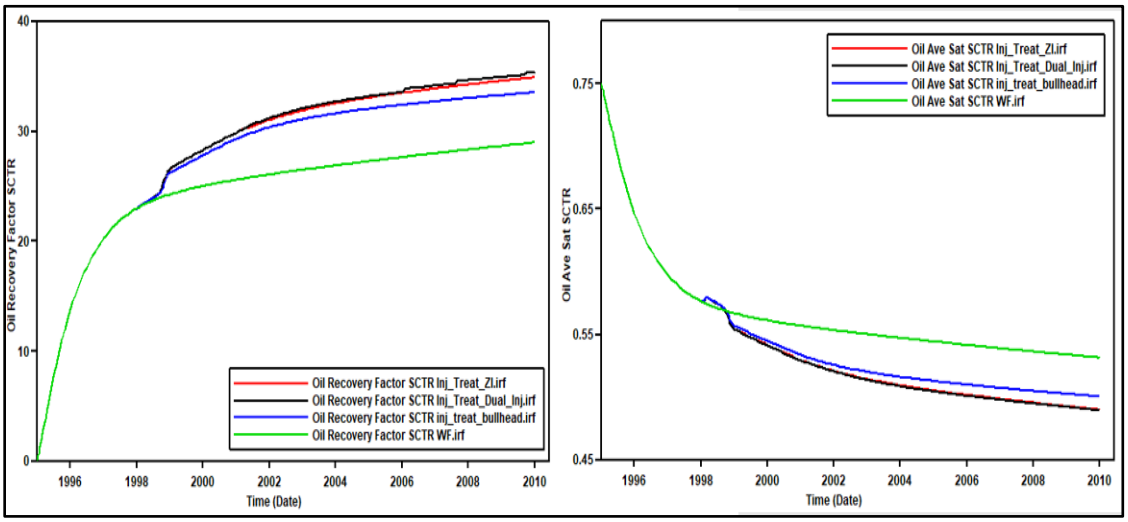

Figure 8. Effect of placement method on oil recovery factor (left) and average oil saturation (right).

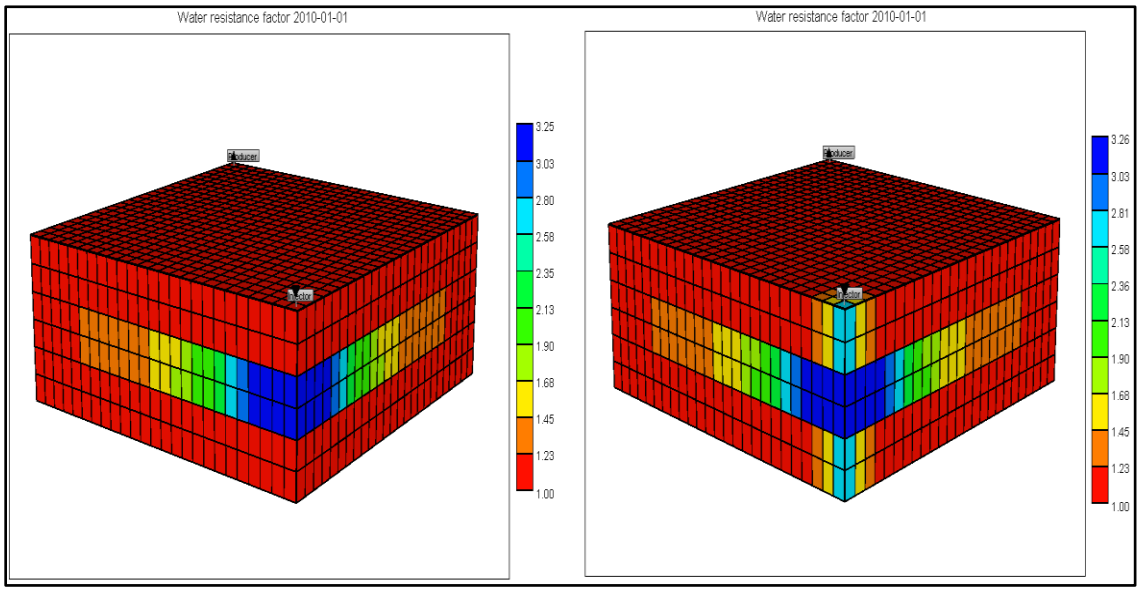

Figure 9. Comparison of permeability reduction between dual injection method (left) and bullhead injection (right).

12.4. EFFECT OF HCL CONCENTRATION

As mentioned previously, in a silicate gel system, polymerization is triggered by lowering the solution's pH by adding acids such as HCl (Pham and Hatzignatiou, 2016). Thus, any variation on pH would have a big influence on the gelation time. Hatzignatiou et al. (2014) showed experimentally that by adjusting the HCl concentration, it was possible to control the gelation time. Therefore, a low concentration of HCl is necessary to make the gelation time long enough, which allows the sodium silicate solution to penetrate deep into the thief zones (Krumrine and Boyce, 1985; Skrettingland et al., 2012). The importance of the HCl concentration comes from its effect on the gelation time (Stavland et al., 2011a). Therefore, two models were run and their results are shown in Table 12 and Figure 10, respectively.

Table 12. Dependence of recovery factor and cumulative recovery on the concentration of HCl.

Parameter	Water flood	Low HCL Conc.	High HC Conc.
Recovery Factor, %	29.00	34.70	33.50
Cumulative Oil, Bbl.	363,101	434,654	419,389
Incremental Oil, Bbl.		71,553	56,288

Figure 10 shows that using a low HCl concentration will enable the sodium silicate solution to penetrate deeper into layer 3 with a low value of RRF compared to the high HCl model. These results indicate that by lowering the activator concentration (i.e., HCl), the sodium silicate solution has a longer gelation time.

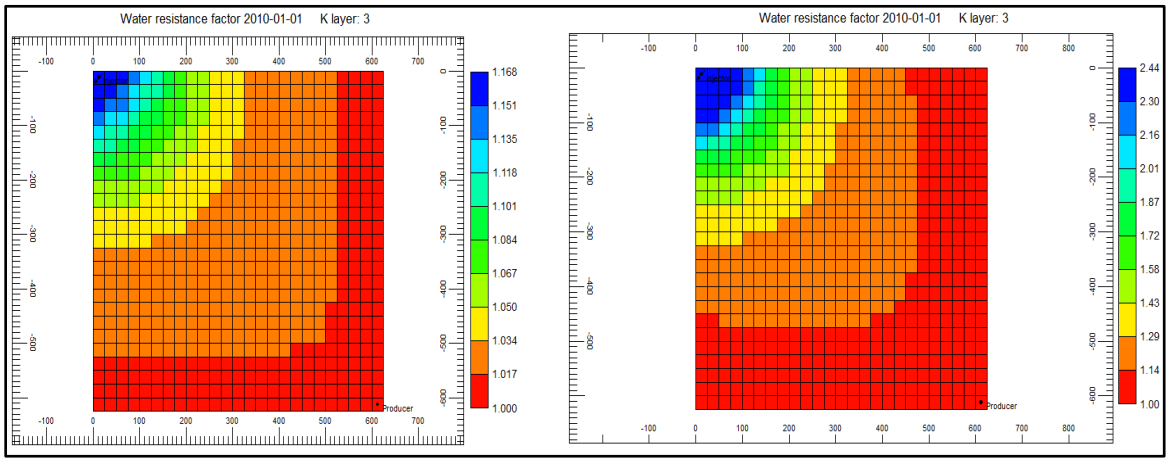

Figure 10. Comparison of permeability reduction between low HCl (left) and high HCl (right) concentrations.

12.5. EFFECT OF PRE-FLUSH

The existence of divalent cations could jeopardize the success of a sodium silicate application as a deep reservoir treatment by accelerating the gelation process (Krumrine and Boyce, 1985; Hamouda and Amiri, 2014). Thus, it is necessary to pre-flush the reservoir to soften the formation water before implementing the treatment. There is a possible white precipitation of sodium silicate and unwanted plugging when it is mixed with a formation brine containing divalent cations, which results in insoluble metal silicate precipitation (Amiri et al., 2014). Pham and Hazignatiou (2016) stated that the effect of Mg^{2+} on precipitation of sodium silicate was higher than the effect of Ca^{2+}. Therefore, the reservoir's ions are diluted by pre-flushing with low-salinity water. Moreover, the gelation time was reduced and the gel strength and shrinkage increased with increasing brine salinity (Hatzignatiou et al., 2014; Amiri, 2014).

To illustrate the effect of pre-flush in controlling the ion exchange and removing unwanted divalent cations, two models were run: with pre-flush and without pre-flush. The

results are shown in Table 13 and Figure 11, respectively. Thus, injecting a sodium silicate solution without conditioning the reservoir will result in a lower recovery compared to a pre-flush run.

Table 13. Effect of pre-flush on reservoir performance.

Parameter	Water flood	With pre-flush	Without pre-flush
Recovery Factor, %	29.00	34.90	34.10
Cumulative Oil, Bbl.	363,101	437,393	426,440
Incremental Oil, Bbl.		74,292	63,339

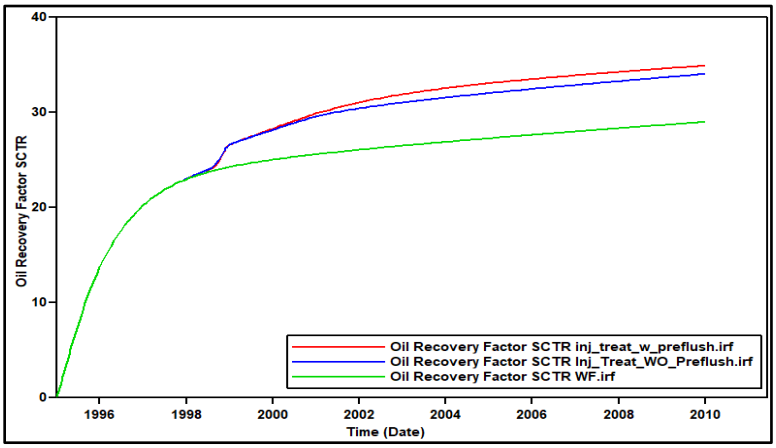

Figure 11. Oil recovery factor showing the effect of pre-flushing the reservoir before sodium silicate injection.

Another model was run to show the difference of pre-flushing all layers versus pre-flushing high permeability streaks only. The injected pore volume of the pre-flush fluid is presented in Table 14. The results showed a difference in the recovery factor (Table 15) when only the thief zones pre-flushed. This finding supports the importance of pre-flushing

the well to condition the sodium silicate solution inflow paths in the targeted layers before the injection of the treatment.

Table 14. KCl pre-flush injected PV.

Parameter	Total volumes, ft^3	Injected PV
Pre-flushing all layers	32,635	0.020
Pre-flushing thief zones only	32,635	0.059

Table 15. Effect of pre-flush on reservoir performance.

Parameter	Water flood	Pre-flush all layers	Pre-flush thief zones only
Recovery Factor, %	29.00	34.90	35.40
Cumulative Oil, Bbl.	363,101	437,393	442,967
Incremental Oil, Bbl.		74,292	79,866

12.6. VOLUME OF PRE-FLUSH

Sizing the volume of pre-flush is a vital factor from an economic point of view because in the pre-flush stage, a diluted brine or low salinity water (i.e., soft water) is injected. Thus, the time span or length of pre-flush injection should be optimized to get better results. Three models with different pre-flush volumes, as shown in Table 16, were run and compared.

Note that in Table 3, the injected PV of pre-flush was calculated based on total pore volumes of the model, whereas in Table 16 the calculated injected PV was based on the pore volume of thief zones only (i.e., layers 3 and 4). The results in Table 17 and Figure

12 show that the optimum time length to inject pre-flush fluid into high permeability streaks was only two months.

Table 16. Pre-flush volumes based on pore volume of thief zones only.

Time span of pre-flush injection	Injected volume, Bbl.	Injected PV
One month	16,585	0.030
Two months	32,635	0.059
Three months	49,220	0.088

Table 17. Effect of pre-flush time span on the performance of sodium silicate solution.

Parameter	Water flood	Pre-flush for one month	Pre-flush for two months	Pre-flush for three months
Recovery Factor, %	29.00	35.04	35.40	35.15
Cumulative Oil, Bbl.	363,101	438,737	442,967	440,155
Incremental Oil, Bbl.		75,636	79,866	77,054

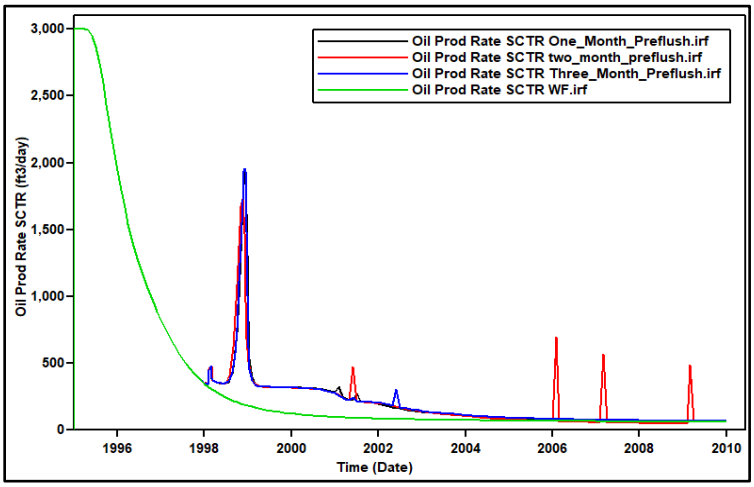

Figure 12. Oil production rate showing the effect of different pre-flush duration.

12.7. EFFECT OF ADSORPTION

Adsorption of polymers is defined as the attachment of polar groups along the polymer chain to many different polar points on the rock surface (Manichand and Seright, 2014). In a sodium silicate solution, the level of adsorption affects the solution's concentration, which affects the success of the treatment. Amiri (2014) suggested that the silicate adsorption is a reversible process, in which the adsorbed mass is retrieved in post-treatment water injection. Hellern (2011) proposed the following equation to calculate the amount of adsorbed gel (m_{gel}):

$$m_{gel} = V_{pore}.Ads_{max} \quad (11)$$

The amount of adsorbed gel is different from high to low permeability layers. In high permeability layers, the adsorbed amount was calculated based on the pore volume of the thief zones only. In low permeability layers, the amount of adsorbed gel was calculated based on the pore volume of these layers. Moreover, Scott et al. (1987) stated that if gel penetrated into low permeability layers, the amount of adsorbed gel would be higher than this amount in the thief zones. This assumption stated that if gel penetrated into low permeability layers, the permeability reduction would be high compared to permeability reduction in the thief zones.

In this study, three levels of adsorption were considered: irreversible, partial reversible, and reversible adsorption. As shown previously, Table 6 presented the irreversible and reversible adsorption of silicate gel that was used in this study. Therefore, at 2 wt% sodium silicate concentration, two values were used for irreversible and reversible adsorption, respectively. Moreover, a mid-value between irreversible and reversible was considered as partial reversible. In these models, prolonged chase-water was injected and

the simulation was ended at 01/01/2050 compared to other models where the chase-water injection was ended at 01/01/2010. Table 18 shows the calculated gel mass by Equation 11 in the low- and high-permeability layers, respectively.

Table 19 shows a big difference in single-well treatment between irreversible and reversible adsorption, whereas there is only a small difference between irreversible and partial reversible. Thus, determining the value of silicate adsorption is vital in field applications where multiple wells are involved in the treatment. Moreover, reversible adsorption will desorb all the sodium silicate solution from the high-permeability streaks as suggested by Amiri (2014). However, damage to the adjacent oil layers will occur as shown in the right-hand side of Figure 13, as compared to no damage in the same layer when assuming irreversible adsorption (left-hand side of Figure 13). Table 18 shows that the amount of adsorbed gel in case of reversible adsorbtion in both zones is zero. The only explanation to this discrepancy between Table 18 and the right-hand side of Figure 13 is that the reversible adsorption assumption will remove silicate from high permeability layers, but damage will occur to low permeability layers due to the dispersion of sodium silicate.

Table 18. Amount of adsorbed gel.

	Amount of adsorbed gel, lb	
Adsorption	Low permeability zones	High permeability streaks
Reversible	0	0
Partial reversible	16.51	4.13
Irreversible	330.2	82.60

Table 19. Oil recovery factor and incremental oil between three levels of adsorption.

Parameter	Water flood	Irreversible adsorption	Partial reversible adsorption	Reversible adsorption
Recovery factor, %	38.20	45.50	44.80	41.40
Cumulative oil, Bbl.	478,048	569,090	560,563	517,918
Incremental oil, Bbl.		91,042	82,515	39,870

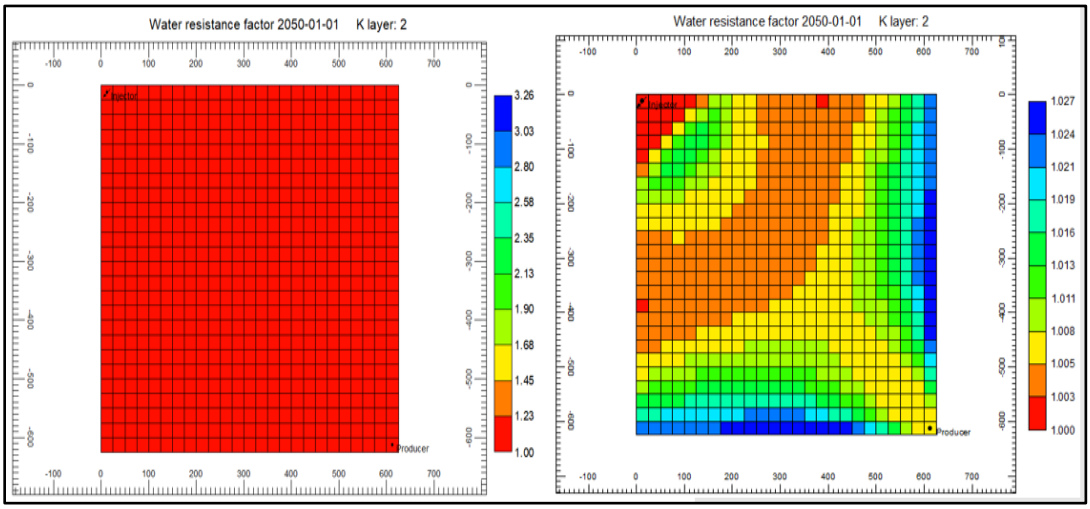

Figure 13. Comparison between irreversible adsorption (left) and reversible adsorption (right) showing damage in layer 2 caused by permeability reduction.

12.8. COMPARISON OF SODIUM SILICATE AND XANTHAN BIOPOLYMER MIXTURE MODEL VERSUS SODIUM SILICATE AND HPAM SYNTHETIC POLYMER MIXTURE MODEL

In CEOR processes, two types of polymer solutions are commonly used: xanthan and partially hydrolyzed polyacrylamide (HPAM), which exhibit non-Newtonian flow behavior. Xanthan biopolymer solutions exhibit shear thinning or pseudoplastic behavior in porous media in which the viscosity is decreasing with an increase of the shear rate (Seright et al., 2010). On the other hand, synthetic polymer solution (e.g., HPAM) exhibits

both shear-thinning behavior at low to moderate flow velocity and shear-thickening behavior (also called dilatant, pseudodilatant, and viscoelastic) at a very high shear rate (Chauveteau, 1981). The shear-thickening behavior is predominant for an HPAM solution with a molecular weight higher than 20 million (Delshad et al., 2008; Kim et al., 2010; Li and Delshad, 2014). Thus, the xanthan solution will preferentially enter high permeability streaks since it exhibits shear-thinning behavior, whereas HPAM will assist diverting of fluids into low permeability layers due to its shear-thickening behavior (Clarke et al., 2015). Hatzignatiou et al. (2016) performed laboratory measurements of mixing sodium silicate with xanthan biopolymer and HPAM that has a low molecular weight. In some cases, crosslinkers were added to a synthetic polymer to study their combination effects.

In this study, two polymer solutions, xanthan biopolymer and HPAM synthetic polymer, were separately mixed with sodium silicate, and the resultant mixtures were injected into high permeability layers for 30 days at the same injection rate (i.e., 535 bbl/day). Table 20 and Figure 14 show the properties of these two solutions, where the molecular weight of xanthan biopolymer is unkown; however, xanthan biopolymer exhibited a close behavior as HPAM with 18 million Dalton molecular weight (Clarke et al., 2015).

Table 20. Properties of HPAM synthetic polymer and xanthan biopolymer solution.

Polymer solution	MW, Million Dalton	Concentration, ppm	Rheological properties
Xanthan biopolymer	Unkown	1300	Shear-thinning behavior only
HPAM synthetic polymer	8	1200	Combined shear thinning and shear-thickening behavior

The results in Table 21 show that mixing sodium silicate with xanthan biopolymer neither increased the recovery factor too much nor improved the blocking efficiency of the sodium silicate solution (Figure 15), despite the fact that xanthan biopolymer is a good viscosifying agent. Hatzignatiou et al. (2016) showed that more shear-thinning behavior resulted when xanthan was added to sodium silicate. On the other hand, adding the HPAM solution to the sodium silicate solution not only increased the recovery factor and cumulative oil, but also improved permeability reduction in high permeability layers.

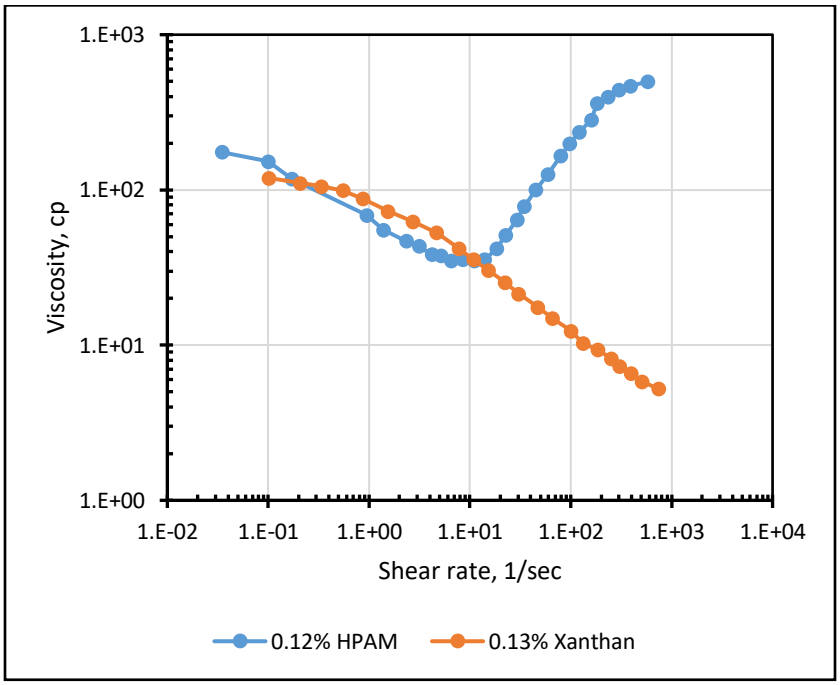

Figure 14. Viscosity versus shear rate for xanthan biopolymer and HPAM synthetic polymer (Clarke et al., 2015).

HPAM polymer solution, when added to sodium silicate, increased the strength of the produced gelant. Thus, the incremental oil is attributed to the shear-thickening behavior of this type of polymer solution.

Table 21. Effect of adding xanthan and HPAM polymer to sodium silicate.

Parameter	Water flood	Na-Silicate only	Mix of Na-Silicate and Xanthan	Mix of Na-Silicate and HPAM
Recovery Factor, %	29.00	34.90	35.22	36.52
Cumulative Oil, Bbl.	363,101	437,393	441,044	457,309
Incremental Oil, Bbl.		74,292	77,943	94,208

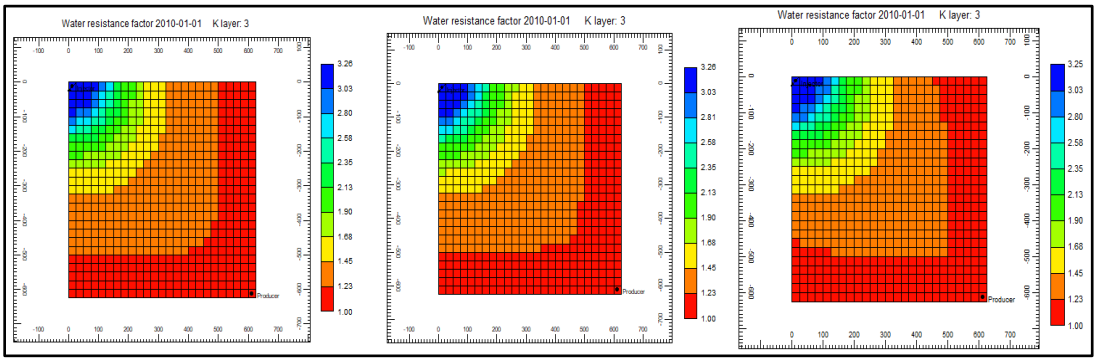

Figure 15. Comparison of permeability reduction in layer 3 between sodium silicate model only (left), mixture of sodium silicate with xanthan mode (center), and mixture of sodium silicate with HPAM model (right).

12.9. EFFECT OF TEMPERATURE AND ACTIVATION ENERGY

It is well known that fast gelation of silica gel occurrs at high temperatures (Krumrine and Boyce, 1985; Helleren, 2011). Hunt et al. (2013) concluded that a low-temperature reservoir is more preferable to apply a silica gel system. Because not only the elevated temperatures accelerate the gelation, but also lower the gel strength (Hamouda and Amiri, 2014). Experiments conducted by Hamouda and Amiri (2014) showed that at 113 °F (45 °C) the gelation time was 215 min compared to 26 min at 158 °F (70 °C). In addition, Pham and Hatzignatiou (2016) tabulated the sol-gel transition time at different

temperatures. In this table, the transition time decreased from 5.09 hr at 104 °F (40 °C) to 1.43 hr at 140 °F (60 °C). Moreover, when the reservoir temperature increased, the activation energy also increased. The activation energy is defined as the minimum energy the molecules must have in order to react and form gel. Thus, the higher the temperature, the higher the activation energy. Arrhenius' equation (Equation 1) best describes the relationship between the sol-gel transition time and the inverse of absolute temperature (Pham and Hatzignatiou, 2016). The researchers proposed different activation energies, for instance, Pham and Hatzignatiou (2016) suggested an activation energy of 55.8 kJ/mol, while Jurinak and Summers (1991) assumed an activation energy of 73.27 kJ/mol. Moreover, Hamouda and Amiri (2014) estimated 70 kJ/mol for a temperature above 104 °F (40 °C), and Stavland et al. (2011) calculated the activation energy to be 77 kJ/mol. Thus, an activation energy between 55.8 kJ/mol and 77 kJ/mol was assumed and calculated by previous studies. Thus, in this study, two activation energies were assumed: 70 kJ/mole at 120 °F and 90 kJ/mol at 160 °F. Table 22 and Figure 16 show that increasing the activation energy at a higher temperature will lower the recovery factor due to the fast gelation of sodium silicate, which prevents gel from penetrating further into high-permeability layers.

Table 22. Effect of temperature and activation energy.

Parameter	Water flood	Activation energy 70 kJ/mol at 120 °F	Activation energy 90 kJ/mol at 160 °F
Recovery Factor, %	29.00	34.90	34.13
Cumulative Oil, Bbl.	363,101	437,393	427,395
Incremental Oil, Bbl.		74,292	64,294

12.10. EFFECT OF SHUT-IN PERIOD

In field applications of gel treatment, the injection well should be shut-in after gel placement for a pre-determined time to allow the gelation process to complete and to produce a strong gel. Thus, the stronger the gel, the more that gel can withstand the differential pressure after the treatment. In addition, injection treatment has an advantage over the production treatment, because during injection treatment, there is no need to close the production well.

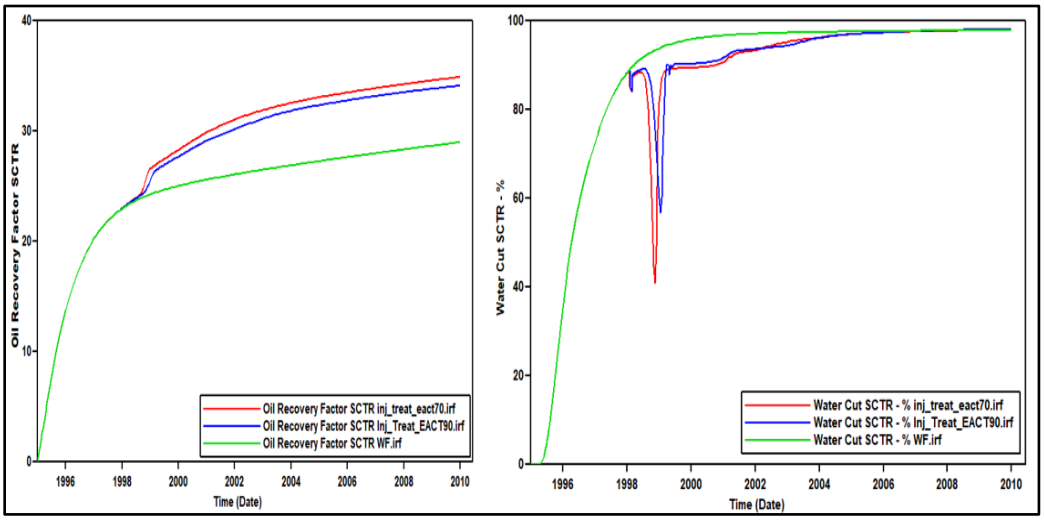

Figure 16. Oil recovery factor (left) and water cut (right) for different values of activation energy.

In this study, the sodium silicate solution was injected for 30 days and the injection well was shut-in for 30 days, which is normal procedure in field applications. A shorter shut-in time (i.e., 10 days) was examined to shorten the closure time of the injection well. In addition, no shut time was modeled and the post-treatment water was resumed directly after placement of the sodium silicate solution. The results in Table 23 and Figure 17

clearly demonstrate the importance of shut-in time; thus, the longer the shut-in time, the higher the recovery factor. The reason is that the gelation process did not fully complete, and a weaker gel resulted with no shut-in model. Thus, shut-in the well was very important in improving the gel strength.

Table 23. Effect of shut-in time.

Parameter	Water flood	No shut-in	10-day shut-in	30-day shut-in
Recovery Factor, %	29.00	34.30	34.70	34.90
Cumulative Oil, Bbl.	363,101	429,991	434,917	437,393
Incremental Oil, Bbl.		66,890	71,816	74,292

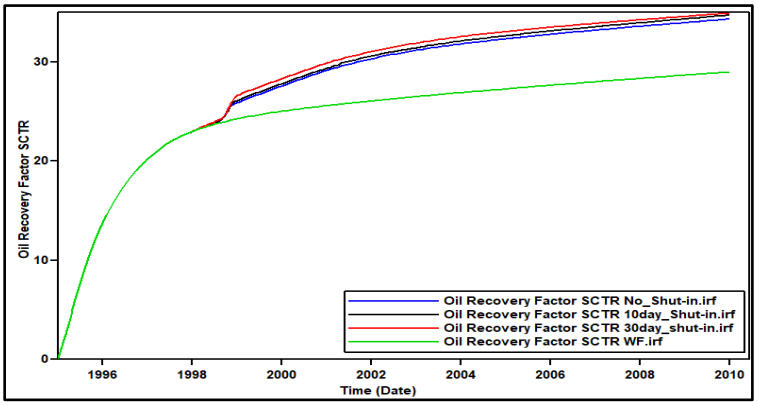

Figure 17. Oil recovery factor showing the effect of shut-in time.

12.11. EFFECT OF RESERVOIR WETTABILITY

The efficiency and success of any flooding process depends on reservoir wettability, where the distribution and movement of fluid inside the porous media is controlled by this property. The reservoir wettability affects both relative permeability and

capillary pressure. For example, the capillary desaturation curve, which is considered the most important parameter of designing a water-flooding process, is affected by wettability as shown in Figure 18. This figure shows a high capillary number is required to mobilize the wetting phase rather than non-wetting phase.

In water-wet conditions, the connate water saturation is low, occupies small pores, and exists as a film around the grain surfaces, while oil is located in the large pores. Thus, there is oil phase continuity in water-wet conditions; in addition, endpoint oil relative permeability is higher than endpoint water relative permeability. The distribution of fluid is completely different in oil-wet conditions, where water is considered as a non-wetting phase and occupies the larger pores. Thus, water relative permeability is high, and when flooding oil-wet reservoirs, the water cut in the production wells increases rapidly.

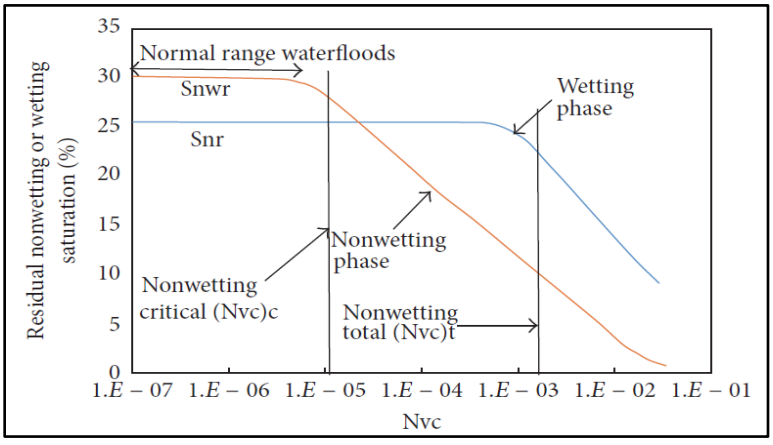

Figure 18. Typical capillary desaturation curve (CDC) showing the effect of wettability (Green and Willhite, 1998).

Sodium silicate is considered as a wetting phase in a water-wet porous media, since 90% or more of the content of sodium silicate is water; thus, a higher mobility reduction

might occur (Askarinezhad et al. 2017). To illustrate the effect of reservoir wettability on the performance of sodium silicate, water-wet and oil-wet conditions were assumed. The relative permeability curves are shown in Figure 19.

The relative permeability curves used in this section were different from the relative permeability curves used in the previous sections; thus, the results from these two models are not comparable with other models. Table 24 and Figure 20 show the results obtained from these models, which clearly demonstrates that a higher recovery factor and good performance were obtained under water-wet conditions compared to oil-wet conditions.

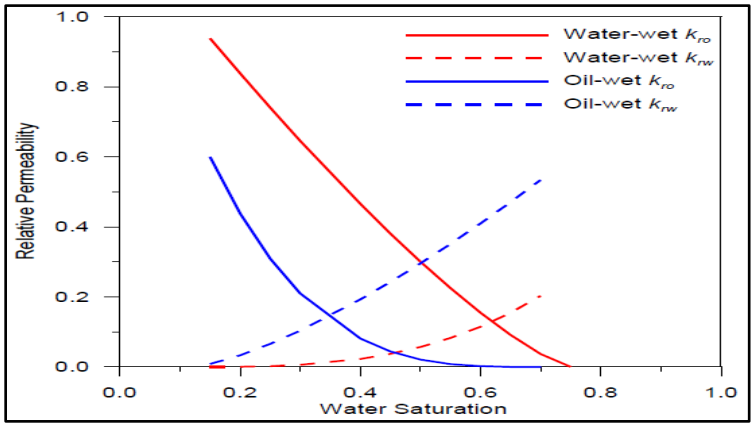

Figure 19. Relative permeability curves for water-wet and oil-wet conditions (Shen et al., 2014).

Table 24. Effect of reservoir wettability.

Parameter	Water-wet		Oil-wet	
	WF	Gel	WF	Gel
Recovery Factor, %	30.00	37.30	21.20	26.40
Cumulative Oil, Bbl.	440,148	548,016	310,736	387,275
Incremental Oil, Bbl.		107,868		76,539

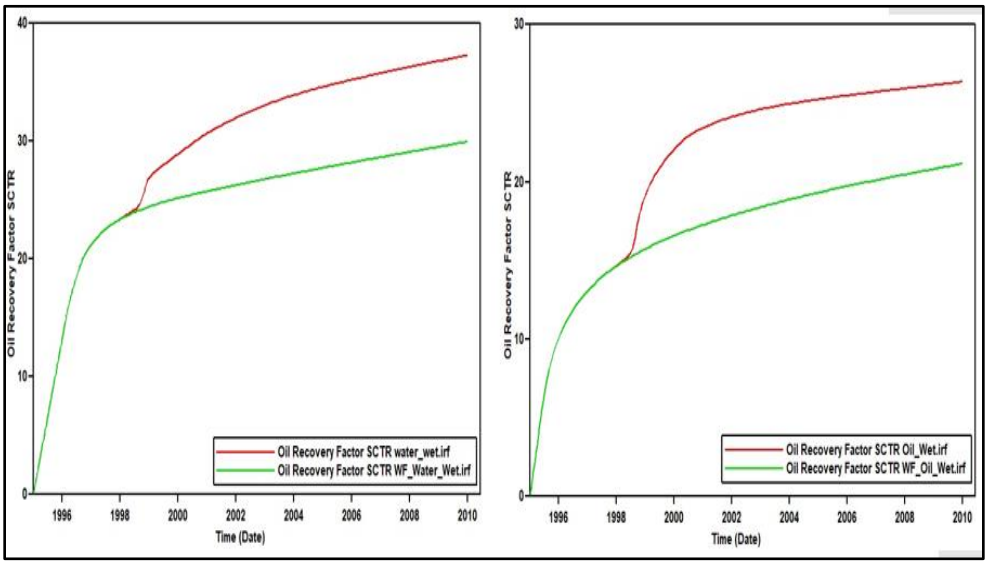

Figure 20. Oil recovery factor for water-wet (left) and oil-wet systems (right).

13. CONCLUSIONS

1. Sensitivity analysis showed that the fewer the gridblock's number, the better the performance of the gel system.
2. Applying the treatment on the injection well yielded higher results than the production well, yet the simultaneous treatment of injection and production well was even more efficient.
3. In all gel systems, including sodium silicate gel, zonal isolation was better than bullhead injection. In addition, dual injection was more efficient than zonal isolation.
4. A low concentration of HCl is necessary to make the gelation time long enough, which allows the sodium silicate solution to penetrate deep into the formation.
5. The existence of divalent cations could jeopardize the success of sodium silicate application as a deep reservoir treatment by accelerating the gelation process. Thus, it

is necessary to pre-flush the reservoir to soften the formation water before implementing the treatment.

6. Pre-flushing only high-permeability layers has more effects on the recovery factor rather than pre-flushing all layers.
7. A two-month pre-flush period was selected to run the rest of the scenarios because this length of pre-flush injection was better than one month and three months.
8. Irreversible adsorption yielded higher results than reversible and partial reversible adsorption. In addition, assuming reversible adsorption caused damage to low permeability layers.
9. Mixing a sodium silicate solution with either xanthan biopolymer or HPAM polymer solutions enhanced the performance of sodium silicate. However, the mixture of sodium silicate with HPAM polymer solution was more efficient.
10. Increasing the reservoir temperature will cause the activation energy to increase; therefore, there is a faster gelation rate and a lower penetration distance in the thief zones.
11. No shut-in or short shut-in period after the treatment resulted in weak gel that was not strong enough to divert post-water treatment to low permeability layers. Therefore, the best shut-in period was 30 days.
12. Sodium silicate gel is considered as a wetting agent in water-wet system; therefore, the gel performed better when it was applied to water-wet conditions rather than oil-wet conditions.

ACKNOWLEDGMENTS

The authors would like to acknowledge Iraq Ministry of Oil and the ExxonMobil Iraq Training Technology & Scholars Program (ExxonMobil Iraq) for their financial support.

REFERENCES

Al-Muntasheri, G.A., Nasr-El-Din, and Zitha, P.L.J. 2008. Gelation Kinetics and Performance Evaluation of an Organically Crosslinked Gel at High Temperature and Pressure. *SPE J* **13** (03): 337-345. https://doi.org/10.2118/104071-PA.

Amiri, H.A.A., Hamouda, A.A., and Roostaei, A. 2014. Sodium Silicate Behavior in Porous Media Applied for In-Depth Profile Modifications. *Energies* **7** (4): 2004-2026. http://dx.doi.org/10.3390/en7042004.

Amiri, H.A.A. 2014. *Evaluation of Alkaline Sodium Silicate Gel for Reservoir In-Depth Profile Modifications to Enhance Water Sweep Efficiency in Sandstone Reservoirs*. PhD Dissertation, University of Stavanger, Stavanger, Norway (2014). http://hdl.handle.net/11250/226251.

Askarinezhad, R., Hatzignatiou, D.G. et al. 2017. Disproportionate Permeability Reduction of Water-Soluble Silicate Gelants: Importance of Formation Wettability. *SPE Prod & Oper* **32** (03): 362- 373. https://doi.org/10.2118/179589-PA.

Bai, B., Wang, Q., Du, Y. et al. 2004. Factors Affecting In-Depth Gel Treatment for Reservoirs with Thick Heterogeneous Oil Layers. Presented at the 55th Canadian International Petroleum Conference, Calgary, Alberta, Canada, 8-10 June, PETSOC-2004-140. https://dx.doi.org/10.2118/2004-140.

Boreng, R. and Svendsen, O.B. 1997. A Successful Water Shut Off. A Case Study from the Statfjord Field. Presented at the SPE Production Operations Symposium, Oklahoma City, Oklahoma, USA, 9-11 March, SPE-37466-MS. https://doi.org/10.2118/37466-MS.

Chauveteau, G. 1981. Molecular Interpretaion of Several Different Properties of Flow of Coiled Polymer Solutions through Porous Media in Oil Recovery Conditions. Presented at the SPE 56th Annual Technical Conference and Exhibition, San Antonio, Texas, USA, 5-7 October. SPE-10060-MS. https://doi.org/10.2118/10060-MS.

Clarke, A., Howe, A.M., Mitchell, J. et al. 2015. How Viscoelastic Polymer Flooding Enhances Displacement Efficiency. Presented at the SPE Asia Pacific Enhanced Oil Recovery Conference, Kuala Lumpur, Malaysia. 11-13 August, SPE-174654-MS. https://doi.org/10.2118/174654-MS.

CMG-STARS Technical Manual, 2015.

Delshad, M., Kim, D.H., Magbagbeola, O.A. et al. 2008. Mechanistic Interpretation and Utilization of Viscoelastic Behavior of Polymer Solutions for Improved Polymer-Flood Efficiency. Presented at SPE/DOE Improved Oil Recovery Symposium, Tulsa, Oklahoma, USA, 19-23 April. SPE-113620-MS. http://doi.org/10.2118/113620-MS.

Fletcher, A.J.P, Flew, S., Forsdyke, I.N. et al. 1992. Deep diverting gels for very cost-effective waterflood control. *J Petrol Sci & Eng* **7** (1-2): 33-43. https://doi.org/10.1016/0920-4105(92)90006-M.

Green, D.W. and Willhite, G.P. 1998. Enhanced Oil Recovery, SPE Textbook Series 6. Richardson, TX, USA: SPE.

Hamouda, A.A. and Amiri, H.A.A. 2014. Factors Affecting Alkaline Sodium Silicate Gelation for In-Depth Reservoir Profile Modification. *Energies* **7** (2): 568-590. https://doi.org/10.3390/en7020568.

Hatzignatiou, D.G., Helleren, J., and Stavland, A. 2014. Numerical Evaluation of Dynamic Core-Scale Experiments of Silicate Gels for Fluid Diversion and Flow-Zone Isolation. *SPE Prod & Oper* **29** (02): 122- 138. https://doi.org/10.2118/170240-PA.

Hatzignatiou, D.G., Giske, N.H., and Stavland, A. 2016. Polymers and Polymer-Based Gelants for Improved Oil Recovery and Water Control Applications in Naturally Fractured Chalk Formations. Presented at the SPE Bergen One-Day Seminar, Bergen, Norway, 20 April. https://doi.org/10.2118/180024-MS.

Hatzignatiou, D.G., Askarinezhad, R., Giske, N.H. et al. 2016. Laboratory Testing of Environmentally Friendly Sodium Silicate Systems for Water Management Through conformance Control. *SPE Prod & Oper* **31** (04): 337-350. https://doi.org/10.2118/173853-PA.

Helleren, J. 2011. *Numerical Simulation of Chemical Flow-Zone Isolation*. Master Thesis, University of Stavenger, Stavenger, Norway (2011).

Herring, G.D., Milloway, J.T., and Wilson, W.N. 1984. Selective Gas Shut-Off Using Sodium Silicate in the Prudhoe Bay Field, AK. Presented at the SPE Formation Damage Control Symposium, Bakersfield, California, USA, 13-14 February, SPE-12473-MS. https://doi.org/10.2118/12473-MS.

Hunt, J.D., Ezzedine, S.M., Bourcier, W. et al. 2013. Kinetics of the Gelation of Colloidal Silica at Geothermal Conditions, and Implications for Modification and Management. Presented at the 38th Workshop on Geothermal Reservoir Engineering, Stanford, California, USA, 11–13 February. https://digital.library.unt.edu/ark:/67531/metadc830320/.

Iler, R. K., 1979. The Chemistry of Silica, Solubility, Polymerization, Colloid and Surface Properties and Biochemistry. New York, NY: John Wiley-InterScience Publisher. http://doi.org/10.1002/ange.19800920433.

Jurinak, J.J. and Summers, L.E. 1991. Oilfield Applications of Colloidal Silica Gel. *SPE Prod Eng* **6** (04): 406-412. https://doi.org/10.2118/18505-PA.

Khamees, T., Flori, R.E., and Wei, M. 2017. Simulation Study of In-Depth Gel Treatment in Heterogeneous Reservoirs with Sensitivity Analyses. Presented at the SPE Western Regional Meeting, Bakersfield, California, USA, 23-27 April. SPE-185716-MS. https://doi.org/10.2118/185716-MS.

Kim, H.S. 1995. *Simulation Study of Gel Conformance Treatments*. PhD Dissertation, the University of Texas, Austin, Texas, USA (1995).

Krumrine, P.H. and Boyce, S.D. 1985. Profile Modification and Water Control with Silica Gel-Based Systems. Presented at the SPE Oilfield and Geothermal Chemistry Symposium, Phoenix, Arizona, USA, 9-11 March. SPE-13578-MS. https://doi.org/10.2118/13578-MS.

Lakatos, I., Lakatos-Szabo, J., Tiszai, Gy. et al. 1999. Application of Silicate-Based Well Treatment Techniques at the Hungarian Oil Fields. Presented at the SPE Annual Technical Conference and Exhibition, Houston, Texas, USA, 3-6 October. SPE-56739-MS. https://doi.org/10.2118/56739-MS.

Lakatos, I. and Lakatos-Szabo, J. 2012. Reservoir Conformance Control in Oilfields Using of Silicate: State-of-the-Arts and Perspectives. Presented at the SPE Annual Technical Conference and Exhibition, San Antonio, Texas, USA, 8-10 October, SPE-159640-MS. https://doi.org/10.2118/159640-MS.

Li, Z. and Delshad, M. 2014. Development of an Analytical Injectivity Model for Non-Newtonian Polymer Solution. *SPE J.* **19** (03): 381-389. http://doi.org/10.2118/163672-PA.

Manichand, R.N., and Seright, R. 2014. Field vs. Laboratory Polymer-Retention Values for a Polymer Flood in the Tambaredjo Field. *SPE Res Eval & Eng* **17** (03): 314-325. https://doi.org/10.2118/169027-PA.

Mills, R.V.A. 1922. U. S. Patent 1421706.

Nasr-El-Din, H.A., Bitar, G.E., Bou-Khamsin, F.I. et al. 1998. Field Application of Gelling Polymers in Saudi Arabia, Presented at the SPE/DOE Improved Oil Recovery Symposium, Tulsa, Oklahoma, USA, 19-22 April. SPE-39615-MS. https://doi.org/10.2118/39615-MS.

Pham, L.T. and Hatzignatiou, D.G. 2016. Rheological evaluation of a sodium silicate gel system for water management in mature, naturally fractured oilfields. J Petrol Sci & Eng 138: 218- 233. https://doi.org/10.1016/j.petrol.2015.11.039.

Prud'homme, R.K. and Uhl, J.T. 1984. Kinetics of Polymer/Metal-Ion Gelation. Presented at the SPE Enhanced Oil Recovery Symposium, Tulsa, Oklahoma, USA, 15-18 April. SPE-12640-MS. https://doi.org/10.2118/12640-MS.

Robertson Jr., J.O. and Oefelein, F.H. 1967. Plugging Thief Zones in Water Injection Wells. *J Pet Technol* **19** (08): 999- 1004. https://doi.org/10.2118/1524-PA.

Rolfsvag, T.A., Jakobsen, S.R., Lund, T.A.T. et al. 1996. Thin Gel Treatment of an Oil Producer at the Gullfaks Field: Results and Evaluation. Presented at the European Production Operations Conference and Exhibition, Stavanger, Norway, 16-17 April. SPE-35548-MS. https://doi.org/10.2118/35548-MS.

Scott, T., Roberts, L.J., Sharpe, S.R. et al. 1987. In-situ Gel Calculations in Complex Reservoir Systems using a New Chemical Flood Simulator. *SPE Res Eng* **2** (4): 634-646. http://dx.doi.org/10.2118/14234-PA.

Seright, R.S. 1996. Improved Methods for Water Shutoff. PRRC Report 96-23, Semi-Annual Technical Report, Submitted to BDM-OKLAHOMA/The US DOE, Sept. 30.

Seright, R.S., Lane, R.H., and Sydansk, R.D. 2003. A Strategy for Attacking Excess Water Production. *SPE Prod & Fac* **18** (03): 158- 169. https://doi.org/10.2118/84966-PA.

Seright, R.S., Fan, T., and Balaban, R. d C. 2010. New Insights into Polymer Rheology in Porous Media. Presented at the SPE IOR Symposium, Tulsa, Oklahoma, USA, 24-28 April. https://doi.org/10.2118/129200-MS.

Shen, G.X., Lee, J.H., and Lee, K.S. 2014. Influence of Temperature on Gel Treatment under Various Reservoir Wettability Conditions. Presented at Offshore Technology Conference-Asia, Kuala Lumpur, Malaysia, 25-28 March. OTC-24853-MS. https://doi.org/10.4043/24853-MS.

Sheng, J. J. 2011. Modern Chemical Enhanced Oil Recovery: Theory and Practice. Amsterdam: Elsevier, Print.

Skrettingland, K., Giske, N.H., Johnsen, J.H. et al. 2012. Snorre In-depth Water Diversion Using Sodium Silicate- Single Well Injection Pilot. Presented at the SPE Improved Oil Recovery Symposium, Tulsa, Oklahoma, USA, 14-18 April. SPE-154004-MS. https://doi.org/10.2118/154004-MS.

Smith, J.E. 1999. Practical Issues With Field Injection Well Gel Treatments. Presented at the SPE Rocky Mountains Regional Meeting, Gillette, Wyoming, USA, 15-18 May. SPE-55631-MS. https://doi.org/10.2118/55631-MS.

Smith, L.R., Fast, C.R., and Wagner, O.R. 1969. Development and Field Testing of Large Volume Remedial Treatment for Gross Water Channeling. *J Pet Technol* **21** (08): 1015-1025. https://doi.org/10.2118/2217-PA.

Southard, M.Z., Green, D.W., and Willhite, G.P. 1984. Kinetics of the Chromium (VI)/Thiourea Reaction in the Presence of Polyacrylamide. Presented at the SPE Enhanced Oil Recovery Symposium, Tulsa, Oklahoma, USA, 15- 18 April. SPE-12715-MS. https://doi.org/10.2118/12715-MS.

Stavland, A., Jonsbraten, H.C., Vikane, O. et al. 2011a. In-Depth Water Diversion Using Sodium Silicate on Snorre – Factors Controlling In-Depth Placement. Presented at the SPE European Formation Damage Conference, Noordwjik, The Netherlands, 7-10 June, SPE-143836-MS. http://dx.doi.org/10.2118/143836-MS.

Stavland, A., Jonsbraten, H.C., Vikane, O. et al. 2011b. In-Depth Water Diversion Using Sodium Silicate – Preparation for Single Field Pilot on Snorre. Presented at the 16th European Symposium on Improved Oil Recovery, Cambridge, UK, 12-14 April.

Willhite, G.P. and Dominguez, J.G. 1977. Mechanisms of Polymer Retention in Porous Media. In: Improved Oil Recovery by Surfactant and Polymer Flooding, ed. Shah, D.O. and Schechter, R.S., 511- 554, Academic Press.

Yang, X., Zhu, W., and Yang, Q. 2007. The Viscosity Properties of Sodium Silicate Solutions. J Solution Chem 37: 73-83. http://doi.org/10.1007/s10953-007-9214-6.

SECTION

3. CONCLUSIONS AND RECOMMENDATIONS

3.1. CONCLUSIONS

In this dissertation, different polymer gel systems have been investigated through numerical modeling using CMG-STARS and UTGEL simulators. The results of polymer gel systems were compared with polymer flooding to prove the importance of injecting polymer gels.

The following conclusions are the most important points that could be drawn from this study:

- In-depth gel treatment should be considered the only method of blocking the high-permeability layers and diverting the post-water injection into the low-permeability layers for thick heterogeneous reservoir with crossflow.
- Injecting gel into the high permeability layers only (i.e., zone isolation method) have better results than injecting gel into all layers (i.e., bullhead method).
- The higher the heterogeneity, the lower the performance of gel treatment.
- The lower the polymer/crosslinker ratio, the higher the penetration into the high permeability layers and the higher the recovery factor.
- It is necessary to initiate the treatment based on the heterogeneity of the reservoir and fluid properties, such as the viscosity of the reservoir fluids. For example,

- For thick heterogeneous reservoirs with crossflow, the optimum time to start gel treatment is when the water cut reaches 80% because prior to this value, high volume of oil is still available in the high permeability layers.
- The optimum crossflow determined from this study was 0.1.
- In addition, the low crossflow model (0.01) with high permeability contrast would perform better than the high crossflow model (0.2) with the high permeability contrast.
- Polymer rheology plays an important role of the strength of the formed gel. Therefore, the viscoelastic properties of the HPAM yielded higher recovery factor and assisted the diversion of post-treatment water into the low-permeability layers, thus improving the sweep efficiency.
- Regardless of the salinity, it is important to consider shear-thinning and shear-thickening behavior together (UVM model).
- The higher the salinity of the injected brine and/or the brine of the reservoir, the lower the recovery factor. Therefore,
- As the salinity of the makeup water and/or the reservoir brine increased, the adsorption of the HPAM increased and the viscosity decreased, which affects the strength of the formed gel.
- Low-salinity post-treatment water greatly improves the sweep efficiency, especially when the initial reservoir salinity was too high.
- The presence of divalent cations (hardness) in the brine lowers the recovery factor; however, low-salinity post-treatment water improves the recovery in the presence of hardness.

- The presence of the clays in the reservoir affected the crosslinking process by removal of the crosslinkers from the gelant solution. Thus, no gel will be formed in the presence of the clay.
- If there are clays in the reservoir, the reaction rate between the crosslinkers and polymer solution to form gel must be high enough to overcome the removal of the crosslinkers by the clay.
- If the treatment was applied in a reservoir with water-wet condition, it would yielded higher recovery factor and higher incremental oil compared to oil-wet conditions.
- A damage to low-permeability layers would occur if the treatment injected in an oil-wer reservoir.
- The effect of low-salinity post-treatment water on oil-wet was higher than water-wet models.
- The dip angle has a great impact on the treatment. Thus, higher recovery factor was yielded if the dip angle was from the injector to the producer (i.e., positive dip angle).
- The higher the mobility ratio, the lower the recovery factor and incremental oil. However, injection of polymer solution after gel treatment improves the performance of gel treatment in case of unfavorable mobility ratio.
- The negative or the positive skin factor in the injection well would increase or decrease the recovery factor after the gel treatment if high injection rate was used compared to low injection rate.
- Increasing the reservoir temperature will cause the activation energy to increase; therefore, there is a faster gelation rate and a lower penetration distance in the thief zones.

- Combining more than conformance control technologies together is promoting the recovery factors and enhancing sweep efficiencies more than applying single conformance control method. For example,
- Mixing a sodium silicate solution with either xanthan biopolymer or HPAM polymer solutions enhanced the performance of sodium silicate.
- However, the mixture of sodium silicate with HPAM polymer solution was more efficient. Moreover,
- Improving the sweep efficiency form heterogeneous reservoir saturated with viscous oil requires combining more than chemical EOR processes. Furthermore,
- Starting the treatment with gel followed by polymer makes the remaining crosslinkers from gel treatment attach to the subsequent injected polymer; therefore, it creates a higher recovery factor and higher incremental oil,
- The effects of high molecular weight HPAM polymer solutions on both displacement and volumetric sweep efficiency could make them to compete with polymer gel system.

3.2. RECOMMENDATIONS

In this study, conceptual models were built by implementing real polymer and gel properties. Therefore, it is recommended to:

- Study real reservoir geometries and applying the conclusions that were obtained from this research.
- A fictitious (not real) fracture geometries were implemented in these models. Therefore, another code to create more accurate and more representative fracture networks, such as embedded discrete fracture model (EDFM), is required.

- Since the onset of the shear-thickening behavior is very essential to the strength of the form gel, it is necessary to study the parameters that could affect the onset of shear-thickening behavior by using artificial neural network (ANN).
- It is important to run an economical evaluation of each polymer gel that has been modeled in this research.

APPENDIX

The following is the input data file for modeling polymer/chromium chloride in-depth gel system using UTGEL simulator. This data file is one of many data files that used to produce the results of article that published in Fuel journal, which is presented in this dissertation. KGOPT flag in the input file should be set KGOPT=1. This data file is for salinity = 10,000 mg/l and UVM rheology model.

```
CC*************************************************************************
CC                                                                        *
CC    BRIEF DESCRIPTION OF DATA SET: UTGEL                                *
CC                                                                        *
CC*************************************************************************
CC                                                                        *
CC                                                                        *
CC                                                                        *
CC  LENGTH (FT) :1875                PROCESS :                            *
CC  THICKNESS (FT) :220              INJ. RATE (FT3/DAY) :                *
CC  WIDTH (FT) :1875                 COORDINATES : CARTESIAN              *
CC  POROSITY :VARIABLE                                                    *
CC  GRID BLOCKS : 19×19×6                                                 *
CC  DATE : 03/08/2017                                                     *
CC                                                                        *
CC*************************************************************************
```

```
CC
CC*************************************************************************
CC                                                                       *
CC    RESERVOIR DESCRIPTION                                              *
CC                                                                       *
CC*************************************************************************
CC
CC
*----RUNNO
CK_S10000
CC
CC
*----HEADER
In-Depth Gel Treatment
Polymer Chromium Chloride Gel
Tariq Dissertation
CC
CC SIMULATION FLAGS
*----IMODE   IMES   IDISPC   IREACT   ICOORD   ITREAC   ITC   IENG
         1.0       2.0       3.0         1.0          1.0          0.0        1.0       1.0
CC
CC  NUMBER OF GRID BLOCKS AND FLAG SPECIFIES CONSTANT OR
VARIABLE GRID SIZE
```

```
*----NX   NY   NZ   IDXYZ   IUNIT

        19       19       6      2       0

CC

CC  GRID SIZE OF BLOCK IN X DIRECTION

*----DX(I), I=1, NX

          25.0    50.0    75.0    75.0   100.0   100.0   125.0   150.0   150.0
175.0   150.0   150.0   125.0   100.0   100.0    75.0    50.0    50.0    50.0

CC

CC  GRID SIZE OF BLOCK IN Y DIRECTION

*----DY(J), J=1, NY

          25.0    50.0    75.0    75.0   100.0   100.0   125.0   150.0   150.0
175.0   150.0   150.0   125.0   100.0   100.0    75.0    50.0    50.0    50.0

CC

CC  GRID SIZE OF BLOCK IN Z DIRECTION

*----DZ(K), K=1, NZ

     50.0   50.0   10.0   10.0   50.0   50.0

CC

CC  TOTAL NO. OF COMPONENTS, NO. OF TRACERS, NO. OF GEL
COMPONENTS

*----N   NTW   NG

     14.0   0.0     6.0

CC

CC  ALL species must be present even for standard waterflood

*----SPNAME(IT),IT=1,N
```

WATER

OIL

none

POLYMER

ANION

CALCIUM

none

none

none

Dichromate

Thiourea

Cr3+

GEL

H+

CC

CC FLAG INDICATING IF THE COMPONENT IS INCLUDED IN CALCULATIONS OR NOT

*----ICF(KC) FOR KC=1,N

1.0 1.0 0.0 1.0 1.0 0.0 0.0 0.0 0.0 1.0 1.0 1.0 1.0 1.0

CC

CC**********

CC *

CC OUTPUT OPTIONS *

```
CC                                                                    *
CC*********************************************************************
CC
CC
CC  FLAG FOR PV OR DAYS FOR OUTPUT AND STOP THE RUN
*----ICUMTM   ISTOP
          0.0          0.0
CC
CC  FLAG INDICATING IF THE PROFILE OF KCTH COMPONENT SHOULD BE
WRITTEN
*----IPRFLG(KC),KC=1,N
      1.0   1.0   0.0   1.0   1.0   0.0   0.0   0.0   0.0   1.0   1.0   1.0   1.0   1.0
CC
CC  FLAG FOR PRES,SAT.,TOTAL CONC.,TRACER CONC.,CAP.,GEL,
ALKALINE PROFILES
*----IPPRES   IPSAT   IPCTOT   IPGEL   IPTEMP
         1.0        1.0         1.0          1.0          1.0
CC
CC  FLAG FOR WRITING SEVERAL PROPERTIES
*----ICKL  IVIS  IPER  ICNM  ICSE
        1.0     1.0     1.0     1.0       0.0
CC
CC  FLAG FOR WRITING SEVERAL PROPERTIES TO PROF
*----IADS  IVEL  IRKF  IPHSE
```

```
      1.0     0.0     1.0     0.0

CC

CC*****************************************************************

CC                                                                 *

CC    RESERVOIR PROPERTIES                                         *

CC                                                                 *

CC*****************************************************************

CC

CC

CC  MAX. SIMULATION TIME (DAYS)

*----TMAX

      7300.0

CC

CC  ROCK COMPRESSIBILITY (1/PSI), STAND. PRESSURE(PSIA)

*----COMPR   PSTAND

     0.000008      14.7

CC

CC  FLAGS INDICATING CONSTANT OR VARIABLE POROSITY, X,Y,AND Z
PERMEABILITY

*----IPOR1   IPERMX   IPERMY   IPERMZ   IMOD   ITRNZ   INTG

        2.0        2.0         3.0         3.0         0.0      0.0        0.0

CC

CC  Constant POROSITY
```

```
*----PORC1, I=1,NX*NY*NZ
    361*0.25
    361*0.25
    361*0.20
    361*0.20
    361*0.25
    361*0.25
CC
CC  VARIABLE X-PERMEABILITY (MILIDARCY)
*----PERMX(I), I=1,NX*NY*NZ
    361*100
    361*100
    361*1500
    361*1500
    361*100
    361*100
CC
CC  VARIABLE Y-PERMEABILITY (MILIDARCY)
*----FACTY
       1.0
CC
CC CONSTANT Z-PERMEABILITY (MILIDARCY)
*----FACTZ
```

```
      0.01

CC

CC  FLAG FOR CONSTANT OR VARIABLE DEPTH, PRESSURE, WATER
SATURATION

*----IDEPTH   IPRESS   ISWI

        0.0        1.0        0.0

CC

CC  DEPTH OF TOP GRID BLOCK AND THE RESERVOIR DIP ANGLES

*----D111

      5000.0

CC

CC  INITIAL PRESSURE AND THE CORRESPONDING DEPTH ARE SPECIFIED

*----PINIT   HINIT

     2500.0    5000.0

CC

CC  CONSTANT INITIAL WATER SATURATION

*----SWI

      0.3

CC

CC  CONSTANT CHLORIDE AND CALCIUM CONCENTRATIONS (MEQ/ML)

*----C50   C60

   0.7165    0.0

CC
```

```
CC*********************************************************************
CC                                                                    *
CC    PHYSICAL PROPERTY DATA                                          *
CC                                                                    *
CC*********************************************************************
CC
CC
CC  OIL CONC. AT PLAIT POINT FOR TYPE II(+) AND TYPE II(-), CMC
*----EPSME
      0.0000001
CC  SLOPE AND INTERCEPT OF BINODAL CURVE AT ZERO, OPT., AND
2XOPT SALINITY
CC  FOR ALCOHOL 1
*----HBNS70   HBNC70   HBNS71   HBNC71   HBNS72   HBNC72
         0.0          0.0          0.0          0.0          0.0          0.0
CC
CC
*---- HBNT0   HBNT1   HBNT2   CSET
         0.0         0.0         0.0         0.0
CC  SLOPE AND INTERCEPT OF BINODAL CURVE AT ZERO, OPT., AND
2XOPT SALINITY
CC  FOR ALCOHOL 2
*----HBNS80   HBNC80   HBNS81   HBNC81   HBNS82   HBNC82
          0.0         0.0          0.0          0.0          0.0          0.0
```

```
CC

CC  LOWER AND UPPER EFFECTIVE SALINITY FOR ALCOHOL 1 (7) AND
ALCOHOL 2 (8)

*----CSEL7   CSEU7   CSEL8   CSEU8

         0.0       0.0         0.0         0.0

CC

CC  THE CSE SLOPE PARAMETER FOR CALCIUM AND ALCOHOL 1 AND
ALCOHOL 2

*----BETA6   BETA7   BETA8

         0.0        0.0         0.0

CC

CC  FLAG FOR ALCOHOL PART. MODEL AND PARTITION COEFFICIENTS

*----IALC   OPSK7O   OPSK7S   OPSK8O   OPSK8S

       0.0         0.0         0.0         0.0           0.0

CC

CC  NO. OF ITERATIONS, AND TOLERANCE

*----NALMAX   EPSALC

         0.0           0.0

CC

CC  ALCOHOL 1 PARTITIONING PARAMETERS IF IALC=1

*----AKWC7   AKWS7   AKM7   AK7   PT7

        0.0         0.0         0.0       0.0      0.0

CC

CC ALCOHOL 2 PARTITIONING PARAMETERS IF IALC=1
```

```
*----AKWC8   AKWS8   AKM8   AK8   PT8
         0.0         0.0        0.0       0.0     0.0
CC
CC  0 = Healy and Reed and 1 is Chun-Huh
*----IFT
      1.0
CC
CC  INTERFACIAL TENSION PARAMETERS
*----CHUH   AHUH
         0.5      10.0
CC
CC  LOG10 OF OIL/WATER INTERFACIAL TENSION
*----XIFTW
        1.6
CC
CC  CAPILLARY DESATURATION PARAMETERS FOR PHASE 1, 2, AND 3
*----ITRAP   T11    T22    T33
         0.0       0.0      0.0     0.0
CC
CC  REL. PERM. AND PC CURVES
*----IPERM   IRTYPE
         0.0         0.0
CC
```

CC FLAG FOR CONSTANT OR VARIABLE REL. PERM. PARAMETERS

*----ISRW IPRW IEW

0.0 0.0 0.0

CC

CC CONSTANT RES. SATURATION OF PHASES 1, 2, AND 3 AT LOW CAPILLARY NO.

*----S1RWC S2RWC S3RWC

0.3 0.26 0.0

CC

CC CONSTANT ENDPOINT REL. PERM. OF PHASES 1, 2, AND 3 AT LOW CAPILLARY NO.

*----P1RWC P2RWC P3RWC

0.3 0.7 0.0

CC

CC CONSTANT REL. PERM. EXPONENT OF PHASES 1, 2, AND 3 AT LOW CAPILLARY NO.

*----E1WC E2WC E3WC

2.0 2.0 0.0

CC

CC WATER AND OIL VISCOSITY , RESERVOIR TEMPERATURE

*----VIS1 VIS2 TSTAND

0.86 6.0 60.0

CC

CC TEMPERAURE DEPENDENCY OF VISCOSITY (IENG=1)

*----BVI(1) BVI(2)

0.0 0.0

CC

CC VISCOSITY PARAMETERS

*----ALPHA1 ALPHA2 ALPHA3 ALPHA4 ALPHA5

0.0 0.0 0.0 0.0 0.0

CC

CC PARAMETERS TO CALCULATE POLYMER VISCOSITY AT ZERO SHEAR RATE

*----AP1 AP2 AP3

105.5 25.7 1644.6

CC

CC PARAMETER TO COMPUTE CSEP, MIN. CSEP, AND SLOPE OF LOG VIS. VS. LOG CSEP

*----BETAP CSE1 SSLOPE

10.0 0.01 -0.665

CC

CC PARAMETER FOR SHEAR RATE DEPENDENCE OF POLYMER VISCOSITY

*----GAMMAC GAMHF POWN IPMOD ISHEAR RWEFF GAMHF2 IWREATH

0.0 0.0 0.0 1.0 1.0 0.4 0.0
0

CC

CC UVM MODEL

*----BETAV1 BETAV2 EXPN1 TETAV TAU0 TAU1 EXPN2 AP11 AP22

```
      0.0192   18.522        0.78        0.01   0.0089   0.2992   3.5    21.76    3.49
CC
CC  FLAG FOR POLYMER PARTITIONING, PERM. REDUCTION PARAMETERS
*----IPOLYM   EPHI3   EPHI4   BRK   CRK   RKCUT
        0.0       1.0       0.8    1000.0  0.0186  10.0
CC
CC  SPECIFIC WEIGHT OF BRINE, OIL, SURFACTANT, AND ALCOHOL 1,2
*----DEN1   DEN2   DEN3   DEN7   DEN8  IDEN  IODEN
      0.433   0.368   0.0       0.0       0.0       1.0       0.0
CC
CC  FLAG FOR CHOICE OF UNITS ( 0:BOTTOMHOLE CONDITION , 1: STOCK
TANK)
*----ISTB
      1.0
CC
CC  FVF(L), for L=1, NPHAS
*----FVF1  FVF2  FVF3
     1.0     1.0      0.0
CC
CC  COMPRESSIBILITY FOR VOL. OCCUPYING COMPONENTS 1,2,3,7,AND 8
*----COMPC(1)   COMPC(2)   COMPC(3)   COMPC(7)   COMPC(8)
    0.0000027     0.00005         0.0                0.0             0.0
CC
CC  CONSTANT OR VARIABLE PC PARAM., WATER-WET OR OIL-WET PC
```

CURVE FLAG

*----ICPC IEPC IOW

0.0 0.0 0.0

CC

CC CAPILLARY PRESSURE PARAMETER, CPC0

*----CPC0

0.0

CC

CC CAPILLARY PRESSURE PARAMETER, EPC0

*----EPC0

5 0

CC

CC MOLECULAR DIFFUSIVITY OF KCTH COMPONENT IN PHASE 1 (D(KC),KC=1,N)

*----D(1) D(2) D(3) D(4) D(5) D(6)

1.875E-3 1.875E-3 1.875E-3 1.875E-3 1.875E-3 1.875E-3 1.875E-3 1.875E-3 1.875E-3 1.875E-3 1.875E-3 1.875E-3 1.875E-3 1.875E-3 1.875E-3

CC

CC MOLECULAR DIFFUSIVITY OF KCTH COMPONENT IN PHASE 2 (D(KC),KC=1,N)

*----D(1) D(2) D(3) D(4) D(5) D(6)

1.875E-3 1.875E-3 1.875E-3 1.875E-3 1.875E-3 1.875E-3 1.875E-3 1.875E-3 1.875E-3 1.875E-3 1.875E-3 1.875E-3 1.875E-3 1.875E-3 1.875E-3

CC

CC MOLECULAR DIFFUSIVITY OF KCTH COMPONENT IN PHASE 3

(D(KC),KC=1,N)

*----D(1) D(2) D(3) D(4) D(5) D(6)

0.0 0.0 0.0 0.0 0.0 0.0 0.0 0.0 0.0 0.0 0.0 0.0 0.0 0.0

CC

CC LONGITUDINAL AND TRANSVERSE DISPERSIVITY OF AQUEOUS PHASE

*----ALPHAL(1) ALPHAT(1)

0.0 0.0

CC

CC LONGITUDINAL AND TRANSVERSE DISPERSIVITY OF OLEIC PHASE

*----ALPHAL(2) ALPHAT(2)

0.0 0.0

CC

CC LONGITUDINAL AND TRANSVERSE DISPERSIVITY OF MICROEMULSION PHASE

*----ALPHAL(3) ALPHAT(3)

0.0 0.0

CC

CC SURFACTANT AND POLYMER ADSORPTION PARAMETERS

*----AD31 AD32 B3D AD41 AD42 B4D IADK IADS1 FADS REFK

0.0 0.0 0.0 1.0 0.0 1000 0.0 0.0 0.0 0.0

CC

CC PARAMETERS FOR CATION EXCHANGE OF CLAY AND SURFACTANT

*----QV XKC XKS EQW

```
      0.0     0.0     0.0       0.0
CC
CC  PARAMETERS FOR GELATION KINETICS (THIS LINE ONLY IF IREACT
=1)
*----KGOPT
         1.0
CC
CC
*----AK1   AK2     SCR   X4     X13    X14    X16   WM4
   0.00001   15.0    0.25   0.8     0.0     1.32    1.0    6.E+6
CC
CC  Temperature DEPENDECNCY FOR REACTION RATE
*----AK1T   AK2T
      0.0   -22344
CC
CC  PARAMETERS FOR GEL VISCOSITY (THIS LINE ONLY IF IREACT = 1)
*----AG1      AG2      CRG   AGK   BGK
    0.00008   2.7E-5    5.0     0.06    0.099
CC
CC  PARAMETERS FOR GEL RETENTION, NA-H & NA-CR EXCHANGE, INIT.
H+ CONC.
*----A15D   B15D   ICREX   A14D   B14D   CRNAK   HNAK   C160
    1157.0    100.0     1.0         0.0       0.0       1.57E+7      2.0    0.1258E-7
```

```
CC
CC  I NITIAL RESERVOIR TEMPERATURE IN F
*----TEMPI
     140.0
CC
CC  THERMAL PROPERTY OF ROCK AND FLUID
*----DENS   CRTC   CVSPR  CVSPL(L) L=1,NPHAS
     165.43   67.2       0.20       1.0   0.5   1.0
CC
CC  HEAT LOSS TO OVERBURDEN
*----IHLOS
       1.0
CC
CC  HEAT LOSS PARAMETER
*----TCONO    DENO    CVSPO   TCONU   DENU   CVSPU
        72.0      165.43       0.20        72.0      165.43      0.20
CC
CC*************************************************************************
CC                                                                        *
CC   WELL DATA                                                            *
CC                                                                        *
CC*************************************************************************
CC
```

```
CC

CC  TOTAL NUMBER OF WELLS, WELL RADIUS FLAG, FLAG FOR TIME OR
COURANT NO.

*----NWELL   IRO   ITIME  NWREL

        2.0         2.0      1.0       2.0

CC

CC  WELL ID, LOCATION, AND FLAG FOR SPECIFYING WELL TYPE, WELL
RADIUS, SKIN

*----IDW   IW   JW   IFLAG   RW   SWELL   IDIR   IFIRST   ILAST   IPRF

     1.0      1.0    1.0     1.0        0.4       0.0        3.0        1.0        6.0        0.0

CC

CC  WELL NAME FOR THE WELL ID SPECIFIED IN IDW(M) FOR THE Mth
WELL

*---- WELNAM

INJ

CC

CC  MAX. AND MIN. ALLOWABLE BOTTOMHOLE PRESSURE AND RATE

*----ICHEK   PWFMIN   PWFMAX   QTMIN   QTMAX

        0.0         0.0          20000          0.0         100000

CC

CC  WELL ID,LOCATIONS,AND FLAG FOR SPECIFYING WELL TYPE, WELL
RADIUS, SKIN

*----IDW   IW      JW      IFLAG   RW   SWELL   IDIR   IFIRST    ILAST    IPRF

      2.0    19.0     19.0      2.0       0.4       0.0        3.0        1.0          6.0         0

CC
```

```
CC  WELL NAME FOR THE WELL ID SPECIFIED IN IDW(M) FOR THE Mth
WELL

*----WELNAM

PROD

CC

CC  ICHEK MAX. AND MIN. ALLOWABLE BOTTOMHOLE PRESSURE AND
RATE

*----ICHEK   PWFMIN   PWFMAX   QTMIN   QTMAX

        0.0          0.0          20000          0.0         -100000

CC

CC  ID,INJ. RATE AND INJ. COMP. FOR RATE CONS. WELLS FOR EACH PHASE

(L=1,3)

*----ID   QI(M,L)   (C(M,KC,L),KC=1,N),L=1,3) FOR IFLAG=1 OR 3

 1   6000.0   1.0  0.0  0.0  0.0  0.7165  0.0  0.0  0.0  0.0  0.0   0.0   0.0  0.0  0.1258E-7

 1        0.0   0.0  0.0  0.0  0.0  0.0        0.0  0.0  0.0  0.0  0.0   0.0  0.0   0.0  0.0

 1        0.0   0.0  0.0  0.0  0.0  0.0        0.0  0.0  0.0  0.0  0.0   0.0  0.0   0.0  0.0

CC

CC  INJECTION FLUID TEMPERATURE IN F

*---- WELL ID    TEMINJ

          1.0            70.0

CC

CC  BOTTOMHOLE PRESSURE IS SPECIFIED FOR PROD1

*----WELL ID      PWF,  PSI

          2.0          500.0
```

```
CC

CC  CUM. INJ. TIME , AND INTERVALS (PV OR DAY) FOR WRITING TO
OUTPUT FILES

*----TINJ   CUMPR1   CUMHI1   CUMHI2    WRHPV   WRPRF   RSTC

     1825.0    10.0         10.0          10.0          10.0         10.0       10.0

CC

CC  FOR IMES=2, THE INI. TIME STEP, CONC. TOLERANCE, MAX., MIN.
COURANT NO.

*----DT   DCLIM   CNMAX   CNMIN

      0.01      0.1         0.4          0.04

CC

CC  FLAGS

*----IRO   ITIME   IFLAG

       2.0     1.0     1.0   2.0

CC

CC  NO. OF WELLS WITH CHANGES IN LOCATION OR SKIN OR PWF

*----NWEL1

       1.0

CC

CC  WELL ID, LOCATION, AND FLAG FOR SPECIFYING WELL TYPE, WELL
RADIUS, SKIN

*----IDW   IW   JW   RW   SWELL   IDIR   IFIRST   ILAST   IPRF

       1.0     1.0    1.0    0.4       0.0         3.0         1.0         6.0       1.0

CC
```

```
CC

*----KPRF(M,IWB), for IWB=1,NWBC

        0.0    0.0    1.0    1.0    0.0    0.0

CC

CC  WELL NAME FOR THE WELL ID SPECIFIED IN IDW(M) FOR THE Mth
WELL

*----WELNAM

INJ

CC

CC  MAX. AND MIN. ALLOWABLE BOTTOMHOLE PRESSURE AND RATE

*----ICHEK   PWFMIN   PWFMAX   QTMIN   QTMAX

       0.0         0.0           20000           0.0         100000

CC

CC  NUMBER OF WELLS WITH RATE CHANGES IN RATES, ID

*----NWEL2   ID

        1.0        1.0

CC

CC  ID,INJ. RATE AND INJ. COMP. FOR RATE CONS. WELLS FOR EACH PHASE
(L=1,3)

*----ID  QI(M,L)  (C(M,KC,L),KC=1,N),L=1,3) FOR IFLAG=1 OR 3

 1   6000.0    1.0  0.0  0.0  0.1  0.7165  0.0  0.0  0.0  0.0  0.05  0.07  0.0  0.0  0.502E-2

 1        0.0    0.0  0.0  0.0  0.0  0.0        0.0  0.0  0.0  0.0  0.0    0.0    0.0  0.0  0.0

 1        0.0    0.0  0.0  0.0  0.0  0.0        0.0  0.0  0.0  0.0  0.0    0.0    0.0  0.0  0.0

CC
```

```
CC  INJECTION FLUID TEMPERATURE IN F
*----WELL ID     TEMINJ
        1.0           70.0
CC
CC  FLAGS
*----TINJ   CUMPR1   CUMHI1   CUMHI2   WRHPV   WRPRF   RSTC
     1875.0    10.0         10.0          10.0          10.0         10.0       10.0
CC
CC  AUTOMATIC TIME STEP SELECTOR (IMES=3)
*----DT    DCLIM    CNMAX   CNMIN
     0.01     0.1           0.2        0.02
CC
CC  FLAGS
*----IRO   ITIME   IFLAG
     2.0      1.0       1.0    2.0
CC
CC  NO. OF WELLS WITH CHANGES IN LOCATION OR SKIN OR PWF
*----NWEL1
       1.0
CC
CC  WELL ID, LOCATION, AND FLAG FOR SPECIFYING WELL TYPE, WELL
RADIUS, SKIN
*----IDW   IW   JW   RW   SWELL  IDIR  IFIRST   ILAST   IPRF
```

```
      1.0   1.0   1.0   0.4      0.0      3.0      1.0      6.0      1.0

CC

CC

*----KPRF(M,IWB), for IWB=1,NWBC

      1.0     1.0     1.0     1.0     1.0     1.0

CC

CC  WELL NAME FOR THE WELL ID SPECIFIED IN IDW(M) FOR THE Mth
WELL

*----WELNAM

INJ

CC

CC  MAX. AND MIN. ALLOWABLE BOTTOMHOLE PRESSURE AND RATE

*----ICHEK   PWFMIN   PWFMAX   QTMIN   QTMAX

       0.0         0.0         20000         0.0       100000

CC

CC  NUMBER OF WELLS WITH RATE CHANGES IN RATES, ID

*----NWEL2   ID

      1.0       1.0

CC

CC  ID,INJ. RATE AND INJ. COMP. FOR RATE CONS. WELLS FOR EACH PHASE
(L=1,3)

*----ID  QI(M,L)  (C(M,KC,L),KC=1,N),L=1,3) FOR IFLAG=1 OR 3

 1  6000.0  1.0  0.0  0.0  0.0  0.7165  0.0  0.0  0.0  0.0  0.0  0.0  0.0  0.0  0.1258E-7

 1       0.0  0.0  0.0  0.0  0.0  0.0       0.0  0.0  0.0  0.0  0.0  0.0  0.0  0.0  0.0
```

```
 1        0.0   0.0  0.0  0.0  0.0  0.0  0.0         0.0  0.0  0.0  0.0  0.0  0.0  0.0  0.0  0.0  0.0
CC
CC  INJECTION FLUID TEMPERATURE IN F
*----WELL ID    TEMINJ
          1.0           70.0
CC
CC  FLAGS
*----TINJ    CUMPR1   CUMHI1   CUMHI2   WRHPV   WRPRF   RSTC
     7300.0     10.0          10.0          10.0          10.0         10.0        10.0
CC
CC  AUTOMATIC TIME STEP SELECTOR (IMES=3)
*----DT    DCLIM   CNMAX   CNMIN
       0.01     0.1          0.4          0.04
```

REFERENCES

Abdulbaki, M., Huh, C., Sepehrnoori, K., et al. 2014. A Critical Review on use of Polymer Microgels for Conformance Control Purposes. *J Petrol Sci Eng* **122**: 741-753. https://doi.org/10.1016/j.petrol.2014.06.034.

Ahmed, T. 2001. *Reservoir Engineering Handbook* 3rd Edition, Gulf Professional Publishing. Gulf Professional Publishing, Elsevier, Massachusetts, USA.

Ahmed, T. and Meehan, N. 2012. *Advanced Reservoir Management and Engineering*, Second edition, Gulf Professional Publishing, Elsevier, Massachusetts, USA.

Alhuraishawy, A.K, Sun, X., Bai, B. et al. 2018. Areal sweep efficiency improvement by integrating preformed particle gel and low salinity water flooding in fractured reservoirs. Fuel J 221: 380-392. https://doi.org/10.1016/j.fuel.2018.02.122.

Alvarado, V. and Manrique, E. 2010. *Enhanced Oil Recovery: Field Planning and Development Strategies*, Gulf Professional Publishing, Elsevier, Massachusetts, USA.

Bai, B., Li, L., Liu, Y. et al. 2007a. Preformed particle gel for conformance control: factors affecting its properties and applications. *SPE Res Eval & Eng* **10** (04): 415-422. SPE-89389-PA. https://doi.org/10.2118/89389-PA.

Bai, B., Liu, Y., Coste, J.-P et al. 2007b. Preformed particle gel for conformance control: Transport Mechanism through Porous Media. *SPE Res Eval & Eng* **10** (02): 176-184. SPE-89468-PA. https://doi.org/10.2118/89468-PA.

Bai, B., Huang, F., Liu, Y. et al. 2008. Case Study on Preformed Particle Gel for In-depth Fluid Diversion. Presented at SPE Symposium on Improved Oil Recovery, 20-23 April, Tulsa, Oklahoma. SPE-113997-MS. https://doi.org/10.2118/113997-MS.

Bai, B., Wei, M., and Liu, Y. 2012. Injecting Large Volumes of Preformed Particle Gel for Water Conformance Control. *Oil & Gas Sci and Technol* **67** (06): 941-952. http://doi.org/10.2516/ogst/2012058.

Bai, B., Zhou, J., and Yin, M. 2015. A Comprehensive Review of Acrylamide Polymer Gels for Conformance Control *Petrol Explor & Develop* **42** (04): 525-532. https://doi.org/10.1016/S1876-3804(15)30045-8.

Bailey, B., Tyrie, J., Elphick, J. et al. 2000. Water Control. *Oilfield Review* **12** (1), 30-51.

Bhasker, R.K., Stinson, J.A., Willhite, G.P. et al. 1988. The Effects of Shear History on the Gelation of Polyacrylamide/Chromium VI/Thiourea Solutions. *SPE Res Eval* **3** (04): 1251-1256. SPE-17472-PA. https://doi.org/10.2118/17472-PA.

Chang, H.L., Zhang, Z.Q., Wang, Q.M. et al. 2006. Advances in Polymer Flooding and Alkaline/Surfactant/Polymer Processes as Developed and Applied in the People's Republic of China. *J Pet Technol* **58** (02): 84- 89. SPE-89175-JPT. https://doi.org/10.2118/89175-JPT.

Chauveteau, G., and Kohler, N. 1974. Polymer Flooding: The Essential Elements for Laboratory Evaluation. Presented at SPE Improved Oil Recovery Symposium, 22-24 April, Tulsa, Oklahoma, SPE-4745-MS. https://doi.org/10.2118/4745-MS.

Chen, Z. 2016. *Polyacrylamide and its derivative for oil recovery*. PhD dissertation. Missouri University of Science and Technology, Rolla, Missouri (2016).

Clampitt, R.L. and Hessert, J.E. 1974. Method for Controlling Formation Permeability. U.S. Patent No. 3,785,437.

Coste, J.-P., Liu, Y., Bai, B. et al. 2000. In-Depth Fluid Diversion by Pre-Gelled Particles. Laboratory Study and Pilot Testing. Presented at the SPE/DOE Improved Oil Recovery Symposium, Tulsa, Oklahoma, 3-5 April. SPE-59362-MS. https://doi.org/10.2118/59362-MS

Cozic, C., Rousseau, D., and Tabary, R. 2008. Broadening the Application Range of Water Shutoff/Conformance-Control Microgels: An Investigation of Their Chemical Robustness. SPE Annual Technical Conference and Exhibition, Denver, Colorado, USA, 21-24 September. SPE-115974-MS. http://doi.org/10.2118/115974-MS.

Delshad, M., Kim, D.H., Magbagbeola, O.A. et al. 2008. Mechanistic Interpretation and Utilization of Viscoelastic Behavior of Polymer Solutions for Improved Polymer-Flood Efficiency. Presented at the 2008 SPE/DOE Improved Oil Recovery Symposium, Tulsa, Oklahoma, 19-23 April. SPE-113620-MS. http://doi.org/10.2118/113620-MS.

Diaz, D., Somaruga, C., Norman, C. et al. 2008. Colloidal Dispersion Gels Improve Recovery in a Heterogeneous Argentina Waterflood. Presented at the SPE Symposium on IOR, Tulsa, Oklahoma, 20-23 April. SPE-113320-MS. https://doi.org/10.2118/113320-MS.

Feng, Y., Tabary, R. Renard, M. et al. 2003. Characteristics of Microgels Designed for Water Shutoff and Profile Control. Presented at the International Symposium on Oilfield Chemistry, Houston, Texas, 5-7 February. SPE-80203-MS. http://doi.org/10.2118/80203-MS.

Frampton, H., Morgan, J.C., Cheung, S.K. et al. 2004. Development of a novel waterflood conformance control system. Presented at the SPE/DOE Fourteenth Symposium on Improved Oil Recovery, Tulsa, Oklahoma, 17-21 April. SPE-89391-MS. https://doi.org/10.2118/89391-MS.

Galli, G., Morra, D., Ghaddab, F. et al. 2012. Thermally Activated Particle Treatment to Improve Sweep Efficiency: Pilot Test Results and Field Scle Application Design in ElBorma Filed (Tunisia). Presented at the SPE Improved Oil Recovery Symposium, Tulsa, Oklahoma, 14-18 April. SPE-154042-MS. https://doi.org/10.2118/154042-MS.

Garmeh, R., Izadi, M., Salehi, M. et al. 2012. Thermally Active Polymer to Improve Sweep Efficiency of Waterfloods: Simulation and Pilot Design Approaches. *SPE Res Eval & Eng* 15 (01): 86-97, SPE-144234-PA. https://doi.org/10.2118/144234-PA.

Glenat, Ph., Zaborowski, G., and Loppinet, A. 1996. Profile Modification in Water Injection Wells by Polymer Treatments. Presented at the SPE Abu Dhabi International Petroleum Exhibition and Conference, Abu Dhabi, UAE, 13-16 October. SPE-36212-MS. http://doi.org/10.2118/36212-MS.

Goudarzi, A. 2015. *Modeling Conformance Control and Chemical EOR Processes Using Different Reservoir Simulators*. PhD dissertation, The University of Texas at Austin, Austin, Texas, USA (2015).

Goudarzi, A., Delshad, M., and Sepehrnoori, K. 2016. A chemical EOR benchmark study of different reservoir simulators. *Computers & Geosciences* **94**: 96-109. https://doi.org/10.1016/j.cageo.2016.06.013.

Green, D.W., and Willhite, G.P. 1998. *Enhanced Oil Recovery*. Henry L. Doherty Memorial Fund of AIME, Society of Petroleum Engineers. Texas, USA.

Guo, Z., Dong, M., Chen, Z. et al. 2013. A fast and effective method to evaluate the polymer flooding potential for heavy oil reservoirs in Western Canada. *J Pet Sci Eng* **112**: 335-340. https://doi.org/10.1016/j.petrol.2013.11.023.

Han, M., Alshehri, A.J., Krinis, D. et al. 2014. State-of-the-Art of In-Depth Fluid Diversion Technology: Enhancing Reservoir Oil Recovery by Gel Treatments. Presented at the SPE Saudi Arabia Section Technical Symposium and Exhibition, Al-Khobar, Saudi Arabia, 21-24 April. SPE-172186-MS. https://doi.org/10.2118/172186-MS.

Hasan, S.F, Han, M., Zhou, X. et al. 2013. Study of Polyacrylamide/Cr (III) Hydrogels for Conformance Control in Injection Wells to Enhance Chemical Flooding. Presented at the SPE Saudi Arabia Section Technical Symposium and Exhibition, 19-22 May, Al-Khobar, Saudi Arabia. SPE-168069-MS. http://doi.org/10.2118/168069-MS.

Herbas, J., Kumar, S., Moreno, R. et al. 2004. Reservoirs Simulations of Gel Treatments to Control Water Production, Improve the Sweep Efficiency and the Conformance Factor in Eastern Venezulean HPHT Fractured Reservoirs. Presented at SPE International Petroleum Conference, Puebla, Mexico, 8-9 November. SPE-92003-MS. https://doi.org/10.2118/92003-MS.

Hessert, J.E. and Fleming, P.D. 1979. Gelled Polymer Technology for Control of Water in Injection and Production Wells. Presented at the University of Kansas Third Tertiary Oil Recovery Conference. Wichita, Kansas, 25-26 April.

Hirasaki, G.J. and Pope, G.A. 1974. Analysis of Factors Influencing Mobility and Adsorption in the Flow of Polymer Solution through Porous Media. *SPE J.* **14** (04): 337-346. SPE-4026-PA. https://doi.org/10.2118/4026-PA.

Hirasaki, G.J., Miller, C.A., and Puerto, M. 2008. Recent Advances in Surfactant EOR. Presented at the SPE Annual Technical Conference and Exhibition, Denver, Colorado, USA, 21-24 September. SPE-115386-MS. http://doi.org/10.2118/115386-MS.

Hoteit, H., Alexis, D., Adepoju, O.O. et al. 2016 .Numerical and Experimental Investigation of polymer-Induced Resistance to Flow in Reservoirs Undergoing a Chemical Flood. Presented at the SPE Annual technical Conference and Exhibition, 26-28 September, Dubai, UAE. SPE-181720-MS. https://doi.org/10.2118/181720-MS.

Izgec, O. and Shook, G.M. 2012. Design Considerations of Waterflood Conformance Control with Temperature-Triggered, Low-Viscosity, Submicron Polymer. *SPE Res Eval & Eng* 15 (05): 533-540, SPE-153898-PA. https://doi.org/10.2118/153898-PA.

Kristensen, R., Lund, T., Titov, V.I. et al. 1993. Laboratory Evaluation and Field Tests of a Silicate Gel System Aimed to be under North Sea Conditions. *Geological Society London special Publications* 84 (01): 251-259. http://doi.org/10.1144/GSL.SP.1995.084.01.25.

Laherrere, J. 2003. Future of oil supplies. *Energy Exploration & Exploitation 21* (3): 227-267. http://doi.org/10.1260/014459803769520061.

Lake, L. 1989. *Enhanced Oil Recovery*. Prentice Hall, New Jersey, USA

Liu, Y., Bai, B., and Shuler, P.J. 2006. Application and Development of Chemical-Based Conformance Control Treatments in China Oil Fields. Presented at the SPE/DOE Symposium on Improved Oil Recovery, Tulsa, Oklahoma, USA, 22-26 April. SPE-99641-MS. http://doi.org/10.2118/99641-MS.

Liu, Y., Bai, B., and Wang, Y. 2010. Applied Technologies and Prospects of Conformance Control Treatments in China. *Oil & Gas Sci Technol* **65** (06): 859-878. http://doi.org/10.2516/ogst/2009057.

Lockhart, T.P. 1994. Chemical Properties of Chromium/Polyacrylamide Gels. SPE Adv Technol Series 2 (02): 199-205. SPE-20998-PA. https://doi.org/10.2118/20998-PA.

Lotfollahi, M., Farajzadeh, R., Delshad, M., et al. 2016. Mechanistic Simulation of Polymer Injectivity in Field Tests. *SPE J.* **21** (4): 1178-1191. SPE-174665-PA. http://doi.org/10.2118/174665-PA.

Luo, H.S, Delshad, M., Li, Z.T. et al. 2015. Numerical simulation of the impact of polymer rheology on polymer injectivity using a multilevel local grid refinement method. *Petrol Science* **13** (01): 110-125. https://doi.org/10.1007/s12182-015-0066-1.

Mack, J.C. and Smith, J.E. 1994. In-Depth Colloidal dispersion Gels Improve Oil Recovery Efficiency. Presented at the SPE/DOE Ninth Symposium on IOR, Tulsa, OK., USA, April 17-20. SPE-27780-MS. https://doi.org/10.2118/27780-MS.

Maitin, B.K. 1992. Performance Analysis of Several Polyacrylamide Floods in North German Oil Fields. Presented at the SPE/DOE Eighth Symposium on Enhanced Oil Recovery, Tulsa, Oklahoma, 22-24 April. SPE-24188-MS. https://doi.org/10.2118/24118-MS.

Manichand, R.N., and Seright, R. 2014. Field vs. Laboratory Polymer-Retention Values for a Polymer Flood in the Tambaredjo Field. *SPE Res Eval & Eng* **17** (03): 314-325, SPE-169027-PA. https://doi.org/10.2118/169027-PA.

Mustoni, J.L., Norman, C.A., and Denyer, P. 2010. Deep Conformance Control by a Novel Thermally Activated Particle System to Improve Sweep Efficiency in Mature Waterfloods of San Jorge Basin. Presented at the SPE Improved Oil Recovery Symposium, Tulsa, Oklahoma, 24-28 April. SPE-129732-MS. http://doi.org/10.2118/129732-MS.

Needham, R.B., Threlkeld, C.B., and Call, J.W. 1974. Control of Water Mobility Using Polymers and Multivalent Cations. Presented at the SPE Improved Oil Recovery Symposium, Tulsa, Oklahoma, 22-24 April. SPE-4747-MS. http://doi.org/10.2118/4747-MS.

Needham, R.B. and Doe, P.H. 1987. Polymer Flooding Review. *J Pet Technol* **39** (12):1503-1507. SPE-17140-PA. https://doi.org/10.2118/17140-PA.

Ohms, D., Mcleod, J., Graff, C.J. et al. 2010. Incremental-Oil Success from Waterflood Sweep Improvement in Alaska. *SPE Prod & Oper* **25** (03): 247-254. SPE-121761-PA. https://doi.org/10.2118/121761-PA.

Onbergenov, U. 2012. *Simulation of Thermally Active and pH-Sensitive Polymers for Conformance Control*. Master Thesis. The University of Texas at Austin, Austin, Texas, USA (2012)

Pope, G.A., Sepehrnoori, K., and Delshad, M. (Oct. 1, 2002 – March 30, 2003). A New Generation Chemical Flooding Simulator. Semi-annual Report, Center for Petroleum and Geosystems Engineering, The University of Texas at Austin. Austin, Texas, USA.

Pritchett, J., Frampton, H, Brinkman, J. et al. 2003. Field Application of a New In-Depth Waterflood Conformance Improvement Tool. Presented at the SPE International Improved Oil Recovery Conference in Asia Pacific, Kuala Lumpur, Malaysia, 20-21 October. SPE-84897-MS. https://doi.org/10.2118/84897-MS.

Pye, D.J. 1964. Improved Secondary Recovery by Control of Water Mobility. *J Pet Technol* **16** (08): 911-916. SPE-845-PA. https://doi.org/10.2118/845-PA.

Ranganathan, R. Lewis, R., McCool, C.S. et al. 1998. Experimental Study of the Gelation Behavior of a Polyacrylamide/Aluminum Citrate Colloidal-Dispersion Gel System. *SPE J* **3** (04): 337-343. SPE-52503-PA. https://doi.org/10.2118/52503-PA.

Rego, F.B., Botechia, V.E., and Schiozer, D.J. 2017. Heavy oil recovery by polymer flooding and hot water injection using numerical simulation. *J Pet Sci Eng* **153**: 187-196. https://doi.org/10.1016/j.petrol.2017.03.033.

Salehi, M., Thomas, C.P., Kevwitch, R.M. et al. 2012. Performance Evaluation of Thermally-Activated Polymers for Conformance Correction Applications. Presented at the SPE Improved Oil Recovery Symposium, Tulsa, Oklahoma, 14-18 April. SPE-154022-MS. https://doi.org/10.2118/154022-MS.

Sandiford, B.B. 1964. Laboratory and Field Studies of Water Floods Using Polymer Solutions to Increase Oil Recoveries. *J Pet Technol* **16** (08): 917-922. SPE-844-PA. https://doi.org/10.2118/844-PA.

Seright, R.D. and Martin, F.D. 1993. Impact of Gelation pH, Rock Permeability, and Lithology on the Performance of a Monomer-Based Gel. *SPE Res Eng* **8** (01): 43-50. SPE-20999-PA. https://doi.org/10.2118/20999-PA.

Seright, R.S. (October 1, 1996 to September 30, 1997). Improved methods for water shutoff. Report No. DOE/PC/91008—4. Semi-Annual Technical Report submitted to BDM-OKLAHOMA/The US DOE. http://doi.otg/10.2172/555333.

Seright, R.S., Lane, R.H., and Sydansk, R.D. 2003. A Strategy for Attacking Excess Water Production. *SPE Prod & Fac* **18** (03): 158-169. SPE-84966-PA. http://doi.org/10.2118/84966-PA.

Seright, R.S., Seheult, M., and Talashek, T. 2009. Injectivity Characteristics of EOR Polymers. *SPE Res Eval & Eng* **12** (05): 783-792. SPE-115142-PA. http://doi.org/10.2118/115142.PA.

Seright, R.S., Fan, T., Wavrik, K. et al. 2011. New Insights into Polymer Rheology in Porous Media. *SPE J* **16** (01): 35-42. SPE-129200-PA. http://doi.org/10.2118/129200-PA.

Seright, R.S., Zhang, G., Akanni, O. et al. 2012. A Comparison of Polymer Flooding with In-Depth Profile Modification. *J Can Pet Technol* **51** (05): 393-402. SPE-146087-PA. https://doi.org/10.2118/146087-PA.

Schulte, W.M. 2005. Challenges and Strategy for Increased Oil Recovery. Presented at the International Petroleum Technology Conference held in Doha, Qatar, 21-23 November. http://doi.org/10.2523/IPTC-10146-MS.

Sheng, J.J. 2011. *Modern Chemical Enhanced Oil Recovery: Theory and Practice*. Gulf Professional Publishing, Elsevier, Massachusetts, USA.

Sheng, J.J. 2015. Status of surfactant EOR technology. *Petroleum* **1** (02): 97-105. https://doi.org/10.1016/j.petlm.2015.07.003.

Shiyi, Y., Dong, H., Qiang, W. et al. 2000. Numerical Simulation on Weak Gel Injection. Presented at the SPE Asia Pacific Oil and Gas Conference and Exhibition, Brisbane, Australia, 16-18 October. SPE-64291-MS. https://doi.org/10.2118/64291-MS.

Smith, J.E., Liu, H., and Guo, Z. D. 2000. Laboratory Studies of In-Depth Colloidal Dispersion Gel Technology for Daqing Oil Field. Presented at the SPE/AAPG Western Regional Meeting, Long Beach, California, 19-22 June. SPE-62610-MS. https://doi.org/10.2118/62610-MS.

Sorbie, K.S. 1991. *Polymer-Improved Oil Recovery*. CRC Press Boca Raton, Florida, USA.

Southwell, G.P. and Posey, S.M. 1994. Applications and Results of Acrylamide-Polymer/Chromium (III) Carboxylate Gels. Presented at the APE/DOE Improved Oil Recovery Symposium, Tulsa, Oklahoma, 17-20 April. SPE-27779-MS. https://doi.org/10.2118/27779-MS.

Spildo, K, Skauge, A., Aarra, M.G. et al. 2009. A New Polymer Application for North Sea Reservoirs. *SPE Res Eval & Eng* **12** (03): 427-432. https://doi.org/10.2118/113460-PA.

Standnes, D.C. and Skjevark, I. 2014. Literature review of implemented polymer field projects. *J Pet Sci Eng* **122**: 761-775. https://doi.org/10.1016/j.petrol.2014.08.024

Sydansk, R.D. 1988. A New Conformance-Improvement-Treatment Chromium (III) Gel Technology. Presented at the SPE Enhanced Oil Recovery Symposium, Tulsa, Oklahoma, 16-21 April. SPE-17329-MS. https://doi.org/10.2118/17329-MS.

Sydansk, R.D. and Moore, P.E. 1990. Production Responses in Wyoming's Big Horn Basin Resulting from Application of Acrylamide-Polymer/Cr(III) Carboxylate Gels. SPE-21894-MS.

Sydansk, R.D. and Southwell, G.P. 2000. More Than 12 Years of Experience with a Successful-Conformance Control Polymer-Gel Technology. *SPE Prod & Fac* **15** (04): 270-278. SPE-66558-PA. https://doi.org/10.2118/66558-PA.

Sydansk, R. D. and Romero-Zeron, L. 2011. *Reservoir conformance improvement*. Society of Petroleum Engineers.

Terry, R.E., Huang, C.G., Green, D.W. et al. 1981. Correlation of Gelation Times for Polymer Solutions Used as Sweep Improvement Agents. *SPE J* **21** (02): 229-235. https://doi.org/10.2118/8419-PA.

UTGEL Technical Manual, 2015.

Veil, J.A., Puder, M.G., Elcock, D. et al. (January 2004). A White Paper Describing Water from Production of Crude Oil, Natural Gas, and Coal Bed Methane. Argonne National Laboratory. Final Report, Contract W-31-109-Eng-38, US DOE NETL, Argonne, Illinois.

Wang, D., Xia, H., Liu, Z. et al. 2001. Study of the Mechanism of Polymer Solution with Visco-Elastic Behavior Increasing Microscopic Oil Displacement Efficiency and the Forming of Steady 'Oil Threads' Flow Channels. Presented at the SPE Asia Pacific Oil and Gas Conference and Exhibition, Jakarta, Indonesia, 17-19 April. SPE-68723-MS. https://doi.org/10.2118/68723-MS.

Wang, D., Seright, R., Zhenbo, S. et al. 2007. Key Aspects of Project Design for Polymer Flooding. Presented at the SPE Annual Technical Conference and Exhibition, Anaheim, California, 11-14 November. SPE-109682-MS. https://doi.org/10.2118/109682-MS.

Wang, J. and Dong, M. 2009. Optimum effective viscosity of polymer solution for improving heavy oil recovery. *J Pet Sci Eng* **67**: 155-158. https://doi.org/10.1016/j.petrol.2009.05.007.

Wang, D. Xia, H., Yang, S. et al. 2010. The Influence of Visco-elasticity on Micro Forces and Displacement Efficiency in Pores, Cores and in the Field. Presented at the SPE Enhanced Oil Recovery Conference at Oil and Gas West Asia, Muscat, Oman, 11-13 April. SPE-127453-MS. https://doi.org/10.2118/127453-MS.

Wang, D., Wang, G., and Xia, H. 2011. Large Scale High Visco-Elastic Fluid Flooding in the Field Achieves High Recoveries. Presented at the SPE Enhanced Oil Recovery Conference, Kuala Lumpur, Malaysia, 19-21 July. SPE-144294-MS. https://doi.org/10.2118/144294-MS.

Yanez, P.A.P. Mustoni, J.L., Relling, M.F. et al. 2007. New Attempt in Improving Sweep Efficiency at the Mature Koluel Kaike and Piedra Clavada Waterflooding Projects of the S. Jorge Basin in Argentina. Presented at the Latin American & Caribbean Petroleum Engineering Conference, Buenos Aires, Argentina, 15-18 April. SPE-107923-MS. http://doi.org/10.2118/107923-MS.

Zaitoun, A., Tabary, R., Rousseau, D. et al. 2007. Using Microgels to shutoff Water in a Gas Storage Well. Presented at the International Symposium on Oilfield Chemistry, Houston, Texas, USA, 28 February- 2 March. SPE-106042-MS. http://doi.org/10.2118/106042-MS.

Zhang, H. and Bai, B. 2011. Preformed particle gel transport through open fractures and its effect on water flow. *SPE J* **16** (02): 388-400. SPE-129908-PA. https://doi.org/10.2118/129908-PA.

Zhao, G., Dai, C., Zha, M. et al. 2013. Investigation and Preparation and Mechanisms of a Dispersed Particle Gel Formed from a Polymer Gel at Room Temperature. *PLOS ONE* **8** (12): 1-9. https://doi.org/10.1371/journal.pone.0082651.

VITA

Tariq Khalaf Khamees was born in Baghdad, Iraq. He received his B.Sc. and M.Sc. degrees in Petroleum Engineering from University of Baghdad, Baghdad, Iraq in 1994 and 1998, respectively. He joined Iraq Ministry of Oil (IMoO) as a reservoir engineer in 1999. His main area of interest included, but were not limited to, integrated reservoir studies of Iraqi oil fields using reservoir simulators such as CMG and ECLIPSE. He was the principal investigator of Kirkuk and Bai Hassan Tertiary reservoir studies.

Tariq was granted a PhD scholarship by the Iraq Ministry of Oil and ExxonMobil Iraq in 2013 through Iraq Training Technology and Scholars Program (ITTSP). He joined Missouri University of Science and Technology in Fall Semester 2014.

His PhD research included an investigation of different parameters that could affect the gelation process of in-depth fluid diversion (IFD) using reservoir simulators applying different polymer gel systems, such as in-situ and preformed gels. He received his Doctor of Philosophy from Missouri University of Science and Technology in May 2020.